

CHARACTERIZATION OF SHORT  
TEMPLATE-NUCLEATED HELICAL PEPTIDES

by

Sherri L. Oslick

B.A., Cornell University

(1989)

Submitted in Partial Fulfillment

of the Requirements for the

Degree of

Doctor of Philosophy

at the

Massachusetts Institute of Technology

June, 1996

Copyright © Massachusetts Institute of Technology 1996  
All Rights Reserved

Signature of Author \_\_\_\_\_

Department of Chemistry  
March 1, 1996

Certified by \_\_\_\_\_

Professor Daniel S. Kemp  
Thesis Supervisor

Accepted by \_\_\_\_\_

Professor Dietmar Seyferth  
Chairman, Departmental Committee on Graduate Students

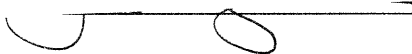
MASSACHUSETTS INSTITUTE  
OF TECHNOLOGY

JUN 12 1996

Science

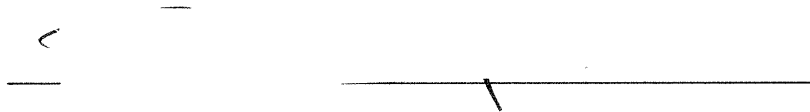
This doctoral thesis has been examined by a Committee of the Department of Chemistry as follows:

Professor John M. Essigmann



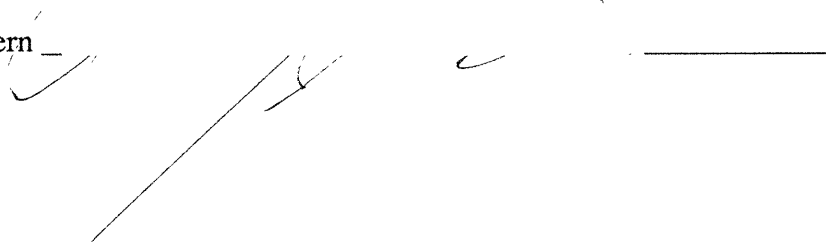
Chairman

Professor Daniel S. Kemp



Thesis Supervisor

Professor Lawrence J. Stern



# CHARACTERIZATION OF SHORT TEMPLATE-NUCLEATED HELICAL PEPTIDES

by

SHERRI L. OSLICK

Submitted to the Department of Chemistry  
at the Massachusetts Institute of Technology on March 1, 1996  
in partial fulfillment of the requirements for the degree of Doctor of Philosophy

## ABSTRACT

Knowledge of the properties of conjugates of the *N*-terminal helix nucleating template Ac-Hel<sub>1</sub> has been expanded through an <sup>1</sup>H-NMR analysis of a series of nonpeptide derivatives of the template. The effects of temperature, salt, and trifluoroethanol have been investigated and are in accord with prior findings for peptide derivatives. The rate of *s*-cis (c)→*s*-trans (t) isomerization of the *N*-acetyl group of the template has been determined and has been shown to be solvent dependent.

These derivatives have been examined by circular dichroism (CD) spectroscopy as well and reveal a strong absorption in the region of interest for the study of secondary structure. The spectra are shown to vary with the relative ratio of nucleating and nonnucleating conformational states of the template. The limiting spectra of the pure conformational states of the template have been determined by a linear regression analysis on a series of CD spectra of a simple monoamide derivative of the template in various concentrations of trifluoroethanol, providing a first step toward the analysis of peptide segments of peptide conjugates of the template. The mole fractions of the nucleating state of the template, required for the linear regression analysis, were calculated directly from the t/c ratio of the template as measured by NMR integration.

Potential discrepancies between NMR and CD data, including concentration, temperature, perchlorate, and isotope effects, have been investigated and are shown to be insignificant. An assay has been developed to provide an accurate determination of CD sample concentrations of template derivatives.

CD spectra of the alanine series Ac-Hel<sub>1</sub>-A<sub>1-6</sub>-OH and Ac-Hel<sub>1</sub>-A<sub>1-6</sub>-NH<sub>2</sub> in varying concentrations of trifluoroethanol have been recorded along with the t/c ratios of these compounds measured by NMR. The template contribution to these CD spectra has been eliminated by calculations utilizing the t/c ratios, and the resultant spectra corresponding to the peptide portion only of these derivatives are given. A linear regression analysis on these corrected spectra has been performed and has yielded the peptide spectra corresponding to the nonnucleating state of the template. These have been shown to be random coil in nature, providing the first direct evidence that peptides attached to the nonnucleating state of the template are in fact unstructured. These spectra have been used to determine the peptide spectra corresponding to the nucleating state of the template, and additional derivations have been performed to calculate for the first time the value of  $[\theta]_{222}$  corresponding to 100% helix for a five and six residue peptide.

Thesis Supervisor: Professor Daniel S. Kemp

Title: Professor of Chemistry

## Acknowledgments

Of all the sections of this thesis, this is perhaps the hardest to write. There are numerous people to whom I have become indebted over the years and who have helped make this thesis a reality. I know that I will be remiss in my acknowledgments and apologize to those who deserve to be included but elude me at the moment. Having said that, I would like to acknowledge and thank the following.

I am grateful for financial support from the Department of Chemistry in the form of a teaching assistantship (1989-1990). I also appreciate financial support in the form of a research assistantship (1990-1996) from Professor D. S. Kemp. I would also like to thank Dr. Kemp for the opportunity to conduct this research in his laboratories.

I am very grateful to the staff of the Chemistry Department Spectroscopy Laboratory, Jim Simms, Jeanne Owens, Scott Gardner, and Debbie Western, for addressing my constant barrage of questions and problems with patience and understanding. Large portions of this thesis would not have been possible without their assistance.

To the past members of the Kemp group, I would like to give thanks not only for a great deal of help over the years, but also for their companionship. Nader Fotouhi deserves special recognition for helping me get started in the lab. I must also thank Chris Arico-Muendel and Dan Blanchard; I very much enjoyed the time I spent in their bay and am grateful for their friendships. Jeff Rothman, in that zany way of his, was rather endearing and added much necessary humor to the group. And I would like to acknowledge Tom Allen; although we had our differences, I am very glad to have had the opportunity to know him.

The present members of the Kemp group must also be acknowledged. I would like to thank Linda Szabo Shimizu and Evan Powers for performing the tedious task of proofreading this thesis. Furthermore, I must give special thanks to Linda, with whom I have shared a lab during the majority of my graduate career. Through music compromises, coffee runs, and everyday interactions, it has truly been a pleasure sharing space with her. Evan never ceases to amuse me, and for that I am extremely grateful. His unique brand of humor certainly helped me get through many grim days; I am thankful for his friendship as well. I wish Linda, Evan, Janette Lee, and Z. Q. Li all the best with their theses and for the future.

My roommate throughout graduate school, Elizabeth Trimmer, deserves a special acknowledgment. I am not an easy person to live with, and Elizabeth managed to do so for over six years. I thank her, and wish her the best of luck in the completion of her own dissertation.

Over the years, I have had the privilege of friendship with some very special people, and I cannot adequately express my gratitude for what they have added to my life. Nevertheless, I would like to give heartfelt thanks to the following: To Rachael Berman, whom I wish I had gotten to know sooner; I have very much enjoyed our discussions and the time we have spent together. To Shannon Storm Blanchard, who is one of the most kind and genuine people I have ever known and who is a wonderful listener and friend. To Natasha Kablaoui, with whom I have had a great deal of fun over the years but has also been a good friend on a more serious level. To Beth Powers, my very dear friend from college, who always provided a haven in which to take refuge when I needed to get away

and who was always there for me despite my inability to devote much time to our friendship. And to Kelly Suber, whose cheerful disposition was always appreciated and who made my time here very much more enjoyable.

Most importantly, however, I must thank my family. They have been, and always will be, the most important people in my life. I thank my grandmother, Mom-mom Mary, for her pride in her granddaughter and her love; both have put a smile on my face and made the days a bit brighter. I also thank my brother, Mitchell, whom I have always respected and admired and whose own successes I have always tried to emulate.

My largest debt of gratitude goes to my parents, Ted and Irene, who instilled in me not only the belief that I could accomplish anything I wanted but also the strength with which to do so. They have been there for me so many times and in so many ways that it is impossible to recount them all here. Suffice it to say that I am deeply grateful for everything they have done for me. It is to my parents that I dedicate this thesis.

To Mom and Dad

*with gratitude, appreciation, and love*

## Table of Contents

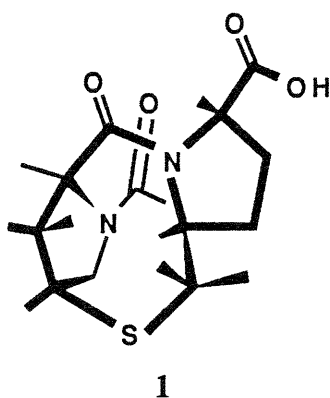
	Page
Chapter 1: Introduction .....	8
Chapter 2: Characterization of Small Nonpeptide Template Derivatives .....	17
Chapter 3: Characterization of the Series Ac-Hel <sub>1</sub> -A <sub>n</sub> -OH and Ac-Hel <sub>1</sub> -A <sub>n</sub> -NH <sub>2</sub> .....	41
Experimental .....	105
Appendix A: Development of the Ninhydrin Assay for Concentration Determination ..	140
Appendix B: CD Data Analysis: Derivations and Results .....	154
References .....	192

## **Chapter 1**

Introduction



It has been previously demonstrated that the helix nucleating template Ac-Hel<sub>1</sub>, **1**, designed to mimic the spacing and carbonyl orientation of  $\alpha$ -helices, can be conveniently synthesized (McClure *et. al.*, 1995) and utilized to induce helical structure in covalently linked short peptides in a variety of solvents, including water (Curran, 1988; Boyd, 1989; Allen, 1993; Groebke *et. al.*, 1996). An *s*-trans (*t*) conformation of the *N*-acetyl, as demonstrated below, is required for helix formation, but a nonnucleating *s*-cis (*c*) population also exists. Extensive analysis has shown that the *t/c* state ratio of the template, easily measured by NMR integration, can be directly related to the fractional helicity of the attached peptide. Thus Ac-Hel<sub>1</sub> serves not only to initiate helices but also to report on their relative stability. An expansion of the utility of the *t/c* ratio as a measure of helicity is presented in this thesis.



Ever since its first use by Doty and coworkers in their analysis of soluble polyamino acids (Holzwarth *et. al.*, 1962; Holzwarth & Doty, 1965), circular dichroism (CD) has been widely accepted as the fundamental tool for the structural analysis of both peptides and proteins. For helices, the spectrum is distinctive, consisting of a maximum at 190 nm and minima at 208 and 222 nm; the ellipticity at 222 nm ( $\theta_{222}$ ) is used to measure fractional helicity by comparison to the per residue value of  $[\theta]_{222}$  corresponding to 100% helix. That value, however, approximately  $-35,000 \text{ deg}\cdot\text{cm}^2/\text{dmole}$  for polylysine (Greenfield & Fasman, 1969), is not as well defined. Theoretical calculations suggest a strong length dependence for helices containing fewer than 3-4 turns or 11-15 residues (Manning *et. al.*, 1988) and the experimentally derived values used in the literature have ranged from  $-26,500 \text{ deg}\cdot\text{cm}^2/\text{dmole}$  (Bierzynski *et. al.*, 1982) to  $-39,400 \text{ deg}\cdot\text{cm}^2/\text{dmole}$  (Todd & Millhauser, 1991), with isolated instances of values as high as  $-49,000 \text{ deg}\cdot\text{cm}^2/\text{dmole}$  (Albert & Hamilton, 1995). Despite these uncertainties, the ease and convenience of CD analysis has led to its widespread acceptance for the quantitation of

helicity. Clearly an independent means is needed to determine the value of  $[\theta]_{222}$  for 100% helix and resolve this dilemma, thereby ensuring maximal accuracy and precision in CD measurements of helicity.

This thesis provides such a means by relating the CD spectra of various Ac-Hel<sub>1</sub> derivatives to their corresponding t/c ratios. In light of the current surge of interest in the study of short peptides, accurate assignments of their helicity by CD is essential, and the template system provides an ideal matrix in which to study the ellipticity of such peptides. Chapter 3 presents the per residue ellipticities of peptides with as few as five and six residues.

Before this information is presented, it is necessary to address broader issues and to place it in the context of previous work of others investigating the formation of polypeptide helices. The remainder of this chapter will address these issues, including methods of helical quantitation, but will begin with the importance of studying short unaggregated helices in solution.

## **Helix Formation and the Protein Folding Problem**

The significance of the protein folding problem cannot be underestimated. The fact that a protein, comprised of a linear sequence of amino acids, is able to consistently adopt a specific, unique, and highly compact three dimensional structure within a matter of minutes is truly an amazing feat of nature. A predictive understanding of the strategy employed in the transition from primary to tertiary structure is not only an intellectual challenge, but has widespread implications in numerous areas of medicinal chemistry and structural biology.

To date, such an understanding does not exist. Numerous strides have been made, but owing to the magnitude of the problem, current knowledge can still be regarded as preliminary. Early investigations, however, have provided key information regarding the pathway of protein folding and indicate that elements of protein secondary structure are formed early in the pathway. This information has led to the development of a model in which short segments of secondary structure serve as the foundation upon which further rearrangement leads to the final folded form. Certainly any understanding of the pathway and mechanism of protein folding as a whole must therefore begin with an understanding of the factors governing the formation of short regions of secondary structure in water. Helices, for which a substantial body of both theoretical and experimental information exists, are obvious targets for study. Hence techniques for their investigation are essential, and are presented in the next section.

## Quantitation of Helical Structure

Alternate means may be and have been employed, but despite its drawbacks, CD is currently the best technique for the quantitation of helical structure.

The helix→coil transition may be effected by either an increase in temperature or an increase in the concentration of a denaturant such as urea. Techniques such as CD or UV/Vis spectroscopy are used to monitor the resultant melting, or loss of structure. Most melting curves, for peptides in the realm of 50 residues or larger, show sharp, highly cooperative transitions, and the melting temperature of a particular helix may therefore be regarded as a measure of its robustness. For short peptides, however, the melting curve is usually broad, and the melting temperature cannot be evaluated with precision.

NMR measurements are able to evaluate helical structure at particular residues, and therefore can be used for the analysis of local effects such as fraying, which serves to decrease the overall helical content of a peptide. Rates of amide H-D proton exchange in D<sub>2</sub>O are expected to be minimal for a tightly coiled helix, and relative exchange rates for individual residues can be used to estimate overall fraying and structure. The relationship between fraying and stability, however, can depend in a complex manner on particular interhelical interactions, and hence exchange rates have rarely been used as a simple or direct measure of helicity. Chemical shift values and coupling constants have also been used as indicators of helical structure but are often inconclusive and difficult to relate to overall helicity. They serve better as support for other findings than as definitive evidence of helicity.

2D <sup>1</sup>H-NOE NMR can provide a wealth of three dimensional structural information, and is an ideal technique for the analysis of helices, which exhibit a comprehensive set of through-space connectivities owing to their highly compact, regular structure (Wüthrich, 1986). The strength of an NOE interaction, however, is dependent on abundance, on local chemical and magnetic environment, and on distance in a nonlinear fashion. Hence characteristic NOEs indicate only the presence of helical structure, not the magnitude. While NOE experiments are extremely valuable as structural probes, except in rare cases, they cannot provide quantitative information.

The above techniques are able to indicate the presence of helical structure in short peptides, but cannot reliably quantitate it. Only CD can be used to assign numbers to helical content, and as such has been used extensively by investigators probing the formation of helices.

## Systems to Probe Helix Formation

While it is not yet possible to predict accurately what peptide segments will likely become helical, notable progress has been made toward an understanding of how helices form. This section will provide a brief review of such progress.

Early investigations by Doty and coworkers focused on soluble polyamino acids and revealed a sharp temperature or solvent dependent helix→coil transition. It was possible to synthesize polyamino acids of controlled molecular weights (Blout *et. al.*, 1954; Blout & Karlson, 1956; Idelson & Blout, 1957; Katchalski & Sela, 1958), and the dependence of the helical character of these compounds on solvent, temperature, pH, various additives, and peptide chain length was established (Doty *et. al.*, 1954; Doty & Yang, 1956; Doty *et. al.*, 1956; Moffit & Yang, 1956; Doty *et. al.*, 1957; Yang & Doty, 1957; Doty *et. al.*, 1958; Gratzer & Doty, 1963; Fasman *et. al.*, 1964; Davidson & Fasman, 1967).

From these studies evolved a basic understanding of  $\alpha$ -helix formation, which in turn led to the development of a body of theoretical models directed at explaining the observed transitions. The best known of these models was developed by Zimm & Bragg (Zimm & Bragg, 1959) and later extended by others, including Lifson & Roig (Lifson & Roig, 1961) and Scheraga (Poland & Scheraga, 1969). In these models, a peptide chain of length  $n$  is viewed as a composite chain of one helical (h) segment flanked by two random coil (c) segments of varying length that can be denoted  $c_x h_y c_z$ , where  $x$  and  $z \geq 0$  and  $x+y+z=n$ . Random coil residues are assigned a statistical weight of 1; helix weight is dependent on two parameters. The first is entropically based and represents the difficulty in aligning the peptide backbone angles to form the first turn of the helix. This factor corresponds to the first three residues of a helical sequence and is assigned a weight of  $\sigma$ . The second parameter is an enthalpic factor denoting the likelihood that each subsequent amino acid in the chain will join the preexisting helix and is assigned a weight of  $s$  for each of the  $y-3$  remaining helical residues. The essence of their theory is summarized by approximating the helical function to be a sum of terms of the form  $\sigma s^{n-2}$ . For the homopolymers studied by Doty, the nucleation factor  $\sigma$  was best fit with values in the range of  $10^{-3}$  to  $10^{-4}$ , and the propagation factor  $s$  for the individual amino acids was slightly greater than 1.

Experimental determination of  $\sigma$  and  $s$  values for each of the naturally occurring amino acids was obtained in an extensive analysis by Scheraga and coworkers (Sueki *et. al.*, 1984). The amino acid of interest was randomly incorporated as a "guest" into a homopolymer host of poly-hydroxybutyl-glutamine, the change in melting temperature was

monitored, and the result was applied to a model similar to the above to compute the values for the helical parameters. While this work is extremely significant, the model must be regarded as preliminary as it does not account for short range neighboring effects, as pointed out by Scheraga.

Early attempts to detect secondary structure in short peptide segments in water, even those known to be helical within a protein, were unsuccessful (Epanand & Scheraga, 1968). It was believed that for short peptides the gain in enthalpy from hydrogen bond formation was insufficient to overcome the loss in entropy of nucleation and thus they simply did not develop helical character. In the context of the model discussed above, a calculation demonstrates the observed length dependence of helix formation. For a homopolypeptide of alanine, assigned an  $s$  value of 1.06 and a  $\sigma$  of  $8 \times 10^{-4}$  (Scheraga, 1978), the probability of forming a helical peptide sequence of length ten calculates to be  $(8 \times 10^{-4})(1.06)^8 = .00128$ . In a peptide sequence of only ten residues, this state is in equilibrium with a random coil state with a probability of  $(1)^{10} = 1$ . In a very simple model in which this is the only helical state, the fractional helicity, or helical content relative to the total population, is then  $(.00128)/(1 + .00128) = 0.00128$  and the helical percentage is 0.128%. For a helical peptide sequence of a hundred residues, the corresponding state probability is  $(8 \times 10^{-4})(1.06)^{98} = 0.242$  and the helical percentage is 19.5%. This crude model ignores the contribution to the helical state of shorter helical sequences, but it clearly predicts that helicity should only be detectable in long polypeptides (on the order of 50-100 residues), in accordance with experimental results.

A notable exception was discovered by Brown and Klee with the observation that the C-peptide, a 13 residue fragment of the 20 residue S-peptide cleaved from the N-terminus of RNase A, exhibited significant helical structure in aqueous solution at low temperatures (Brown & Klee, 1971). Only later, however, was it recognized by Baldwin and coworkers that this peptide could be used to investigate the formation and stabilization of helices, providing the first system by which short peptides could be used experimentally toward this purpose (Bierzynski *et al.*, 1982). A comprehensive study of the helical structure of this peptide, of sequence KETAAAKFERQHHse(lactone), was conducted by both NMR and CD and confirmed that this peptide did in fact exhibit a high level of helicity at very low temperatures in water (Bierzynski & Baldwin, 1982; Bierzynski *et al.*, 1982; Kim *et al.*, 1982). Later work by Baldwin and others on analogs of the S- and C-peptides revealed that the high degrees of helicity observed for the parent peptides were not anomalies but could be extended to a larger class of similar peptides (Shoemaker *et al.*, 1985; Shoemaker *et al.*, 1987; Fairman *et al.*, 1989; Osterhout *et al.*, 1989; Merutka & Stellwagen, 1989; Fairman *et al.*, 1990; Shoemaker *et al.*, 1990; Fairman *et al.*, 1991).

It was not readily apparent, however, why such peptides exhibited high levels of helical character while others of similar size exhibited none, nor was it clear to what extent this class of peptides could be extended.

Calculations based on  $s$  and  $\sigma$  values obtained from oligopeptides do not predict the observed helical content, but the possibility still existed that short range neighboring effects were responsible for helical enhancement. In fact, early investigations focused on the role of specific side chain stabilizing effects such as salt bridges and interactions with the helix dipole. The pH profile of the C-peptide suggested that a salt bridge was in fact responsible for helix stabilization (Bierzynski & Baldwin, 1982), and additional studies clarified the role of side chain salt bridges in this peptide and its analogs (Osterhout *et al.*, 1989; Fairman *et al.*, 1990; Shoemaker *et al.*, 1990). Analysis of the role of side chains at the two termini confirmed the ability of a favorable interaction between charged side chains and the helix dipole to provide additional stability to the helix (Shoemaker *et al.*, 1985; Shoemaker *et al.*, 1987; Fairman *et al.*, 1989).

With these principles in mind, Baldwin and Marqusee were able to create short peptides of *de novo* design, containing only alanine (A), lysine (K), and glutamic acid (E) residues, constructed to maximize  $\text{Glu}^- \cdots \text{Lys}^+$  salt bridges as well as dipole interactions (Marqusee & Baldwin, 1987). These EAK peptides exhibited a high helical content in water at low temperatures, again suggesting the importance of side chain electrostatic effects in helix stabilization.

This idea was brought firmly into question, however, when Baldwin and Marqusee simplified the EAK peptides to sequences containing only alanine and lysine, such as  $\text{Ac}-(\text{AAAAK})_3\text{A}-\text{NH}_2$ , or only alanine and glutamic acid, such as  $\text{Ac}-\text{A}(\text{EAAAA})_3-\text{NH}_2$ ; these peptides exhibited a high helical content similar to the EAK peptides (Marqusee *et al.*, 1989). With only one type of charged side chain, stabilization could not be attributed to salt bridges, and pH profiles indicated that dipole interactions were not responsible either. Additionally, a similar neutral peptide, containing only alanine and glutamine residues, was also highly helical (Scholtz *et al.*, 1991a). Clearly an explanation other than electrostatic interactions was needed to explain the innate stability of these short peptides, such as a discrepancy in alanine and/or lysine  $s$  values determined in host oligopeptides versus short peptide systems.

Noting that a decrease in helicity was observed for the incorporation of additional lysine residues into the  $\text{A}_4\text{K}$  peptide, Baldwin and coworkers concluded that lysine had a low  $s$  value and attributed the stability of the  $\text{A}_4\text{K}$  peptide to an intrinsically high helical propensity of alanine (Marqusee *et al.*, 1989), ignoring the potential for destabilizing interactions among proximal lysine residues. They have quoted  $s_{\text{Ala}}$  values ranging from

1.35 (Scholtz *et al.*, 1991b) to 1.54 (Chakrabartty *et al.*, 1994). Further investigation of the Marqusee peptide series established the connection and applicability of amide exchange data, thermal melting curves and calorimetric enthalpic data of these peptides to a modified Lifson-Roig theory (Scholtz *et al.*, 1991b; 1991c; Rohl *et al.*, 1992). An extension of this analysis led to the determination of  $s$  values for the 20 natural amino acids in the A<sub>4</sub>K matrix using their Lifson-Roig model (Chakrabartty *et al.*, 1994).

Other researchers have utilized host matrices other than oligopeptides as well in order to determine the relative helix forming propensities of the natural amino acids. These matrices include proteins, such as barnase, studied by Fersht (Serrano *et al.*, 1992a; 1992b) and T4 lysozyme, investigated by Matthews (Bell *et al.*, 1992; Blaber *et al.*, 1993), the helix bundles of DeGrado (O'Neil & DeGrado, 1990), and EAK containing *de novo* peptides of Kallenbach (Lyu *et al.*, 1990; Gans *et al.*, 1991) and Stellwagen (Merutka *et al.*, 1990; Park *et al.*, 1993a; 1993b). While the relative helix forming tendencies of the neutral amino acids measured in these systems correlate somewhat qualitatively with the host-guest studies of Scheraga and with each other, quantitative agreement is poor, and questions have been raised regarding the practicality of using  $s$  values to predict helical structure. Clearly more analysis is needed to resolve this dispute.

Baldwin finds reasonable correlation of his results with those of Kallenbach and Stellwagen (Chakrabartty *et al.*, 1994), and current opinion leans toward an acceptance of the Baldwin values and a belief that the oligopeptide matrix of the Scheraga analysis possesses significant side chain interactions that interfere with the ability to properly determine  $s$  values of the guest amino acids (Padmanabhan *et al.*, 1994). Doubts have surfaced, however, regarding the validity of the Baldwin analysis.

Millhauser and coworkers have modified the EAK peptides of Baldwin with the incorporation of spin-labels to monitor the helix→coil transition by ESR spectroscopy; results indicate that the helices formed in these peptides are primarily  $3_{10}$  and not  $\alpha$ -helical in nature (Miick *et al.*, 1992). Scheraga has attributed the high helical character of the AK peptides to an interaction between the lysine side chain and the helix backbone (Vila *et al.*, 1992). In fact, recent research in these laboratories has indicated this to be the case and attributes the unusually high helicity to high  $s_{\text{Lys}}$  values, in stark contrast to the suggestion of Baldwin that it is founded in high  $s_{\text{Ala}}$  values (Groebke *et al.*, 1996). Initial studies of Ac-Hel<sub>1</sub> were aimed at developing a consistent understanding of the behavior of its peptide derivatives, and current focus has centered on peptides containing one or more lysine residues in an alanine base. Naturally, it is of interest to reconcile our results with those of Baldwin and coworkers.

Helical assignments of the Baldwin-Marqusee peptides and their analogs have all been made by CD measurement as compared to a value of  $[\theta]_{222}$  representing 100% helix. The value employed, however, has been inconsistent. Before direct comparisons may be made between our data and that of Baldwin and coworkers, this value must be determined.

Hence the major aim of this thesis has been in the development of CD methodology for its application to Ac-Hel<sub>1</sub> derivatives and the independent determination of  $[\theta]_{222}$  based on t/c values. The template itself has a considerable absorption in the region of interest for helices and a correction for its contribution must be made prior to helical comparison of the peptide portions of its derivatives. This process is less than straightforward, however, owing to the presence of three conformational states of the template, discussed in Chapter 2, each with its own CD absorption. The solution to this problem through the use of a simple amide conjugate of the template, Ac-Hel<sub>1</sub>-NH<sub>2</sub>, is presented in Chapter 2, along with results that clarify our understanding of the properties of Ac-Hel<sub>1</sub> conjugates.

A precise and accurate concentration measurement is essential for the proper determination of helical values by CD, and as such has been the focus of much attention, with varied success. Appendix A of this thesis presents a reliable solution to this problem as developed for the peptide derivatives of Ac-Hel<sub>1</sub>.

The CD spectra of the alanine series Ac-Hel<sub>1</sub>-A<sub>n</sub>-OH and Ac-Hel<sub>1</sub>-A<sub>n</sub>-NH<sub>2</sub>, n=1-6, are presented in Chapter 3 and used in conjunction with carefully measured t/c ratios to determine for the first time the molar per residue ellipticity of a completely helical penta- and hexaalanine peptide.



## **Chapter 2**

### Characterization of Small Nonpeptide Template Derivatives

## INTRODUCTION

As related in Chapter 1, the primary goal of this thesis is the application of CD spectroscopy to the study of short peptides linked to the helix nucleating template Ac-Hel<sub>1</sub>. In this chapter, two sets of results will be presented. In the first, NMR data, designed to expand the analysis by Dr. T. Allen (1993) of the effects of salt, temperature, and trifluoroethanol (TFE, a known helix stabilizer) on templated peptides, is presented. In the second, the CD spectra of simple monoester and monoamide derivatives of the template are given, as well as a linear regression analysis on one of these derivatives that yields the limiting CD spectra of pure conformational states of the template. Prior to presenting these findings, it is necessary to provide an overview of previous results regarding the structural features of the template and its derivatives. This section will relate the relevant information and provide the foundation upon which this thesis is built.

The helix nucleating template Ac-Hel<sub>1</sub> was designed to be covalently attached to short peptides at their *N*-termini, thereby circumventing the energetic difficulties of helix formation in short peptides by separating helix initiation from helix propagation. The spacing and carbonyl orientation of Ac-Hel<sub>1</sub> resembles that of an  $\alpha$ -helix and as such it is able to pre-nucleate a helical conformation in covalently linked peptides. As propagation is a relatively favorable event, the attached short peptides are able to develop helical character. The template is diproline derived; proline was selected as its fixed  $\phi$  angle of  $-60^\circ$  is close to the value of  $-57^\circ$  for  $\alpha$ -helices and because proline is frequently observed at the termini of helices. It is *N*-acetylated to provide an additional carbonyl for hydrogen bond formation, and the thiomethylene bridge was incorporated to populate the otherwise inaccessible helix-inducing conformation.

Through an extensive investigation of the template and its peptide derivatives, a three state model has been developed. The template, while designed to be conformationally rigid, contains two important sites of conformational flexibility. The first is the *N*-acetyl, which can adopt either an *s*-cis (c) or an *s*-trans (t) conformation, and the second is the thiomethylene bridge, which can be either staggered (s) or eclipsed (e). Of the four possible conformers, only three have been observed experimentally. These are shown in Figure 2.1.

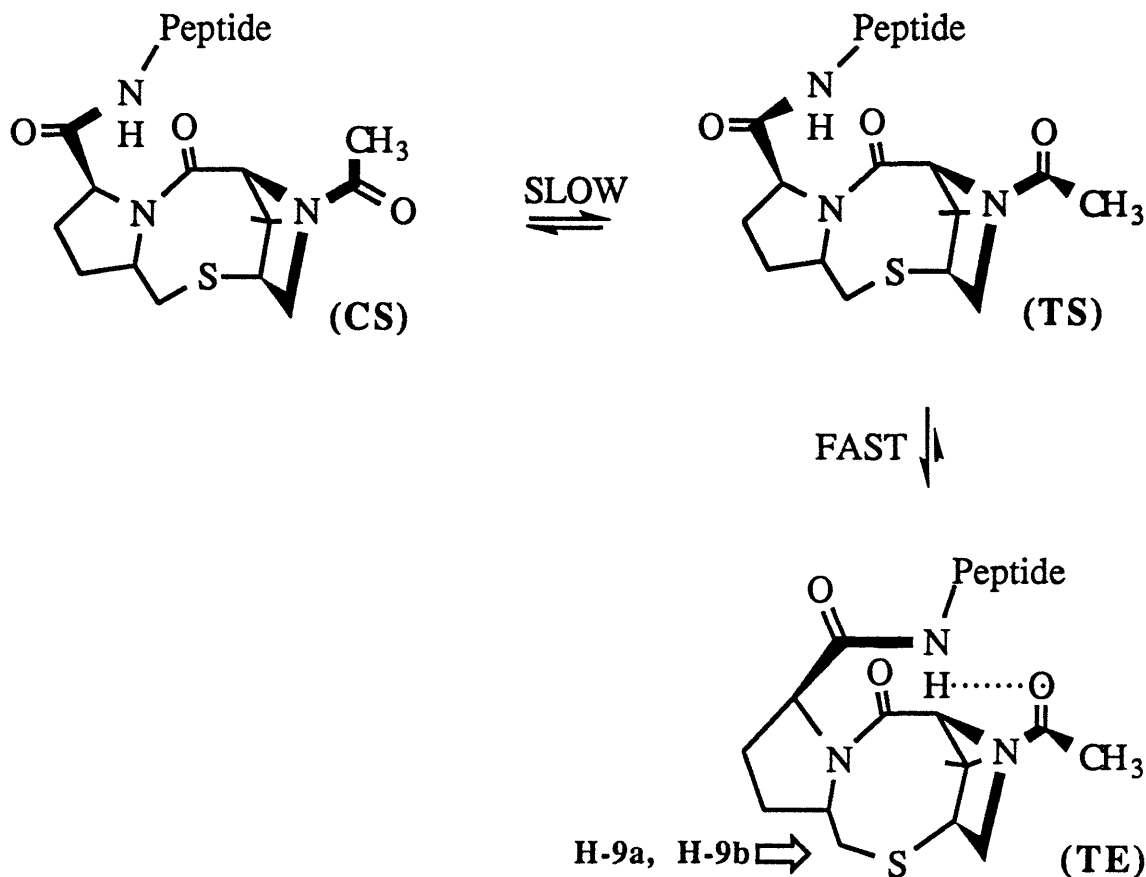


**Figure 2.1:** The three conformational states of Ac-Hel<sub>1</sub>.

The acetyl isomerization is slow on the NMR time scale, and thus a doubling of resonances is observed in the NMR spectra. The  $s \leftrightarrow e$  equilibration is fast on the NMR time scale and all t state resonances therefore exist as a weighted average of s and e state populations. Thus these states are easily monitored by NMR. The cs and ts states do not have the proper carbonyl orientation and geometry to induce helical structure and are therefore nonnucleating states of the template. Only the te state is able to nucleate helical structure in an attached peptide, yet it is only accessible with the coupling of amino acids to the template. Furthermore, the equilibrium proportions of the three helical states are dependent on the specific peptide attached. Figure 2.2 illustrates the change in the NMR spectra as the relative proportions of the three conformational states change. (This data has been previously recorded by Dr. T. Allen, but in 9:1 H<sub>2</sub>O:D<sub>2</sub>O; it was remeasured in D<sub>2</sub>O to avoid the effects of water suppression. In addition, delay times were increased to more appropriate values than used by Dr. T. Allen. These modifications provide more reliable and accurate data.) An increase in peptide chain length is correlated with an increase of the

template *t*e state relative to the *c*s and *t*s states. The doubling of resonances and the shift of the *t* state protons from a pure *s* state to a more *e* containing state is most apparent in the H-9<sub>a<sub>t</sub></sub> and H-9<sub>b<sub>t</sub></sub> protons, the methylene protons adjacent to the sulfur; their local environment is most strongly affected by the *s*↔*e* equilibration. Moreover, the abundance of *t* state resonances relative to *c* state resonances increases. Thus, the degree of helical character in the peptide is mirrored by the extent of *t*e character of the template, and this can be applied to the evaluation of these systems. Extensive analysis has shown that the fractional helicity of the peptide can be directly related to the *t*/*c* ratio of the template, easily measured by NMR integration. A shift in the conformation of the template toward more *t*e character is reflected in an increase in the *t*/*c* ratio. This inherent property of the template has greatly simplified the structural characterization of its derivatives and has provided the means by which to compare and contrast different sequences and conditions.

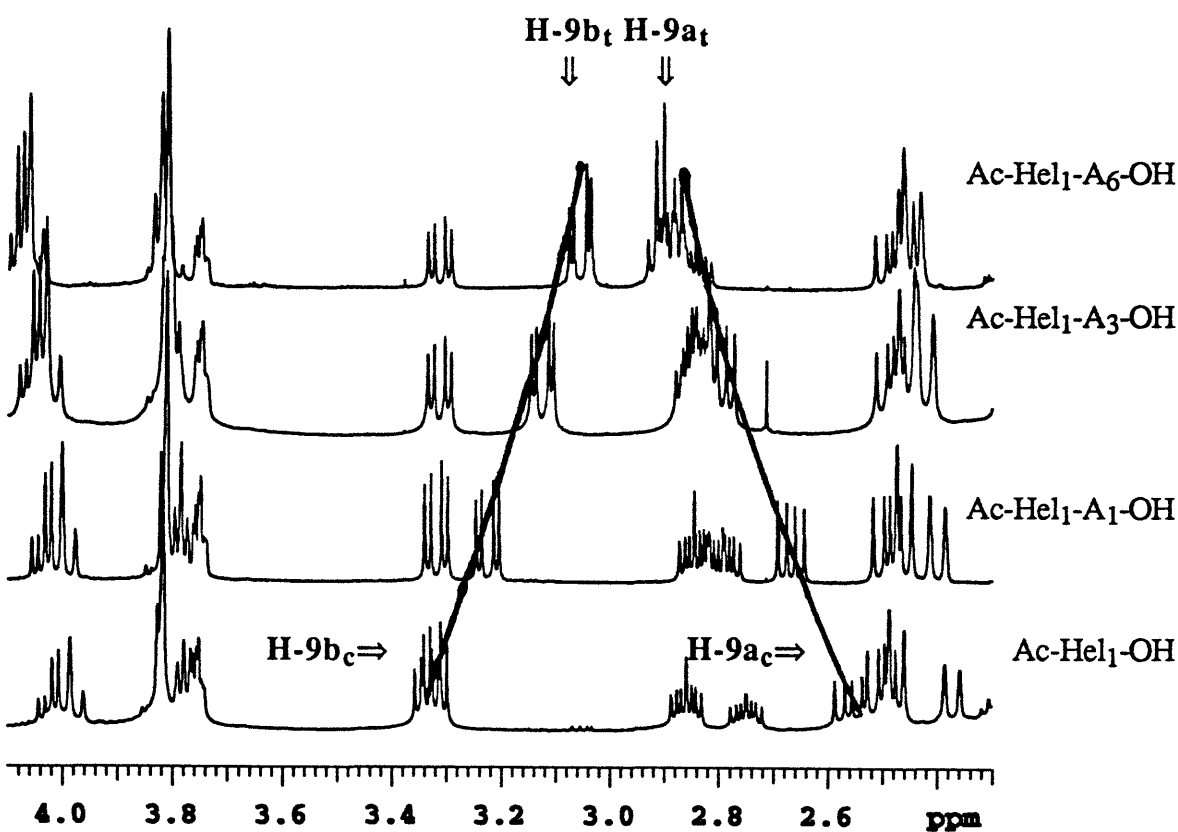


**Figure 2.2:** A portion of the  $^1\text{H}$ -NMR spectra of the series  $\text{Ac-Hel}_1\text{-A}_n\text{-OH}$  ( $n=0, 1, 3, 6$ ) in  $\text{D}_2\text{O}$ , demonstrating the separate *t* and *c* state resonances, as well as the *s*↔*e* shift of the H-9<sub>a<sub>t</sub></sub> and H-9<sub>b<sub>t</sub></sub> protons (shown by the curves).

An additional feature of the template further simplifies the analysis of its derivatives. Through a linear regression analysis of 16 separate series of a wide variety of template derivatives in both water alone and in TFE-water mixtures, the equilibrium constant  $K_1$  was found to be constant, with a value of 0.79 (Kemp *et. al.*, 1995). Using the expressions of 2.1 it is possible to derive equation 2.2, which relates the inverse of the t/c ratio to the observed chemical shift of a given derivative.

$$\delta_{\text{obs}} = \delta_{\text{te}} \frac{[\text{te}]}{[\text{te}] + [\text{ts}]} + \delta_{\text{ts}} \frac{[\text{ts}]}{[\text{te}] + [\text{ts}]}; \quad \frac{[\text{c}]}{[\text{t}]} = \frac{[\text{cs}]}{[\text{ts}] + [\text{te}]}; \quad K_1 \equiv \frac{[\text{ts}]}{[\text{cs}]} \quad 2.1$$

$$\delta_{\text{obs}} = \delta_{\text{te}} + (\delta_{\text{ts}} - \delta_{\text{te}}) K_1 \frac{[\text{c}]}{[\text{t}]} = A + B \frac{[\text{c}]}{[\text{t}]} \quad 2.2$$

For all series,  $\delta_{\text{obs}}$  did in fact depend on c/t in a linear fashion, and using a  $\delta_{\text{ts}}$  value obtained from derivatives incapable of developing te character, linear regression analysis provided a solution for both A and B, from which  $K_1$  could easily be computed.

The importance of this result is threefold. First, it provides an understanding of the equilibrium relationship between the two nonnucleating states of the template. Secondly, it enables the mole fractions of the individual template states of any derivative to be directly solved from its t/c ratio; expressions found in 2.3 can be derived to give 2.4.

$$t/c = \frac{ts + te}{cs}; \quad \frac{ts}{cs} = 0.79; \quad \chi_{\text{te}} = \frac{te}{cs + ts + te} \quad 2.3$$

$$\chi_{\text{cs}} = \frac{1}{1 + t/c}; \quad \chi_{\text{ts}} = \frac{K_1}{1 + t/c}; \quad \chi_{\text{te}} = 1 - \frac{1.79}{1 + t/c} \quad 2.4$$

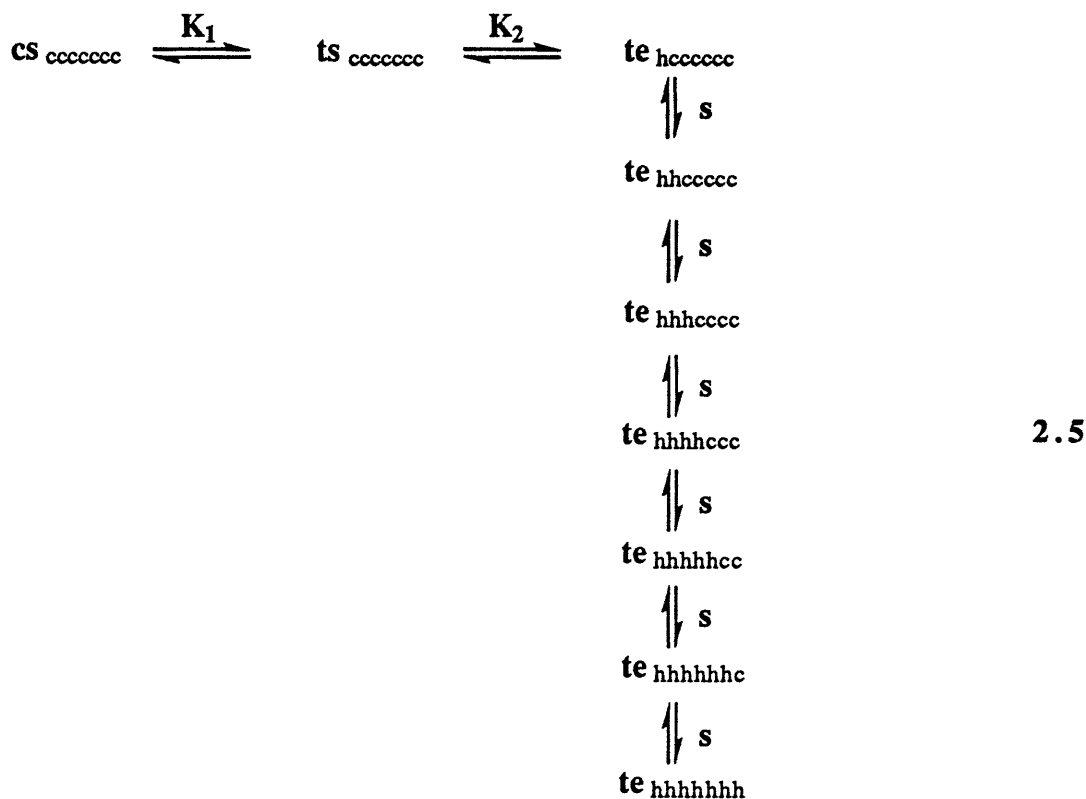
And lastly, a constant  $K_1$  links the cs and ts states of the template in an invariant manner, enabling these two states to be grouped together and regarded as one. Thus the three state model of the template may be reduced to a two state model, consisting of a nonnucleating (cs+ts) state and a nucleating te state.

The preceding discussion has focused on the structural analysis of the template portion of Ac-Hel<sub>1</sub>-peptide conjugates, but the conformational features of the peptide portions have been extensively characterized as well. Dr. T. Curran initiated these studies through an <sup>1</sup>H NMR analysis of the series Ac-Hel<sub>1</sub>-A<sub>n</sub>-OtBu, n=1-6, in various organic

solvents. Through a study of amide proton chemical shifts, vicinal coupling constants, and NOE interactions, Dr. T. Curran demonstrated that in these solvents, the c state peptides exhibit random coil properties while the t state peptides are helical in nature (Kemp & Curran, 1988; Kemp *et. al.*, 1991a). This analysis was extended to aqueous solution by Dr. J. Boyd, whose analysis of Ac-Hel<sub>1</sub>-A<sub>6</sub>-OH in water supported the conformational evidence obtained in organic solution. In addition, the peptide of this derivative was shown to be most helical at the template junction, with structure diminishing gradually with increasing distance from the template (Kemp *et. al.*, 1991b).

The most extensive characterization of templated peptides in aqueous solution was performed by Dr. T. Allen (Allen, 1993; Kemp *et. al.*, 1996a). Analysis of the amide protons of Ac-Hel<sub>1</sub>-A<sub>6</sub>-OH, including chemical shift dependencies on temperature and additives as well as vicinal coupling constants, was in accord with earlier findings. The most compelling evidence was obtained from a comprehensive 2D ROESY analysis, which again demonstrated that peptides of the c state are unstructured, while the t state peptides assume an  $\alpha$ -helix conformation. In addition, an invariance of the ts/cs ratio with changes in solvent and peptide structure was noted, suggesting the peptides of these two states to be similar in conformation. Furthermore, very large t/c ratios were shown to be consistent only with the absence of a significant population of structured peptides in the cs and ts states. In short, peptides in the cs and ts states may be regarded as random coils, while peptides in the te state are  $\alpha$ -helices, most structured at the template junction and least structured at the C-terminus.

This fraying effect in the te state of the peptide is consistent with the model for peptide helicity developed by Zimm & Bragg as discussed in the previous chapter. Under the plausible assumption that the peptide length is too short for spontaneous initiation at sites other than the template juncture, the peptide substates can be easily defined. By definition of the te state of the template, the amide of the first amino acid is necessarily hydrogen bonded and therefore helical in nature. The remaining amino acids may then exist in either a helical or a coiled state as seen in expression 2.5, which demonstrates the relationship among the template and peptide states shown below for the derivative Ac-Hel<sub>1</sub>-A<sub>6</sub>-NH<sub>2</sub>.



While there are only six amino acids, there are in fact seven possible peptides states as the *N*-terminal amide may hydrogen bond in a helical conformation. For a peptide with a free carboxylic acid at its *N*-terminus, the final peptide state must then end with a "c" residue. In this model, the values of *s*, the helix propagation parameter, are assumed to be identical for this homopeptide. (For an analysis of the validity and consequences of this assumption, see Kemp *et. al.*, 1996b).

While the results above provide an extensive knowledge base upon which the properties of the template system can be understood, there are still some remaining experiments necessary to expand upon current knowledge of the solution dynamics of the template. These center on the effects of environmental perturbations on small nonpeptide template derivatives and will be presented in the next section of this chapter. Furthermore, as outlined in Chapter 1, it is essential that CD methodology be developed for its application to Ac-Hel<sub>1</sub> derivatives and the value of  $[\theta]_{222}$  be determined based on *t/c* values. As the template itself has a considerable absorption in the region of interest for helices, a correction for its contribution must be made. CD analysis of the alanine series will be introduced in the final section of this chapter through a procedure to correct for the template CD contribution.

## ANALYSIS OF SMALL NONPEPTIDE TEMPLATE DERIVATIVES

The study of small nonpeptide derivatives of the template is useful as it provides an understanding of how the template functions without interference from linked peptides. This was initially addressed by Drs. T. Curran, J. Boyd, and T. Allen (Kemp *et al.*, 1991c; Curran, 1988; Boyd, 1989; Allen, 1993) and has been extended for this thesis. The template alone exists solely in the *cs* and *ts* conformations, limiting the range of analysis. Two simple derivatives of the template, Ac-Hel<sub>1</sub>-NH<sub>2</sub> and Ac-Hel<sub>1</sub>-NHMe, circumvent this problem. Both are nonpeptide derivatives with hydrogen bonding capacity and are therefore able to access the *te* state of the template. The methyl ester of the template has also proven useful for study. Figure 2.3 shows the structures of the small nonpeptide template derivatives of interest.

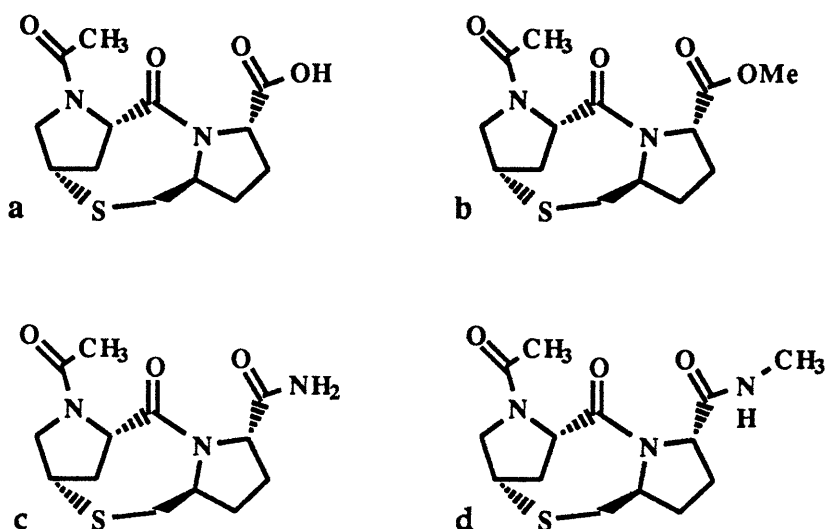


**Figure 2.3:** Small nonpeptide Ac-Hel<sub>1</sub> derivatives: (a) Ac-Hel<sub>1</sub>-OH; (b) Ac-Hel<sub>1</sub>-OMe; (c) Ac-Hel<sub>1</sub>-NH<sub>2</sub>; (d) Ac-Hel<sub>1</sub>-NHMe.

### Rate of Isomerization

Proline *cis-trans* isomerization is regarded as a late step in the protein folding process, and as such, its rate in water has been investigated in both protein and peptide systems. The template, derived from proline, has a rate of interconversion slow on the NMR time scale, and it was of interest to determine its isomerization rate specifically. In order to do so, it is necessary to find conditions in which initial and final equilibrium states



are measurably different. The template has been found to exist solely in the cs state in chloroform solution and in one crystalline form as determined by X-ray analysis. Very nearly the same equilibrium mixture of cs and ts states is found in aqueous solution and in acetonitrile ( $t/c = 0.63$  in  $D_2O$ ,  $0.62$  in  $CD_3CN$ ). It was hoped that it would be possible to exploit these differences to monitor the cis-trans interconversion. Kinetics were initially performed by rapid dissolution of crystalline template into  $D_2O$  and monitored by NMR at  $5^\circ C$ ; all solutions and materials had been equilibrated to  $5^\circ C$  prior to dissolution. Due to the nature of the experiment, the first data point could not be acquired until three minutes after mixing, but a relaxation of a more cs containing mixture to the final equilibrium conditions was nevertheless observed (see Figure 2.4).

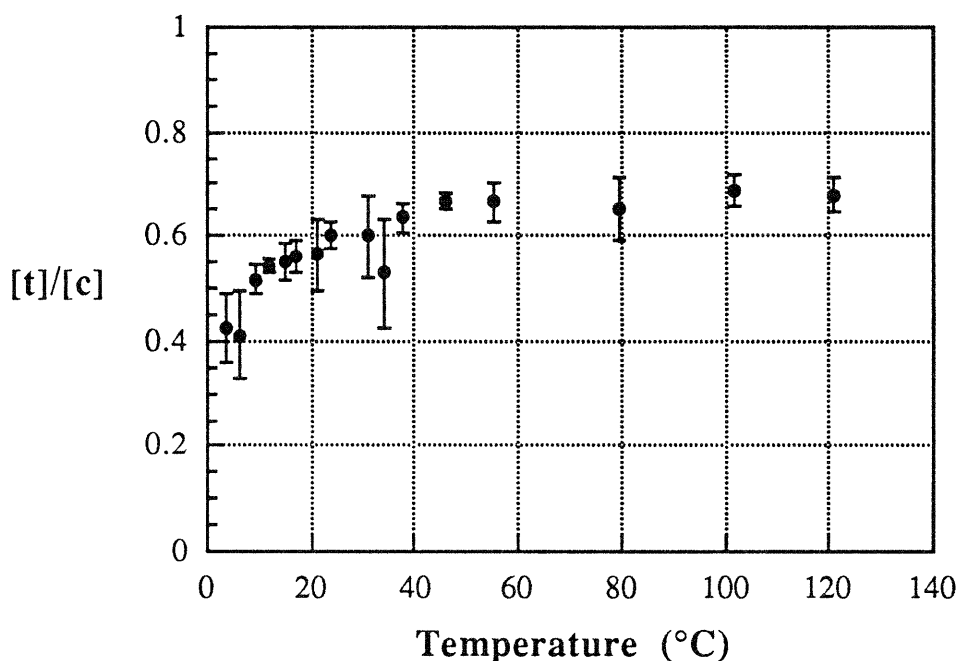


**Figure 2.4:** Change in  $[t]/[c]$  after rapid dissolution of crystalline template into aqueous solution,  $D_2O$ ,  $5^\circ C$ , pD 1.

The data may be fitted to a standard first-order rate analysis. The equilibrium  $t/c$  value of 0.68 is equal to  $k_1/k_{-1}$ , the ratio of the forward and reverse rate constants for  $c \leftrightarrow t$ .

Conversion of  $t/c$  to  $t/(c+t)$ , followed by first-order rate analysis, gives an equation of  $t/c = [4.029 - \exp(-0.045t)] / [5.587 + \exp(-0.045t)]$ , with a value for  $(k_1 + k_{-1})$  of  $0.045 \text{ min}^{-1}$ , corresponding to a half life of isomerization of 15 minutes at  $5^\circ C$ . From their ratio

and sum,  $k_1$  is calculated as  $0.026 \text{ min}^{-1}$  and  $k_{-1}$  as  $0.019 \text{ min}^{-1}$ ; this rate is similar to those found in peptide and protein systems.

A similar experiment was performed in acetonitrile at a lower temperature in an attempt to slow the rate of interconversion, but equilibrium was reached within the three minutes necessary prior to the initial reading. The question of solvent dependence of the cis-trans isomerization was raised, and a series of experiments involving organic solvents ensued. These experiments are summarized in Table 2.1.

Template Portion	Bulk Solution	Interconversion	Temperature	Results
Crystalline Ac-Hel <sub>1</sub> (all cs)	Acetonitrile	cs→cs+ts	-15 °C	equilibrium reached by first data point
Aliquot Ac-Hel <sub>1</sub> in CDCl <sub>3</sub> (all cs)	Acetonitrile	cs→cs+ts	5 °C	equilibrium reached by first data point
Aliquot Ac-Hel <sub>1</sub> in CDCl <sub>3</sub> (all cs)	Acetonitrile	cs→cs+ts	-15 °C	equilibrium reached by first data point
Aliquot Ac-Hel <sub>1</sub> in CDCl <sub>3</sub> (all cs)	Water	cs→cs+ts	5 °C	<i>solution inhomogeneity rendered readings impossible</i>
Aliquot Ac-Hel <sub>1</sub> in CD <sub>3</sub> CN (cs+ts)	Chloroform	cs+ts→cs	-15 °C	equilibrium reached by first data point

**Table 2.1: Summary of kinetics experiments to monitor the cis-trans isomerization of Ac-Hel<sub>1</sub>-OH using organic solvents.**

For all cases involving only organic solvents, equilibrium was reached before it was possible to take the first reading; the cis-trans interconversion in acetonitrile and chloroform proceeds much faster than in water, in general agreement with observations of others for similar systems (Radzicka *et. al.*, 1992; Eberhardt *et. al.*, 1992).

### Analysis of Ac-Hel<sub>1</sub>-OH

The degree of helicity of aqueous peptides is sensitive to environmental perturbations, including temperature and the presence of salts, denaturants such as urea, and alcohols, particularly TFE. While the analysis by Dr. T. Allen of alanine derivatives of Ac-Hel<sub>1</sub> is extensive, a number of key experiments were not performed. Dr. T. Allen reports a negligible effect of TFE on the t/c ratio of Ac-Hel<sub>1</sub>-OH, but did not analyze the effects of other environmental conditions on this molecule.

Dr. T. Allen observed a very small temperature dependence for the t/c ratio of the hexaalanine template derivative over a range of 10 to 65 °C, suggesting a minimal enthalpic

contribution to the stabilization of the helical state. This is a somewhat unusual result given that thermal denaturation has frequently been employed as a means to monitor the helix→coil transition, but not unreasonable for a homoalanine peptide. The question remains, however, whether such a minimal effect could be attributed to a temperature dependence of the template counteractive to a dependence of the peptide segment. In order to examine this possibility, the t/c ratio of the template alone was monitored over a range of 5 to 65 °C. These results are shown in Figure 2.5.

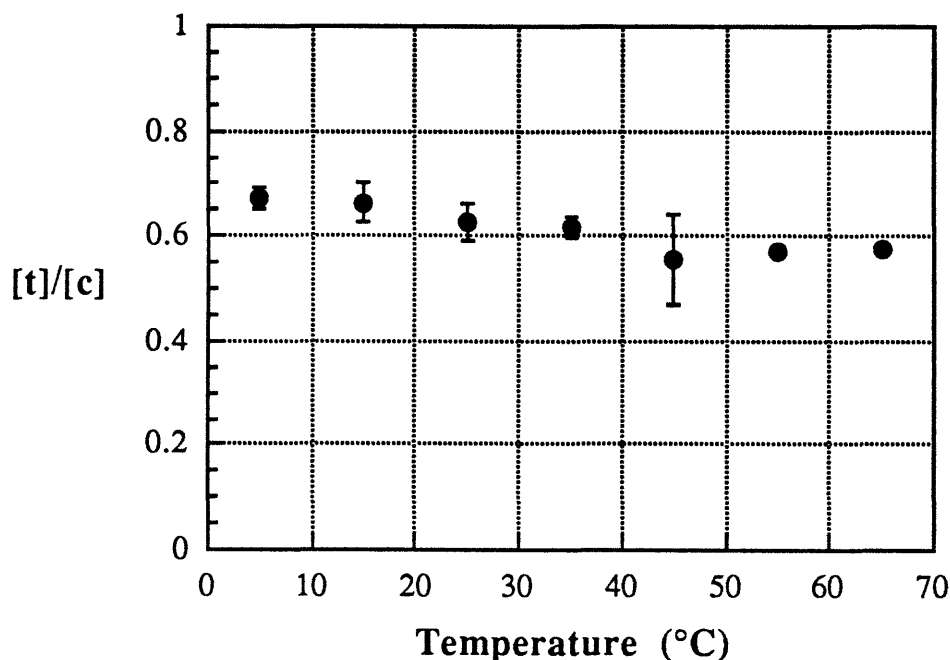


**Figure 2.5:** Effect of temperature on [t]/[c] for Ac-Hel<sub>1</sub>-OH. Measurements were performed from 5 to 65 °C, D<sub>2</sub>O, pD 1.

Clearly the temperature dependence is nominal, and the enthalpy of the cis to trans isomerization must therefore be small.

Dr. T. Allen observed a strong helix strengthening effect at relatively high concentrations of NaCl for Ac-Hel<sub>1</sub>-A<sub>6</sub>-OH, a finding that is consistent with literature reports suggesting that salts act by supporting the macrodipole of the helix (Scholtz *et. al.*, 1991b). In fact, the template alone responds in a similar fashion; Figure 2.6 shows the template region of the spectra. Chemical shift changes are minor, but the change in relative abundances of the t and c state resonances is apparent, in particular for the H-13b ( $\delta$  2.7-2.9 ppm) and the H-8 ( $\delta$  4.2-4.4 ppm) protons. The dependence of the t/c ratio of the

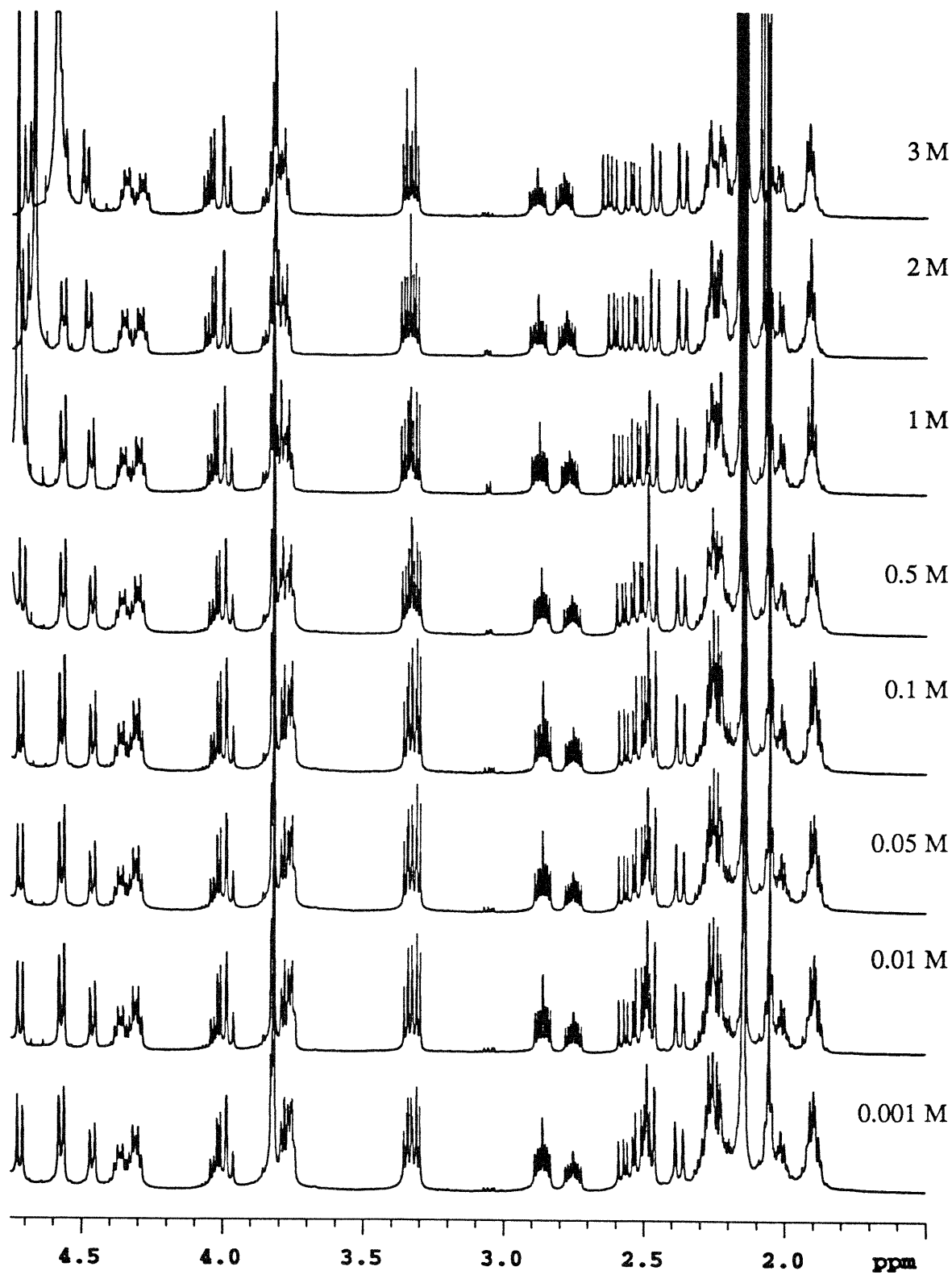
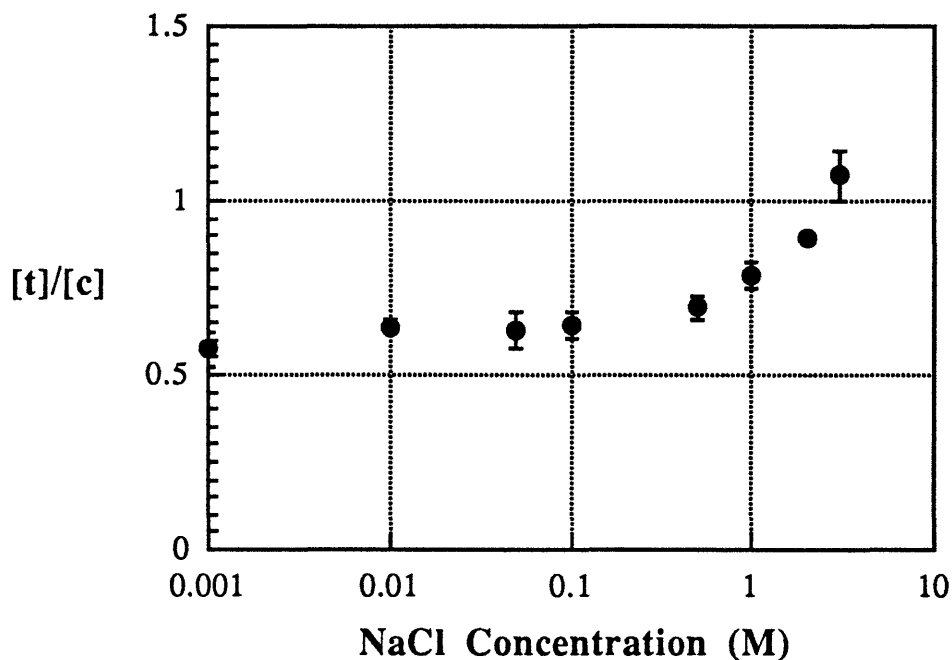


Figure 2.6: NaCl dependence of template resonances of Ac-Hel<sub>1</sub>-OH, 0.001 to 3 M, D<sub>2</sub>O, 27 °C, pH 1.

template on NaCl concentration in the range of 0.001 to 3 M is demonstrated in Figure 2.7.



**Figure 2.7:** Effect of NaCl on  $[t]/[c]$  for Ac-Hel<sub>1</sub>-OH. Measurements were performed in concentrations ranging from 0.001 to 3 M, D<sub>2</sub>O, 27 °C, pD 1.

Much like the alanine derivative, the template alone shows a marked increase in  $t/c$  with NaCl concentration, primarily in the higher concentration range. Two or three carbonyls are aligned in the trans isomers versus one or two in the cis, and the higher dielectric constant in solution due to the presence of NaCl is undoubtedly acting by supporting the stronger dipole moment of the trans isomers.

#### **Analysis of Ac-Hel<sub>1</sub>-NHMe**

It was noted by Dr. T. Allen that Ac-Hel<sub>1</sub>-A<sub>6</sub>-OH responds only marginally to an increase in temperature. Likewise, a similar effect has been determined for Ac-Hel<sub>1</sub>-OH. Hence it would be expected that a derivative like Ac-Hel<sub>1</sub>-NHMe would respond in a similar fashion. This was indeed found to be the case, as demonstrated in Figure 2.8.

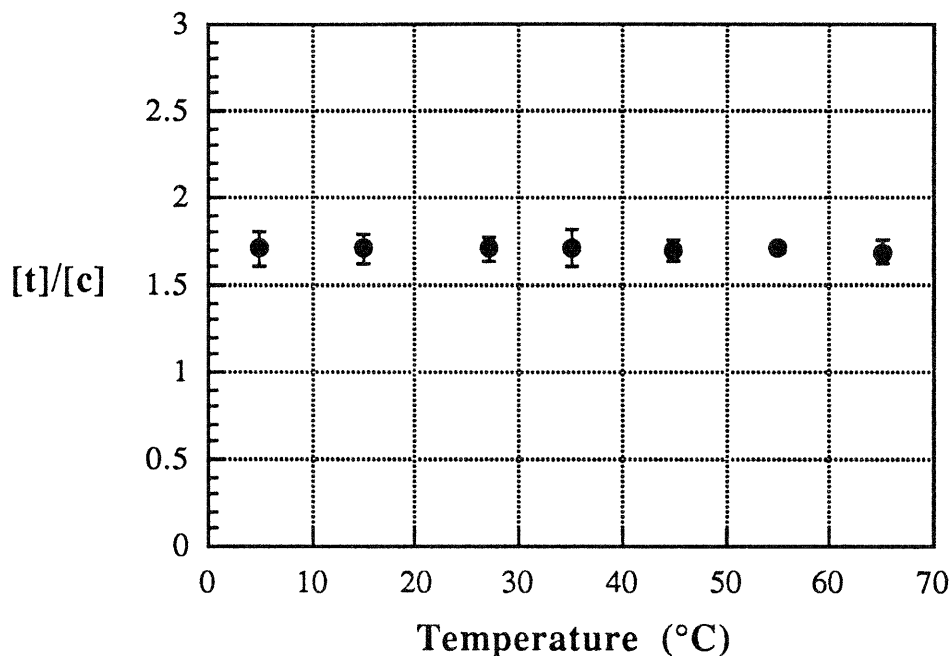


**Figure 2.8:** Effect of temperature on  $[t]/[c]$  for Ac-Hel<sub>1</sub>-NHMe. Measurements were performed from 5 to 65 °C, D<sub>2</sub>O.

The above results indicate that the temperature effect observed for the hexaalanine derivative is not based on an unusual dependence of the template but rather that all elements of the system are nearly temperature independent.

Dr. T. Allen observed a dramatic change in Ac-Hel<sub>1</sub>-A<sub>6</sub>-OH with increasing TFE concentration and none for the template alone. TFE has been widely used to stabilize helices, and Ac-Hel<sub>1</sub>-NHMe provides a system in which the range of TFE effects can be evaluated, as it is capable of hydrogen bond formation but lacks peptide functionalities. Dr. T. Allen has analyzed the TFE dependence of this derivative, but under non-optimal conditions (water suppression, short delay times) that prevent an accurate determination of  $t/c$  ratios. Hence the TFE titration of this derivative was repeated under more appropriate conditions and is shown in Figure 2.9 for the template region of the spectra; the migration of the H-9a<sub>t</sub> and H-9b<sub>t</sub> protons signal a shift of the template to a more  $t_e$  containing state. The dependence of the  $t/c$  ratio on TFE in the range of 0 to 20 mole% is given in Figure 2.10.

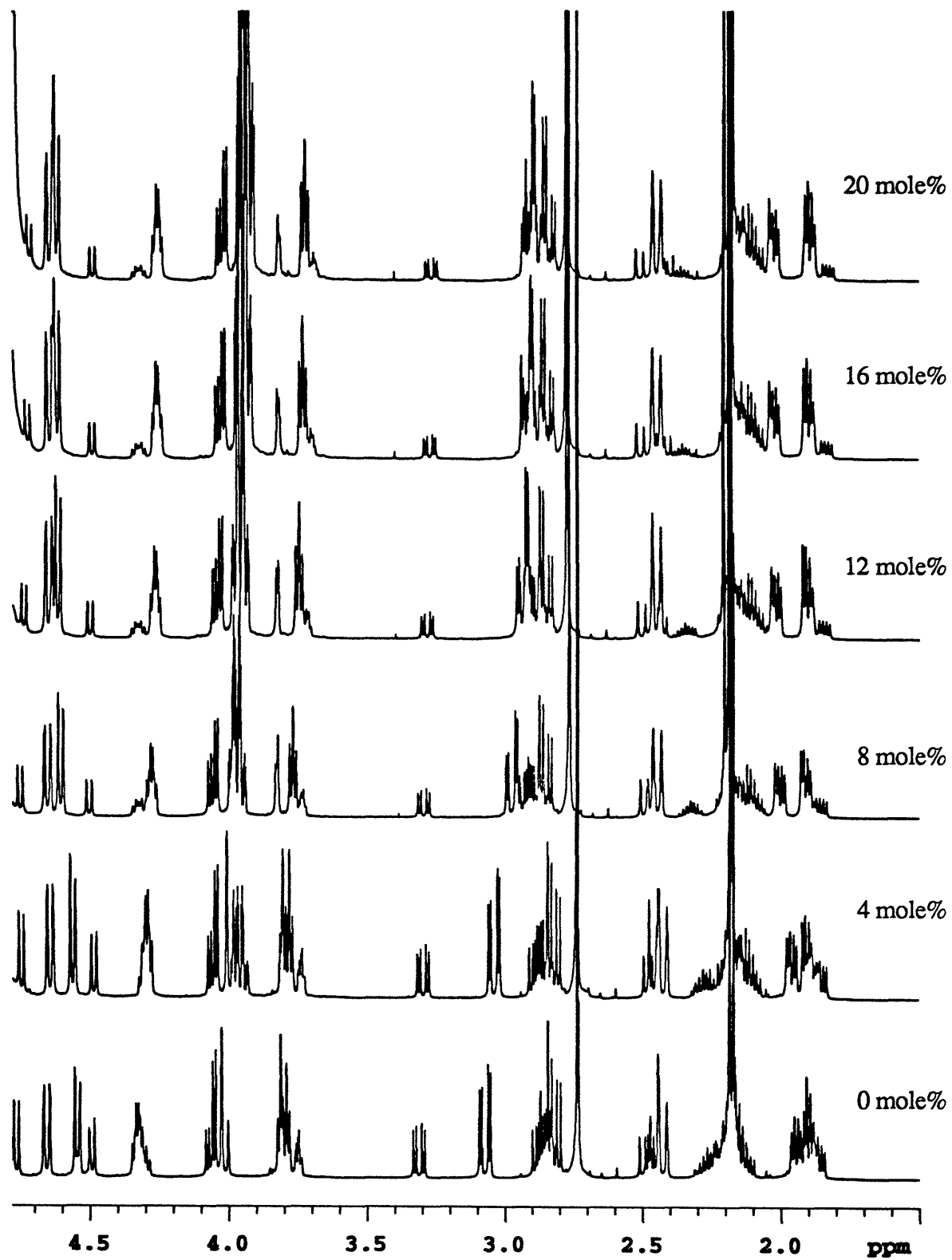
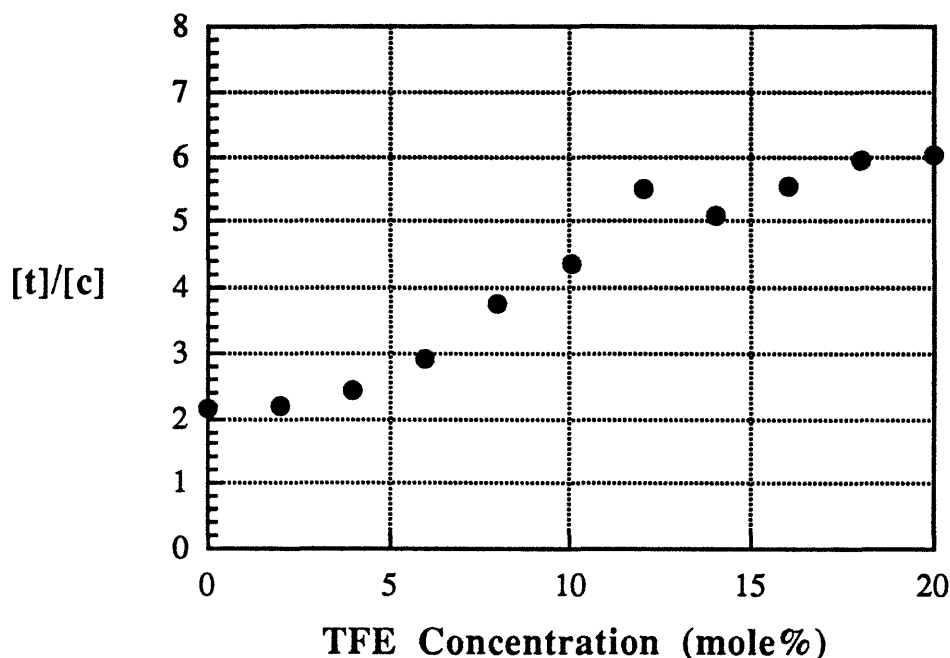


Figure 2.9: TFE dependence of template resonances of Ac-Hel<sub>1</sub>-NHMe, 0 to 20 mole%, D<sub>2</sub>O, 27 °C.



**Figure 2.10:** Effect of TFE on  $[t]/[c]$  for Ac-Hel<sub>1</sub>-NHMe. Measurements were performed in concentrations ranging from 0 to 20 mole%, D<sub>2</sub>O, 27 °C.

Much like the alanine derivative, the  $t/c$  ratio of Ac-Hel<sub>1</sub>-NHMe shows a marked increase in the presence of TFE. Hence TFE is able to exert its effect on a single hydrogen bond. The mechanism by which TFE operates must center on hydrogen bonds, rather than on some type of interaction with amino acid side chains or peptide termini.

### CORRECTION FOR THE CD CONTRIBUTION OF THE TEMPLATE

CD, developed from optical rotary dispersion (ORD) techniques, is founded on the differential absorption of left and right circularly polarized light by peptide amide bonds. The specific orientation of these bonds, different for different elements of secondary structure, gives rise to characteristic spectra. For unpolarized light, absorbance is given by the Beer-Lambert law:

$$A = \epsilon cl$$



where  $c$  is the sample concentration,  $l$  is the path length, and  $\epsilon$  is the molar extinction coefficient. A similar expression can be written for left and right circularly polarized light, where the molar extinction coefficients for each are denoted  $\epsilon_L$  and  $\epsilon_R$ , respectively:

$$\Delta\epsilon = \epsilon_L - \epsilon_R = (A_L - A_R)/cl = \Delta A/cl$$

The molar extinction coefficient for unpolarized light is simply the average of  $\epsilon_L$  and  $\epsilon_R$ . All commercial instruments directly measure  $\Delta A$ , but most report the absorbance values in ellipticity units, an alternative measure that is primarily historic. The ellipticity,  $\theta$ , is an angular measurement that can easily be calculated from  $\Delta A$  by:

$$\theta = 32.98 \Delta A$$

Accounting for sample concentration and path length produces the molar ellipticity, defined below and having the units  $\text{deg}\cdot\text{cm}^2/\text{dmole}$  (Woody, 1995).

$$[\theta]_M = \frac{100\theta}{lc} = 3298\Delta\epsilon$$

The sample concentration must be determined accurately in order to appropriately calculate the molar ellipticity. This issue is particularly problematic for peptide samples, and has been the focus of much attention, with varied success. A solution to this problem as developed for alanine containing conjugates of Ac-Hel<sub>1</sub> is presented in Appendix A of this thesis. The error estimation for this improved analysis is approximately  $\pm 5\%$ . Concentrations of CD samples of Ac-Hel<sub>1</sub>-X, X=OH, OMe, NH<sub>2</sub>, NHMe, were calculated directly from weights of carefully dried samples (see Experimental section for details). Analysis by weight for these samples is more reliable than for peptide containing samples as these small derivatives are much less likely to contain water or other solvents.

The other main potential source of error is the signal to noise ratio of the spectrum itself. Reliable data can be obtained by working in an appropriate concentration range (total optical density in the range of 0.4-1) and by averaging repetitive scans (Johnson, 1985). For samples that are low in concentration, oxygen absorption, as well as signal to noise problems, can become a significant problem, particularly at low wavelengths. Other potential sources of error can be easily eliminated by carefully calibrating the instrument, by allowing sufficient time to warm up the instrument, and by using strain free cells and transparent solvents and buffers.

The CD analysis of template derivatives is complicated by a strong absorption by the template itself in the helical region, and furthermore by the fact that the individual conformations of the template contribute differently to its net CD signal. This is most readily demonstrated by comparing the CD spectra of Ac-Hel<sub>1</sub>-OMe and Ac-Hel<sub>1</sub>-NHMe. The methyl ester in water, like the free acid, is comprised solely of the *cs* and *ts* states of the template. The *N*-methyl amide, on the other hand, is a mixture of all three template states in aqueous solution, which can be altered by the addition of TFE to solution, as was demonstrated in Figure 2.9. The spectra of Ac-Hel<sub>1</sub>-OMe and Ac-Hel<sub>1</sub>-NHMe in water, as well as Ac-Hel<sub>1</sub>-NHMe in TFE-water, are shown in Figure 2.11, and are clearly quite different. An analysis of the peptide segment of a template derivative by simply subtracting the spectrum of Ac-Hel<sub>1</sub> in water is therefore not possible.

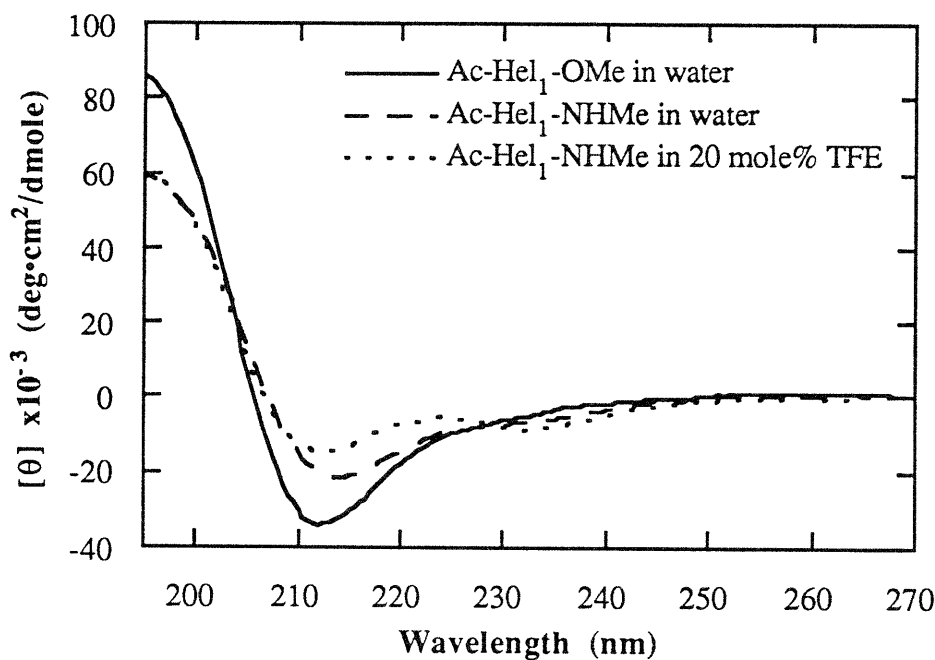


**Figure 2.11:** CD spectra of Ac-Hel<sub>1</sub>-OMe and Ac-Hel<sub>1</sub>-NHMe in water and Ac-Hel<sub>1</sub>-NHMe in 20 mole% TFE, 25 °C.

Before any peptide derivative of the template can be analyzed for helical content in the peptide, an appropriate correction must be made for the contribution of the template. To a reasonable approximation, CD is an additive technique, and the observed spectra of derivatives of Ac-Hel<sub>1</sub> can be viewed as a sum of the independent contributions from the

peptide and the three states of the template, weighted by their mole fractions, as in expression 2.6.

$$\theta_{\text{observed}} = \theta_{\text{peptide}} + \theta_{\text{template}}; \quad \theta_{\text{template}} = \chi_{\text{cs}}\theta_{\text{cs}} + \chi_{\text{ts}}\theta_{\text{ts}} + \chi_{\text{te}}\theta_{\text{te}} \quad 2.6$$

As discussed previously, however, the cs and ts states of the peptide are related by a constant and can therefore be grouped together into one state, (cs+ts). 2.6 then simplifies to expression 2.7.

$$\theta_{\text{observed}} = \theta_{\text{peptide}} + \chi_{(\text{cs+ts})}\theta_{(\text{cs+ts})} + \chi_{\text{te}}\theta_{\text{te}} \quad 2.7$$

The mole fraction of the te state of the template is readily obtained through expression 2.4 (see Appendix B for derivations), and the combined mole fraction of (cs+ts) is simply  $(1-\chi_{\text{te}})$ . Rearrangement of 2.7 gives 2.8, where the only unknowns are  $\theta_{(\text{cs+ts})}$  and  $\theta_{\text{te}}$ .

$$\theta_{\text{peptide}} = \theta_{\text{observed}} - (1 - \chi_{\text{te}})\theta_{(\text{cs+ts})} - \chi_{\text{te}}\theta_{\text{te}} \quad 2.8$$

Knowledge of these unknowns permits a correction for the CD contribution of the template and a means by which to analyze the peptide portion only of a template derivative.

A solution to the problem requires first a way to analyze the template without interference from other chromophores, and second a means to manipulate the relative proportions of the (cs+ts) and te states. The primary amide of the template, Ac-Hel<sub>1</sub>-NH<sub>2</sub>, is the simplest derivative of the template able to populate all three template states. The presence of the te state of this derivative was demonstrated by an analysis of its <sup>1</sup>H NMR spectra in various D<sub>2</sub>O-d<sub>3</sub>-TFE mixtures performed by Dr. K. McClure. The large change in the t/c ratio with the addition of TFE is shown in Figure 2.12. The limiting values of t/c at 0 and 20 mole% TFE correspond to te state populations of 37% and 68%, respectively, as calculated from equation 2.4. TFE in this concentration range has no effect on the CD spectrum of Ac-Hel<sub>1</sub>-OMe; since the t/c ratio is constant under these conditions, it follows that the composite  $\theta_{(\text{cs+ts})}$  state of equation 2.8 must also be invariant. If  $\theta_{\text{te}}$  is similarly invariant, CD spectra of Ac-Hel<sub>1</sub>-NH<sub>2</sub> at varying concentrations of TFE will yield a set of data amenable to a linear regression analysis for the determination of  $\theta_{(\text{cs+ts})}$  and  $\theta_{\text{te}}$ .

Expression 2.9 can be written for this derivative, where  $\theta_{\text{te}}$  and  $\theta_{(\text{cs+ts})}$  are the unknowns of interest.

$$\theta_{\text{obs}} = \theta_{\text{te}}\chi_{\text{te}} + \theta_{(\text{cs+ts})}(1 - \chi_{\text{te}}) \quad 2.9$$

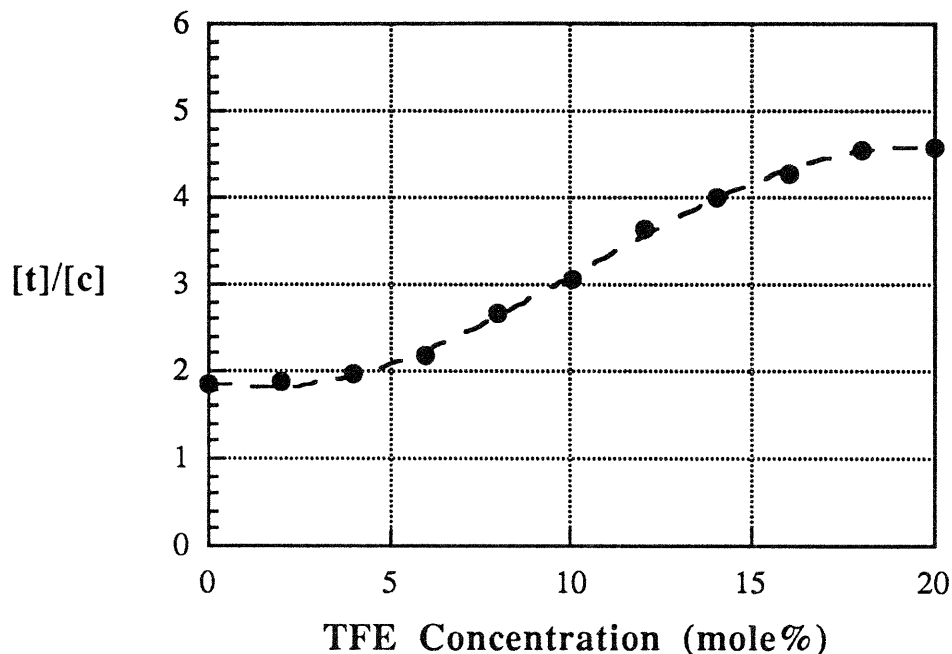


Figure 2.12: Effect of TFE on  $[t]/[c]$  for Ac-Hel<sub>1</sub>-NH<sub>2</sub>. (Data supplied by Dr. K. McClure.)

Only two different spectra, taken for two different proportions of (cs+ts) and te, are needed to solve this expression as a system of two equations in two unknowns. However, a more thorough analysis would include more data, and 2.9 can be rearranged to 2.10 to accommodate this.

$$\theta_{\text{obs}} = (\theta_{\text{te}} - \theta_{(\text{cs}+\text{ts})})\chi_{\text{te}} + \theta_{(\text{cs}+\text{ts})} \quad 2.10$$

The equation 2.10 is in the standard linear form of  $y = mx + b$  and hence a linear regression analysis can be performed for a series of  $\chi_{\text{te}}$  values. Appendix B discusses the relevant derivations and mathematics.

The TFE titration by CD is given in Figure 2.13. The change in the spectrum with increasing TFE concentration reflects the increase in the te state relative to the (cs+ts) state.

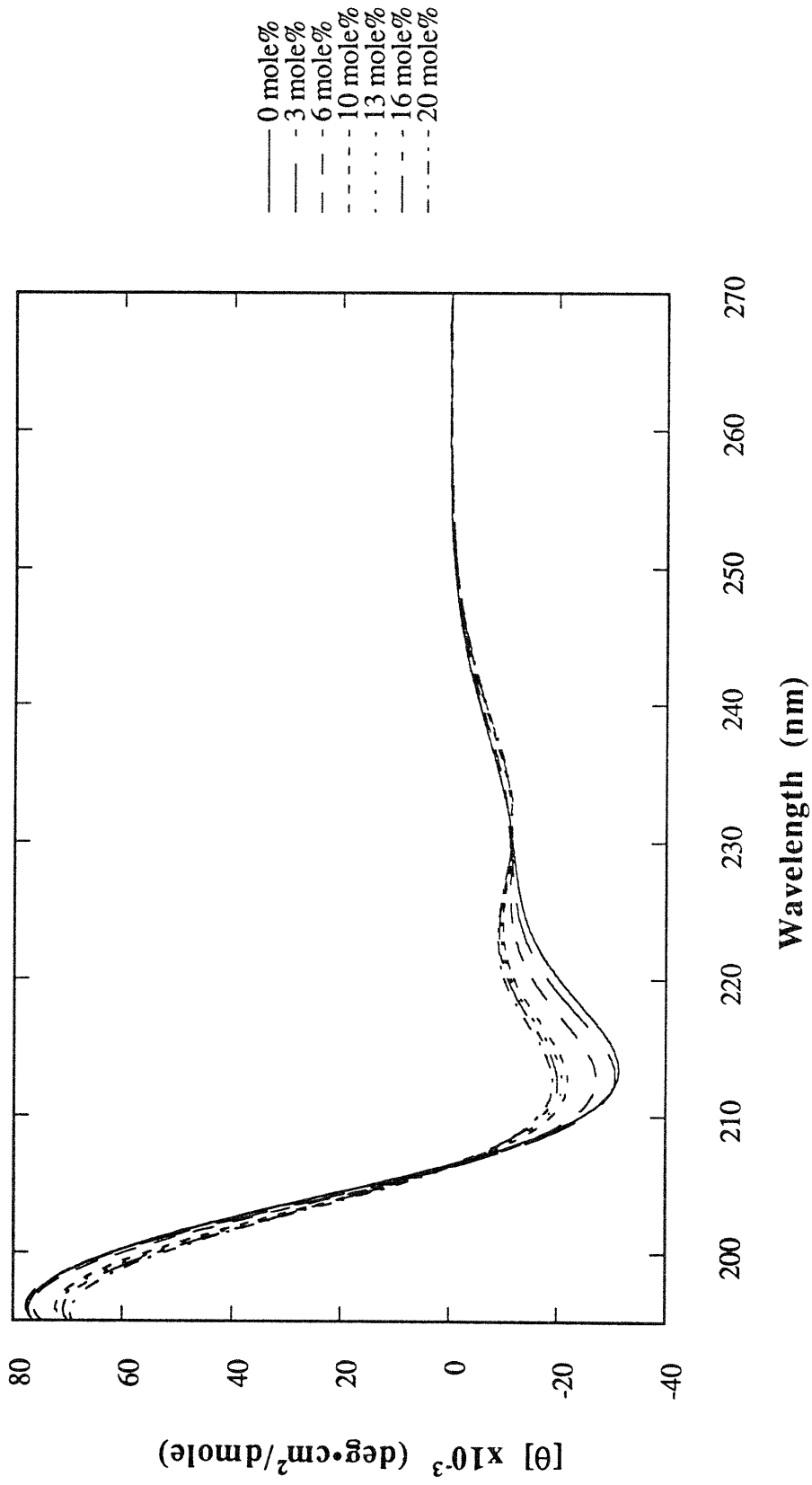
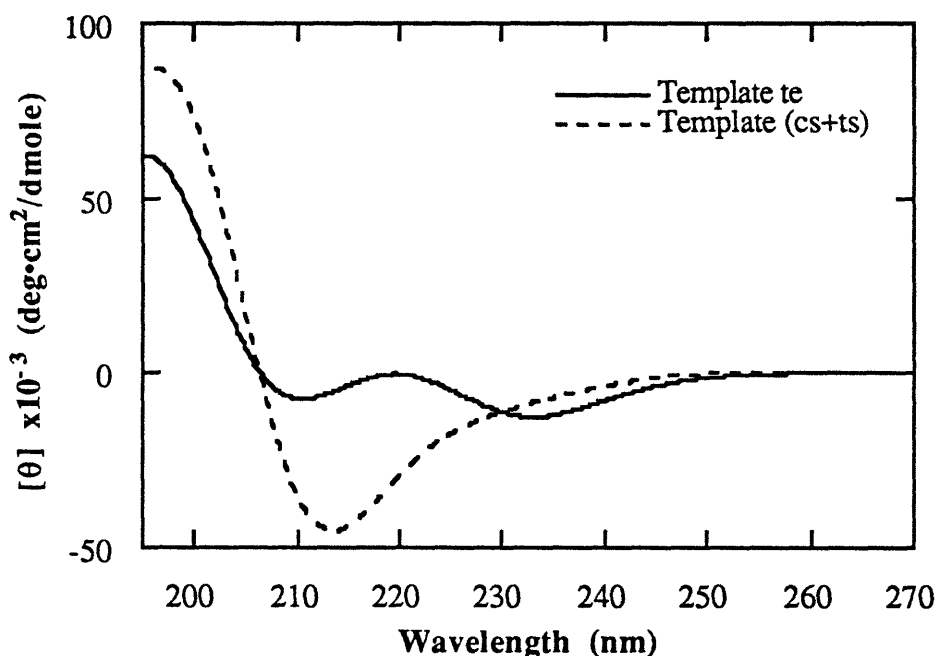


Figure 2.13: TFE titration of Ac-Hel<sub>1</sub>-NH<sub>2</sub>, 25 °C.

The stacked plot of Figure 2.13 exhibits two isoellipsoidal points and shows that in any region, the CD spectrum of Ac-Hel<sub>1</sub>-NH<sub>2</sub> is a simple monotonic function of the mole% TFE, a necessary condition for the success of the linear regression analysis.

The value of  $\chi_{te}$  was calculated for each spectrum using the corresponding t/c ratios (the values for 3 and 13 mole% were obtained by extrapolation). With the aid of a spreadsheet program, these values were used in conjunction with the spectra of Figure 2.13 to perform the linear regression analysis at each wavelength. The results, values for  $\theta_{(cs+ts)}$  and  $\theta_{te}$  of the template, are shown in Figure 2.14.



**Figure 2.14:** CD spectra corresponding to the te state of the template and the (cs+ts) state of the template. Results were computed using a linear regression analysis of Ac-Hel<sub>1</sub>-NH<sub>2</sub> in various TFE concentrations.

Error analysis gave a maximum standard deviation in the ordinate for these calculations of  $\pm 1.3 \times 10^{-3}$  deg·cm<sup>2</sup>/dmole, with most values were considerably lower. The average standard deviation over all wavelengths was  $\pm 0.39 \times 10^{-3}$  deg·cm<sup>2</sup>/dmole, indicating a close fit of the calculated lines to the experimental data. In addition, it is interesting to note that  $\theta_{te}$  is very nearly zero at 222 nm; the correction for  $\theta_{te}$  of the template is minimal at this wavelength.

These results may be compared to the spectra of Ac-Hel<sub>1</sub>-OMe and Ac-Hel<sub>1</sub>-NHMe of Figure 2.11 and are shown in Figure 2.15. The lineshape of the template (cs+ts) spectrum and that of Ac-Hel<sub>1</sub>-OMe are identical, as would be expected. Furthermore, the influence of the template te state is clear in the transition of Ac-Hel<sub>1</sub>-NHMe from water to TFE-water, i.e. to a higher te containing state.

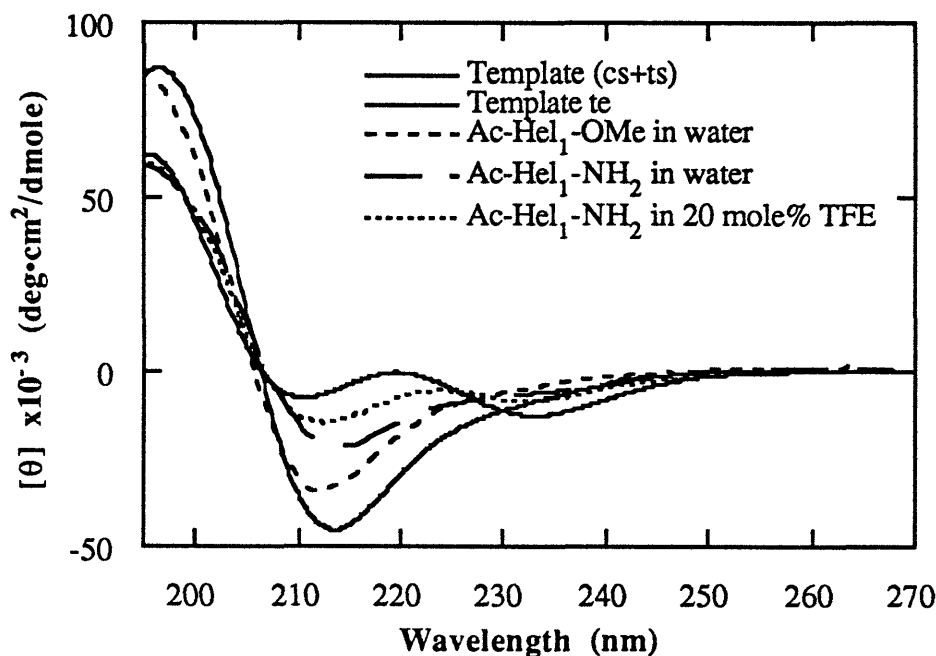


**Figure 2.15:** CD spectra corresponding to the te and (cs+ts) states of the template superimposed with the CD spectra of Figure 2.11.

The results of Figure 2.14 are vital to the analysis of template derivatives; it is now possible to subtract the contribution of the template from the CD spectrum of any given derivative making use of expression 2.8.

## SUMMARY AND CONCLUSIONS

The helix nucleating template Ac-Hel<sub>1</sub> has been shown to follow a three state model, which can be reduced to a two state model by grouping the two nonnucleating conformations (cs+ts) together, separate from the nucleating te conformation. <sup>1</sup>H-NMR analysis of Ac-Hel<sub>1</sub>-A<sub>6</sub>-OH has shown that the te state of the template is correlated with a helical structure in the attached peptide, and while it has not been proven that the (cs+ts)

state peptide is a random coil, all evidence suggests a lack of structure. Furthermore, the response of the hexaalanine derivative to a range of environmental conditions is consistent with the proposed models.

Similar analyses of small nonpeptide derivatives of the template are in accord with the responses of the peptide derivative. Temperature dependence was minimal, while salt showed a strong effect in the high concentration range. TFE was found to act upon some of these small derivatives, supporting a mechanism in which hydrogen bonds are the target of the influence of TFE.

The rate of cis-trans isomerization for the template has been determined in water and has furthermore been shown to be solvent dependent.

Through the use of Ac-Hel<sub>1</sub>-NH<sub>2</sub> in a series of TFE concentrations, the spectra corresponding to the te and (cs+ts) states of the template have been determined for use in the analysis of peptide derivatives of Ac-Hel<sub>1</sub>.



### Chapter 3

Characterization of the Series Ac-Hel<sub>1</sub>-A<sub>n</sub>-OH and Ac-Hel<sub>1</sub>-A<sub>n</sub>-NH<sub>2</sub>

## INTRODUCTION

The previous chapter has demonstrated the importance of studies of small nonpeptide derivatives of Ac-Hel<sub>1</sub> toward a comprehensive understanding of the template system. In particular, analysis of Ac-Hel<sub>1</sub>-NH<sub>2</sub> has provided a picture of the CD contribution of the individual states of the template. This is an essential factor in the analysis of peptide derivatives of the template. With this information in hand, it is possible to examine the peptide portions of templated alanine oligomers, the central goal of this thesis. Prior to presenting this information, however, it is necessary to briefly review previous studies toward an understanding of helical CD spectra, as this serves as the foundation upon which this chapter is based. Historical aspects of CD, factors influencing helical spectra, CD studies of alanine oligomers, and the value of  $[\theta]_{222}$  corresponding to 100% helix will all be discussed.

### History

The phenomena of circular dichroism was first observed by Boit in 1815, but it was not until the 1960s that instruments for its measurement were commercially available (Johnson, 1985). CD was then very quickly accepted as a fundamental technique for the evaluation of secondary structure in both polypeptides and proteins. Prior to CD, optical rotary dispersion (ORD) was often used for this purpose. CD and ORD are closely related, as both are founded in the differential interaction of a chiral molecule with left and right circularly polarized light. The wavelength-dependent rotation of the plane of linearly polarized light gives rise to ORD signals, while a differential absorption of left and right circularly polarized light yields CD spectra. In the far-UV, the primary chromophore of a polypeptide is the amide bond; its specific alignment in space is responsible for the characteristic spectra of peptides and proteins (Adler *et. al.*, 1973). Amide bonds are oriented differently in different elements of secondary structure and therefore generate distinct CD spectra. This is demonstrated in Figure 3.1.

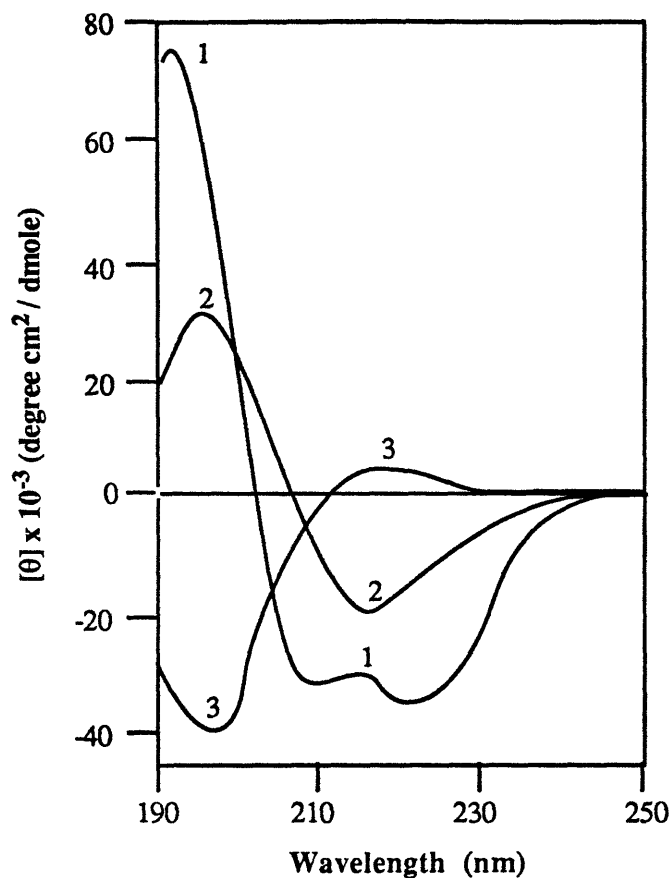


**Figure 3.1:** CD spectra of the three major forms of secondary structure in pure form as derived from poly-L-lysine:  $\alpha$ -helix (1),  $\beta$ -sheet (2), and random coil (3), from Greenfield & Fasman, 1969.

Of these three spectra, the  $\alpha$ -helix CD is the most intense and the most distinctive, with minima at 222 and 208 nm and a maximum at 190 nm, assigned to the  $n$ - $\pi^*$ , parallel  $\pi$ - $\pi^*$ , and perpendicular  $\pi$ - $\pi^*$  transitions, respectively (Tinoco *et al.*, 1963; Woody & Tinoco, 1967). The first helical ORD spectrum was recorded in 1956 (Doty & Yang, 1956), and the measurement of a helical CD followed shortly thereafter (Holzwarth *et al.*, 1962; Holzwarth & Doty, 1965). The advantages of CD over ORD are twofold; first, each transition gives a single band, rather than the positive and negative signals of ORD, and secondly, CD signals are of a finite width, while ORD bands are broad and subject to interference from bands outside the spectral region of interest (Adler *et al.*, 1973).

Furthermore, the helix spectrum is the best characterized, both experimentally and theoretically. Unlike the spectra of  $\beta$ -sheet conformations, the  $\alpha$ -helix CD spectrum is essentially independent of the nature of the side chains and the solvent, provided these factors do not alter the degree of helicity (sequences with aromatic residues at  $\beta$ -carbons are notable exceptions). Models of  $\beta$  structures, including those of  $\beta$ -turns, yield highly variable CD spectra, far more so than those of  $\alpha$ -helices (Woody, 1995). In addition, it has been noted that random coil spectra vary considerably in both magnitude and sign at the higher wavelength transition (Johnson, 1988). While the analysis of helical spectra is not free from complexities, it is more straightforward than that of other forms of secondary structure.

Numerous theoretical approaches to optical activity have been developed and have provided a framework upon which spectroscopic observations can be understood (Crabbé, 1972). In particular, helices have received a great deal of attention and their theories have provided valuable predictions of the expected spectra. The first helical model was developed by Moffit, who applied the exciton theory, treating the  $\alpha$ -helix as an infinitely long molecular crystal (Moffit, 1956a, 1956b; Moffit & Yang, 1956). At about the same time, Fitts & Kirkwood proposed a model based on Kirkwood's polarizability theory (Fitts & Kirkwood, 1956). The discrepancies between these two theories were resolved in a joint publication (Moffit *et. al.*, 1957). Tinoco expanded upon these theories (Tinoco, 1960, 1962); in particular, he developed modifications to model a finite helix and to address the length dependence of optical properties (Tinoco *et. al.*, 1963). Schellman and coworkers also extended these theoretical approaches, developing a matrix method that simplifies the calculation of rotational strength (Schellman & Oriel, 1962; Bayley *et. al.*, 1969). Tinoco and coworkers used this method to extend their analysis to include a model for the  $3_{10}$  helix and a reassessment of length dependence (Woody & Tinoco, 1967). More recent approaches to theoretical models and calculations of helical CD spectra have been made primarily by Woody and coworkers.

### Distorted Helices

One of the major results of the improved models of Woody has been the demonstration of a significant change in the helical CD with deviations from the backbone angles of  $\phi=-48^\circ$ ,  $\psi=-57^\circ$  of the Pauling & Corey helix (Pauling & Corey, 1951). While the  $\alpha$ -helix is a relatively constrained structure, the  $\phi$  and  $\psi$  angles observed for helices in proteins is markedly variant (Barlow & Thornton, 1988). Both an early analysis and an improved model employing four rather than two electronic transitions showed that helices

distorted from the Pauling & Corey parameters produce CD spectra of significantly diminished intensity (Manning *et al.*, 1988; Manning & Woody, 1991). The calculated results for helices with  $\phi$  and  $\psi$  angles comparable to those of model  $\alpha$ -helices and those commonly observed in proteins are, however, notably weaker than their experimental counterparts (Woody, 1994). These qualitative differences reflect the difficulty in adequately modeling these systems, but the trend is nevertheless significant, suggesting that no single CD spectrum can be applied to the range of  $\alpha$ -helices observed.

### Length Dependence

Another important finding from the models of Woody is that there exists a sizable length dependence on the observed CD signal. Early studies have addressed this issue (Tinoco *et al.*, 1963; Woody & Tinoco, 1967), and later studies have provided more details, indicating that at least two turns (*ca.* 7 residues) are required to produce an  $\alpha$ -helical CD spectrum and that a 50 residue peptide adequately represents an infinitely long helix (Manning *et al.*, 1988; Manning & Woody, 1991).

Based on the early work of Woody & Tinoco, Yang and coworkers were able to derive the equation 3.1, relating peptide length to the observed ellipticity at a given wavelength (Chen *et al.*, 1974):

$$\theta_n = \theta_\infty(1 - k/n) \quad 3.1$$

where  $\theta_n$  is the ellipticity per residue of an average helix of  $n$  residues (or amides) within a protein (generally  $n=10$  or  $11$ ),  $\theta_\infty$  is the per residue value of an infinitely long helix, and  $k$  is a wavelength dependent constant ranging from 2-4. Yang and coworkers found reasonable agreement between values calculated from the above equation and experimental values derived from a small protein data base. Woody and coworkers extended this analysis to provide an estimate of the effects of helix length on CD with regard to isolated short peptide segments (13-21 residues); a value for  $k$  of 4.6 was calculated (Gans *et al.*, 1991). This approximation, however, is not applicable to very short helices (*ca.* 5-10 residues).

Experimental results have confirmed the length dependence of the helical CD. Goodman and coworkers have shown that for a series of  $\gamma$ -ethyl-L-glutamate oligopeptides in TFE and in trimethylphosphate, a significant change in the CD spectrum only occurs for the heptamer and larger peptides; these structural changes were confirmed by NMR studies (Goodman *et al.*, 1969). A length dependence in TFE was noted also for alanine based

oligomers with *N*- and *C*- terminal blocking groups incorporated for enhanced solubility (Goodman *et. al.*, 1971; Goodman *et. al.*, 1974).

### Alanine Oligomers

Unstructured alanine oligomers of varying length have been studied by others as well. Toniolo has studied the per residue CD contribution of a single alanine; the internal amide of Ala-Ala was investigated by subtracting the CD spectrum of a blocked alanine trimer from that of a blocked alanine tetramer (Toniolo & Bonora, 1976). Lord and Cox have also measured the per residue ellipticity of alanine by framing alanine with optically inactive glycine residues on both termini (Lord & Cox, 1973). Ac-Ala-NHMe and the series Ac-Ala<sub>*x*</sub>-OMe, *x*=1-4, have been studied by Mattice; some of his results are shown in Figure 3.2 (Mattice, 1974; Mattice & Harrison, 1975).

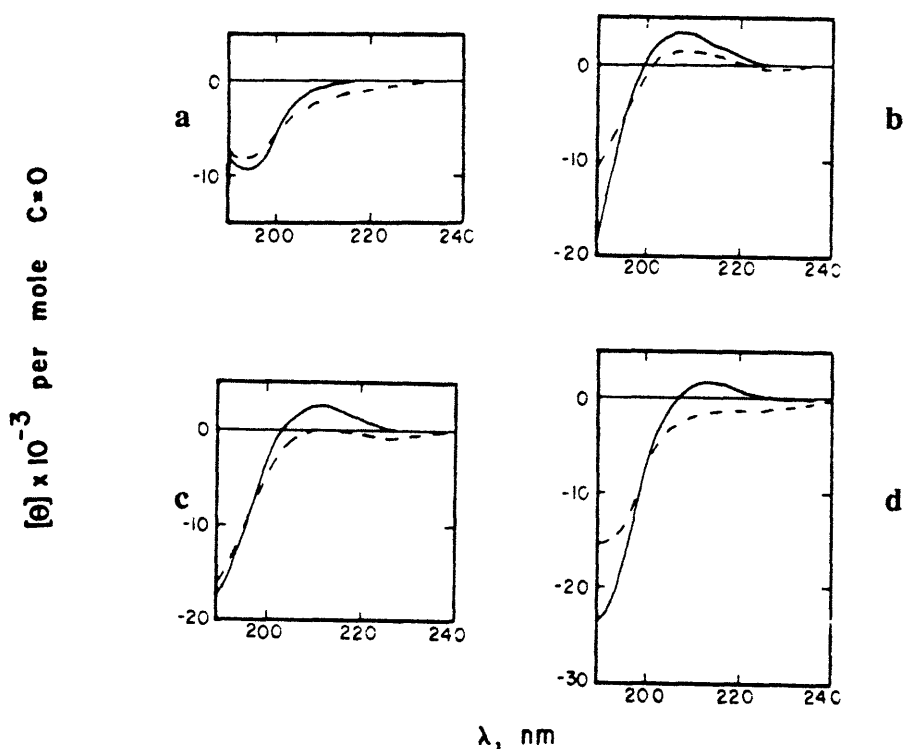


**Figure 3.2:** CD spectra of short alanine oligomers: (a) Ac-Ala-NHMe, (b) Ac-Ala-OMe, (c) Ac-Ala-Ala-OMe, (d) Ac-Ala-Ala-Ala-OMe, H<sub>2</sub>O, 15 °C (solid line) and 75 °C (dashed line), from Mattice, 1974.

The CD curves of Toniolo, Lord & Cox, and Mattice are all qualitatively similar and indicate an unordered structure. Quantitatively, however, the spectra all differ, demonstrating the variability in random coil spectra as discussed earlier.

### Quantitation and the Value of $[\theta]_{222}$

In order to use CD as a quantitative analytical tool, it is necessary to have the appropriate reference spectra, that is, spectra that correspond to 100% of a given form of secondary structure. The first system used for the deconvolution of protein structures into percent helix, sheet, and coil used the polylysine spectra of Figure 3.1 as reference spectra (Greenfield & Fasman, 1969). Yang and coworkers have argued that this system is not directly applicable for use with proteins, which contain shorter elements of secondary structure (Yang *et al.*, 1986). Instead they have derived reference spectra from proteins of known crystal structure, adding additional proteins to the data base as improved Xray data became available (Chen & Yang, 1971; Chen *et al.*, 1972; Chen *et al.*, 1974; Chang *et al.*, 1978). There are flaws in this method, however, including the assumption that the proteins in the database adequately represent a full range of structures, the variability in procedures used in secondary structure determination with Xray data, and the fact that many types of structures within a particular class (i.e.  $\alpha$ - and  $3_{10}$ -helices) are grouped together.

Given this and the helical CD chain length dependence discussed earlier, it follows that neither of the helical reference spectra above would be appropriate for comparison to short helices. Until the work of Baldwin with the C-peptide, this was not an issue, but with the current surge in the study of short helical peptides, it is extremely important. The value of  $[\theta]_{222}$  corresponding to 100% helix is particularly important, as this value is frequently used to monitor helical character. However, no system by which this value could be determined for short peptide segments existed. Many different values of  $[\theta]_{222}$  for 100% helix in short helices have been reported in the literature; a sampling of these is summarized in Table 3.1.

[ $\theta$ ] <sub>222</sub> Cited (deg•cm <sup>2</sup> /dmole)	Method/Source of Value	Citation
-26,500	Average of -25,000 (change observed when unfolded S-peptide is combined with S-protein) and -28,000 (from protein derived data of Yang)	Bierzynski <i>et. al.</i> , 1982
-30,000	Value for complete helix formation of C-peptide	Shoemaker <i>et. al.</i> , 1987
-36,000	Value for complete helix formation of EAK peptide in TFE-water	Marqusee & Baldwin, 1987
-32,000	Maximum value from TFE titration of 3 different Ala, Lys containing peptides	Marqusee <i>et. al.</i> , 1989
-33,000	Maximum value from TFE titration of 7 different Ala based peptides	Padmanabhan <i>et. al.</i> , 1990
-40,000(1-2.5/n)	Based on equation 3.1 (Chen <i>et. al.</i> , 1974)	Chakrabarty <i>et. al.</i> , 1991; Scholtz <i>et. al.</i> , 1991b
-31,500	Value from 12 residue peptide from Forood <i>et. al.</i> , 1993	Jasanoff & Fersht, 1994
-38,000	Value from methionine homopeptide in TFE from Toniolo <i>et. al.</i> , 1979	Nelson & Kallenbach, 1986
-35,000	Approximation of values from Woody, 1985; Johnson, 1988; Greenfield & Fasman, 1969	Lyu <i>et. al.</i> , 1989
-32,000	Value from TFE titration of Glu, Lys based peptides	Lyu <i>et. al.</i> , 1991
-40,000(n-4)/n	Based on equation from Gans <i>et. al.</i> , 1991	Zhou <i>et. al.</i> , 1994
-39,400	Value from TFE titration of EAK modified peptides	Todd & Millhauser, 1991
-38,500	Mean of values from direct measurement of homopolymers (Holzwarth & Doty, 1965; Greenfield & Fasman, 1969; Fillipi <i>et. al.</i> , 1978; Toniolo <i>et. al.</i> , 1979) and values of Yang based on native proteins (Chang <i>et. al.</i> , 1978)	Merutka & Stellwagen, 1989

**Table 3.1: Values cited in the literature for [ $\theta$ ]<sub>222</sub> corresponding to 100% helix.**

What is most readily apparent from Table 3.1 is that no consensus has been reached among those investigating short helices as to what value to use for [ $\theta$ ]<sub>222</sub> for 100% helix.

Furthermore, many of the numbers cited are based on maximum values obtained from TFE titrations of short peptides, without direct evidence that these peptides are in fact completely helical under these conditions.



The uncertainty in the proper value is nevertheless understandable, given that heretofore no system has existed by which to adequately evaluate this per residue ellipticity in a short peptide framework. CD measurements of peptide derivatives of Ac-Hel<sub>1</sub>, however, provide not only this framework, but also a means to evaluate the helical CD length dependence.

The bulk of this chapter is dedicated to an evaluation of the CD spectra of a TFE titration of the series Ac-Hel<sub>1</sub>-A<sub>n</sub>-OH and Ac-Hel<sub>1</sub>-A<sub>n</sub>-NH<sub>2</sub>, n = 1-6, which presents for the first time the values of  $[\theta]_{222}$  for 100% helix of both a five and a six residue peptide. Thus this chapter is in large part composed of the numerous CD spectra measured and calculated for these derivations. The first step in this analysis, however, is a careful NMR measurement of the t/c ratios for these series; this data will be presented prior to the CD calculations.

This chapter will begin, however, by discussing a set of experiments designed to eliminate any potential discrepancies between the NMR and the CD data, as they are used concurrently to determine the values of interest.

## COMPARISON OF NMR AND CD DATA

### Concentration

Alanine oligomers are known to aggregate in solution, yielding a CD spectrum markedly different from the monomeric form (Goodman *et. al.*, 1971). Before the alanine derivatives of Ac-Hel<sub>1</sub> can be studied by CD, their monomeric nature in solution must be demonstrated. Dr. T. Allen demonstrated no variance in the NMR spectra of Ac-Hel<sub>1</sub>-A<sub>6</sub>-OH in aqueous solution over a concentration range of 13.6 mM - 23  $\mu$ M, suggesting that this derivative is in fact unaggregated even at higher concentrations. The possibility still exists, however, that this template derivative is aggregated over the concentration range measured. CD analysis of this derivative extended this concentration range to 6.6  $\mu$ M. In order measure concentrations this low, long path lengths must be employed (see Experimental section); solvent and buffer absorption then becomes a problem. Furthermore, the signal to noise ratio of the spectrum is sacrificed. Thus spectra acquired at very low concentrations can be unreliable, especially at low wavelengths. Recognizing these difficulties, no detectable spectral changes were observed, as shown in the smoothed data of Figure 3.3. In contrast, the spectra of H-Ala<sub>6</sub>-OH in the same general concentration range, presented in Figure 3.4, show a strong concentration dependence

similar to observations for other alanine oligomers (Goodman *et. al.*, 1971). (Spectra of H-Ala<sub>6</sub>-OH at lower concentrations were superimposable with the lowest concentration value shown.) From this information it may be safely concluded that Ac-Hel<sub>1</sub>-A<sub>6</sub>-OH is monomeric in nature in both NMR and CD samples.

### Temperature

NMR analysis of the temperature dependence of the t/c ratio of Ac-Hel<sub>1</sub>-A<sub>6</sub>-OH was performed by Dr. T. Allen; there was a very small change in the t/c ratio over a temperature range of 10 to 65 °C. The temperature dependence of this derivative was evaluated by CD as well; findings were similar, as demonstrated in Figure 3.5. Though small, this temperature dependence cannot be neglected. For this reason, all NMR and CD studies were conducted at identical temperatures.

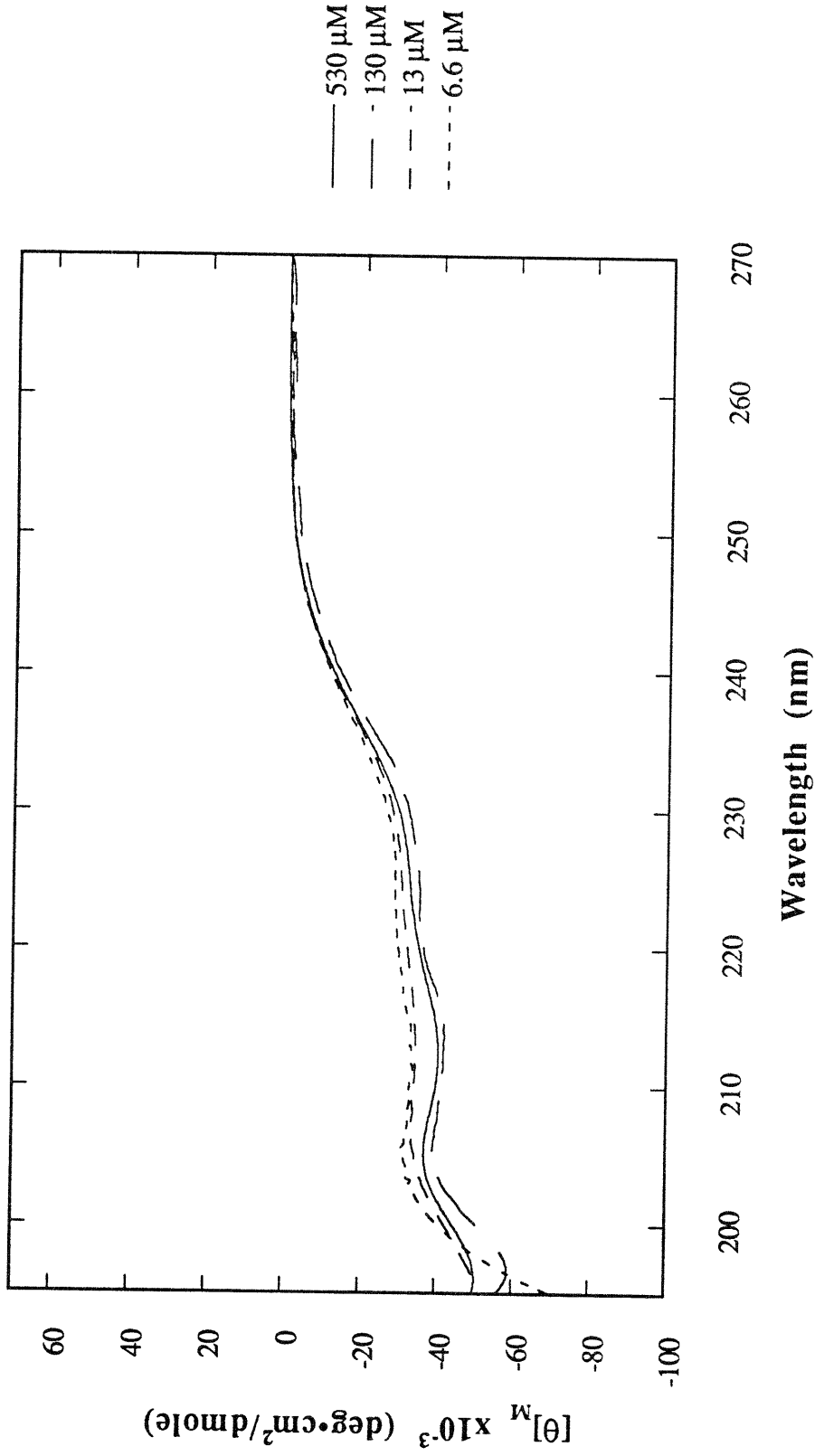


**Figure 3.3:** CD spectra of Ac-Hel<sub>1</sub>-A<sub>6</sub>-OH in the concentration range of 6.6 to 530 μM. Measurements were performed in a perchlorate buffer, 25 °C, pH 1.

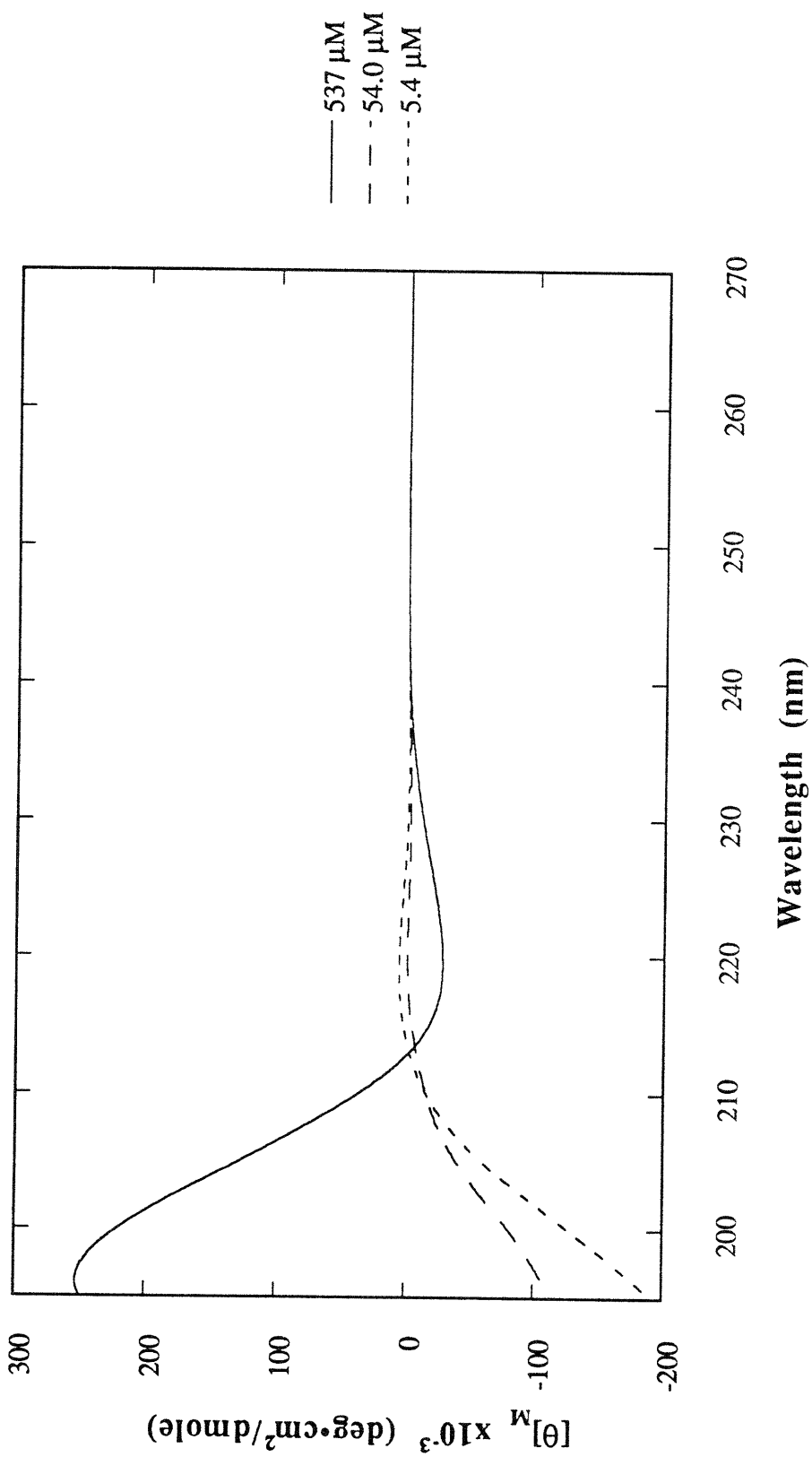
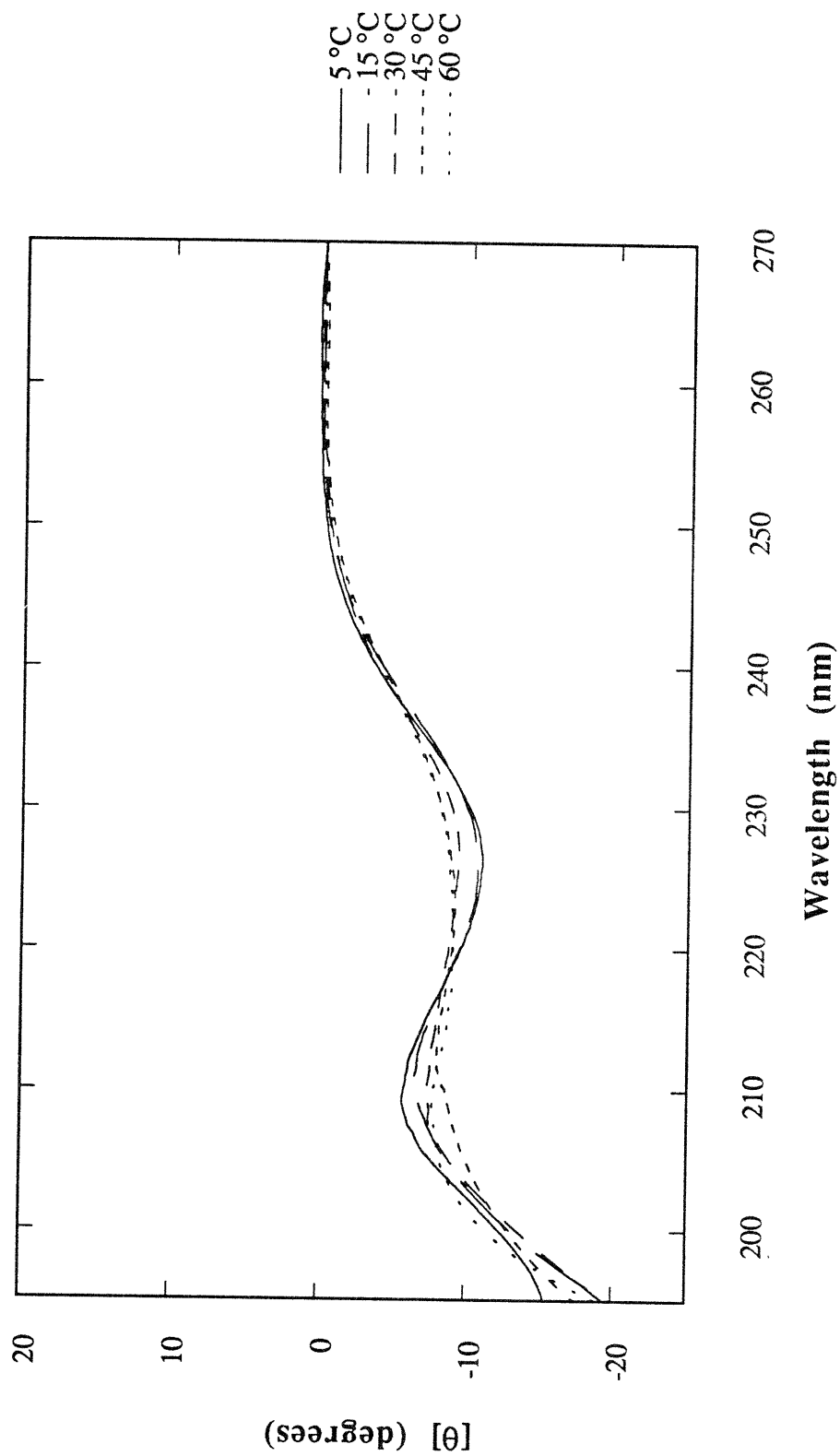


Figure 3.4: CD spectra of H-A<sub>6</sub>-OH in the concentration range of 5.4 to 537 μM. Measurements were performed in water, 25 °C.



**Figure 3.5:** CD spectra of Ac-Hel<sub>1</sub>-A<sub>6</sub>-OH in the temperature range of 5 to 60 °C. Measurements were performed in a perchlorate buffer, 25 °C, pH 1.

## Isotope Effects

Slight solvent based isotope effects have been noted for hydrophobic interactions (Vdovenko *et al.*, 1967; Ben-Naim, 1964; Schneider *et al.*, 1965) as well as hydrogen bonding (Hermans & Scheraga, 1959; Scheraga, 1961; Calvin *et al.*, 1960), suggesting that secondary structure formation in peptides might experience such effects as well. As NMR data was recorded in D<sub>2</sub>O and CD data in H<sub>2</sub>O, the effects, if any, of these differing solvents must be determined. The CD spectrum of Ac-Hel<sub>1</sub>-A<sub>6</sub>-OH was recorded in both the standard H<sub>2</sub>O based perchlorate buffer used for Ac-Hel<sub>1</sub> CD samples and a D<sub>2</sub>O based perchlorate buffer. The two spectra are superimposable, as shown in Figure 3.6, indicating a negligible effect that may be disregarded.

## Perchlorate Concentration

In his analysis of short alanine oligomers, Mattice observed a significant change in the CD spectra of these peptides with sodium perchlorate concentrations of 2, 4, and 6 M (Mattice, 1974). In addition, Baldwin has noted that at concentrations of 2 M and higher, the presence of perchlorate ion can affect the CD spectra of proteins and peptides in such a way as to suggest secondary structure formation where none exists (Scholtz & Baldwin, 1993). In order to suppress ionization of derivatives with a free carboxylic acid at the C-terminus, it is necessary to lower the solution pH to approximately 1. For NMR studies, this is achieved by the addition of a small aliquot of deuterated trifluoroacetic acid (TFA). TFA, however, is not transparent at the wavelengths monitored for CD, and the derivatives are instead analyzed in a perchlorate based buffer. The total perchlorate concentration is small (*ca.* 0.2 M), but the possibility nevertheless exists that the presence of perchlorate could affect resultant CD spectra. (Dr. T. Allen investigated the effects of TFA on the *t/c* ratio in the NMR analyses; no effect was noted at the low concentrations of routine use.) Therefore the CD spectrum of Ac-Hel<sub>1</sub>-A<sub>5</sub>-OH was monitored as a function of [ClO<sub>4</sub><sup>-</sup>] as a test of this potentiality. Figure 3.7 shows the results of this analysis; solution concentrations were low, and the spectra, particularly at low wavelengths, are potentially unreliable in a quantitative sense. Nevertheless, the trend is valid. A significant change in the CD spectra was observed at higher concentrations of perchlorate, but not in the lower range in which CD spectra were recorded.

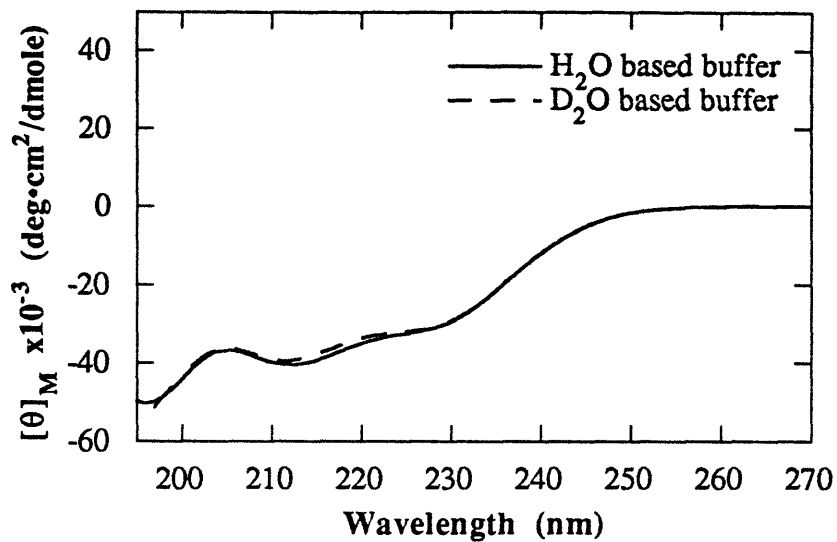


Figure 3.6: CD spectra of Ac-Hel<sub>1</sub>-A<sub>6</sub>-OH in an H<sub>2</sub>O and a D<sub>2</sub>O based perchlorate buffer, 25 °C, pH 1.

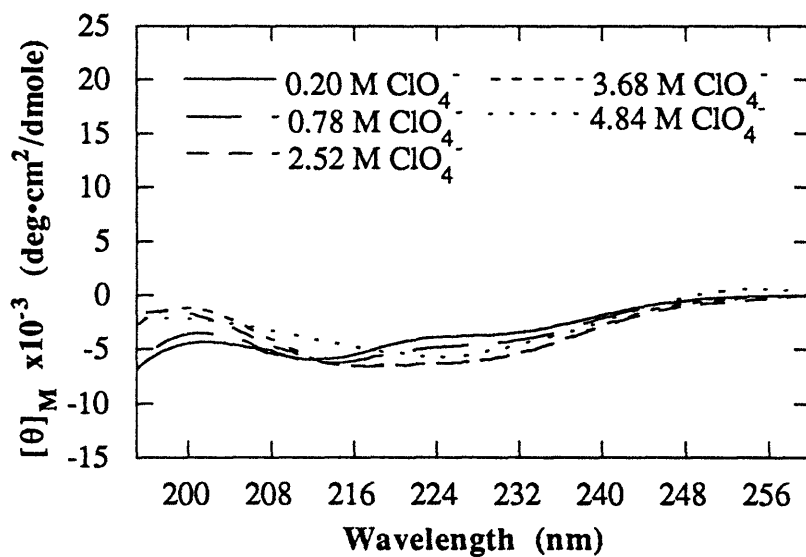


Figure 3.7: CD spectra of Ac-Hel<sub>1</sub>-A<sub>6</sub>-OH in perchlorate concentrations ranging from 0.20 to 4.8 M, 25 °C, pH 1.

## EVALUATION OF $[\theta]_{222}$ FOR 100% HELIX

### TFE Titration of the Series Ac-Hel<sub>1</sub>-A<sub>n</sub>-OH and Ac-Hel<sub>1</sub>-A<sub>n</sub>-NH<sub>2</sub>, n = 1-6: Measurement of the t/c Ratios

Once the discrepancies between the conditions for NMR and CD measurements were established as insignificant, the analysis of the CD spectra of the alanine derivatives of Ac-Hel<sub>1</sub> could be completed. Central to this analysis is an accurate measurement of the t/c ratios of these compounds. Dr. T. Allen has previously measured the t/c ratios of the series Ac-Hel<sub>1</sub>-A<sub>n</sub>-OH, n=1-6, in varying concentrations of TFE, but his data were acquired in 9:1 H<sub>2</sub>O:D<sub>2</sub>O under water suppression conditions, which can strongly affect integration values, and with inadequate delay times. The t/c ratios as a function of TFE concentration were therefore reevaluated in D<sub>2</sub>O, eliminating the need for water suppression, and substantial delays were employed. The results of this analysis are presented in Table 3.2 and Figure 3.8.

Mole% TFE	Ac-Hel <sub>1</sub> - A <sub>1</sub> -OH	Ac-Hel <sub>1</sub> - A <sub>2</sub> -OH	Ac-Hel <sub>1</sub> - A <sub>3</sub> -OH	Ac-Hel <sub>1</sub> - A <sub>4</sub> -OH	Ac-Hel <sub>1</sub> - A <sub>5</sub> -OH	Ac-Hel <sub>1</sub> - A <sub>6</sub> -OH
0	0.7968	1.1706	1.2661	1.3666	1.4707	1.7763
2				1.4607	1.6293	1.9282
3	0.8018	1.3338	1.4728			
4				1.7304	2.3779	2.9442
6	0.9992	1.8162	2.5393	3.0379	3.7750	4.9626
8				4.4462	5.9621	8.8232
10	1.4695	3.5190	4.6263	6.1124	8.8059	14.6367
12				7.4888	11.1080	19.4511
13	1.6792	4.4181	6.1219			
14				8.9730	13.8117	22.4769
16	1.8076	5.3135	7.0584	10.0798	15.4547	24.7681
18				11.8417	17.7777	24.1089
20	1.8896	5.9119	9.0796	12.1568	20.1807	27.5104

**Table 3.2:** [t]/[c] as a function of TFE concentration for the series  
Ac-Hel<sub>1</sub>-A<sub>n</sub>-OH, n=1-6, 0 to 20 mole% TFE, D<sub>2</sub>O, 27 °C.



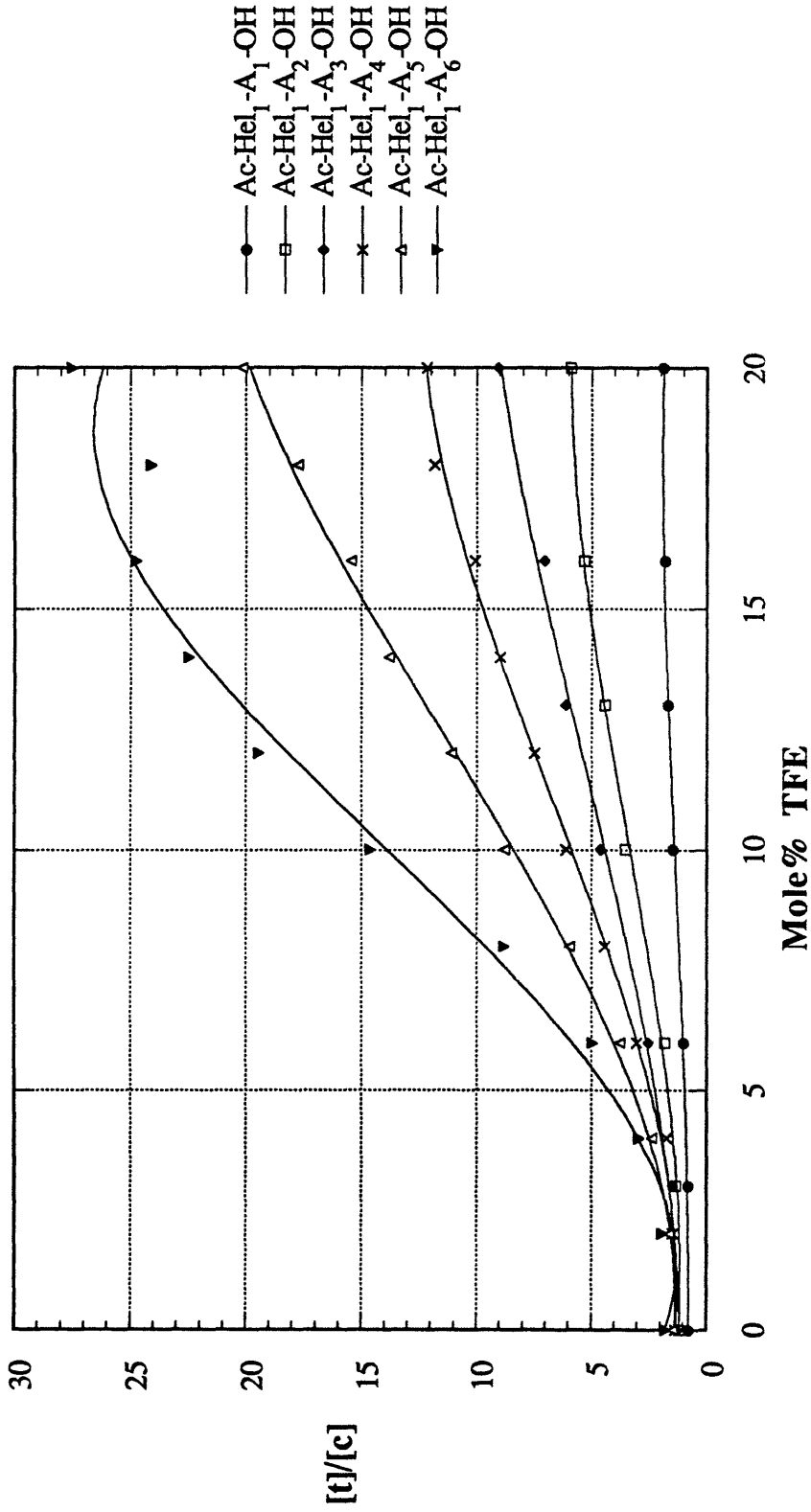


Figure 3.8: TFE titration of the series Ac-Hel<sub>1</sub>-A<sub>n</sub>-OH, n=1-6, for 0 to 20 mole% TFE, D<sub>2</sub>O, 27 °C, pD 1.

Dr. K. McClure measured the  $t/c$  ratios of the series Ac-Hel<sub>1</sub>-A<sub>n</sub>-NH<sub>2</sub>,  $n=1-6$ , in varying concentrations of TFE, and his data are presented in Table 3.3 and Figure 3.9.

Mole% TFE	Ac-Hel <sub>1</sub> - A <sub>1</sub> -NH <sub>2</sub>	Ac-Hel <sub>1</sub> - A <sub>2</sub> -NH <sub>2</sub>	Ac-Hel <sub>1</sub> - A <sub>3</sub> -NH <sub>2</sub>	Ac-Hel <sub>1</sub> - A <sub>4</sub> -NH <sub>2</sub>	Ac-Hel <sub>1</sub> - A <sub>5</sub> -NH <sub>2</sub>	Ac-Hel <sub>1</sub> - A <sub>6</sub> -NH <sub>2</sub>
0	1.19	1.35	1.42	1.54	1.78	1.96
2	1.23	1.41	1.50	1.78	2.05	3.00
4	1.35	1.64	1.85	2.18	2.67	7.38
6	1.67	2.28	2.68	3.54	4.35	10.90
8	2.35	3.53	4.19	5.74	8.78	17.33
10	3.08	5.12	5.97	8.79	13.80	
12	3.88	6.35	8.40	12.02	19.64	
14	4.51	7.39	9.80	15.06		
16	5.28	8.83	11.73	18.01		
18	5.66	9.78	14.08	20.83		
20	6.20	10.62	14.77	27.25		

**Table 3.2:**  $[t]/[c]$  as a function of TFE concentration for the series Ac-Hel<sub>1</sub>-A<sub>n</sub>-NH<sub>2</sub>,  $n=1-6$ , 0 to 20 mole% TFE, D<sub>2</sub>O, from Dr. K. McClure.

These  $t/c$  values allow for the calculation of the relative proportions of the (cs+ts) and the te states from expression 2.4; these calculated values enable the CD spectra to be appropriately corrected for both template and random coil contributions.

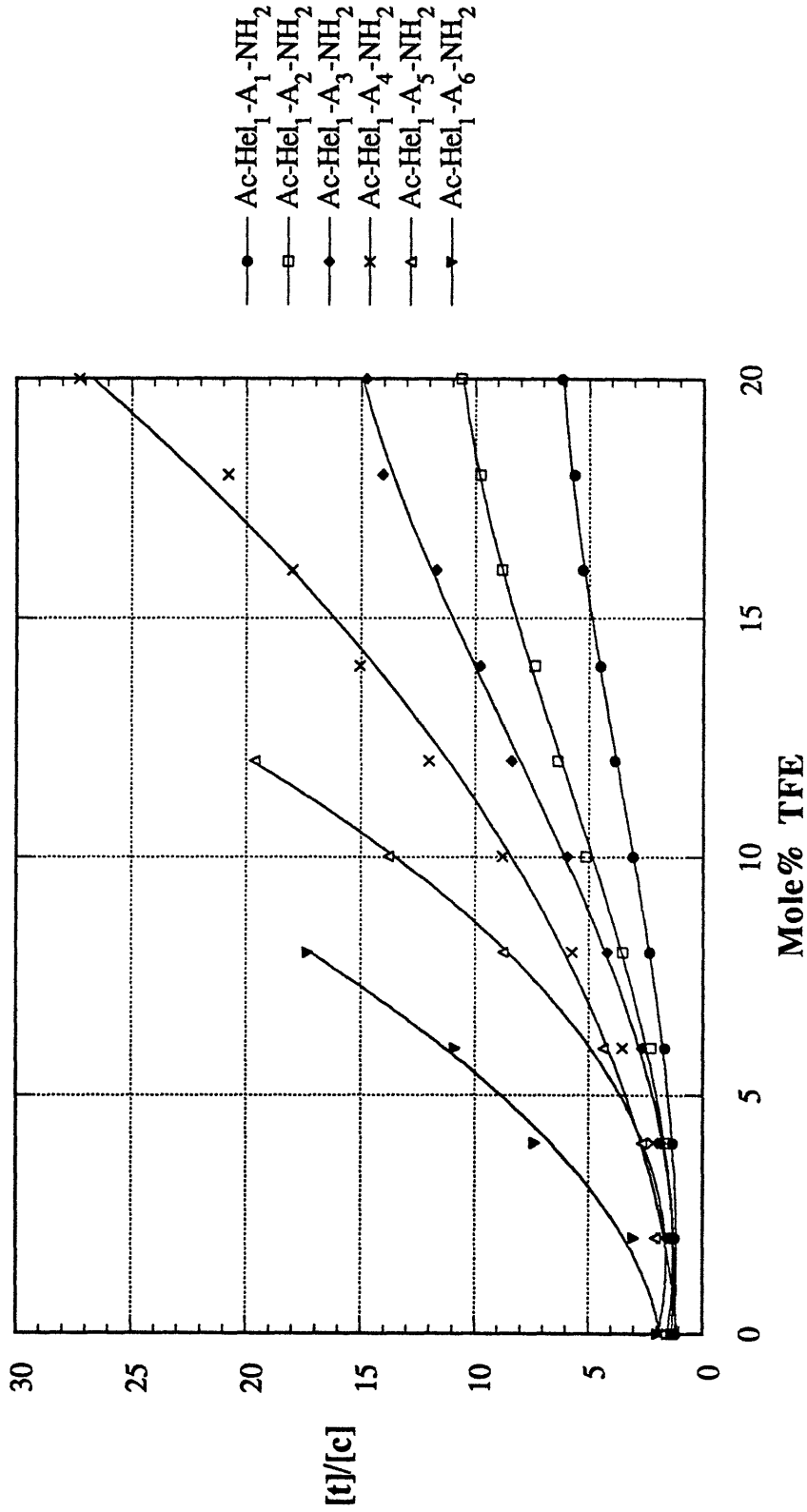


**Figure 3.9:** TFE titration of the series Ac-Hel<sub>1</sub>-A<sub>n</sub>-OH, n=1-6, for 0 to 20 mole% TFE, D<sub>2</sub>O, 27 °C, pD 1, from Dr. K. McClure.

## TFE Titration of the Series Ac-Hel<sub>1</sub>-A<sub>n</sub>-OH and Ac-Hel<sub>1</sub>-A<sub>n</sub>-NH<sub>2</sub>, n = 1-6: CD Spectra

The preliminary computations for the analysis of the CD spectra of Ac-Hel<sub>1</sub> derivatives were presented in Chapter 2 by utilizing the simple amide Ac-Hel<sub>1</sub>-NH<sub>2</sub> to determine  $\theta_{(cs+ts)}$  and  $\theta_{te}$ , the CD spectra corresponding to the composite nonnucleating conformation and the nucleating conformation of the template, respectively. As discussed earlier, this analysis provides the information necessary to appropriately subtract the template contribution from the CD signal of any given derivative to determine the CD spectrum of the peptide segment alone, as seen in equation 2.8.

$$\theta_{\text{peptide}} = \theta_{\text{observed}} - (1 - \chi_{te})\theta_{(cs+ts)} - \chi_{te}\theta_{te} \quad 2.8$$

The CD spectra (i.e.  $\theta_{\text{observed}}$ ) for the series Ac-Hel<sub>1</sub>-A<sub>n</sub>-NH<sub>2</sub>, n = 1-6, are presented in Figure 3.10 on the following six pages; similarly the spectra for Ac-Hel<sub>1</sub>-A<sub>n</sub>-OH, are presented in Figure 3.11 on the subsequent six pages. It must be noted that the data is presented as the molar ellipticity  $[\theta]_M$ , which differs from the mean residue ellipticity  $[\theta]$  most often presented in the literature. The molar ellipticity is computed from the raw ellipticity by accounting for path length and solution concentration. The mean residue ellipticity is the molar ellipticity divided by the number of amino acid residues in the peptide, i.e. the per residue ellipticity. For peptide derivatives of Ac-Hel<sub>1</sub>, it is unclear as to how many residues the diproline derived template should be assigned. Thus values are reported as the molar ellipticity.

These figures reveal the influence of the template on the CD signal, in particular for the shorter derivatives. For these spectra, the curves in water resemble the curve determined in Figure 2.14 for the (cs+ts) state of the template. With increasing TFE concentration, however, the spectra bear a greater resemblance to the te state of the template. For the longer derivatives, the spectra acquired in high TFE concentrations are still reminiscent of the te state of the template, but the spectra at low TFE concentrations are not very similar to the (cs+ts) template spectrum. The decrease in ellipticity at low wavelengths in these spectra is most likely attributed to the decrease in the (cs+ts) state of the template and the corresponding increase in the te state observed for longer derivatives. Thus these mostly aqueous spectra exhibit a template contribution intermediate between the two limiting spectra of Figure 2.14.

These spectra may now be used in conjunction with the t/c ratios as determined by NMR for the first stage of the derivation.

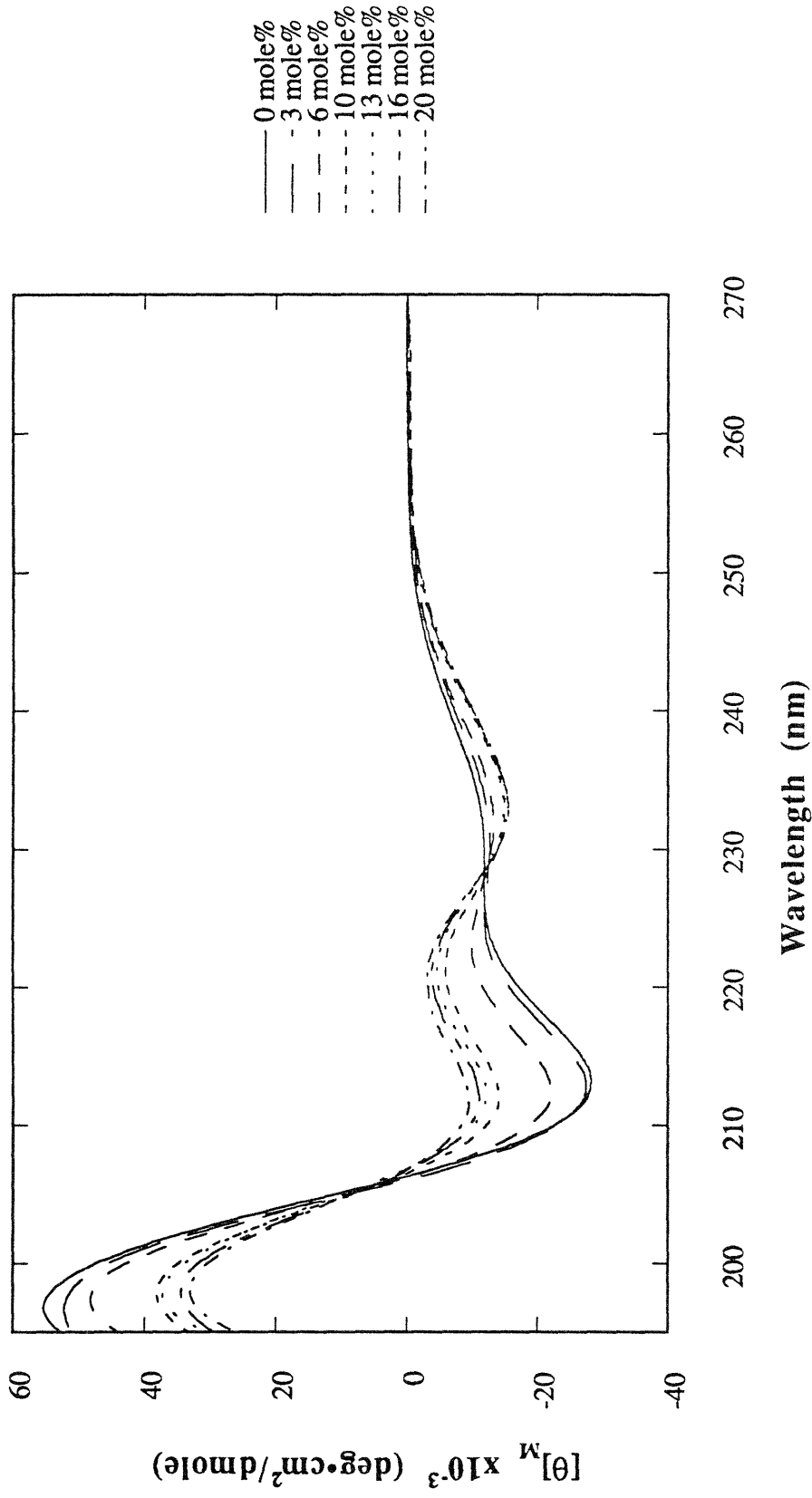
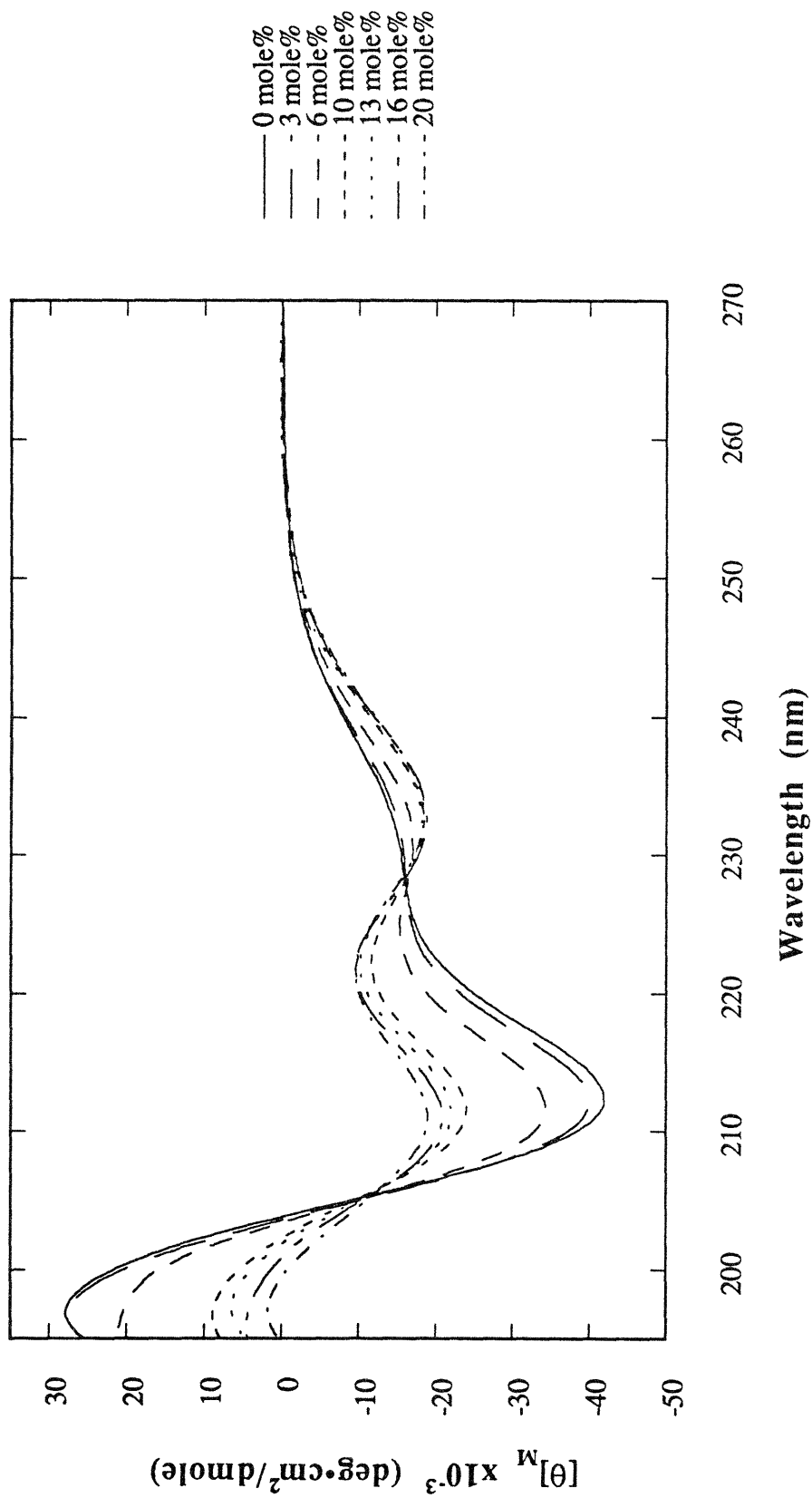


Figure 3.10a: TFE titration of Ac-Hel<sub>1</sub>-A<sub>1</sub>-NH<sub>2</sub>, 25 °C.



**Figure 3.10b:** TFE titration of Ac-Hel<sub>1</sub>-A<sub>2</sub>-NH<sub>2</sub>, 25 °C.

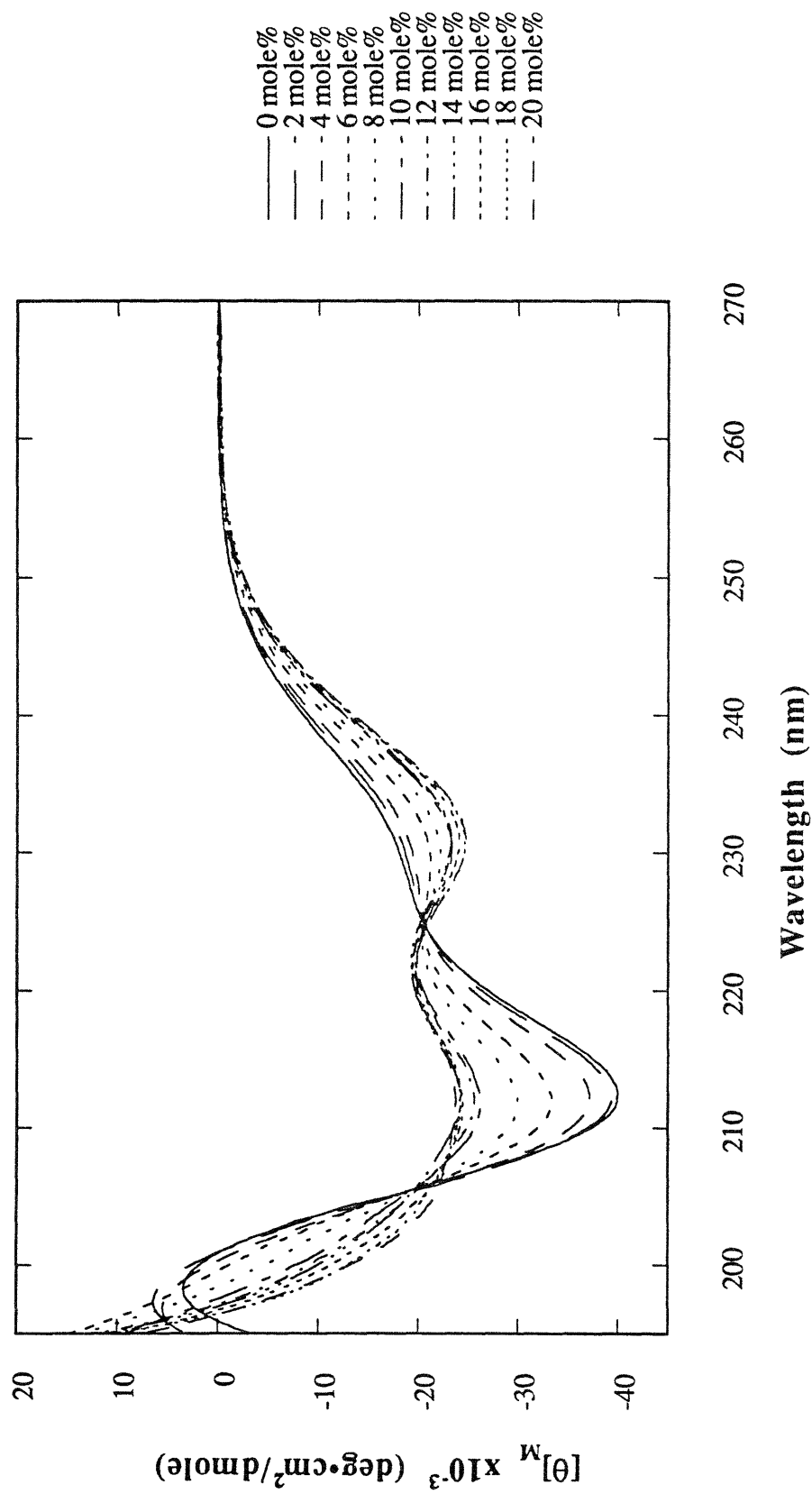


Figure 3.10c: TFE titration of Ac-Hel<sub>1</sub>-A<sub>3</sub>-NH<sub>2</sub>, 25 °C.

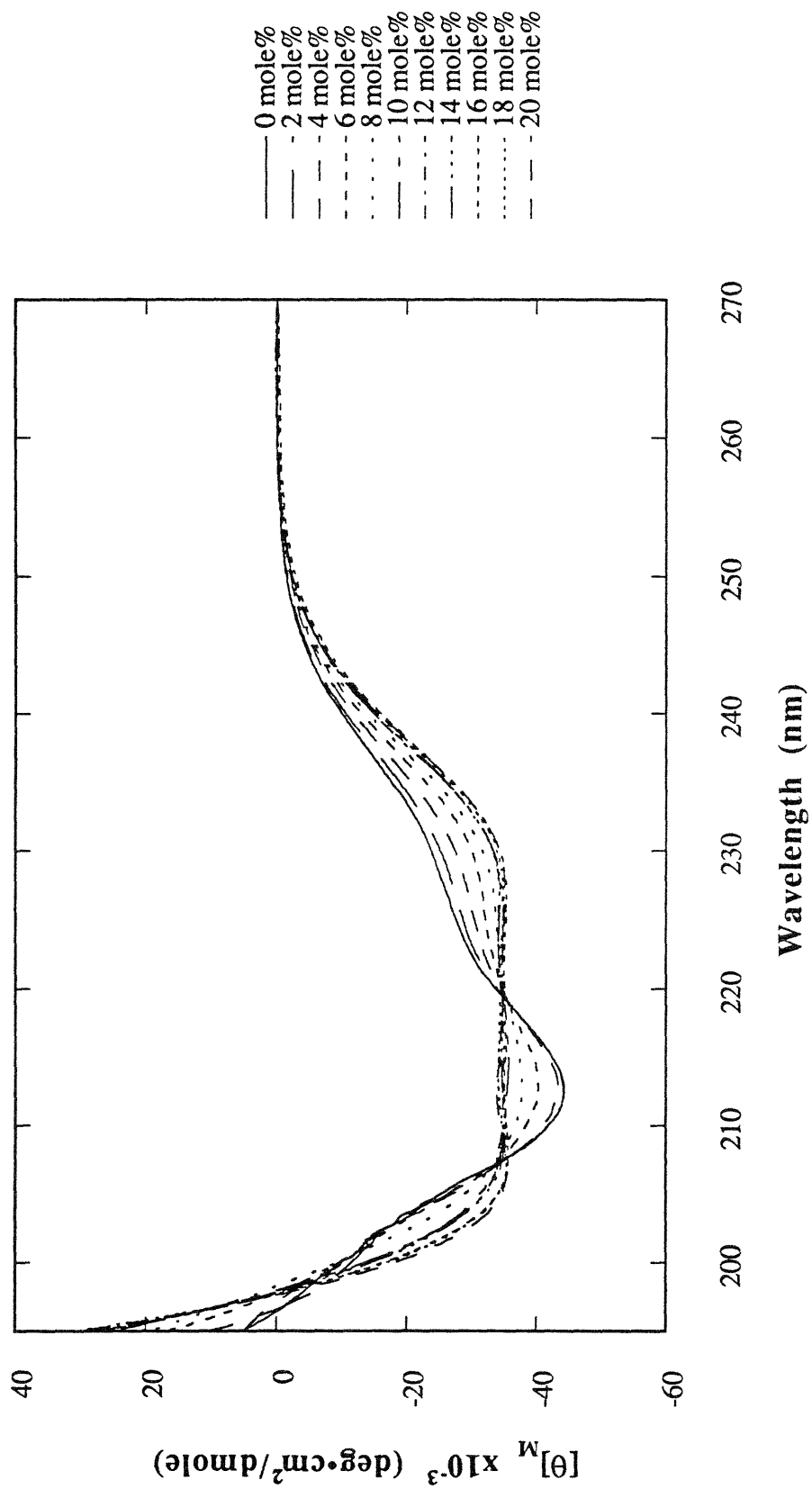


Figure 3.10d: TFE titration of Ac-Hel<sub>1</sub>-A<sub>4</sub>-NH<sub>2</sub>, 25 °C.



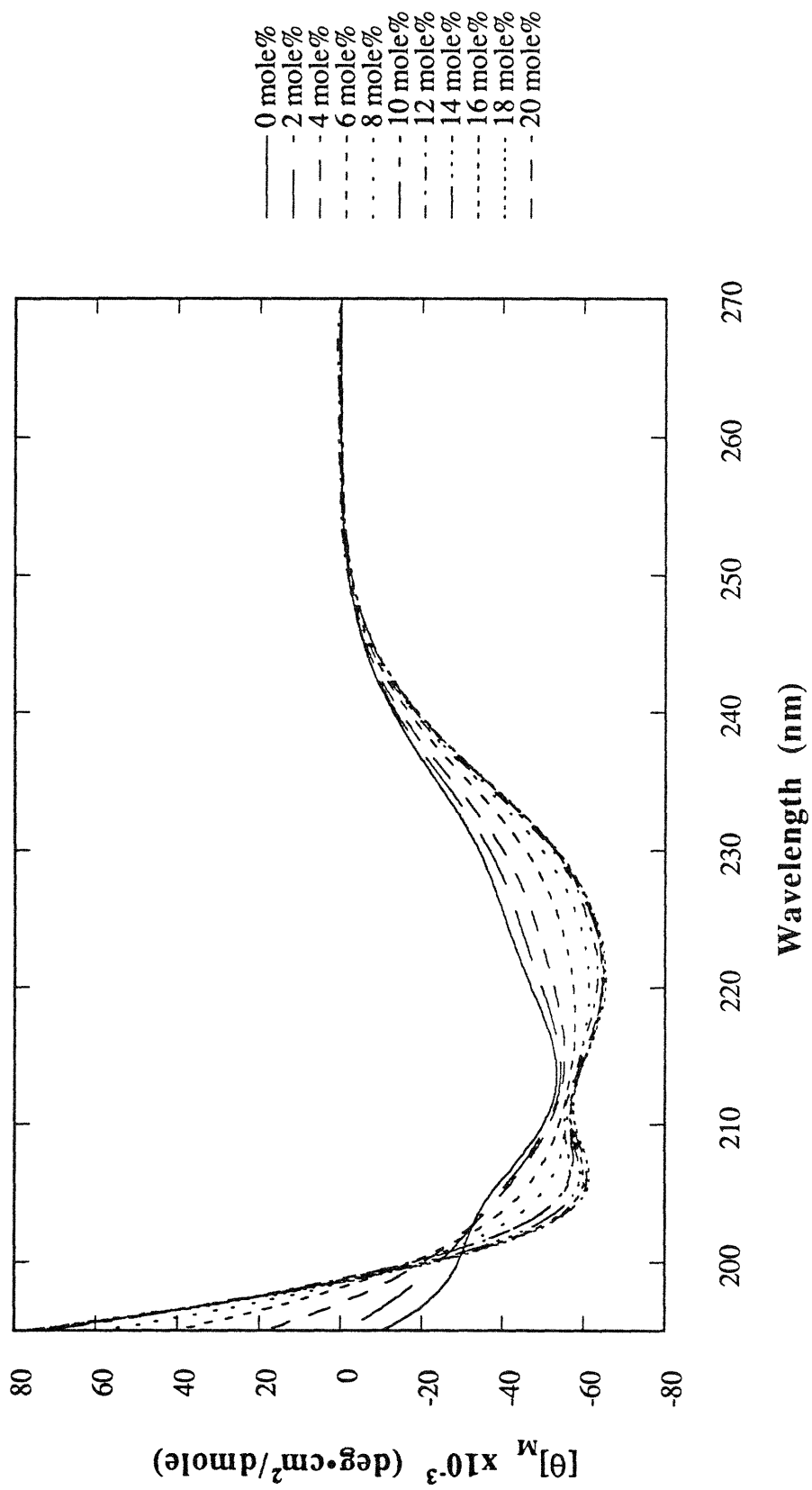


Figure 3.10e: TFE titration of Ac-Hel<sub>1</sub>-A<sub>5</sub>-NH<sub>2</sub>, 25 °C.

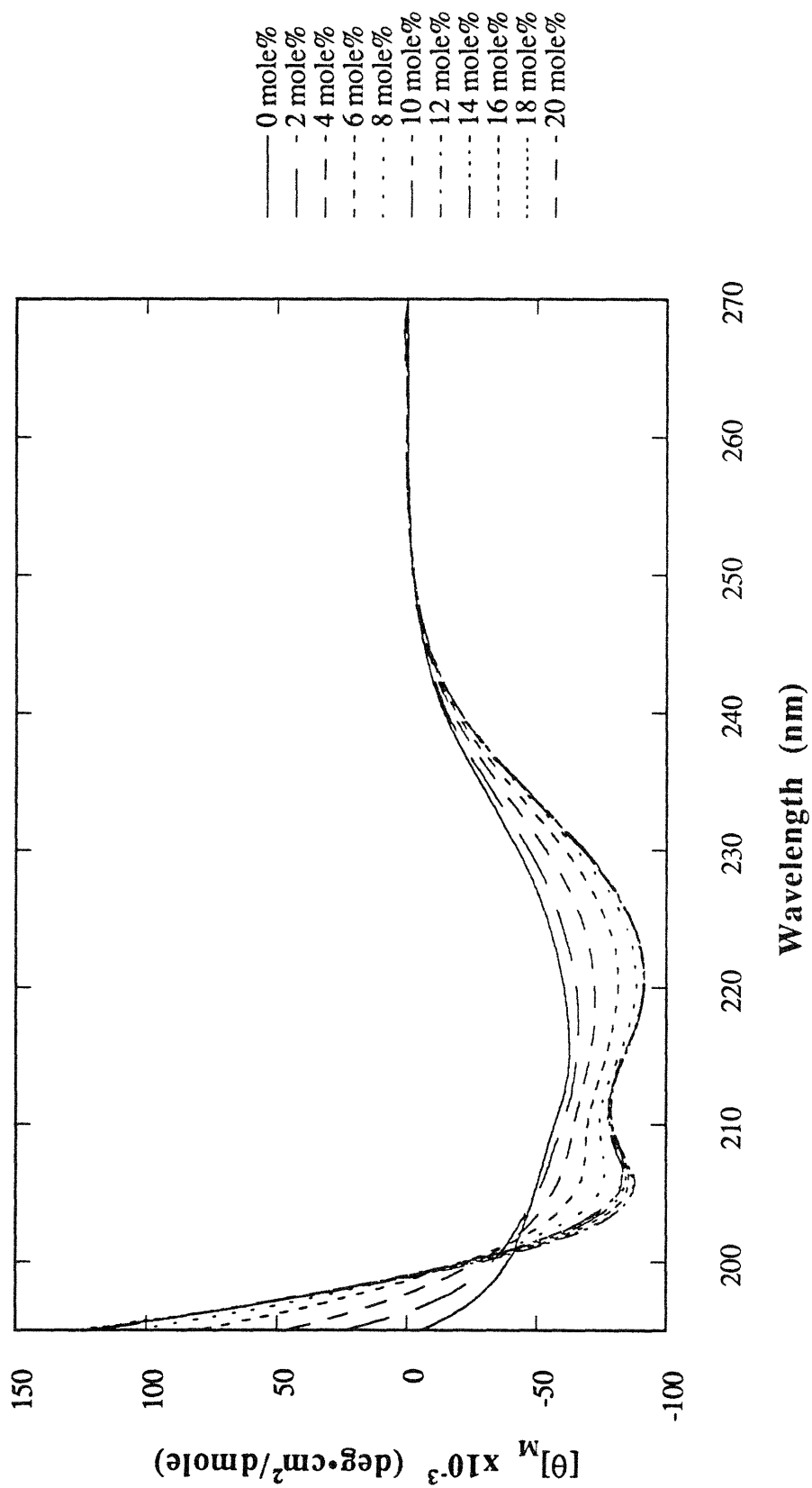


Figure 3.10f: TFE titration of Ac-Hel<sub>1</sub>-A<sub>6</sub>-NH<sub>2</sub>, 25 °C.

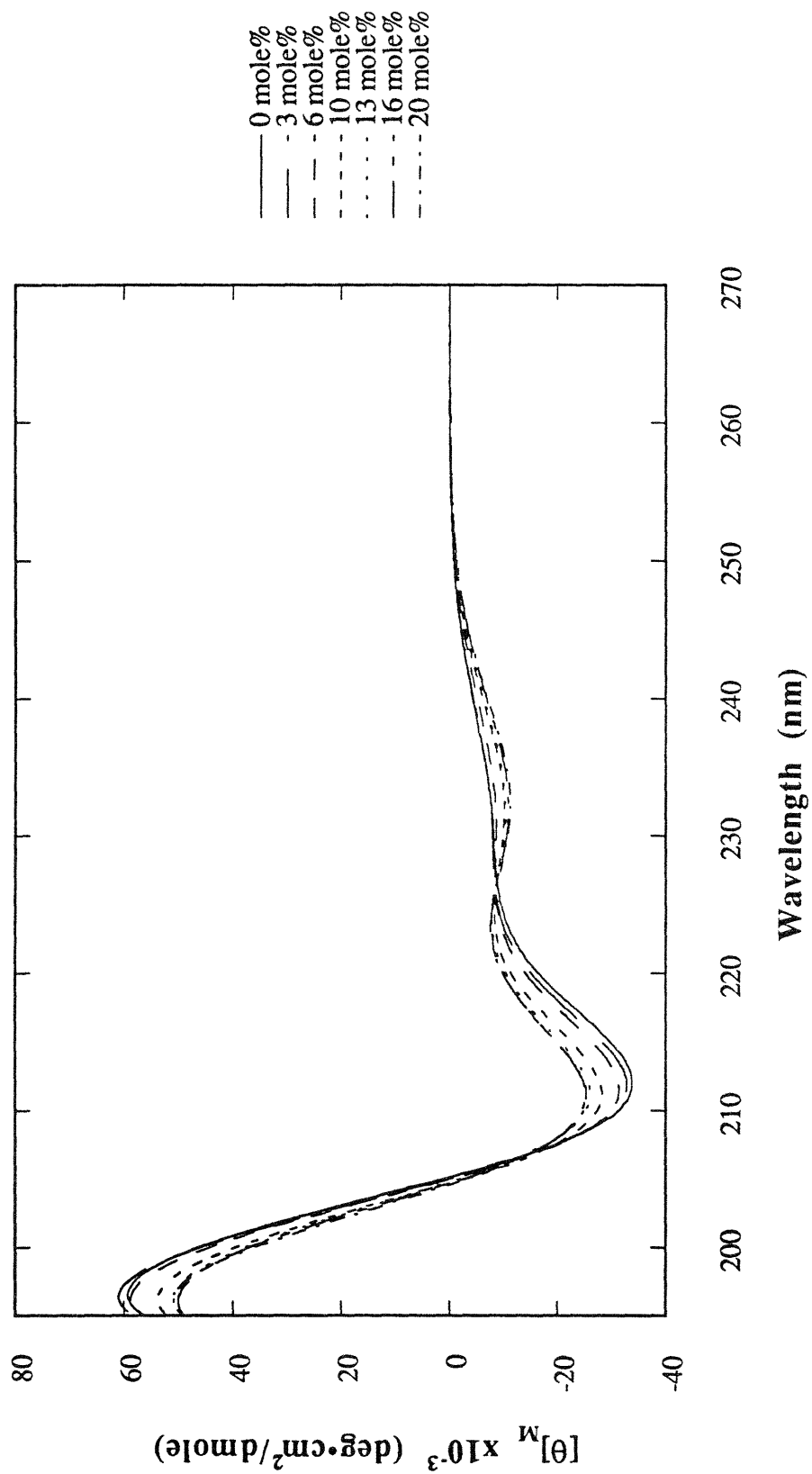
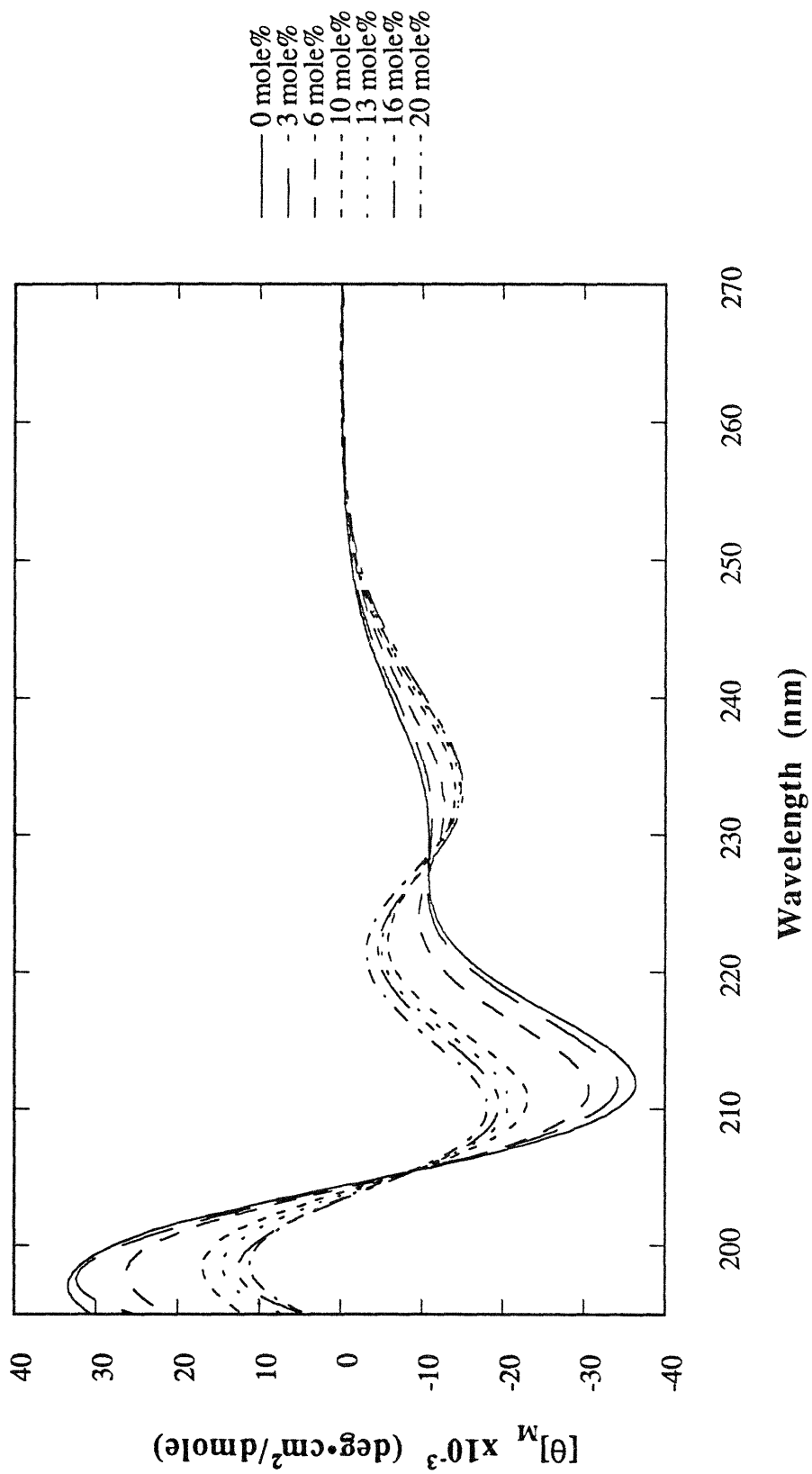


Figure 3.11a: TFE titration of Ac-Hel<sub>1</sub>-A<sub>1</sub>-OH, 25 °C.



**Figure 3.11b:** TFE titration of Ac-Hel<sub>1</sub>-A<sub>2</sub>-OH, 25 °C.

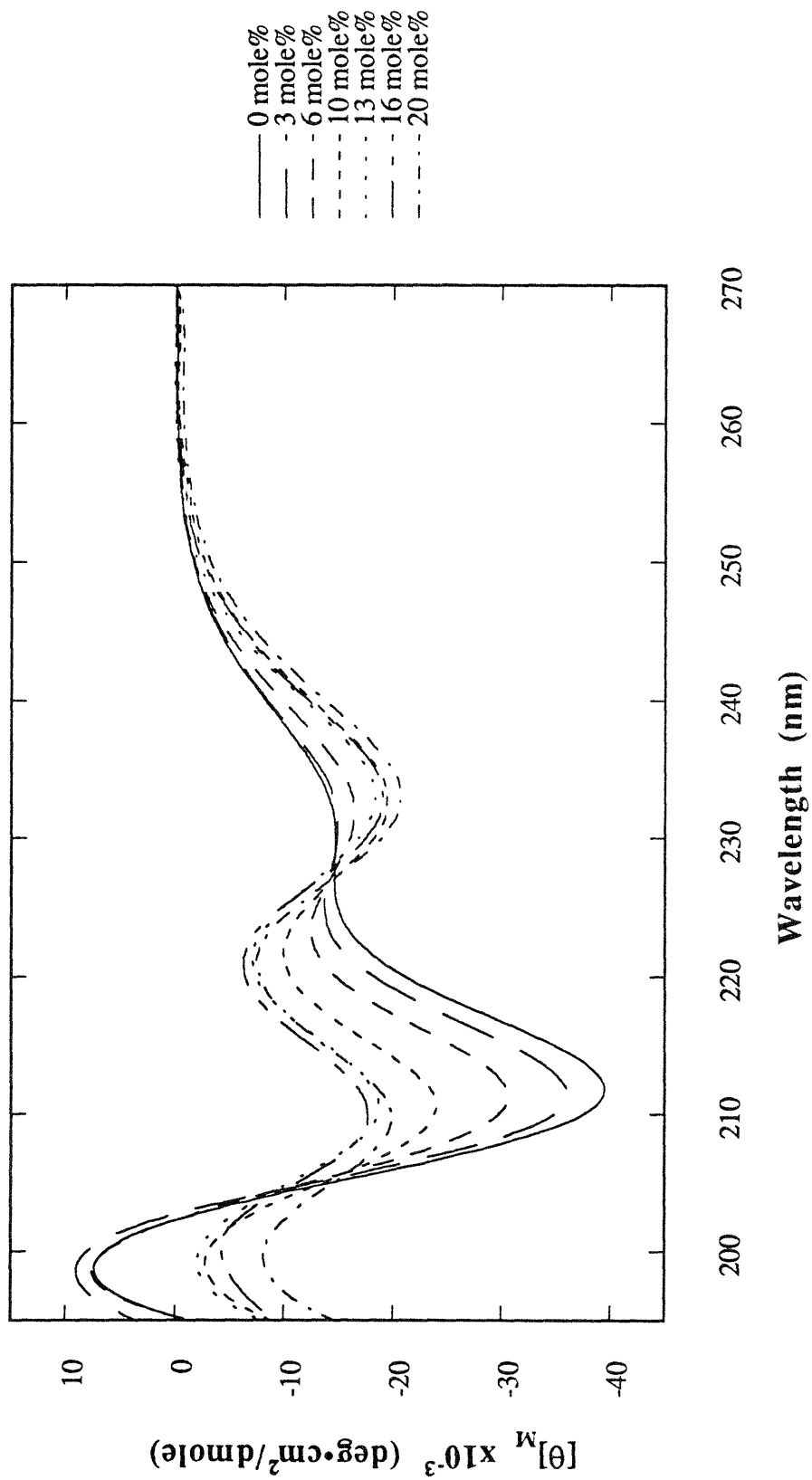


Figure 3.11c: TFE titration of Ac-Hel<sub>1</sub>-A<sub>3</sub>-OH, 25 °C.

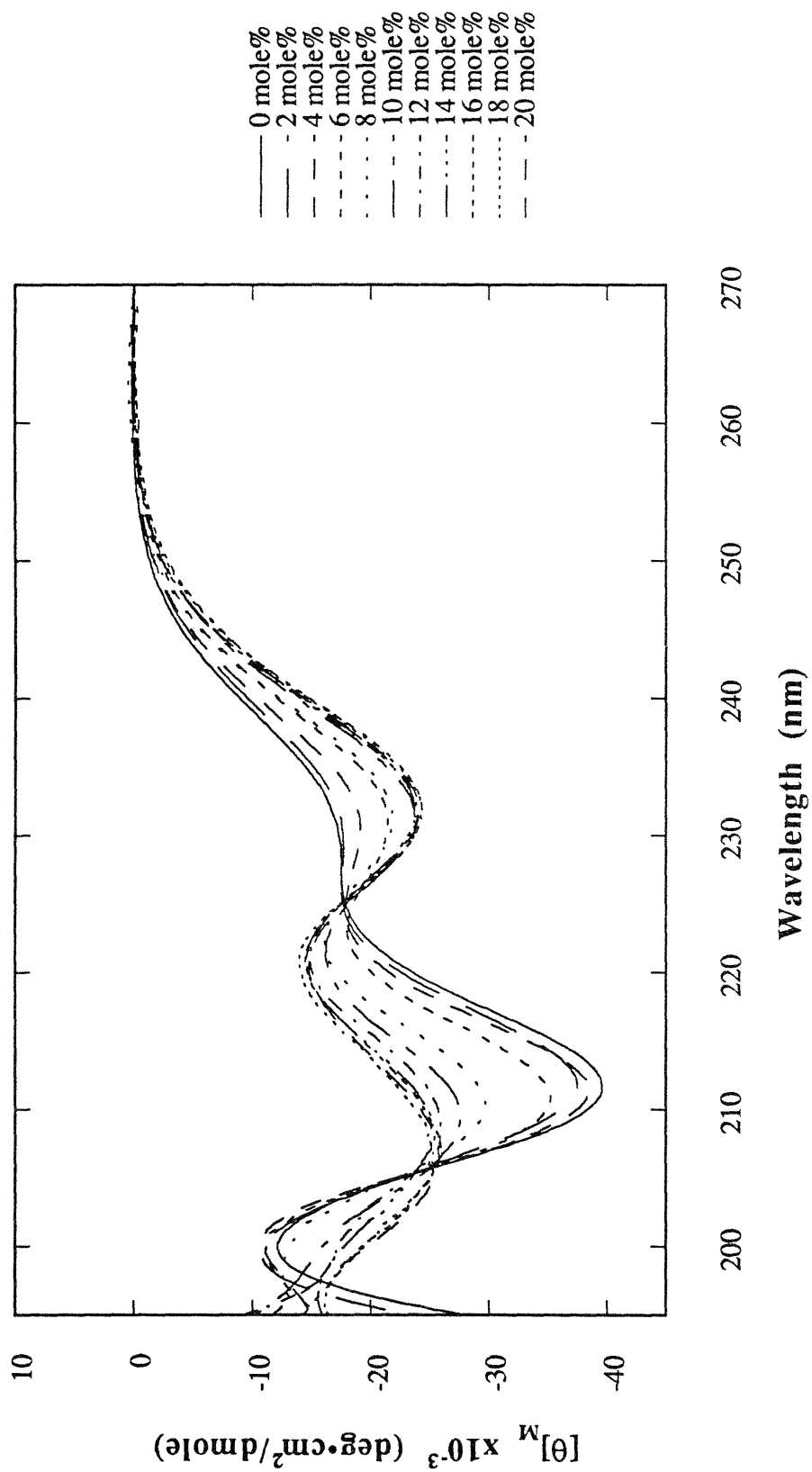


Figure 3.11d: TFE titration of Ac-Hel<sub>1</sub>-A<sub>4</sub>-OH, 25 °C.

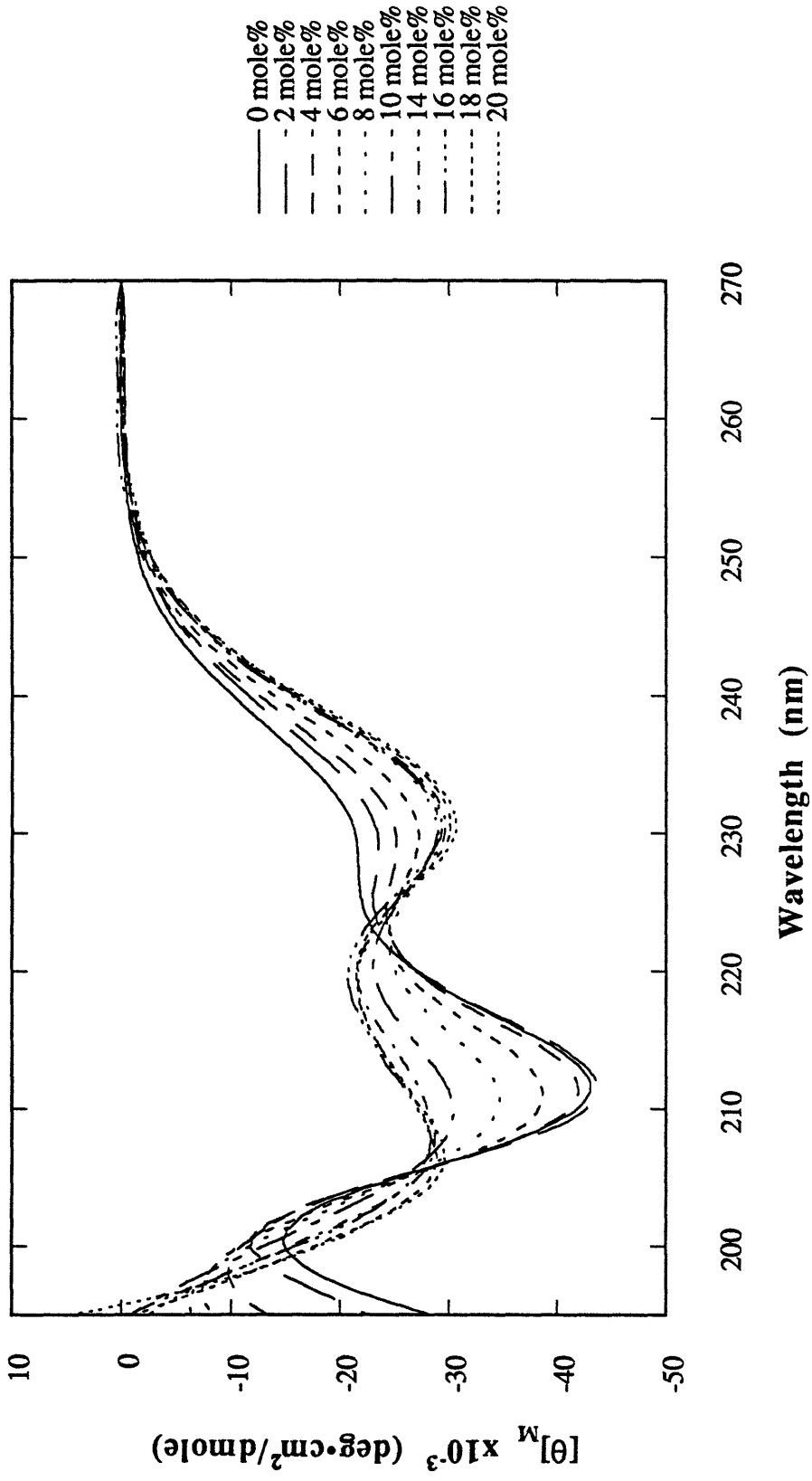
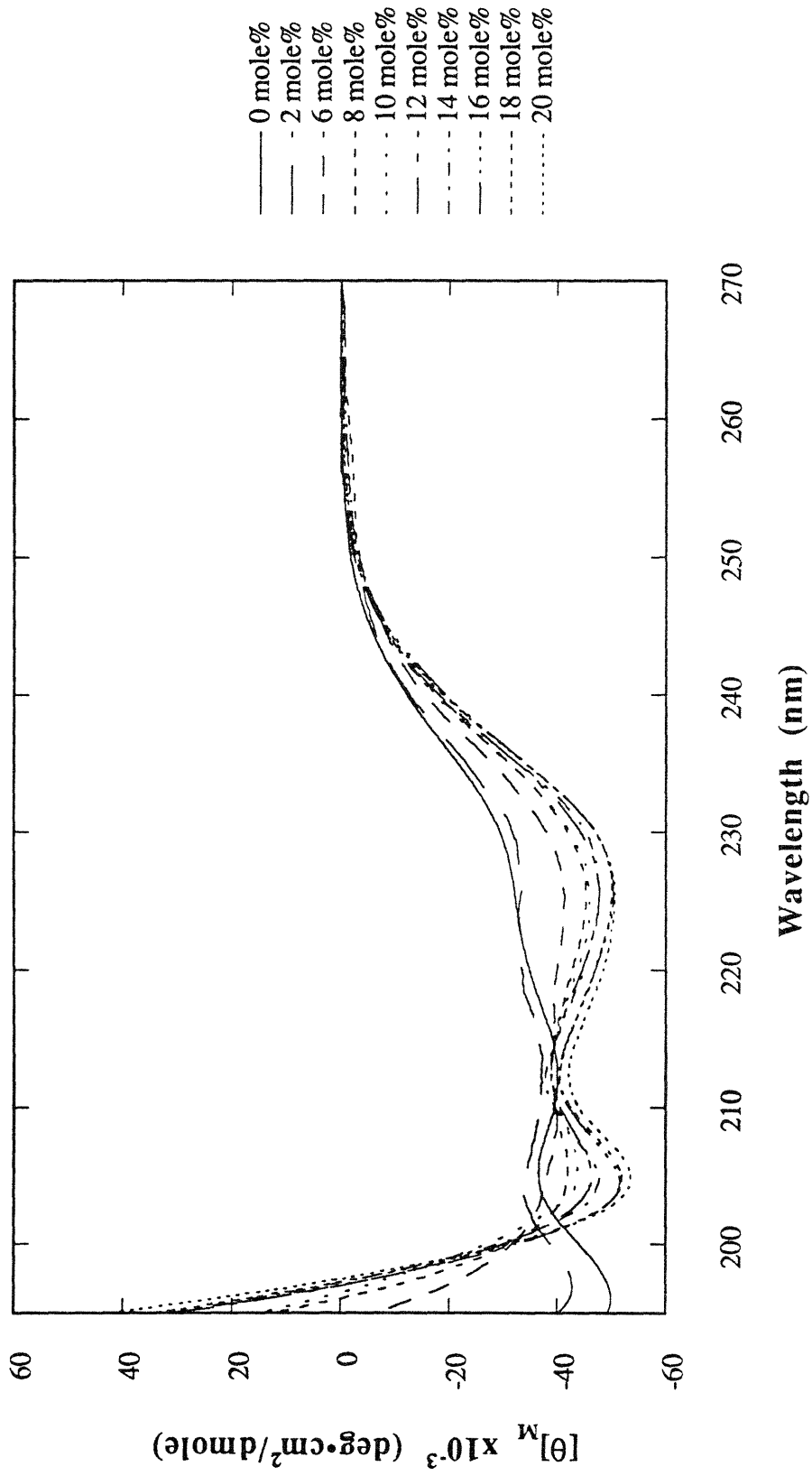


Figure 3.11e: TFE titration of Ac-Hel<sub>1</sub>-A<sub>5</sub>-OH, 25 °C.



**Figure 3.11f:** TFE titration of Ac-Hel<sub>1</sub>-A<sub>6</sub>-OH, 25 °C.



## Correction for the Template Contribution to the Observed CD Signal

This data of the preceding section was corrected for the template contribution as outlined in equation 2.8; the values of  $\chi_{te}$  for each TFE concentration of each derivative were calculated directly from their t/c ratios using expression 2.4. These and all other calculations used in the CD analysis are thoroughly described in Appendix B and will therefore not be discussed in detail in this chapter.

The peptide CD spectra of Ac-Hel<sub>1</sub>-A<sub>n</sub>-NH<sub>2</sub>, n=1,3,6, are presented in Figure 3.12 on the following three pages. The data for Ac-Hel<sub>1</sub>-A<sub>n</sub>-OH, n=1,3,6, is given in Figure 3.13 on the next three pages.

The resultant spectra within the TFE titration for a given shorter derivative (i.e. Ac-Hel<sub>1</sub>-A<sub>1</sub>-NH<sub>2</sub>, Figure 3.12a) are very similar, the large spectral changes observed in the original data of Figures 3.10 and 3.11 for these derivatives are due primarily to changes in the CD signal of the template. For the longer derivatives, this is not the case. The resultant peptide spectra within the TFE titration of Ac-Hel<sub>1</sub>-A<sub>6</sub>-NH<sub>2</sub> (Figure 3.12c), for example, are highly variant and reveal the development of greater helical character in these longer peptides.

With these calculations, the problem of the template contribution to the CD signal of its derivatives has been solved.

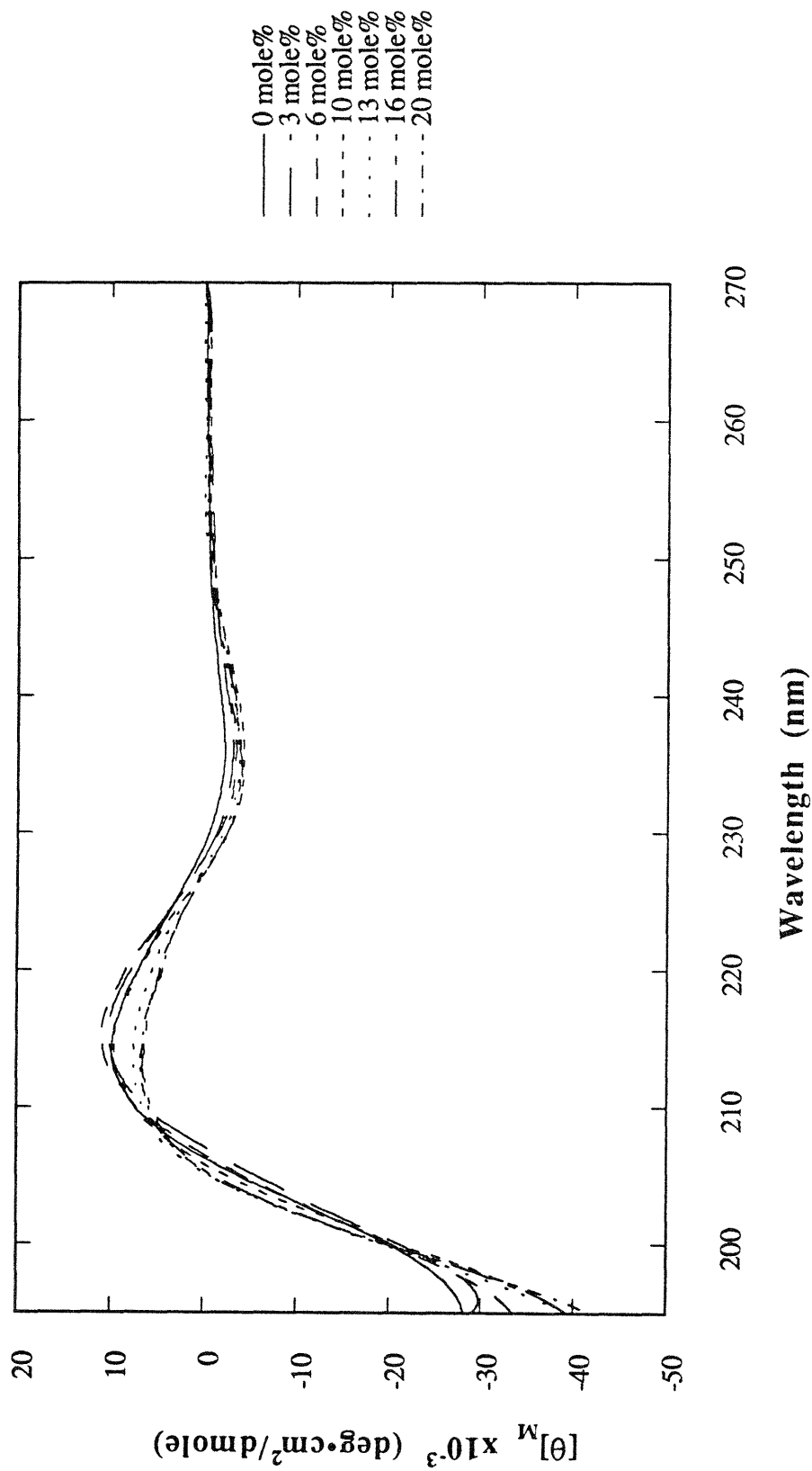


**Figure 3.12a: Peptide portion of the CD spectrum of Ac-Hel<sub>1</sub>-A<sub>1</sub>-NH<sub>2</sub>.**

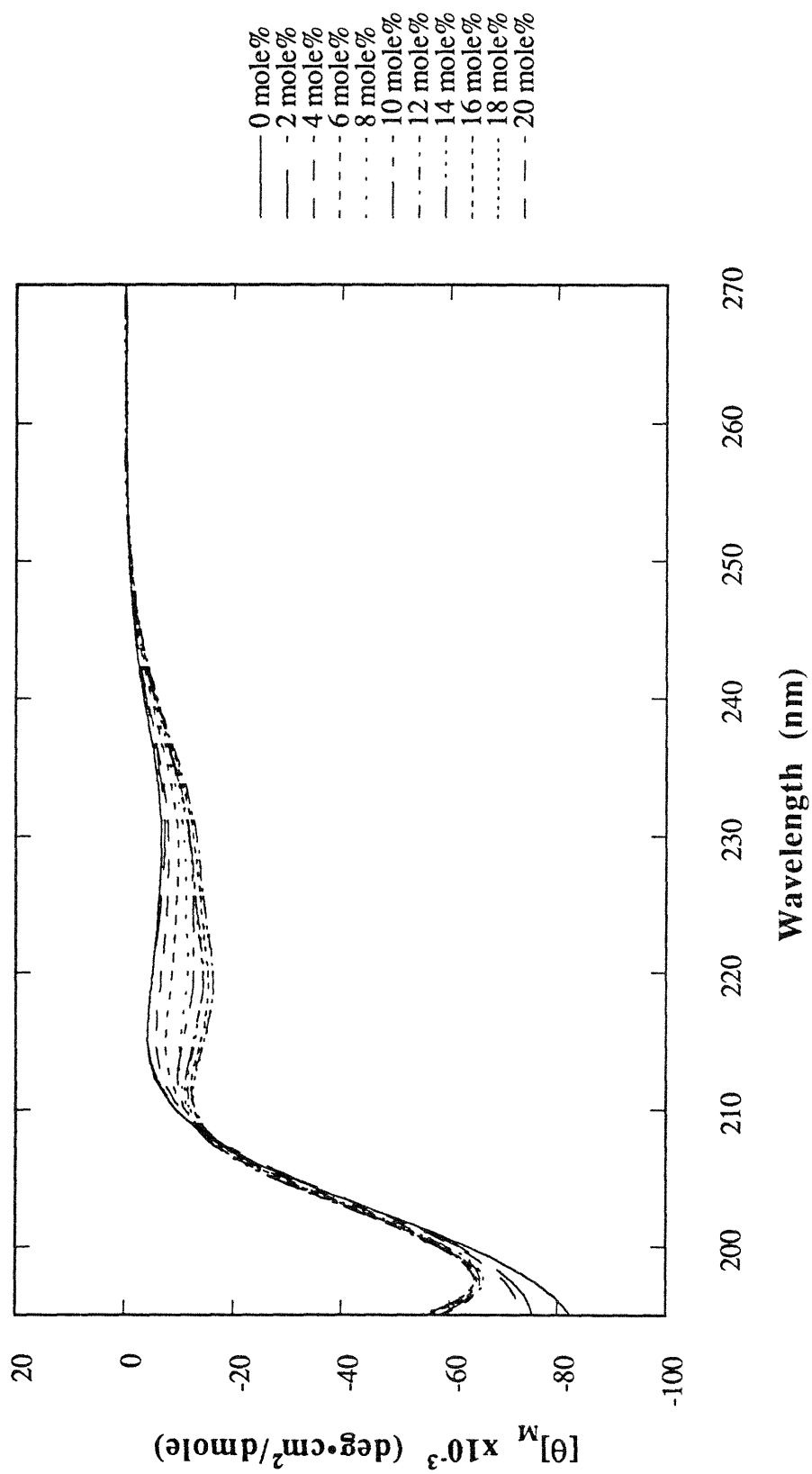


Figure 3.12b: Peptide portion of the CD spectrum of Ac-Hel<sub>1</sub>-A<sub>3</sub>-NH<sub>2</sub>.

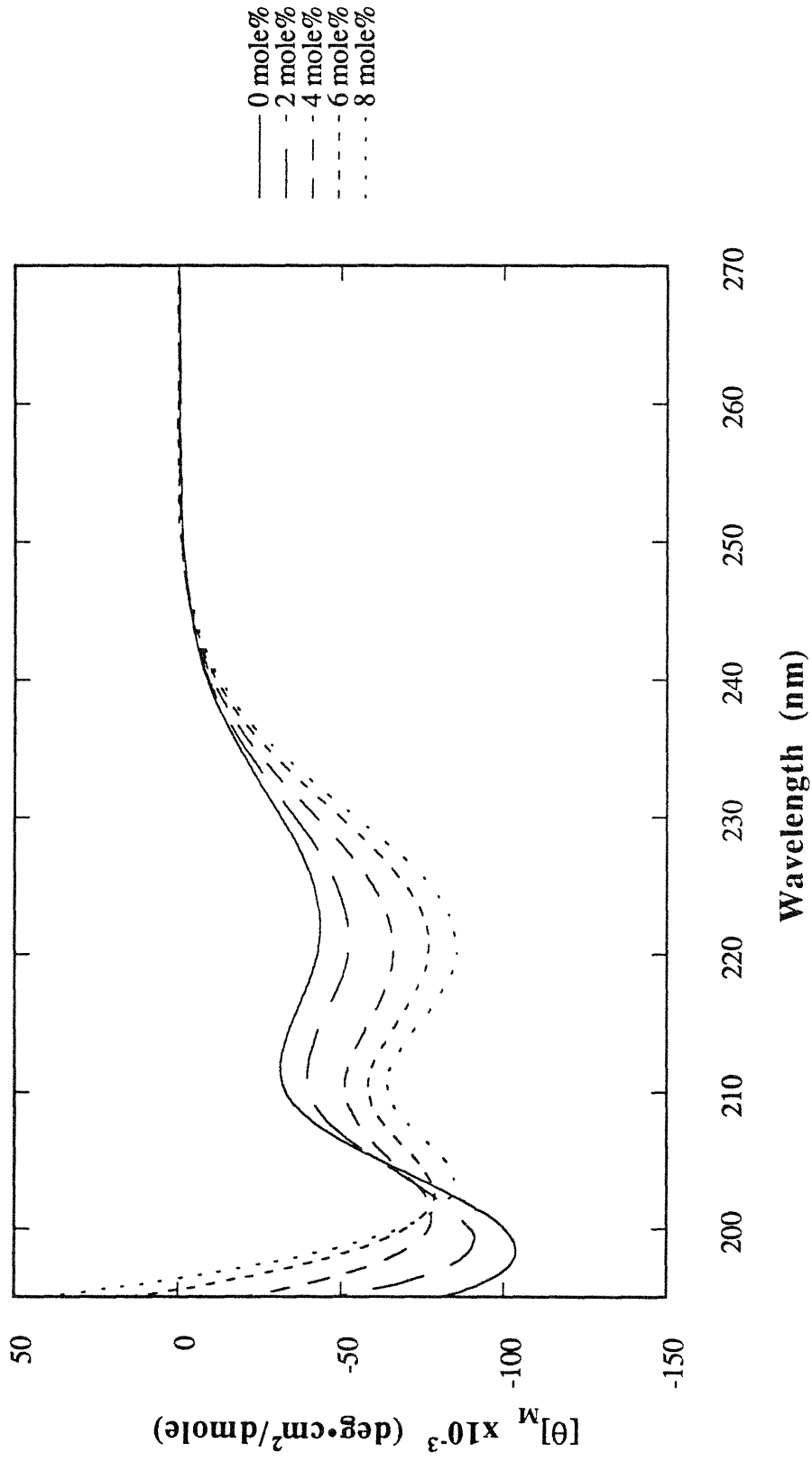


Figure 3.12c: Peptide portion of the CD spectrum of Ac-Hel<sub>1</sub>-A<sub>6</sub>-NH<sub>2</sub>.

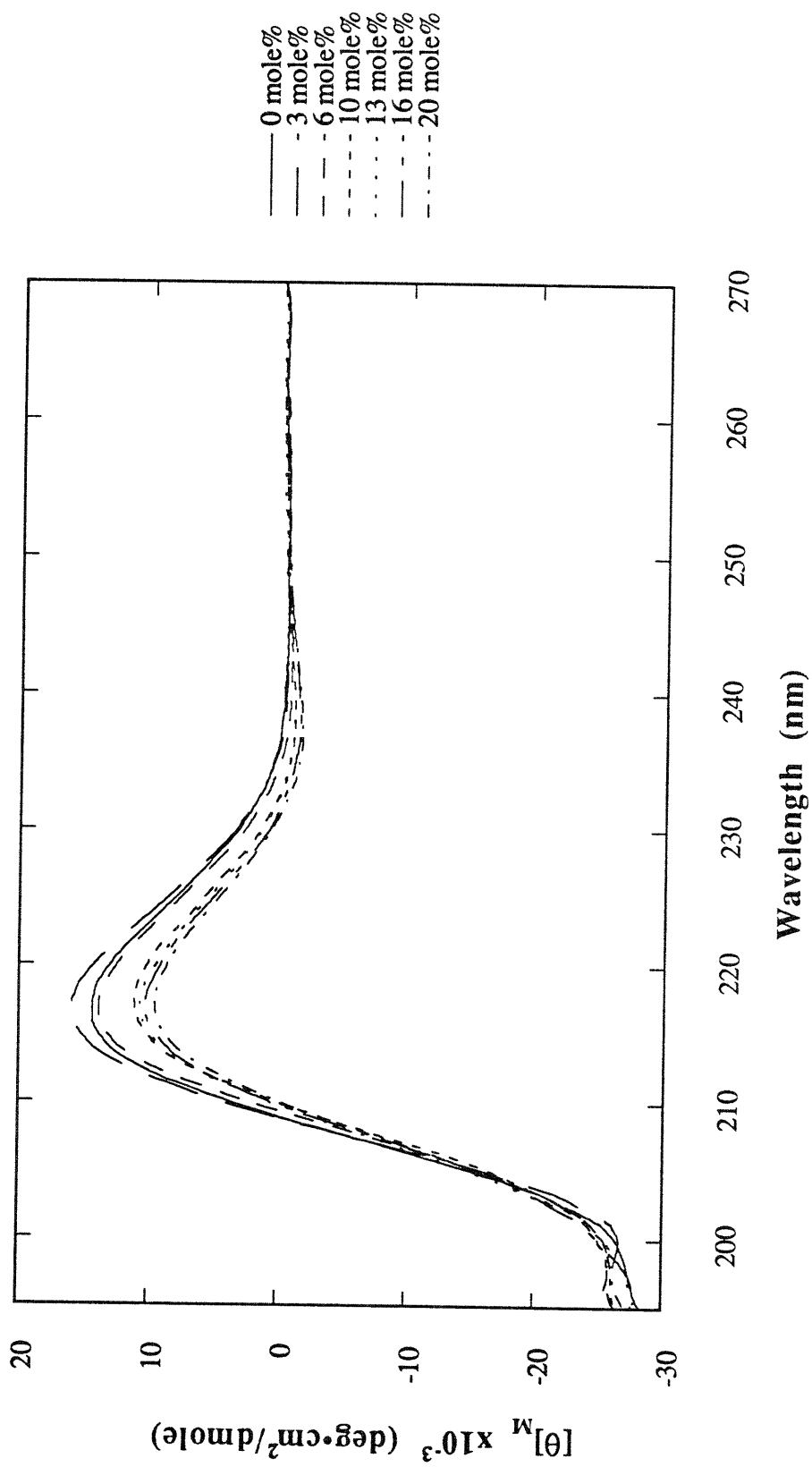


Figure 3.13a: Peptide portion of the CD spectrum of Ac-Hel<sub>1</sub>-A<sub>1</sub>-OH.

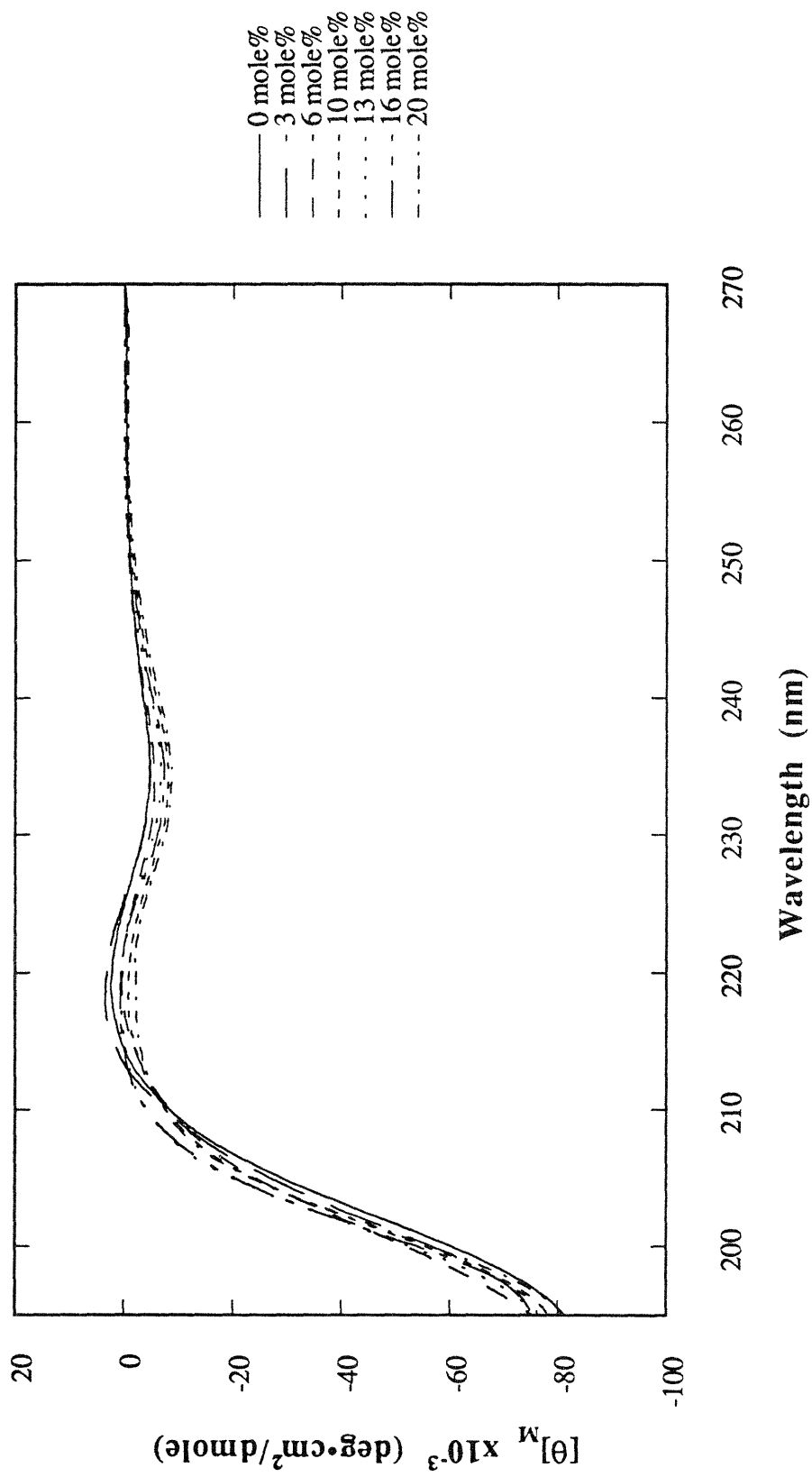
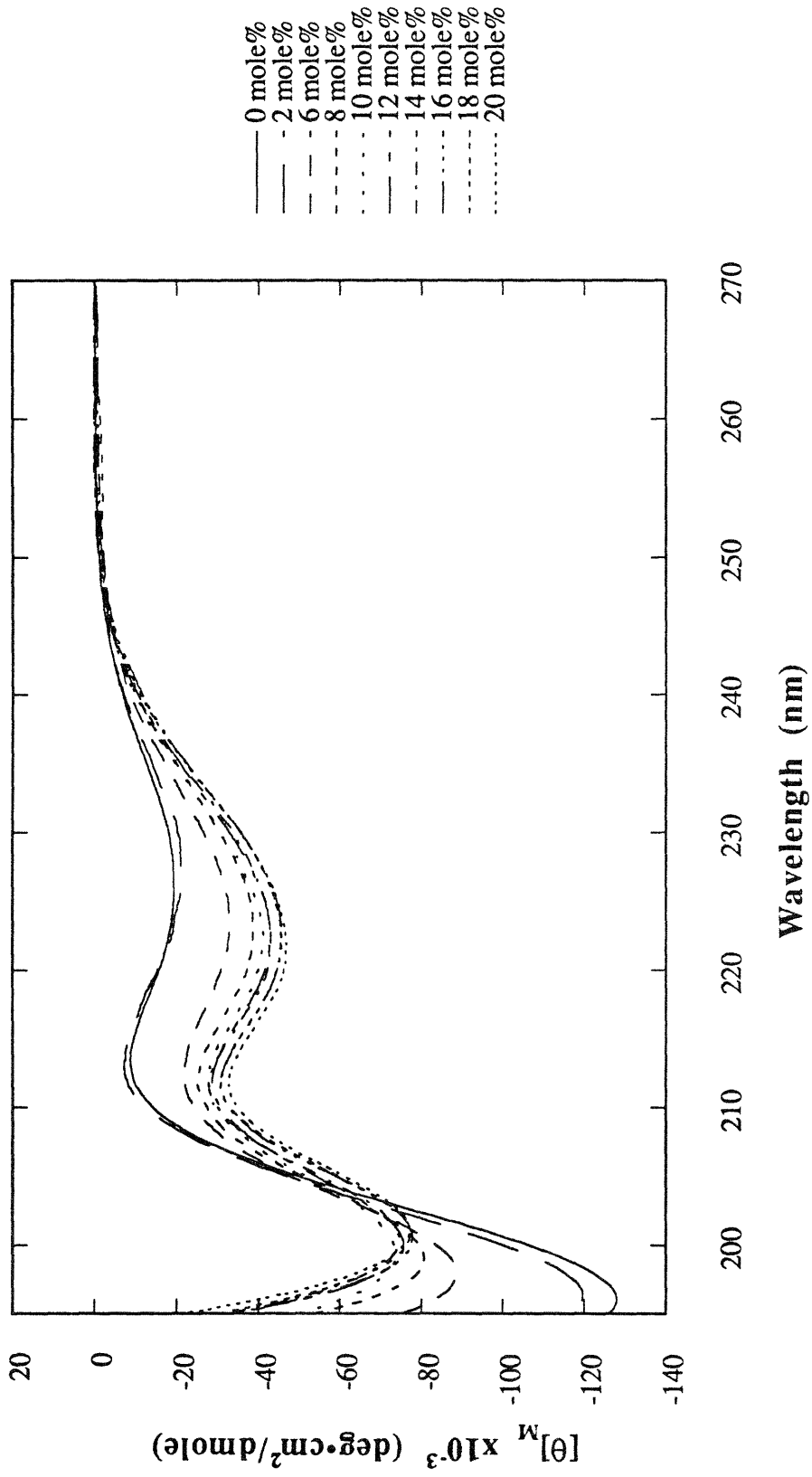


Figure 3.13b: Peptide portion of the CD spectrum of Ac-Hel<sub>1</sub>-A<sub>3</sub>-OH.



**Figure 3.13c:** Peptide portion of the CD spectrum of Ac-Hel<sub>1</sub>-A<sub>6</sub>-OH.

## Calculation of the Peptide Limiting Helical and Non-helical CD Spectra

The CD spectra of Figures 3.12 and 3.13 were calculated based on the assumption that the ellipticity contributions of the template and peptide portions of a given derivative are essentially independent, and that the template contributions are equal to the limiting spectra derived for Ac-Hel<sub>1</sub>-NH<sub>2</sub> in Figure 2.14. These preceding spectra should therefore be equal to the sum of the spectra of the peptide in the (cs+ts) and in the te substates. This is summarized in expression 3.2, where  $\theta_{P-(cs+ts)}$  is the first peptide subset and  $\theta_{P-te}$  the second. The mole fractions of these states at any TFE concentration can be computed from the t/c ratios measured by NMR integration.

$$\theta_{\text{peptide}} = \chi_{(cs+ts)}\theta_{P-(cs+ts)} + \chi_{te}\theta_{P-te} \quad 3.2$$

Under the restrictive assumption that TFE does not affect the average CD spectrum of peptides within these states, a linear regression analysis of the ellipticity at each wavelength of a given derivative would yield the limiting CD spectra of the pure peptide states associated with the template (cs+ts) and te states. This assumption is unlikely to be valid for the te state, as TFE is known from NMR studies to alter the fractional helicity. It is much more plausible for the (cs+ts) state, as direct and indirect evidence shows the peptide conformations associated with this state to be random coils.

Such a linear regression would determine not only whether the observed CD spectra can be accurately represented as a simple function of two limiting spectra, weighted by their relative abundances, but also whether the limiting spectrum for  $\chi_{te}$  is in fact a random coil spectrum. Equation 3.3 summarizes this analysis.

$$\theta_{\text{peptide}} = \text{slope}(\chi_{te}) + \text{intercept} \quad 3.3$$

The values for  $\theta_{P-(cs+ts)}$  of 3.2 were calculated by a linear regression analysis of each TFE series of each derivative, using the linear equation 3.3. When  $\chi_{(cs+ts)} = 1$ ,  $\chi_{te}$  must equal 0, and  $\theta_{P-(cs+ts)} \equiv \text{intercept}$ .

The values computed for  $\theta_{P-(cs+ts)}$  are presented in Figure 3.14 for the amide series and 3.15 for the acid series. Strikingly, the spectra of 3.14 are similar to those reported by Mattice for the series of alanine oligomers shown in Figure 3.2. Furthermore, they exhibit a nearly linear relationship between length and molar ellipticity. Thus these spectra, as well as those of 3.15, can be accurately modeled by a constant per residue random coil molar ellipticity. This is the first direct evidence that the peptides attached to the (cs+ts)



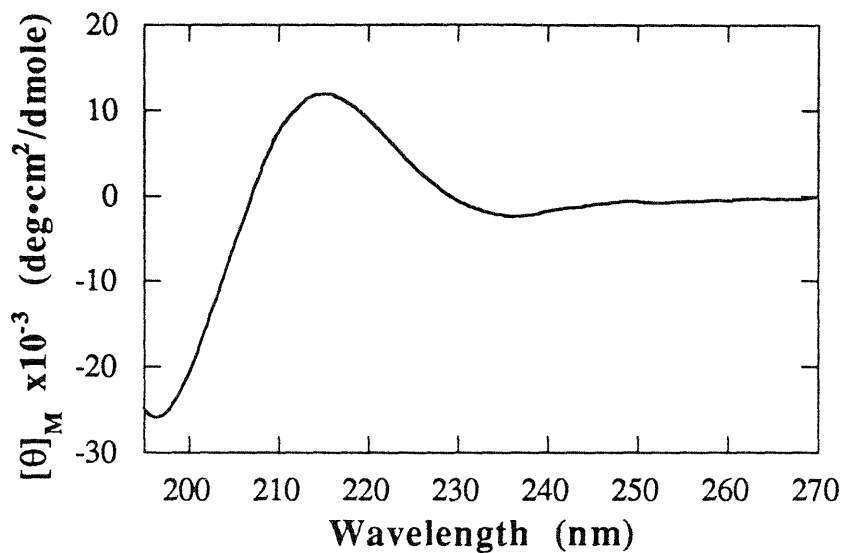


**Figure 3.14a:** CD spectrum of the peptide portion of Ac-Hel<sub>1</sub>-A<sub>1</sub>-NH<sub>2</sub> attached to the nonnucleating (cs+ts) state of the template, 25 °C.

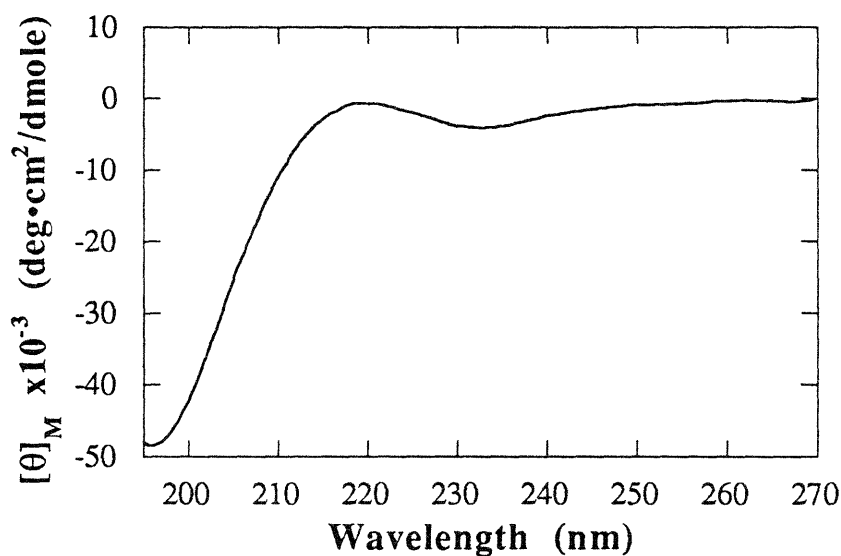


**Figure 3.14b:** CD spectrum of the peptide portion of Ac-Hel<sub>1</sub>-A<sub>2</sub>-NH<sub>2</sub> attached to the nonnucleating (cs+ts) state of the template, 25 °C.

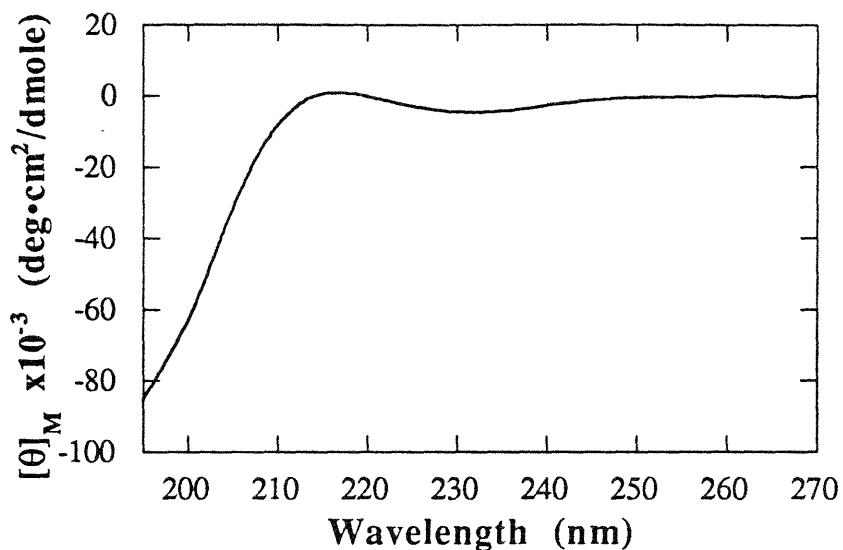


Figure 3.14c: CD spectrum of the peptide portion of Ac-Hel<sub>1</sub>-A<sub>3</sub>-NH<sub>2</sub> attached to the nonnucleating (cs+ts) state of the template, 25 °C.

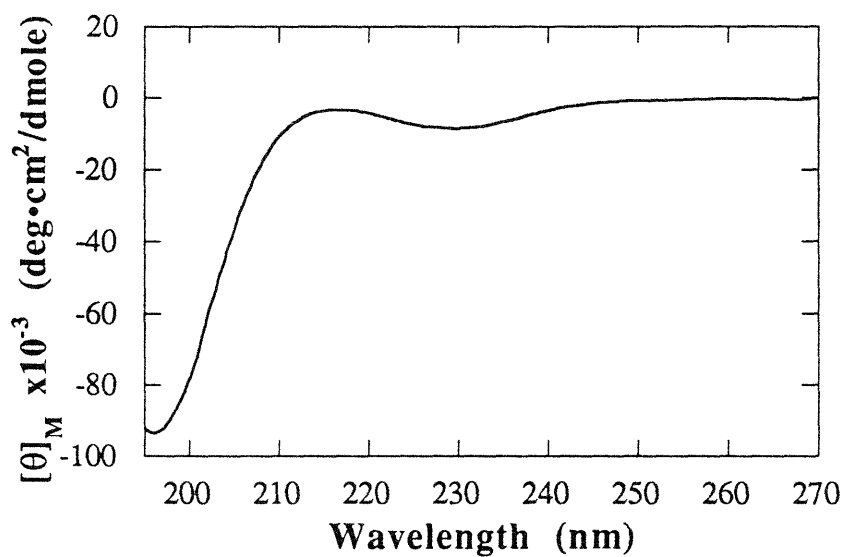
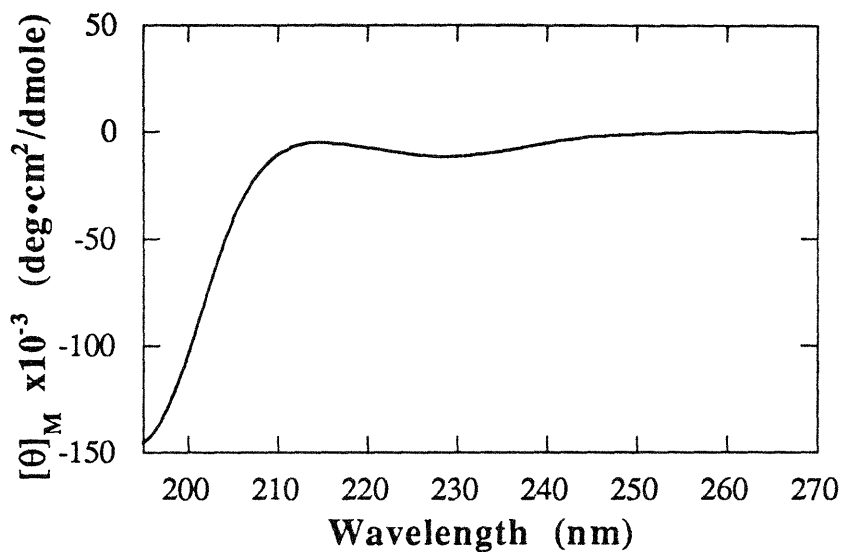
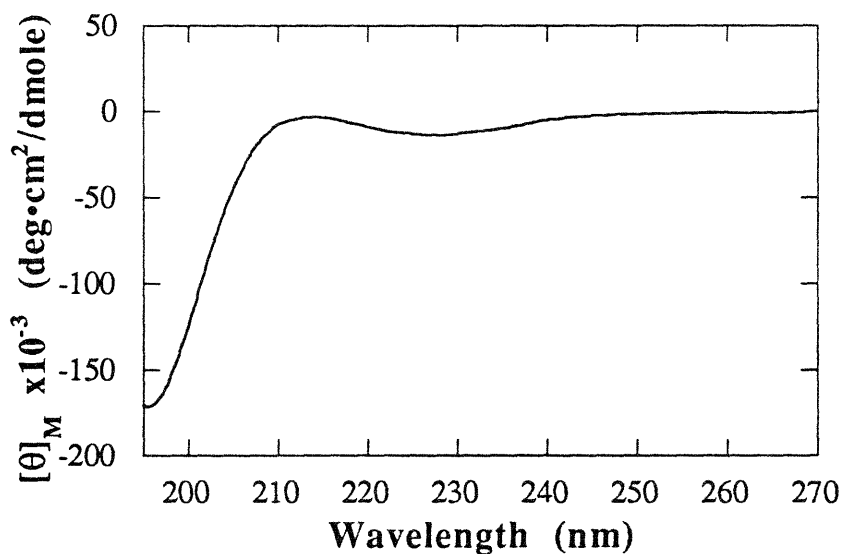


Figure 3.14d: CD spectrum of the peptide portion of Ac-Hel<sub>1</sub>-A<sub>4</sub>-NH<sub>2</sub> attached to the nonnucleating (cs+ts) state of the template, 25 °C.



**Figure 3.14e:** CD spectrum of the peptide portion of Ac-Hel<sub>1</sub>-A<sub>5</sub>-NH<sub>2</sub> attached to the nonnucleating (cs+ts) state of the template, 25 °C.



**Figure 3.14f:** CD spectrum of the peptide portion of Ac-Hel<sub>1</sub>-A<sub>6</sub>-NH<sub>2</sub> attached to the nonnucleating (cs+ts) state of the template, 25 °C.

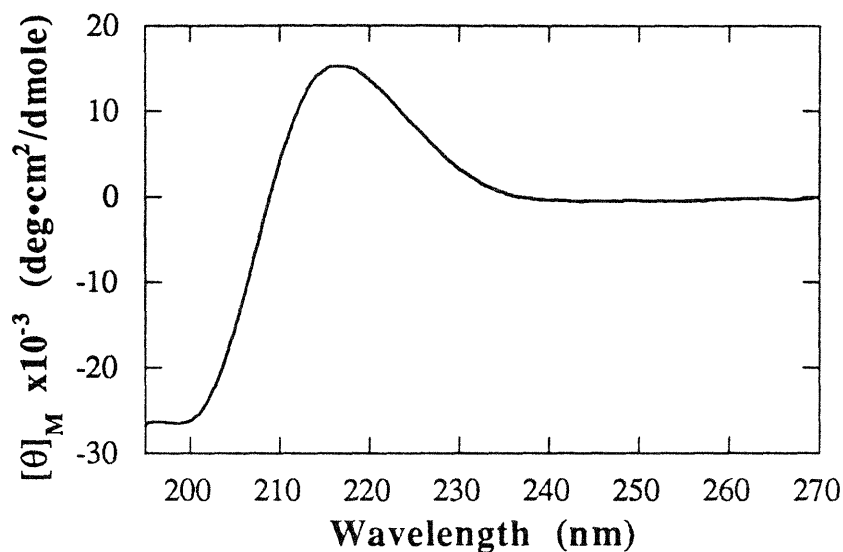


**Figure 3.15a:** CD spectrum of the peptide portion of Ac-Hel<sub>1</sub>-A<sub>1</sub>-OH attached to the nonnucleating (cs+ts) state of the template, 25 °C.

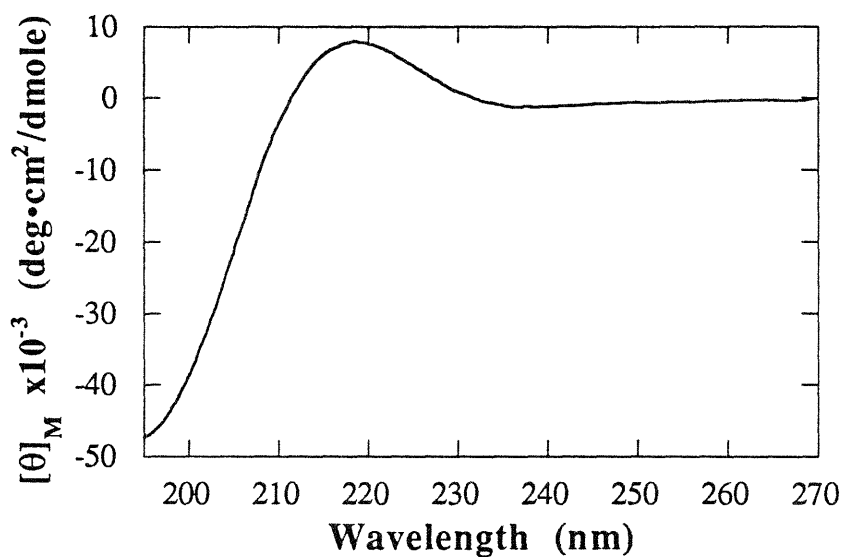


**Figure 3.15b:** CD spectrum of the peptide portion of Ac-Hel<sub>1</sub>-A<sub>2</sub>-OH attached to the nonnucleating (cs+ts) state of the template, 25 °C.

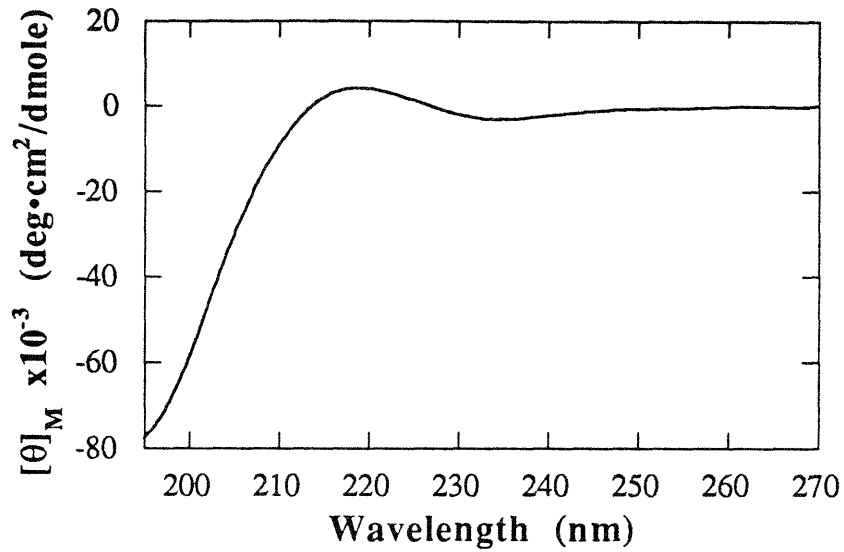


**Figure 3.15c:** CD spectrum of the peptide portion of Ac-Hel<sub>1</sub>-A<sub>3</sub>-OH attached to the nonnucleating (cs+ts) state of the template, 25 °C.

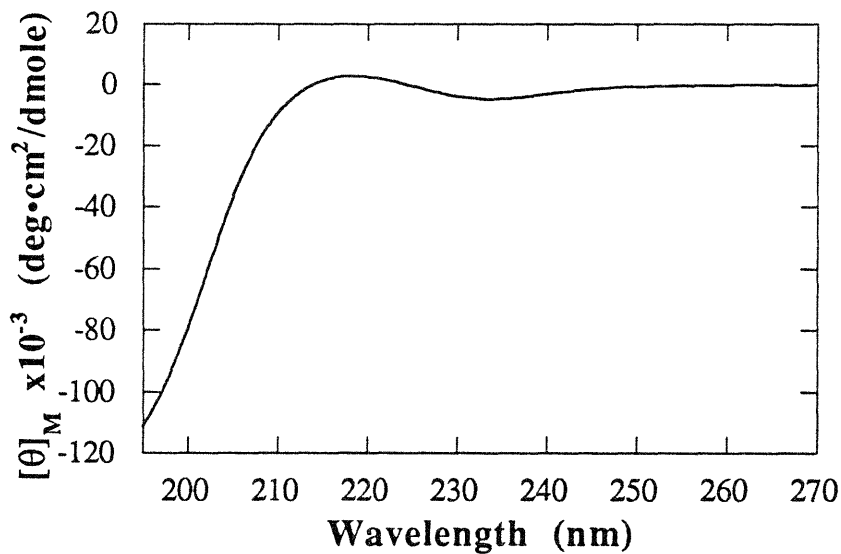


**Figure 3.15d:** CD spectrum of the peptide portion of Ac-Hel<sub>1</sub>-A<sub>4</sub>-OH attached to the nonnucleating (cs+ts) state of the template, 25 °C.

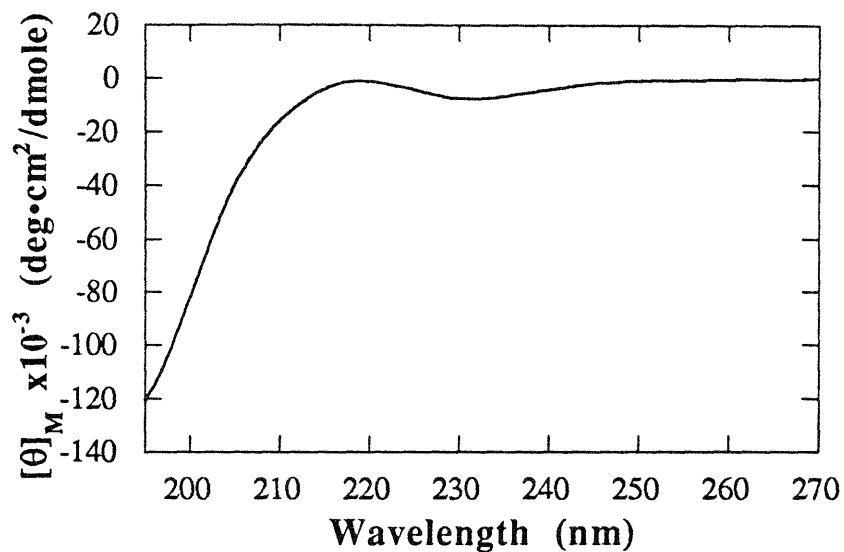


**Figure 3.15e:** CD spectrum of the peptide portion of Ac-Hel<sub>1</sub>-A<sub>5</sub>-OH attached to the nonnucleating (cs+ts) state of the template, 25 °C.

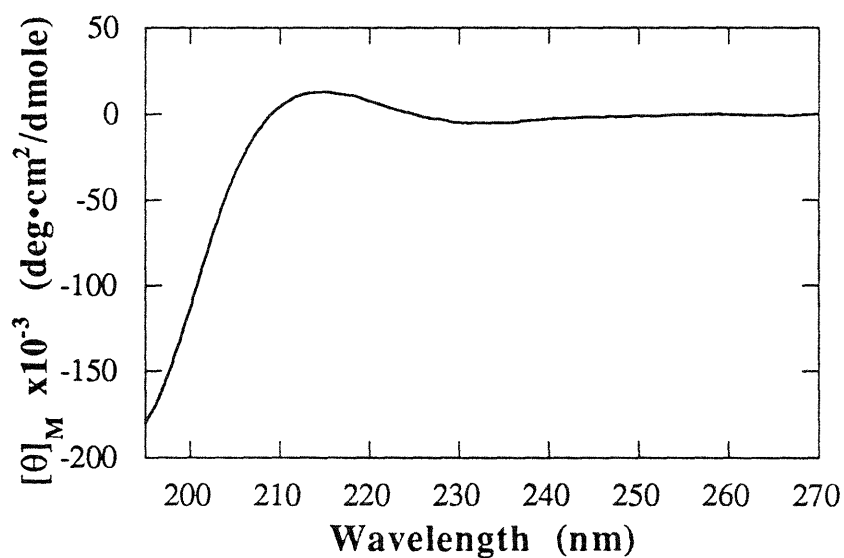


**Figure 3.15f:** CD spectrum of the peptide portion of Ac-Hel<sub>1</sub>-A<sub>6</sub>-OH attached to the nonnucleating (cs+ts) state of the template, 25 °C.

composite state of the template are in fact unstructured; NMR analyses suggested this to be the case but did not prove it so. Figure 3.16 displays the spectra of  $\theta_{P-(cs+ts)}$  of Ac-Hel<sub>1</sub>-A<sub>6</sub>-OH and unaggregated H-A<sub>6</sub>-OH. The spectra, while not identical, are qualitatively similar, in accord with the variance observed for random coil spectra (Johnson, 1988).

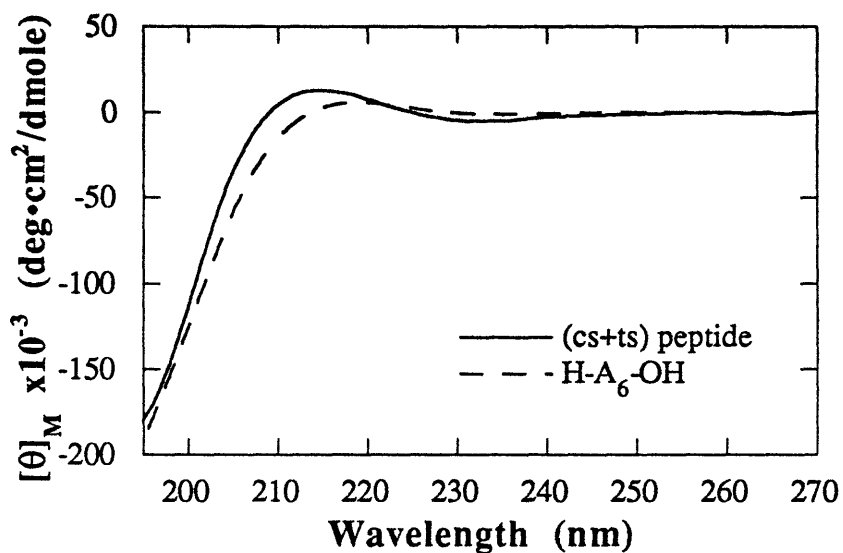


**Figure 3.16:** Comparison of the CD spectra of the (cs+ts) peptide portion of Ac-Hel<sub>1</sub>-A<sub>6</sub>-OH and unaggregated H-A<sub>6</sub>-OH, 25 °C.

### Correction of $\theta_{\text{peptide}}$ for the Contributions of Random Coil Ellipticities

Although the limiting spectra for  $\chi_{\text{te}} = 1$  can also be calculated from the above analysis, a simpler derivation with fewer assumptions can be performed by simply subtracting the random coil contributions of the (cs+ts) state (as determined in the preceding section) from the spectra of Figures 3.12 and 3.13, and normalizing by division by  $\chi_{\text{te}}$ . This alternate method is summarized in equation 3.4, where  $\theta_{\text{P-allte}}$  is the CD spectrum of the peptide if only the te state of the template were present.

$$\theta_{\text{P-allte}} = \frac{\theta_{\text{peptide}} - ((1 - \chi_{\text{te}})\theta_{\text{P-(cs+ts)}})}{\chi_{\text{te}}} \quad 3.4$$

These results are presented in Figure 3.17 for the amide series and 3.18 for the acid series. Owing to fraying effects within the te state, these peptides are not purely helical but rather a mixture of helical and coil residues. It should be noted that the shorter derivatives bear a strong resemblance to the data of Mattice (1974). Given the fraying effects and the fact that very short peptides (ca. 3-4 residues) are expected to exhibit very weak helical CD spectra (Manning *et. al.*, 1988), this was an expected result.



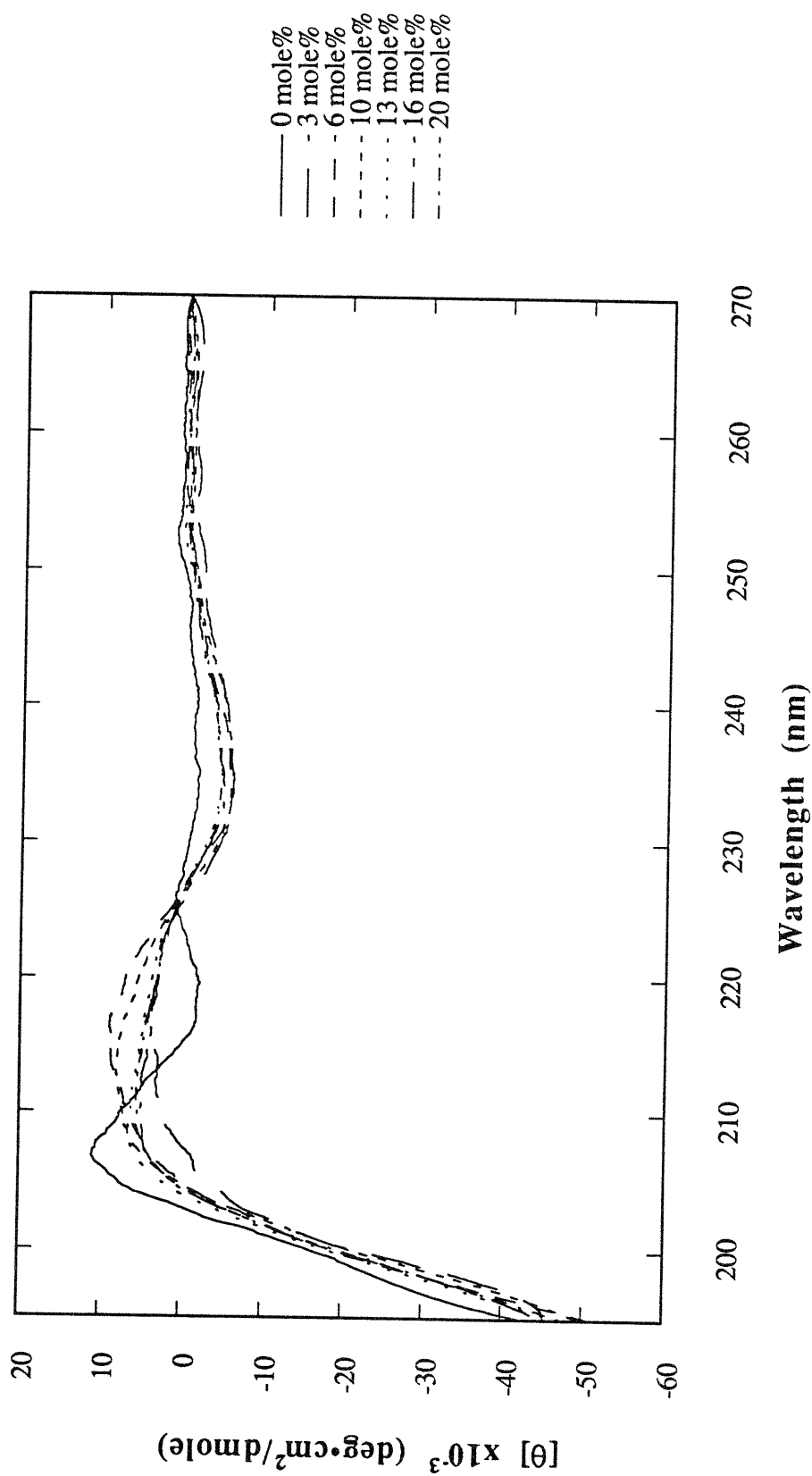


**Figure 3.17a:** CD spectrum of the peptide portion of Ac-Hel<sub>1</sub>-A<sub>1</sub>-NH<sub>2</sub> attached to the nucleating te state of the template, 25 °C.

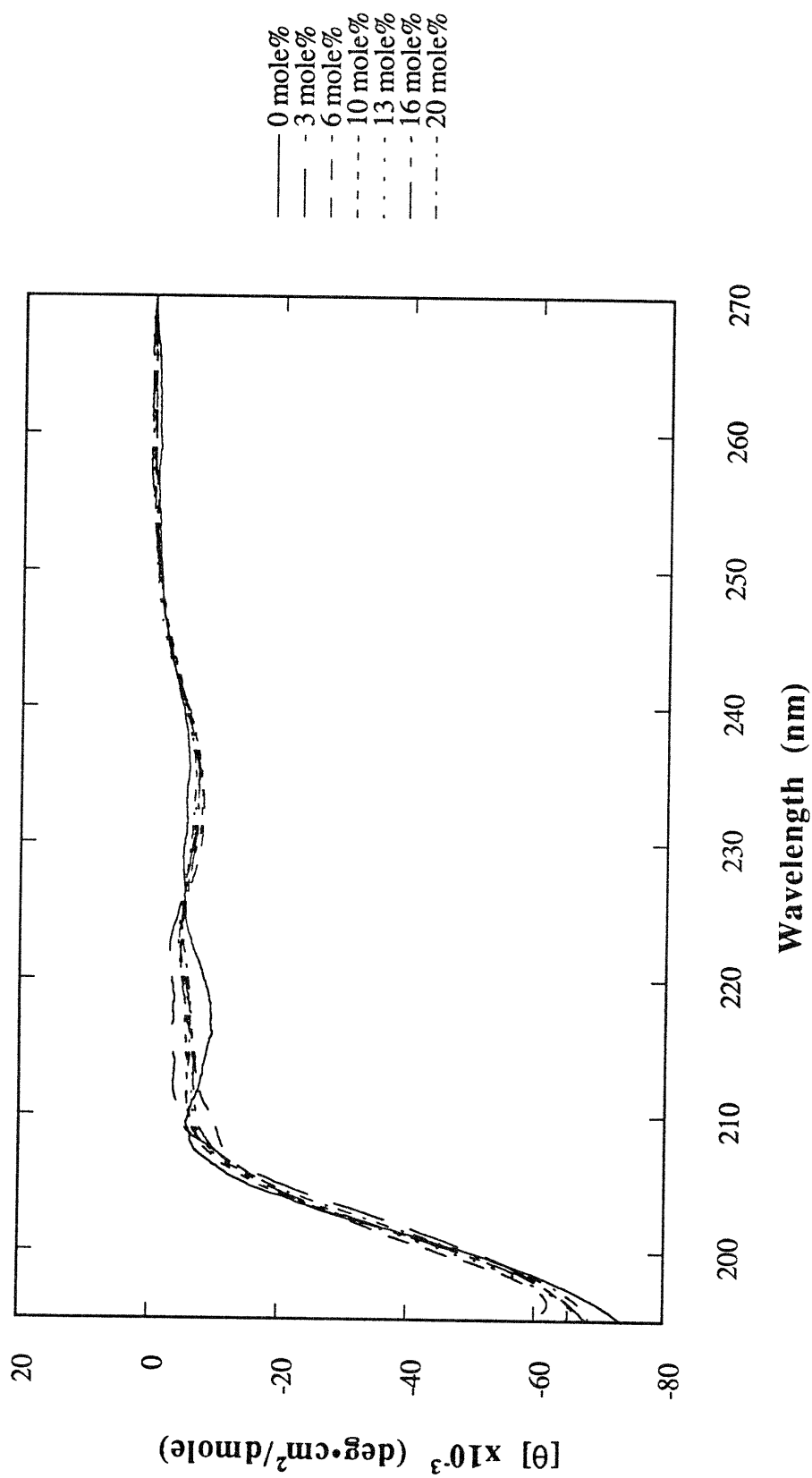


**Figure 3.17b:** CD spectrum of the peptide portion of Ac-Hel<sub>1</sub>-A<sub>2</sub>-NH<sub>2</sub> attached to the nucleating te state of the template, 25 °C.

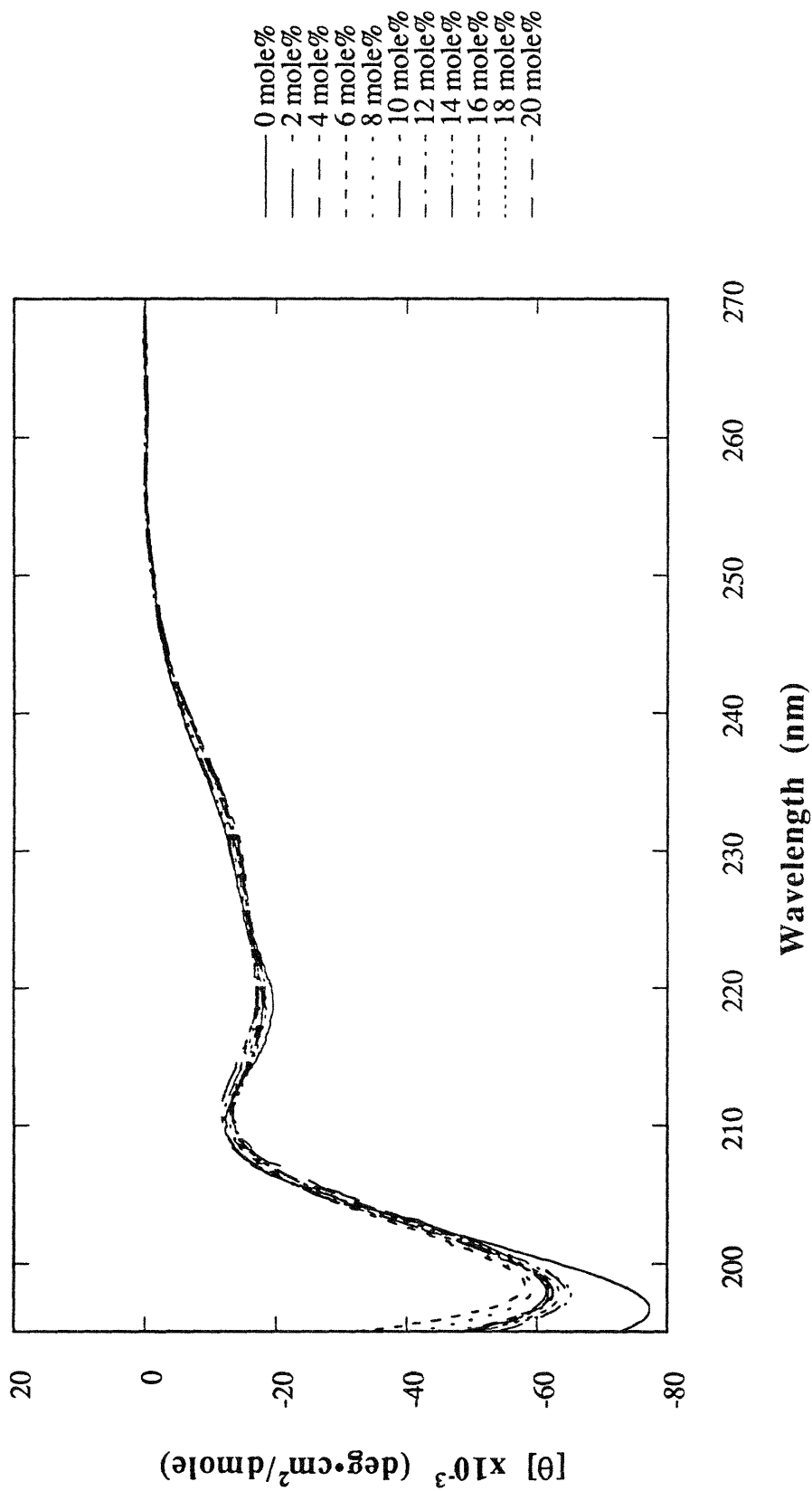


**Figure 3.17c:** CD spectrum of the peptide portion of Ac-Hel<sub>1</sub>-A<sub>3</sub>-NH<sub>2</sub> attached to the nucleating template of the template, 25 °C.

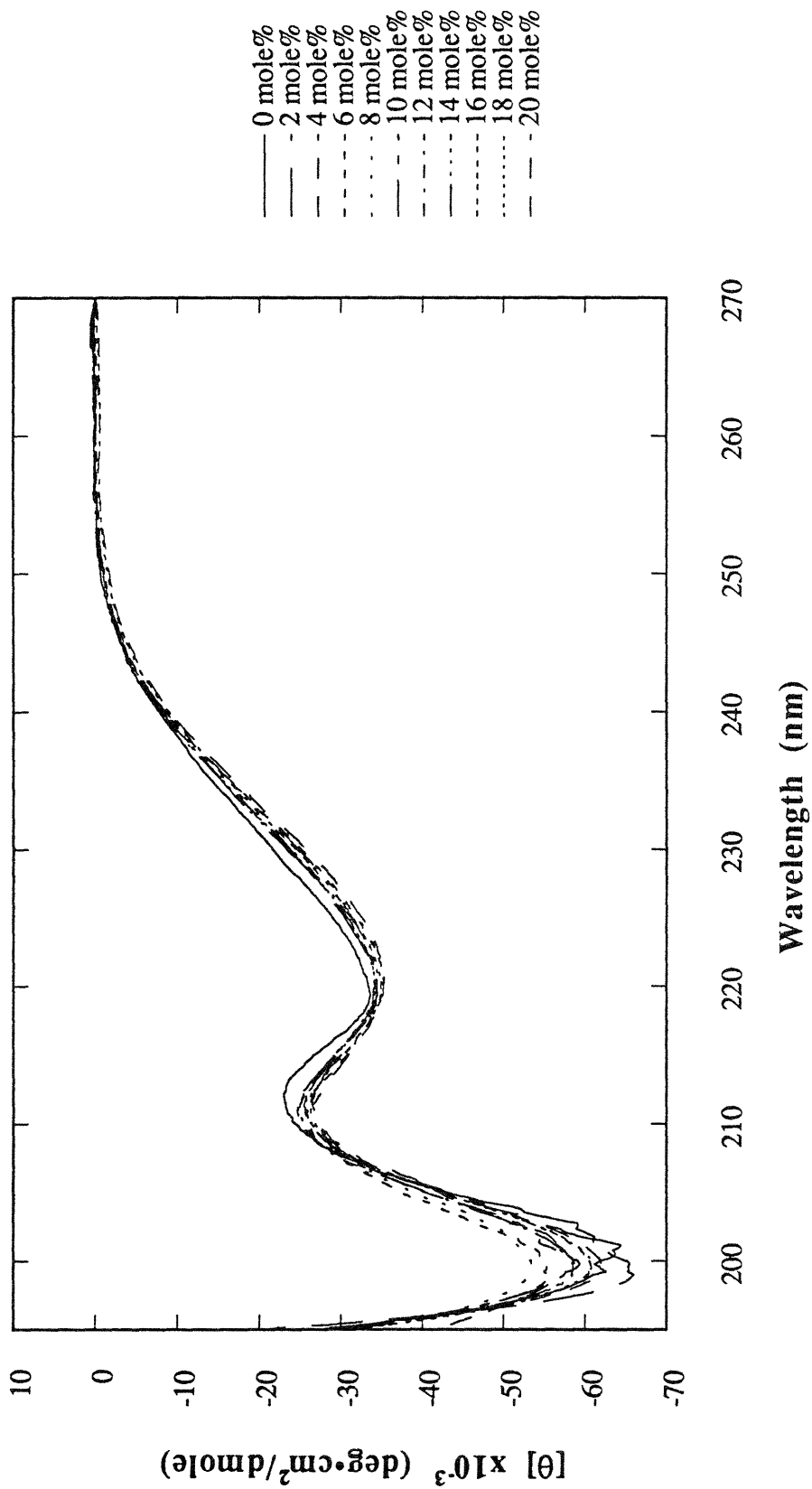


**Figure 3.17d:** CD spectrum of the peptide portion of Ac-Hel<sub>1</sub>-A<sub>4</sub>-NH<sub>2</sub> attached to the nucleating te state of the template, 25 °C.

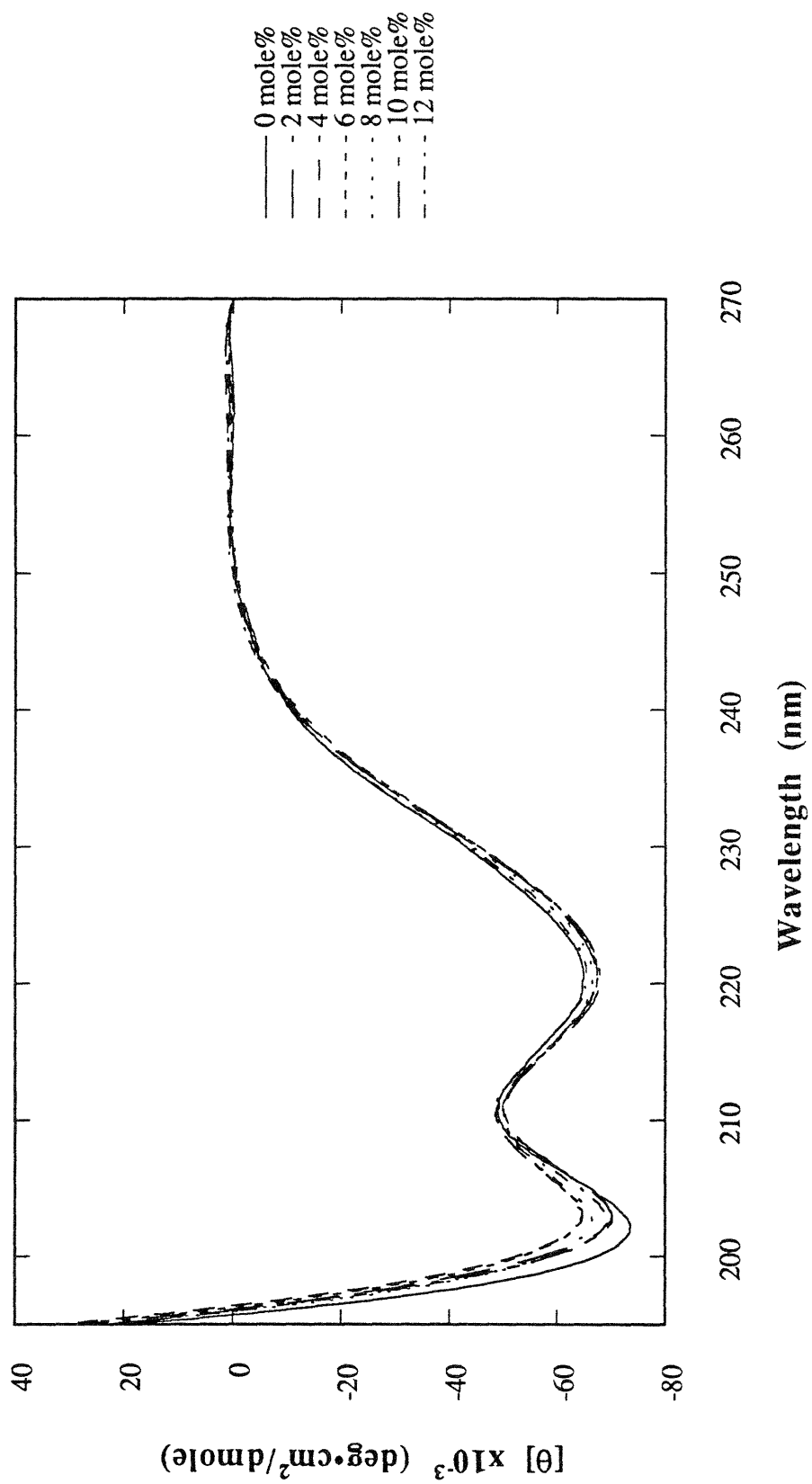


**Figure 3.17e:** CD spectrum of the peptide portion of Ac-Hel<sub>1</sub>-A<sub>5</sub>-NH<sub>2</sub> attached to the nucleating template of the template, 25 °C.

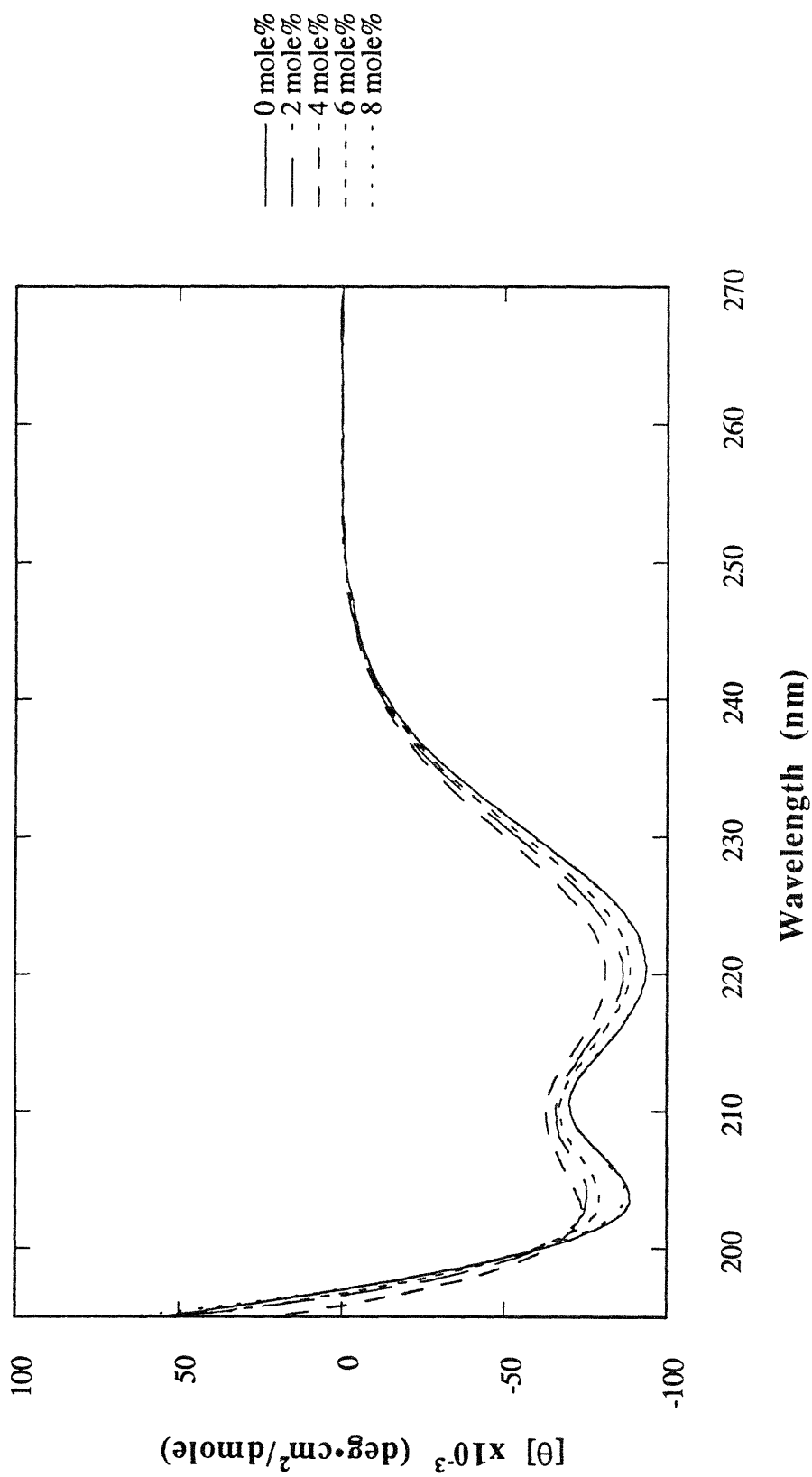


**Figure 3.17f:** CD spectrum of the peptide portion of Ac-Hel<sub>1</sub>-A<sub>6</sub>-NH<sub>2</sub> attached to the nucleating te state of the template, 25 °C.

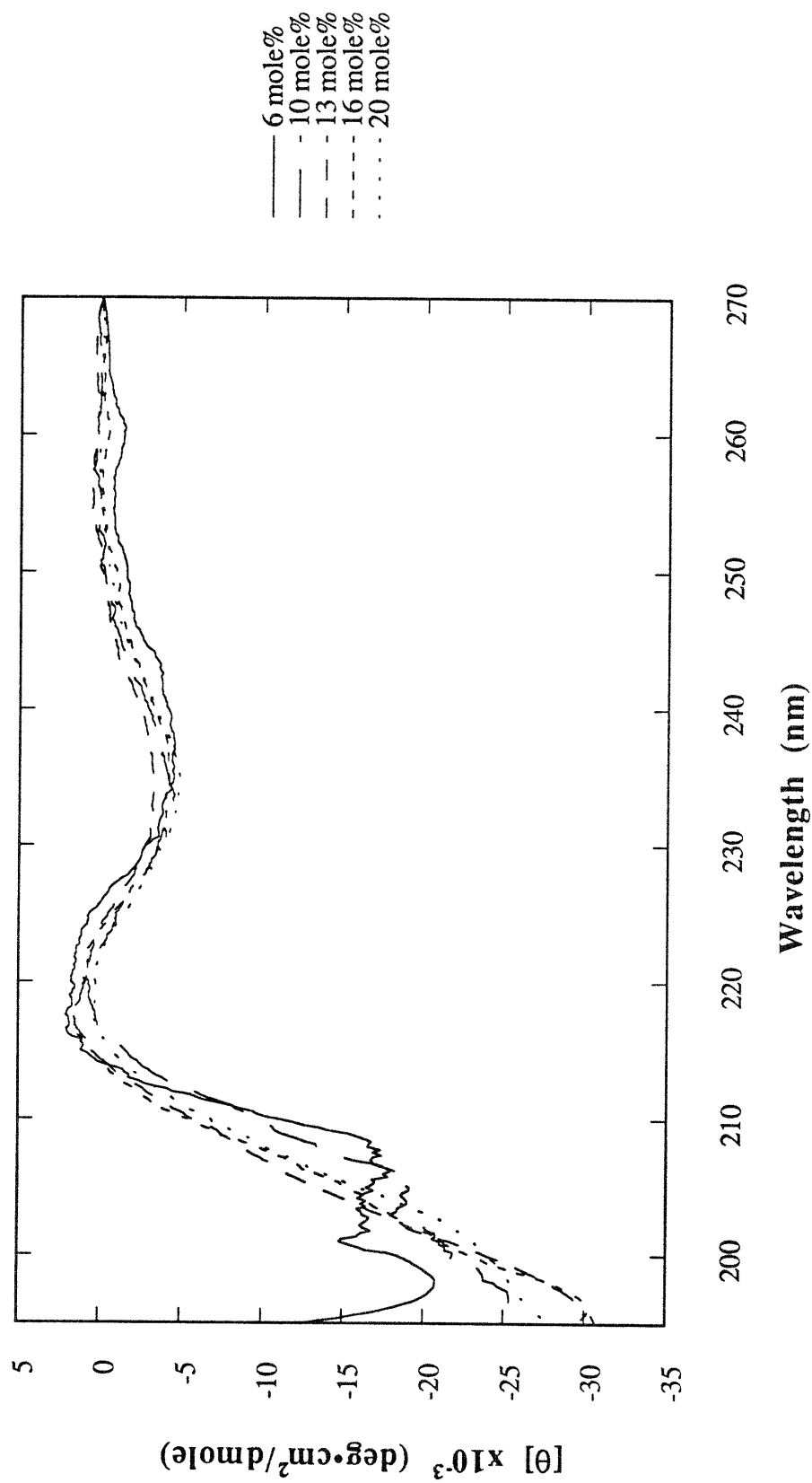


**Figure 3.18a:** CD spectrum of the peptide portion of Ac-Hel<sub>1</sub>-A<sub>1</sub>-OH attached to the nucleating template, 25 °C.

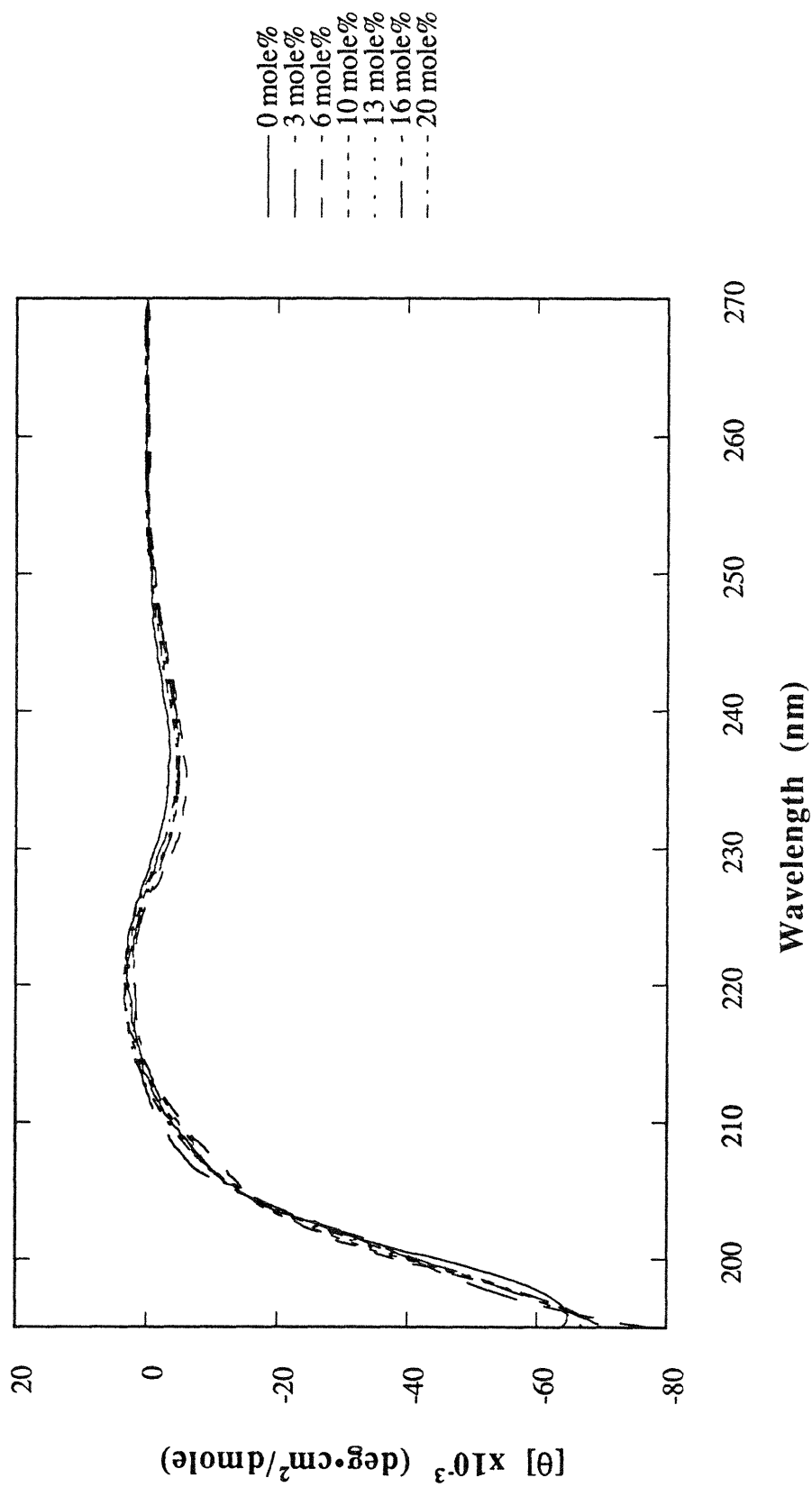


**Figure 3.18b:** CD spectrum of the peptide portion of Ac-Hel<sub>1</sub>-A<sub>2</sub>-OH attached to the nucleating te state of the template, 25 °C.



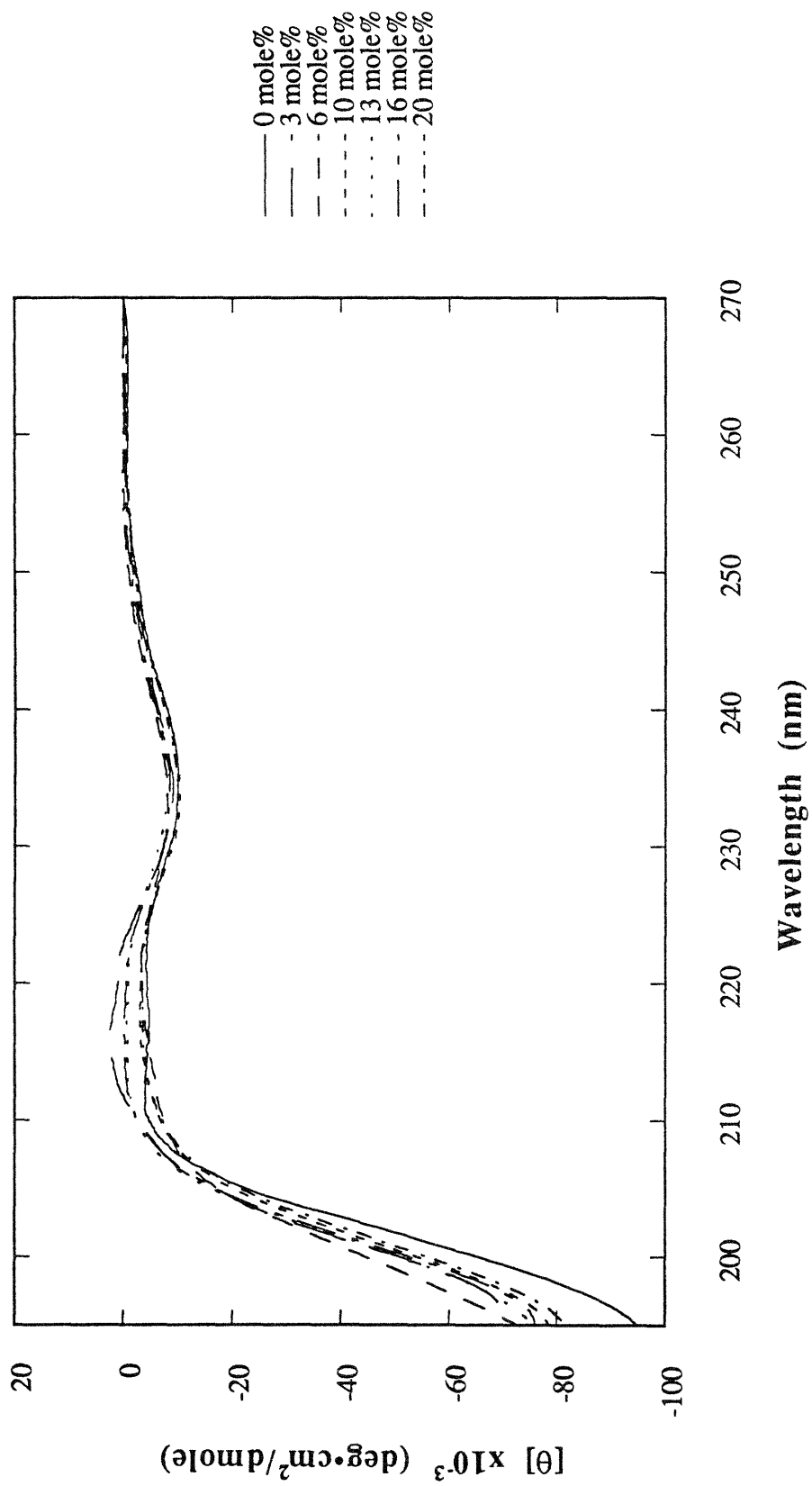


**Figure 3.18c:** CD spectrum of the peptide portion of Ac-Hel<sub>1</sub>-A<sub>3</sub>-OH attached to the nucleating template, 25 °C.

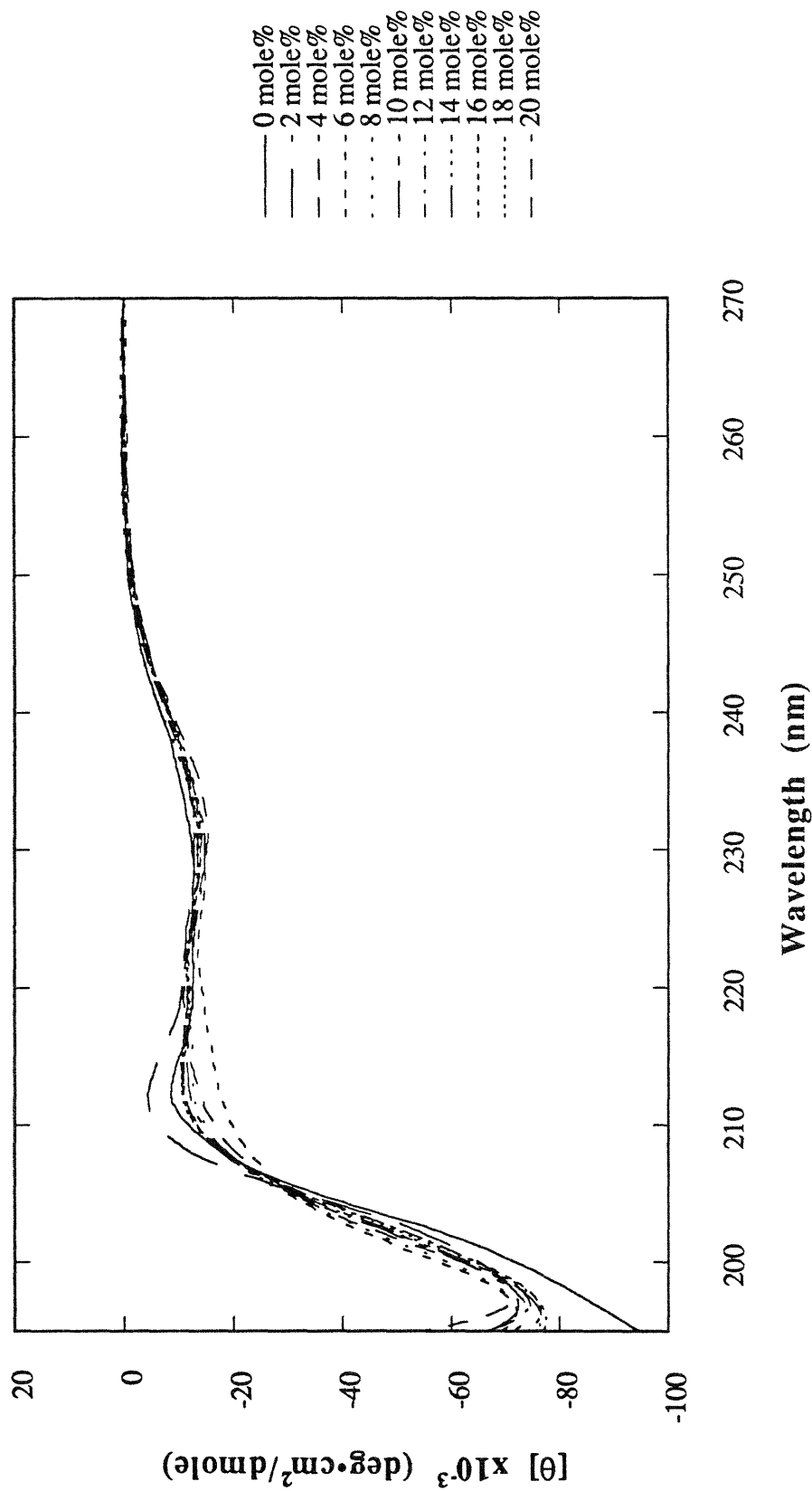


**Figure 3.18d:** CD spectrum of the peptide portion of Ac-Hel<sub>1</sub>-A<sub>4</sub>-OH attached to the nucleating template of the template, 25 °C.

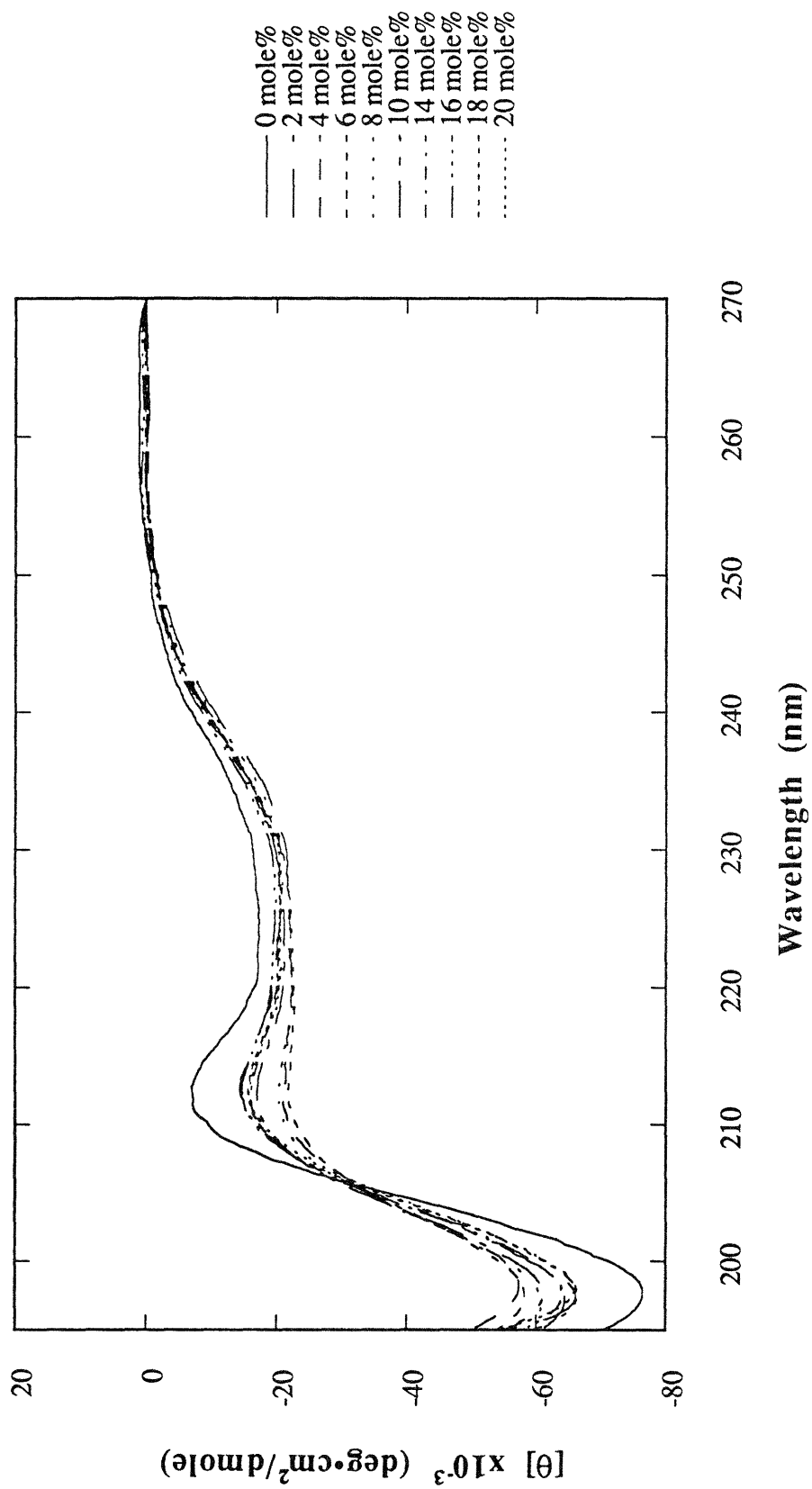


**Figure 3.18e:** CD spectrum of the peptide portion of Ac-Hel<sub>1</sub>-A<sub>5</sub>-OH attached to the nucleating te state of the template, 25 °C.

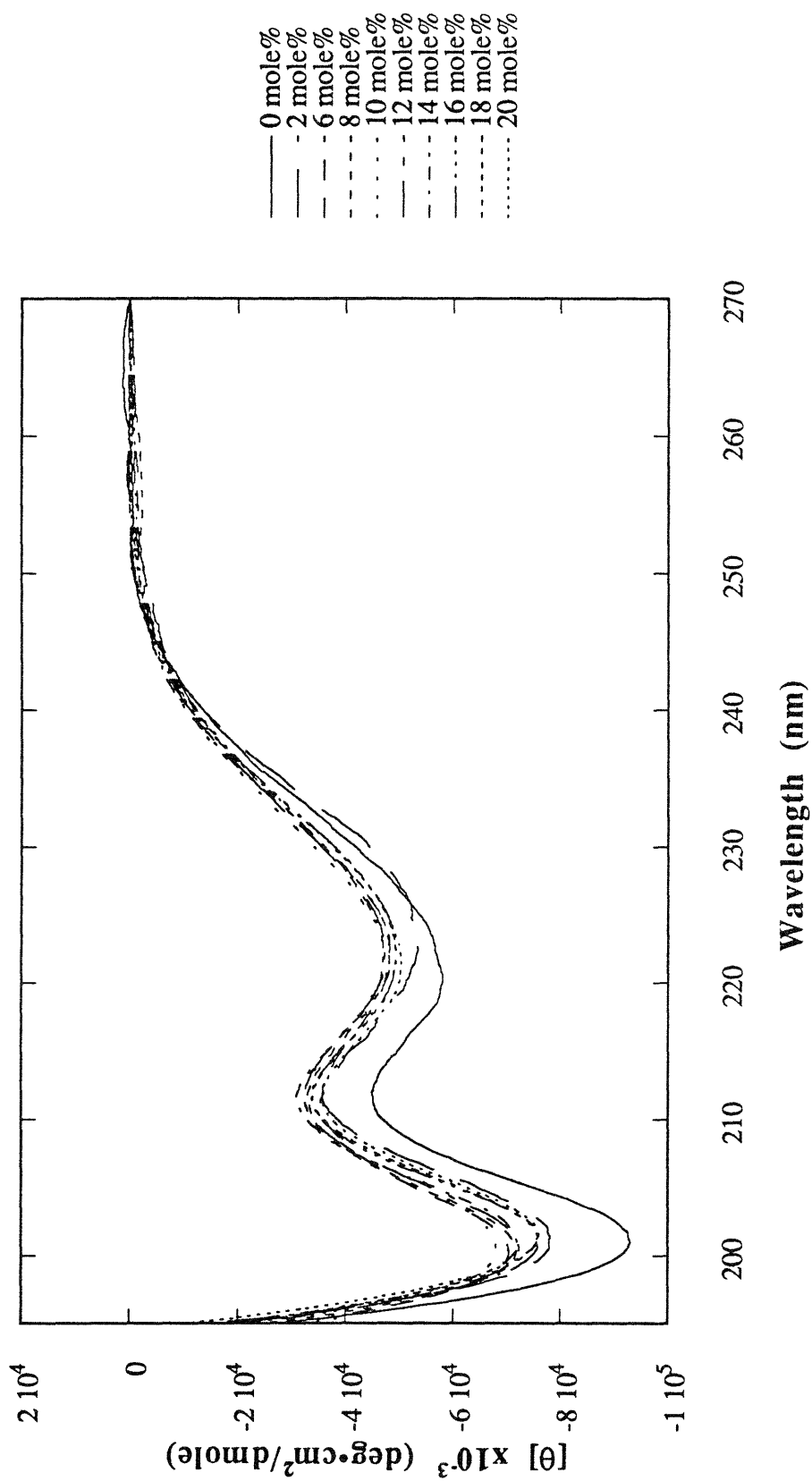


**Figure 3.18f:** CD spectrum of the peptide portion of Ac-Hel<sub>1</sub>-A<sub>6</sub>-OH attached to the nucleating te state of the template, 25 °C.

## Preliminary Calculations of the Ellipticity of a Completely Helical Peptide of Length $n$ ; $s=1$ Analysis

The fraying effects prevent an evaluation of the helical CD for 100% helix, but they can be eliminated based on  $s$  values. As specified in expression 2.5, the equilibrium values of the various frayed states of template peptides are related by their  $s$  values.

Dr. D. S. Kemp has analyzed the  $t/c$  ratios of the series Ac-Hel<sub>1</sub>-Ala <sub>$n$</sub> -OH,  $n=1-6$ ; with a careful iterative linear regression analysis, the values of  $s_{Ala}$  have been determined for various TFE concentrations (Kemp *et al.*, 1996b; Cammers-Goodwin *et al.*, 1996). For spectra recorded in the absence of TFE, the value of  $s_{Ala}$  was found to be very nearly 1.

A preliminary analysis of the per residue helicity of a completely helical residue was completed using the value of  $s_{Ala}=1$ , relying only on spectra acquired in pure water. The complicated analysis is detailed explicitly in Appendix B, section B.7; it centers on a summation of helical and coil residues and a subtraction of the contribution of the coil residues (based on the value of  $\theta_{P-(cs+ts)}$ ). Equations are derived that permit, for the amide series, the calculation of  $[\theta]_{H4}$ ,  $[\theta]_{H5}$ , and  $[\theta]_{H6}$ , where  $[\theta]_n$  corresponds to the per residue ellipticity of a 100% helical peptide of  $n$  residues. For the acid series,  $[\theta]_{H3}$ ,  $[\theta]_{H4}$ , and  $[\theta]_{H5}$  were computed. Figure 3.19 presents the results of this preliminary analysis for the amide series and Figure 3.20 corresponds to the acid series; these spectra are on a per residue basis.

## Calculations of the Ellipticity of a Completely Helical Peptide of Length $n$ ; Variable $s$ Analysis

Both sets of data show not only spectra typical of the 208, 222 double minima  $\alpha$ -helix, but also reveal a significant length dependence. The specific numbers, however, cannot be regarded as accurate. The data for each series is developed from only four different spectra; errors in even one spectrum will significantly impact the analysis. A more thorough analysis provides for the inclusion of spectra recorded in various concentrations of TFE, but is also more complicated as varying  $s$  values must be considered. Table 3.3 gives the  $s$  value of alanine for varying TFE concentrations.

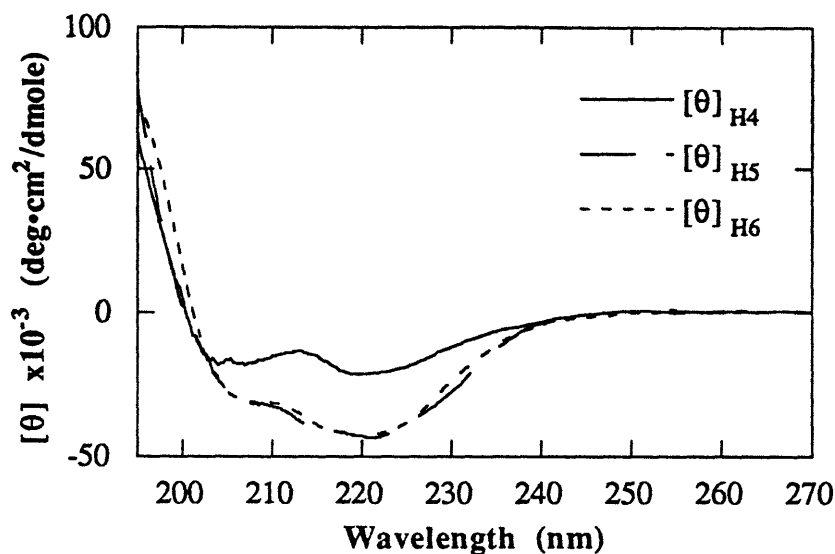


**Figure 3.19:** Per residue CD spectra for 100% helical peptides of 4, 5, and 6 residues using a preliminary  $s=1$  analysis for the series  $\text{Ac-Hel}_1\text{-A}_n\text{-NH}_2$ ,  $n=1-6$ .

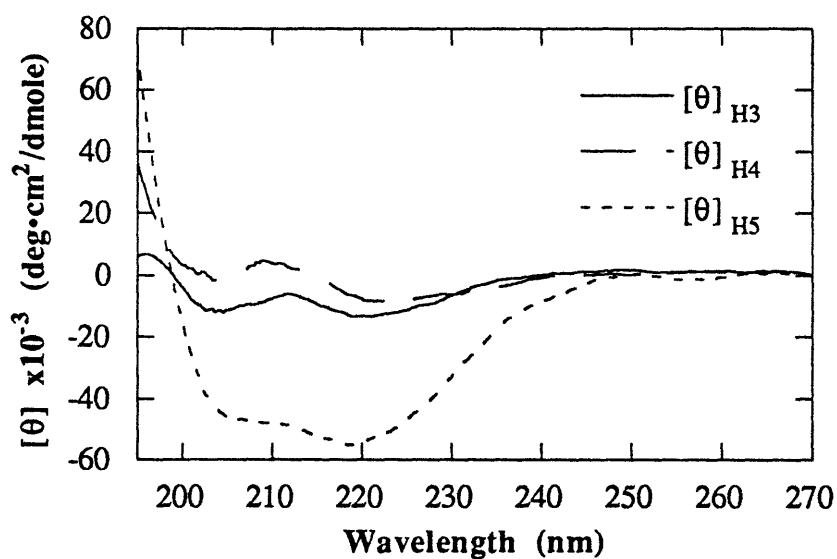


**Figure 3.20:** Per Residue CD spectra for 100% helical peptides of 3, 4, and 5 residues using a preliminary  $s=1$  analysis for the series  $\text{Ac-Hel}_1\text{-A}_n\text{-OH}$ ,  $n=1-6$ .

Mole% TFE	0	2	4	6	8	10
s Value	1	1.03	1.06	1.15	1.29	1.45

**Table 3.3: Values of  $s_{Ala}$  for varying concentrations of TFE, from Cammers-Goodwin *et. al.*, 1996.**

As is evident from Figures 3.8 - 3.11, the effect of TFE levels off at approximately 10 mole% TFE. Beyond this value, TFE no longer induces a significant structural change, and for this reason, the spectra included for the analysis of CD data will not be extended beyond this value.

The analysis involves a multivariable linear regression analysis, which is beyond the scope of the spreadsheet program used for all prior computations. The evaluation was limited to a single wavelength, 222 nm. Section B.8 of Appendix B describes the analysis and the software used to compute the results. For this extended analysis, equations are derived that permit, in theory, the calculation of  $[\theta]_{H4}$ ,  $[\theta]_{H5}$ , and  $[\theta]_{H6}$  for the amide series and  $[\theta]_{H4}$  and  $[\theta]_{H5}$  for the acid series.

Unfortunately, owing to the nature of the analysis, the numbers computed for the shorter helices have associated errors large enough to negate their validity. Nevertheless, the analysis yields values for  $[\theta]_{H5}$  and  $[\theta]_{H6}$  that are summarized in Table 3.4.

Helix Length	Value of $[\theta]_{222}$ for 100% Helix ( $\text{deg}\cdot\text{cm}^2/\text{dmole}$ )	
	Derived from Amide Series	Derived from Acid Series
5 residues	-30,820	-26,955
6 residues	-28,517	

**Table 3.4: Values of  $[\theta]_{222}$  for 100% Helix for a Pentamer and a Hexamer.**

The observed variance is to be expected for an analysis such as this wherein different values are computed from small data bases. Nevertheless, the data provide a first approximation to the value of  $[\theta]_{222}$  for 100% helix determined in a short peptide framework. The values are within the range cited in the literature for short peptides, polypeptides, and proteins, as seen in Table 3.1. They are, however, better suited for assignments of helicity to short peptides than those derived from larger systems.

## SUMMARY AND CONCLUSIONS

Helical CD spectra are quite distinct and have been well characterized both experimentally and theoretically. A dependence of the spectra on backbone angles and on peptide chain length is expected. A variety of values of  $[\theta]_{222}$  corresponding to 100% helix have been used in the quantitation of short helical peptides; these values are derived from a variety of sources.

The ability to directly compare helical measurements for peptide derivatives of Ac-Hel<sub>1</sub> by NMR and by CD has been established through an analysis of the effects of concentration, temperature, solvent isotopic composition, and perchlorate concentration. It has been demonstrated that these issues are unimportant under the conditions employed in the analyses herein and that NMR and CD data may be compared without concern.

Careful NMR determination of the t/c ratios of Ac-Hel<sub>1</sub>-A<sub>n</sub>-OH and Ac-Hel<sub>1</sub>-A<sub>n</sub>-NH<sub>2</sub>, n = 1-6, in various TFE concentrations permits the determination of the values of  $\chi_{te}$  for each of the spectra as well as  $s_{Ala}$  at different TFE concentrations. This data has been used in conjunction with the CD spectra of the alanine series to evaluate the per residue ellipticity at 222 nm in a short peptide framework. For the first time, the value of  $[\theta]_{222}$  for 100% helix has been determined for a pentapeptide and a hexapeptide.



## Experimental

## GENERAL

Elemental analyses were performed by Robertson Microlit Laboratories in Madison, NJ. Amino acid analyses were performed by the MIT Biopolymers Laboratory.

Melting points were measured on a Thomas Hoover Uni-Melt melting point apparatus and are uncorrected.

All pH measurements were conducted on a Cole-Parmer model 5982-00 pH meter equipped with a Hg/Hg<sub>2</sub>Cl<sub>2</sub> calomel electrode. Calibration prior to use was performed using Mallinckrodt "Buffar" solutions, a pH 7.00 phosphate buffer, a pH 4.01 phthalate buffer, and a pH 10.00 carbonate buffer. The pH was adjusted to the pH 7.00 buffer and the slope to either the acidic buffer for acidic samples or to the basic buffer for alkaline samples. No corrections were made for deuterium isotope effects in pH measurements of D<sub>2</sub>O NMR samples.

## SYNTHESIS

### Ac-Hel<sub>1</sub>-OH

The template Ac-Hel<sub>1</sub>-OH was synthesized by the procedure developed by Dr. T. Curran (1988) and improved upon by Dr. J. Boyd (1989). Yields for the template methyl ester with respect to the cyclization reaction were in the range of 6-16%. Crystalline template acid was made by dissolving the template in a minimal amount of acetonitrile in a Wheaton vial (at an approximate ratio of 15 mg template to 1 mL acetonitrile), evenly heating the solution, and scratching the inside of the vial. Upon cooling, needle-like crystals were formed, which were subsequently filtered and dried under high vacuum (m.p. 229-232 °C, dec.).

### Template derivatives

Peptide derivatives of the template were synthesized by solution phase fragment condensation of monomers, dimers or trimers with the template or with templated peptides following the procedures described by Drs. T. Allen (1993) and T. Curran (1988); couplings were carried out in DMF using HOBt and 1-(3-dimethylaminopropyl)-3-ethylcarbodiimide hydrochloride, and DIEA was added as well for cases in which the peptides existed as the HCl salt. Most peptides were purchased from Bachem Bioscience

as the *t*-butyl ester, with Z-group *N*-terminal protection. Z-groups were removed by hydrogenation in ethanol over Pd-black. C-terminal deprotection was performed in dichloromethane/TFA with anisole or thioanisole as a scavenger. In general, couplings were performed using 5-10 mg of template with yields of 65-75%.

Ac-Hel<sub>1</sub>-NH<sub>2</sub> and the series A-Hel<sub>1</sub>-A<sub>n</sub>-NH<sub>2</sub>, n=1-6, synthesized by solid phase peptide synthesis, were kindly supplied by Dr. K. McClure.

H-Ala<sub>6</sub>-OH was purchased from Sigma.

### Preparation of Ac-Hel<sub>1</sub>-NHMe

Synthesis of this derivative was carried out on a milligram scale in a similar fashion to that outlined by Dr. T. Allen (1993) wherein the template and methylamine hydrochloride were dissolved in DMF and treated with 1-(3-dimethylaminopropyl)-3-ethylcarbodiimide hydrochloride and DIEA. It was found that PyBop coupling worked as well as the carbodiimide coupling employed by Dr. T. Allen. It was also found that an alternate purification procedure was necessary. By preparative HPLC alone, it is very difficult to completely separate both residual HOBt and unreacted template from the desired product. Therefore, the crude reaction product was subjected to flash chromatography (8:2 EtOAc:MeOH) to give a clear oil that was further purified by preparative HPLC (isocratic, 8% CH<sub>3</sub>CN). Yields were close to 100%. Properties were identical to those reported by Dr. T. Allen (1993).

### Purification of Ac-Hel<sub>1</sub> Derivatives

All derivatives were purified to homogeneity by preparative HPLC in acetonitrile/water (containing 0.1% TFA). For *t*-butyl ester derivatives, the TFA was omitted. Acetonitrile was JT Baker HPLC grade, water was distilled, deionized supplied from a Millipore MilliQ Plus water filtration system, and TFA was supplied by Aldrich. Water based solvent mixtures were degassed prior to use. Purification was carried out on a Waters system containing a model 590 pump adapted for preparative work, a Rheodyne injector, an Autochrome OPG/S solvent mixer, a model 484 variable wavelength detector, a Houston Instrument Omniscrite strip chart recorder, and a Vydec 2.2 x 25 cm (218TP1022) C<sub>18</sub> reverse-phase column with a Vydec (GCH-10/218GCC1210) guard column. Separation was carried out at a rate of 18 mL/min and monitored at 214 nm. Purification conditions were as follows:

Derivative	Isocratic Conditions (% CH <sub>3</sub> CN)	Gradient Conditions (Initial % CH <sub>3</sub> CN→ Final % CH <sub>3</sub> CN/ Time/Curve)	Retention Time (minutes)
Ac-Hel <sub>1</sub> -OH	11		8.4
Ac-Hel <sub>1</sub> -A <sub>1</sub> -OH		5→100%/25min/2	8.2
Ac-Hel <sub>1</sub> -A <sub>1</sub> -OrBu		5→40%/25min/2	21
Ac-Hel <sub>1</sub> -A <sub>2</sub> -OH		5→100%/25min/2	7.2
Ac-Hel <sub>1</sub> -A <sub>2</sub> -OrBu		5→100%/30min/2	14.2
Ac-Hel <sub>1</sub> -A <sub>3</sub> -OH		5→100%/25min/2	8.4
Ac-Hel <sub>1</sub> -A <sub>3</sub> -OrBu		5→100%/25min/2	12.0
Ac-Hel <sub>1</sub> -A <sub>4</sub> -OH		5→100%/40min/2	10.6
Ac-Hel <sub>1</sub> -A <sub>4</sub> -OrBu		10→50%/25min/2	14.6
Ac-Hel <sub>1</sub> -A <sub>5</sub> -OH		5→100%/40min/2	10.6
Ac-Hel <sub>1</sub> -A <sub>5</sub> -OrBu		5→100%/25min/2	12.2
Ac-Hel <sub>1</sub> -A <sub>6</sub> -OH		5→100%/40min/2	11.4
Ac-Hel <sub>1</sub> -A <sub>6</sub> -OrBu		5→100%/25min/2	12.4
Ac-Hel <sub>1</sub> -NHMe	8		10.8

## NMR SPECTROSCOPY

### General

All <sup>1</sup>H NMR spectra were acquired on a VXR-500S or a VXR-501S Varian spectrometer. FIDs were routed to either a Sun Microsystems Sparc 2 workstation or a Silicon Graphics Iris Indigo workstation and processed using Varian Instruments VNMR 4.3 software. Temperature was maintained with a Varian VTC4 temperature control apparatus and was calibrated for the VXR-501S by Dr. T. Allen (1993) using a methanol standard.

Deuterated solvents were supplied by Cambridge Isotope Laboratories, with the exception of d<sub>1</sub>-TFA 99.5%, which was obtained from Aldrich. Spectra of aqueous samples were acquired in 99.96% grade D<sub>2</sub>O and referenced to 3-(trimethylsilyl) propionic acid - 2,2,3,3,-d<sub>4</sub>, Na salt. Spectra of acetonitrile samples were acquired in 99.96% grade

CD<sub>3</sub>CN and referenced to tetramethylsilane. d<sub>3</sub>-TFE was 99% grade. 535 NMR tubes were supplied by Wilmad Glass.

Aqueous samples were prepared by complete dissolution in and evaporation from 99.9% D<sub>2</sub>O two to three times followed by drying overnight at room temperature under high vacuum. NMR tubes were left under high vacuum overnight as well. Sample quantities were in the range of 2-10 mg. Most samples were prepared by dissolution into approximately 700-800 μL solvent followed by addition of the reference reagent. For template derivatives with a free acid at the C-terminus it was necessary to adjust the pD of the sample to approximately 1 with d<sub>1</sub>-TFA to ensure a fully protonated species; in general, 5 μL of d<sub>1</sub>-TFA in 700 μL D<sub>2</sub>O yields a sample solution in the appropriate pD range. pD values reported are direct pH measurements as their differences are negligible (Bundi & Wüthrich, 1979). For a few derivatives for which there was very little material available it was necessary to prepare the sample in a glove bag under N<sub>2</sub> atmosphere to minimize the residual water peak.

Routine spectra were carried out with temperature regulation just above ambient temperature (i.e. at 25-27 °C) to minimize temperature fluctuations. In general, acquisitions consisted of 256 transients. As integration values are of extreme importance, acquisition parameters were set to enhance resolution and to ensure full relaxation of all nuclei. For every experiment both the pw90° and T<sub>1</sub> were determined and parameters were adjusted accordingly. For most of the derivatives studied, the maximal T<sub>1</sub> found was approximately 3 seconds. Delays set to 5 times that of the longest T<sub>1</sub> ensure full relaxation, thus most spectra were run with an acquisition time of 4 seconds and a d1 of 11 seconds. Spectra of compounds previously studied by Dr. T. Allen (1993) in aqueous medium were repeated under these conditions as it was found that the relaxation times and water suppression utilized by Dr. T. Allen strongly influenced integration values.

## Template Kinetics

Kinetics of the c↔t transition were monitored by NMR in a series of experiments. In the first experiment, crystalline template, D<sub>2</sub>O containing TSP and d<sub>1</sub>-TFA to a pD≈0.9, and all related supplies were equilibrated to 4 °C in a cold room. The instrument was equilibrated to 5 °C and shimmed to a sample of TSP in D<sub>2</sub>O, pD≈0.9. The cold D<sub>2</sub>O solution was added to the crystalline template and timing initiated. The sample was vigorously shaken until fully dissolved, transferred to an NMR tube, and rushed to the instrument where it was placed in the probe. Following an extremely brief period of reshimming, the first time measurement was taken approximately 4 minutes after the start

of timing. Measurements were taken thereafter at approximately 3 minute intervals for 45 minutes, followed by 7 additional readings for a total of a 2 hour experiment. Acquisition time was set at 4 seconds with a d1 of 11 seconds; each measurement consisted of 2 transients. Additional shimming was performed between measurements to optimize the spectra.

The second experiment was conducted in a similar fashion but at  $-15\text{ }^{\circ}\text{C}$ . Crystalline template and  $\text{CD}_3\text{CN}$  containing TMS were equilibrated to  $-15\text{ }^{\circ}\text{C}$  in an ethylene glycol/dry ice bath. The instrument was equilibrated to  $-15\text{ }^{\circ}\text{C}$  and shimmed to an NMR tube containing a sample of TMS in  $\text{CD}_3\text{CN}$ . With the assistance of a second person, the NMR tube was ejected and emptied while the template was dissolved in the  $\text{CD}_3\text{CN}$  solution and timing initiated in order to minimize the amount of time the NMR tube spent outside the probe (*ca.* 30 seconds). The sample was transferred to the NMR tube and inserted into the probe; the first measurement was taken after a very brief period of shimming at a time of approximately 4 minutes. Measurements were taken approximately every 3 minutes for 45 minutes, followed by additional, less frequent readings for a total of a 3 hour experiment. Additional shimming was performed between measurements. Acquisition parameters were identical to those employed in the first experiment.

In the third experiment, a concentrated solution of the template methyl ester in  $\text{CDCl}_3$  was allowed to equilibrate to  $4\text{ }^{\circ}\text{C}$  in a cold room. The instrument was equilibrated to  $5\text{ }^{\circ}\text{C}$  and shimmed to a sample of TMS in  $\text{CD}_3\text{CN}$ . A small aliquot of the template solution was injected into the NMR tube, timing was initiated, and the tube was shaken vigorously. The sample was returned to the probe followed by a brief period of shimming, and the first measurement was taken after approximately 3 minutes. Measurements were taken approximately every 3 minutes for 30 minutes, with five additional readings for a total of a 2 hour experiment. Additional shimming was performed between measurements. Acquisition parameters were identical to those employed in the first experiment.

The fourth experiment was analogous to the second. A concentrated solution of template methyl ester in  $\text{CDCl}_3$  was allowed to equilibrate to  $-15\text{ }^{\circ}\text{C}$  in an ethylene glycol/dry ice bath. The instrument was equilibrated to  $-15\text{ }^{\circ}\text{C}$  and shimmed to a sample of TMS in  $\text{CD}_3\text{CN}$ . The NMR tube was ejected, a small aliquot of the template solution was injected into the solution in the tube, the tube was vigorously shaken, timing was initiated, and the tube was returned to the probe. After a brief period of shimming, the first measurement was taken after approximately 5 minutes. Measurements were taken approximately every 3 minutes for 45 minutes. Additional shimming was performed between measurements. Acquisition parameters were identical to those employed in the first experiment.

In the fifth experiment, an empty syringe and a concentrated solution of template methyl ester in  $\text{CDCl}_3$  were allowed to equilibrate to  $4\text{ }^\circ\text{C}$  in a cold room. The instrument was equilibrated to  $5\text{ }^\circ\text{C}$  and shimmed to a sample of TSP in  $\text{D}_2\text{O}$ . The NMR tube was removed from the probe, an aliquot of the  $\text{CDCl}_3$  solution was injected using the chilled syringe, timing was initiated, and the tube was vigorously shaken and quickly returned to the probe. Attempts were made to shim to adequate resolution but were unsuccessful due to solution inhomogeneity and the presence of droplets of  $\text{CDCl}_3$  along the inner surface of the NMR tube.

In the final experiment, a concentrated solution of template methyl ester in  $\text{CD}_3\text{CN}$  was allowed to equilibrate to  $-15\text{ }^\circ\text{C}$  in an ethylene glycol/dry ice bath. The instrument was equilibrated to  $-15\text{ }^\circ\text{C}$  and shimmed to a sample of TMS in  $\text{CDCl}_3$ . The NMR tube was ejected, an aliquot of the  $\text{CD}_3\text{CN}$  solution was injected into the tube, timing was initiated, and the tube was vigorously shaken and quickly returned to the probe. After a brief period of reshimming, the first measurement was made after approximately 3 minutes. Two additional measurements were made at 6 minutes and 9 minutes, after which experimentation was ceased as final conditions had been reached. Additional shimming was performed between measurements. Acquisition parameters were identical to those employed in the first experiment.

## Temperature

Temperature studies in aqueous solution were carried out in the range of  $5\text{-}65\text{ }^\circ\text{C}$ . Probe temperature was maintained as described above. For each temperature, both probe and sample were allowed to equilibrate to the set temperature for at least 10 minutes prior to shimming and acquisition.

## NaCl

The study of the dependence of the  $t/c$  ratio of Ac-Hel<sub>1</sub>-OH on NaCl concentration was designed to mimic the study of NaCl dependence of the  $t/c$  ratio of Ac-Hel<sub>1</sub>-A<sub>6</sub>-OH performed by Dr. T. Allen (1993). Thus a NaCl concentration range of  $0\text{-}3.0\text{ M}$  was employed, with concentration values identical to those of Allen's experiments.  $\text{D}_2\text{O}$  was altered to an approximate pD of 1 with  $d_1\text{-TFA}$  and used for all solutions in this study. A stock solution of template acid in acidic  $\text{D}_2\text{O}$  was made at a concentration sufficient that the final sample solutions contained template quantities in the range of  $4.8\text{ to }7.2\text{ mg}$ . Three stock solutions of NaCl in acidic  $\text{D}_2\text{O}$  were prepared with concentrations of  $0.05$ ,  $0.5$ , and

5.0 M. Each of the concentrations for analysis was prepared by diluting the appropriate stock NaCl solution with template stock solution. Volumes were calculated to give a final sample volume of 750  $\mu\text{L}$ . Final pD values were in the range of 0.4 to 0.83. A sample calculation is presented below:

For a 0.05 M NaCl solution, the 0.5 M stock solution was used.

$$0.5 \text{ M} / x = 0.05 \text{ M} \quad ; \quad x = 10$$

$$750 \mu\text{L total sample volume} / 10 = 75 \mu\text{L NaCl stock solution}$$

$$750 \mu\text{L total volume} - 75 \mu\text{L NaCl stock solution} = 675 \mu\text{L template stock solution}$$

Thus 675  $\mu\text{L}$  of the template stock solution was combined with 75  $\mu\text{L}$  of the 0.5 M NaCl stock solution to create the final solution for analysis.

The following chart summarizes the calculations for the full series:

Final [NaCl] (M)	Stock NaCl Solution Used (M)	Volume Stock Template Solution ( $\mu\text{L}$ )	Volume Stock NaCl Solution ( $\mu\text{L}$ )
0.001	0.05	735	15
0.01	0.05	600	150
0.05	0.5	675	75
0.1	0.5	600	150
0.5	5.0	675	75
1.0	5.0	600	150
2.0	5.0	450	300
3.0	5.0	300	450

## TFE

For spectra taken in  $\text{D}_2\text{O}/\text{d}_3\text{-TFE}$  mixtures, TFE values are reported as mole percentages. For all TFE titrations, the sample was dissolved in  $\text{D}_2\text{O}$  or in  $\text{D}_2\text{O}$  containing  $\text{d}_1\text{-TFA}$  to a pD $\approx$ 1 for compounds containing a free carboxylic acid. A known volume of the sample was then aliquoted out into an NMR tube, TSP was added, and the NMR tube was equipped with a rubber septum. Aliquots of  $\text{d}_3\text{-TFE}$  were then added sequentially to



the NMR tube via syringe to yield solutions of the desired mole percentage TFE. At 20 mole% TFE, the total sample volume was double that of the original volume. As shimming is more difficult with larger volumes, a portion of the final solution, usually 20 mole% TFE, was removed from the NMR tube prior to obtaining the spectrum. By this procedure it was possible to do an entire TFE series with a single sample.

TFE volumes were computed based on the volume of D<sub>2</sub>O used (no correction was made for the small amount of TFA that was present in some of the solutions). A sample calculation is presented below:

$$\text{D}_2\text{O:} \quad \begin{array}{l} \text{FW} = 20.03 \text{ g/mol} \\ \text{d} = 1.107 \text{ g/mL} \end{array} \quad \frac{1.107 \text{ g/mL}}{20.03 \text{ g/mol}} \times \frac{1000 \text{ mL}}{1 \text{ L}} = 55.3 \text{ mol/L}$$

$$\text{d}_3\text{-TFE:} \quad \begin{array}{l} \text{FW} = 103.06 \text{ g/mol} \\ \text{d} = 1.45 \text{ g/mL} \end{array} \quad \frac{1.45 \text{ g/mL}}{103.06 \text{ g/mol}} \times \frac{1000 \text{ mL}}{1 \text{ L}} = 14.1 \text{ mol/L}$$

For 700  $\mu\text{L}$  sample:

$$700 \mu\text{L D}_2\text{O} \times \frac{1 \text{ L}}{1 \times 10^6 \mu\text{L}} \times \frac{55.3 \text{ mol}}{\text{L}} = 0.03871 \text{ mol}$$

For a 2 mole% TFE solution:  $0.03871 \text{ mol D}_2\text{O} = (0.98) X \text{ mol total}$   
 $X = 0.0395 \text{ mol}$

$$(0.02)(0.0395 \text{ mol total}) = 0.00079 \text{ mol TFE needed}$$

$$0.00079 \text{ mol TFE} \times \frac{1 \text{ L}}{14.1 \text{ mol}} \times \frac{1 \times 10^6 \mu\text{L}}{1 \text{ L}} = 56.0 \mu\text{L TFE}$$

The following chart summarizes the calculations for the full series (for titration by 2 mole% units beginning with a volume of 700  $\mu\text{L}$  D<sub>2</sub>O):

Mole% TFE	Total Vol. TFE Needed ( $\mu\text{L}$ )	Total Vol. TFE to Add ( $\mu\text{L}$ )
0	0	0
2	56.0	56.0
4	114.4	58.4
6	175.2	60.8
8	238.7	63.5
10	305.0	66.3
12	374.4	69.4
14	446.9	72.5
16	522.9	76.0
18	602.6	79.7
20	686.3	83.7

## Integration

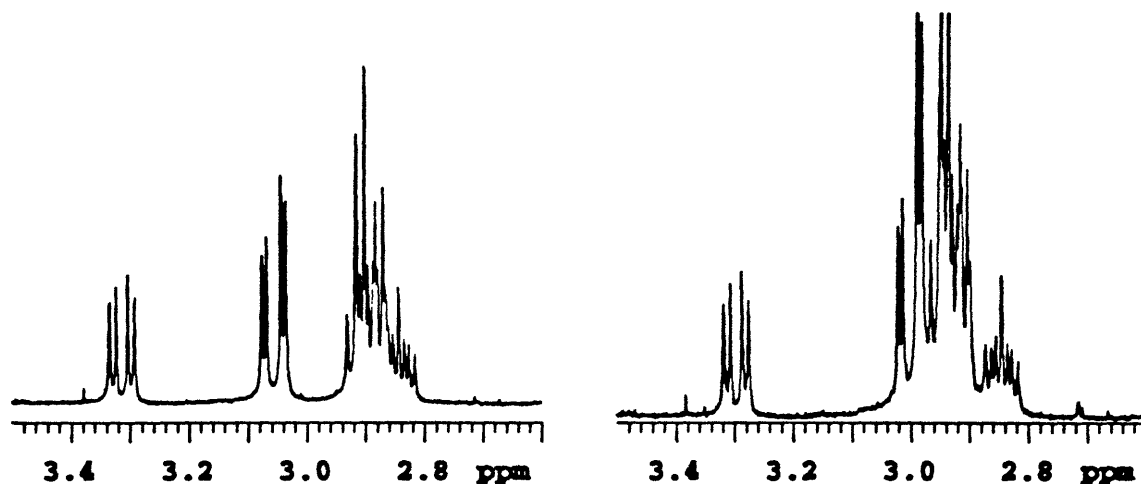
Owing to the heavy reliance on peak integration, spectral acquisition parameters were optimized as described previously and integration values were measured as accurately and precisely as possible. Acquisition parameters were set to both enhance resolution and to provide for full relaxation of all nuclei. Prior to integration, all spectra were phased to pure absorption over the entire spectral range and further adjusted for each specific region of integration when necessary. For each region of interest, a linear baseline correction routine was applied (drift correct) when necessary, and  $lvl/tlt$  values were further adjusted when required. For each peak or set of peaks, integration values were set at 8 Hz outside the outermost peak. In a few instances, it was not possible to achieve baseline resolution with this spectral width; for these cases, a margin of 5 Hz was used.

Dr. T. Allen (1993) developed a systematic approach for the determination of  $t/c$  values that served as a general procedure to measure the  $t/c$  ratio of a wide variety of template derivatives. In his procedure, Dr. T. Allen divides all spectra into three regions; for each a  $t/c$  ratio is determined and the results averaged for a final reported value. The utility of each region is dependent on the specific derivative studied; three independent measurements were employed as an internal standard for the entire series of derivatives studied. The derivatives studied in this thesis are a restricted class for which an alternate approach was utilized to ensure maximal accuracy.

The three regions used by Dr. T. Allen are as follows: Region I, from 4.15 to 3.70 ppm, contains the H-11, H-12a, and H-12b protons of the template. H-11<sub>c</sub> was measured independently for use as the c state value, while the others were measured as a group. The appropriate calculations were made to determine the value for the t state resonance. Region II, spanning 3.40 to 2.70 ppm, contains the H-9b<sub>c</sub>, H-9b<sub>t</sub>, H-9a<sub>t</sub>, H-13b<sub>t</sub>, and H-13b<sub>c</sub> protons. For this region, the H-9b<sub>c</sub> value was measured independently as the value of the c state; the appropriate corrections were made to the integrated value of the remaining protons to determine the t state value. Region III, from 2.60 to 2.05 ppm, contains the H-9a<sub>c</sub>, H-13a<sub>c</sub>, H-13a<sub>t</sub>, H-6, H-7, H-Ac<sub>t</sub>, and H-Ac<sub>c</sub> protons. Here the H-Ac<sub>c</sub> resonance was used as the independent measure of the c state and the t state value was appropriately calculated from the integrated values of the remaining resonances. For the specific set of compounds studied here, Region III was unsuitable owing either to inadequate baseline separation of the H-Ac<sub>c</sub> resonance from that of the H-Ac<sub>t</sub>, or to peak overlap with the H-6 and H-7 protons. For samples containing d<sub>3</sub>-TFE, Region I could not be used due to peak overlap between the H-11<sub>c</sub>/H-11<sub>t</sub>/H-12a<sub>c</sub>/H-12b<sub>c</sub> protons and the residual protonated TFE species. Region II, however, was ideal.

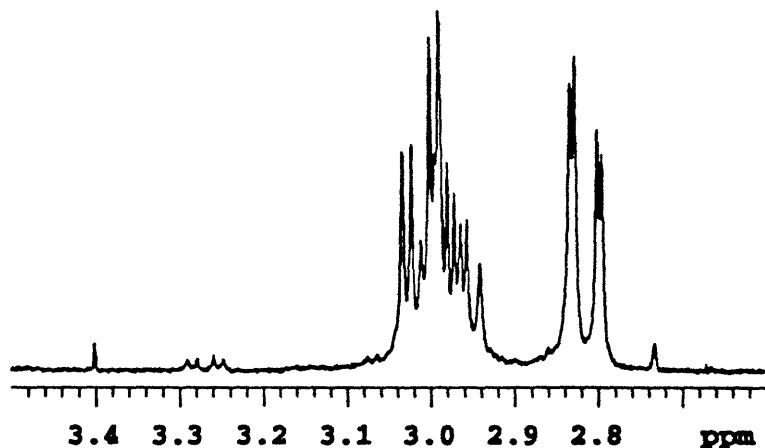
Thus for spectra of Ac-Hel<sub>1</sub>-OH, Ac-Hel<sub>1</sub>-OMe, and Ac-Hel<sub>1</sub>-NHMe, as many clearly resolved regions as possible were integrated to measure a t/c ratio and then averaged for a final number. The following resonances or groups of resonances were used when possible: H-5<sub>c</sub>/H-5<sub>t</sub>, H-2<sub>c</sub>/H-2<sub>t</sub>, H-13b<sub>c</sub>/H-13b<sub>t</sub>, H-9b<sub>c</sub>/H-9b<sub>t</sub>, H-9a<sub>t</sub>+H-9a<sub>c</sub>+H-13a<sub>c</sub>/H-13a<sub>t</sub>, and any of the methods outlined by Dr. T. Allen.

For the TFE titrations of the series Ac-Hel<sub>1</sub>-A<sub>n</sub>-OH, n=1-6, the only feasible region of integration was based on the H-9b protons. For spectra in which the H-9b<sub>t</sub> resonance was downfield from the H-13b resonances by at least 5 Hz, only the H-9b<sub>c</sub> and H-9b<sub>t</sub> protons were integrated. A sample spectrum for which this is the case follows on the left. For instances in which there were fewer than 5 Hz between the H-9b<sub>t</sub> protons and the H-13b protons or where these resonances overlapped, it was necessary to integrate the H-9b<sub>t</sub> protons together with the H-13b<sub>c</sub>, H-13b<sub>t</sub>, and H-9a<sub>t</sub> protons and to make the appropriate corrections. A sample spectrum of this type is given on the right, followed by the equation for calculating the t state value for this type of spectrum.



$$t = \frac{([H-9b_t] + [H-13b_c] + [H-13b_t] + [H-9a_t]) - [H-9b_c]}{3}$$

Thus for these data, the final reported *t/c* ratio is an average of five separate measurements of the H-9b integrations. That is to say, each spectrum was subjected to fourier transform, phasing, baseline correction, and integration five independent times. The five values were then averaged to give the reported ratio as well as the associated error. By this method, standard deviations were, in general, in the range of  $\pm 2-3\%$ . However, there were standard deviations as small as  $\pm 0.3\%$  and as large as  $\pm 9.8\%$ ; high standard deviations were associated with spectra for which there were large differences in the *c* and *t* state populations, such as that of Ac-Hel<sub>1</sub>-A<sub>6</sub>-OH in 20 mole% TFE, shown below.



For comparison, the *t/c* ratio of Ac-Hel<sub>1</sub>-A<sub>1</sub>-OH was determined both by integration of multiple spectral regions as used for the nonpeptidal template derivatives and by integration of the H-9b protons only as described above. The results are as follows:

<u>Multiple Spectral Regions</u>		<u>H-9b Protons Only</u>	
H-5 <sub>c</sub> /H-5 <sub>t</sub>	0.8585		0.7938
H-2 <sub>c</sub> /H-2 <sub>t</sub>	0.8010		0.7932
Region I	0.7840		0.7976
H-9b <sub>c</sub> /H-9b <sub>t</sub>	0.8033		0.7909
Region III	0.7816		0.7905
Average	0.8057	Average	0.7941
Std. Dev.	±3.86%	Std. Dev.	±0.46%

As is evident from the data, the two methods yield comparable results, although there is a larger error associated with the integration of multiple spectral regions.

## CD SPECTROSCOPY

### General

All CD spectra were acquired on an Aviv Model 62-DS Circular Dichroism spectrometer equipped with a Neslab Coolflow CFT-33 cooling unit, a Model RGP-R1-3000 oxygen scrubber, and a GP-240 type liquid nitrogen tank for N<sub>2</sub> gas use. The instrument was housed in a temperature controlled and chemical free room. Instrument calibration was performed using benzene vapors for wavelength calibration and (+)-10-camphorsulfonic acid (CSA); calibration was checked periodically with CSA. All spectra were processed with the instrument software, Aviv 62DS version 4.0s. Unless otherwise specified, all measurements were taken in a 1 mm strain-free quartz cuvette supplied by Hellma Cells, Inc.

All samples were dried under high vacuum prior to use. A buffer consisting of 0.1 M sodium perchlorate in water with the pH adjusted with perchloric acid (Nelson & Kallenbach, 1986), which is transparent in the spectral region of interest, was used to buffer all samples containing a free carboxylic acid to a pH=1. The buffer was prepared by dissolution of 1.4 g NaClO<sub>4</sub>•H<sub>2</sub>O, with enough perchloric acid (*ca.* 0.5 mL) to adjust the pH, to a total volume of 100 mL; the buffer was therefore approximately 0.2 M in perchlorate. The amide series Ac-Hel<sub>1</sub>-A<sub>n</sub>-NH<sub>2</sub>, n=1-6, was also measured in this buffer. Derivatives appeared to be stable in this buffer; in instances where samples were rechecked within a few days, there was no change in the CD spectrum. All other samples were run in pure distilled, deionized water or acetonitrile as indicated. Samples containing visible particulate matter were filtered through a kimwipe plug. All concentration analyses were

performed after this procedure when applied. Sample volumes for the 1 mm cuvette ranged from 250 to 300  $\mu\text{L}$ .

All peptide derivatives of the template were prepared by direct dissolution of the sample into the perchlorate buffer followed by dilution to an appropriate concentration for measurement. For ease in sample preparation, Ac-Hel<sub>1</sub>-OH, Ac-Hel<sub>1</sub>-OMe and Ac-Hel<sub>1</sub>-NHMe were dissolved in a known amount of CH<sub>3</sub>CN to form a stock solution, aliquots of which were carefully diluted into the solvent of interest prior to data collection. After dilution, the Ac-Hel<sub>1</sub>-OH and Ac-Hel<sub>1</sub>-NHMe solutions were 99% by volume in the solvent of interest and 1% in CH<sub>3</sub>CN; the Ac-Hel<sub>1</sub>-OMe sample solutions were 99.8% by volume in the solvent of interest and 0.2% in CH<sub>3</sub>CN. Ac-Hel<sub>1</sub>-NH<sub>2</sub> was prepared by trituration of an oil sample with ethyl acetate to give a solid material, which was subsequently ground to a fine powder and dried under high vacuum overnight. An aliquot was weighed on a microbalance and dissolved in a known volume of water. Sample concentration was determined by weight analysis.

Routine spectra were acquired in wavelength mode, using, for the most part, default parameters, including a temperature of 25 °C, a bandwidth of 0.5 or 0.6 nm, and an averaging time of 1.0 sec. The spectral region was adjusted to scan from 270 nm to 195 nm, as was the step size, which was set to 0.2 nm. Each spectrum was an average of 5 scans. A baseline of the cuvette used for all subsequent samples, containing water or buffer, was measured prior to sample measurements and subtracted from all subsequent spectra. Some degree of instrument drift is to be expected over the course of a day, but it was found that in the controlled temperature environment of the instrument room, the resultant change in the baseline was negligible. Thus a single baseline was acquired per day of instrument use.

## Temperature

The temperature scan of Ac-Hel<sub>1</sub>-A<sub>6</sub>-OH was performed every 5 °C in the range of 5-65 °C. Scans and files were automatically generated using the software macro "twrite." Parameters were set to give an averaging time of 3.0 sec, a step size of 0.5 nm and an equilibration time of 5 minutes.

## Dilution

Dilution studies of Ac-Hel<sub>1</sub>-A<sub>6</sub>-OH were conducted at room temperature by serial dilution of the sample in 1, 10, and 20 mm cylindrical quartz cuvettes using the cell holder

capable of accepting cylindrical cells. Absorption of the perchlorate buffer prevented use of longer cuvettes and thus further dilution.

Dilution studies of H-A<sub>5</sub>-OH were conducted by serial dilution of a sample in pure water in 1, 10, and 100 mm cylindrical quartz cuvettes at room temperature.

### Perchlorate

A sample of Ac-Hel<sub>1</sub>-A<sub>5</sub>-OH was subjected to perchlorate concentrations ranging from approximately 0.20 to 5.42 M and analyzed. Samples were prepared by combining varying aliquots of a stock solution of Ac-Hel<sub>1</sub>-A<sub>5</sub>-OH in the original buffer of approximately 0.20 M perchlorate with a 6.0 M solution of NaClO<sub>4</sub> to a final sample volume of 300 mL. Scans were taken every 0.5 nm. A sample calculation is presented below, and all perchlorate concentrations are approximate owing to the uncertainty in the perchlorate concentration of the original buffer:

$$\frac{240 \mu\text{L Ac-Hel}_1\text{-A}_5\text{-OH} \times 0.2 \text{ M } [\text{ClO}_4^-]}{300 \mu\text{L total volume}} = 0.16 \text{ M } [\text{ClO}_4^-]$$

$$\frac{60 \mu\text{L NaClO}_4 \text{ solution} \times 6.0 \text{ M } [\text{ClO}_4^-]}{300 \mu\text{L total volume}} = 1.20 \text{ M } [\text{ClO}_4^-]$$

$$0.16 \text{ M } [\text{ClO}_4^-] + 1.20 \text{ M } [\text{ClO}_4^-] = 1.36 \text{ M perchlorate total}$$

The following chart summarizes the calculations for the full series:

Volume Stock Ac-Hel <sub>1</sub> -A <sub>5</sub> -OH Solution (μL)	Volume 6.0 M NaClO <sub>4</sub> Solution (μL)	[ClO <sub>4</sub> <sup>-</sup> ] from Ac-Hel <sub>1</sub> -A <sub>5</sub> -OH Solution (M)	[ClO <sub>4</sub> <sup>-</sup> ] from 6.0 M NaClO <sub>4</sub> Solution (M)	Total Perchlorate Concentration (M)
300	0	0.20	0.0	0.20
270	30	0.18	0.6	0.78
240	60	0.16	1.2	1.36
210	90	0.14	1.8	1.94
180	120	0.12	2.4	2.52
150	150	0.10	3.0	3.10
120	180	0.08	3.6	3.68
90	210	0.06	4.2	4.26
60	240	0.04	4.8	4.84
30	270	0.02	5.4	5.42

### D<sub>2</sub>O vs H<sub>2</sub>O

For ease in sample preparation, a sample of Ac-Hel<sub>1</sub>-A<sub>6</sub>-OH was dissolved in the perchlorate buffer (H<sub>2</sub>O based) to form a stock solution. One aliquot of this was diluted into the original perchlorate buffer and another diluted into a D<sub>2</sub>O based perchlorate buffer, pD≈1, to create the samples for analysis. After dilution, the H<sub>2</sub>O sample was in 100% H<sub>2</sub>O, while the D<sub>2</sub>O sample was in 90% D<sub>2</sub>O.

### TFE

For spectra taken in H<sub>2</sub>O/TFE mixtures, TFE values are reported as mole percentages. For all TFE titrations, the sample was dissolved in H<sub>2</sub>O or in the original perchlorate buffer. A known volume of the sample was combined with an appropriate volume of TFE to yield solutions of the desired mole percentage TFE.

TFE volumes were computed based on the volume of solute used (no correction was made for the small amount of NaClO<sub>4</sub>/ClO<sub>4</sub><sup>-</sup> that was present in some of the solutions). A sample calculation is presented below:



$$\text{H}_2\text{O:} \quad \begin{array}{l} \text{FW} = 18.02 \text{ g/mol} \\ \text{d} = 1.00 \text{ g/mL} \end{array} \quad \frac{1.00 \text{ g/mL}}{18.02 \text{ g/mol}} \times \frac{1000 \text{ mL}}{1 \text{ L}} = 55.5 \text{ mol/L}$$

$$\text{TFE:} \quad \begin{array}{l} \text{FW} = 100.04 \text{ g/mol} \\ \text{d} = 1.373 \text{ g/mL} \end{array} \quad \frac{1.373 \text{ g/mL}}{100.04 \text{ g/mol}} \times \frac{1000 \text{ mL}}{1 \text{ L}} = 13.72 \text{ mol/L}$$

For 200  $\mu\text{L}$  of sample:

$$200 \mu\text{L H}_2\text{O} \times \frac{1 \text{ L}}{1 \times 10^6 \mu\text{L}} \times \frac{55.5 \text{ mol}}{\text{L}} = 0.011 \text{ mol}$$

For an 8 mole% TFE solution:  $0.011 \text{ mol H}_2\text{O} = (0.92) X \text{ mol total}$   
 $X = 0.01196 \text{ mol}$

$(0.08)(0.01196 \text{ mol total}) = 0.0009565 \text{ mol TFE needed}$

$$0.0009565 \text{ mol TFE} \times \frac{1 \text{ L}}{13.72 \text{ mol}} \times \frac{1 \times 10^6 \mu\text{L}}{1 \text{ L}} = 69.7 \mu\text{L TFE}$$

The following chart summarizes the calculations for the full series (for titration by 2 mole% units and ending with a final volume of 250 to 300  $\mu\text{L}$ ):

Mole % TFE	Volume Sample ( $\mu\text{L}$ )	Volume TFE ( $\mu\text{L}$ )
2	300	24.6
4	300	50.1
6	300	76.8
8	200	69.7
10	200	100.2
12	200	109.3
14	200	130.5
16	200	152.7
18	200	176.0
20	200	200.4

## Concentration Determination

Concentration determination for CD samples was performed in a two step process. The first step involved complete hydrolysis of the template derivative in solution; in the second step a colorimetric assay was performed using a carefully developed ninhydrin procedure. For each sample, three or four separate analyses were performed and the results averaged.

Materials and reagents used are as listed in the following chart. All reagents used were purchased in the highest possible purity; additional purification was performed in some instances.

Manufacturer specifications for the 50-200  $\mu\text{L}$  pipette were  $\pm 1\%$  in accuracy and  $\pm 0.5\%$  at 50  $\mu\text{L}$  and  $\pm 0.6\%$  at 200  $\mu\text{L}$  in reproducibility; for the 200-1000  $\mu\text{L}$  pipette, the values were  $\pm 1\%$  in accuracy and  $\pm 0.6\%$  at 200  $\mu\text{L}$  and  $\pm 0.5\%$  at 1000  $\mu\text{L}$  in reproducibility. Manufacturer specifications for the Oxford dispensers gave an accuracy level of  $\pm 1\%$  and a precision level of  $\pm 0.5\%$ . For the VWR dispenser, specification values were  $\pm 0.5\%$  in accuracy and  $\pm 0.1\%$  in repeatability.

Sample hydrolysis was conducted in a Pierce "Reacta-therm" block, which is essentially a large metal block fused to a heating element. The metal block is drilled with nine holes, one for a thermometer and the other eight just large enough to accommodate the vacuum hydrolysis tubes. All mixing was carried out using a "Vortex Genie-2" shaker from VWR Scientific. Absorbance readings were measured on a Carl Zeiss UV/Vis Spectrophotometer equipped with an M4QIII monochromator, a PI-2 detector, and a 6V30W tungsten lamp. Prior to any readings, the Zeiss was warmed up for a minimum of one hour. Before the measurement of every set of blank and sample, the slit width and the  $A=0/T=100$  knob were adjusted to give a value of 100.0 in transmittance mode with an empty cell holder in the light path; the instrument was then changed to absorbance mode and readings taken.

Material/Reagent	Use	Special Instructions	Supplier	Catalog Number	Description
1:1 Mixture Hydrochloric:Propionic Acids	Sample hydrolysis		Pierce 1-800-874-3723	27514	
Ninhydrin	Colorimetric ninhydrin assay	Recrystallize from hot water prior to use	Pierce	21000	
Methyl Cellosolve	Colorimetric ninhydrin assay	Test for peroxides using a 10% KI solution prior to use	Aldrich 1-800-558-9160	27,048-2	
Pipettors	Quantitative solution transfer		VWR Scientific 1-800-932-5000	53499-376; 50-200 $\mu$ L 53499-398; 200-1000 $\mu$ L	Variable volume micropipettors; 50-200 $\mu$ L adjusts by 1 $\mu$ L increments; 200-1000 $\mu$ L adjusts by 10 $\mu$ L increments
Vacuum Hydrolysis Tubes	Sample hydrolysis		ChemGlass, Inc. 1-800-843-1794	CG-4506-03 (Chem-Cap Plug, CG-561-01 complete; CG-561-20 stem only)	10 mL total volume with Teflon caps and 3 O-rings for complete vacuum seal
Replacement O-rings for vacuum hydrolysis tubes	Sample hydrolysis	Should be replaced when even slightly deformed	ChemGlass, Inc.	CG-305-05	
Detergent to clean vacuum hydrolysis tubes	Glassware cleaning		Pierce	72288	Specially designed detergent for protein and peptide residue
Oxford Dispensers	Colorimetric ninhydrin assay		VWR Scientific	53519-484	Brown bottle capped with variable volume dispensing unit; adjusts by 5 $\mu$ L increments
VWR Dispenser	Colorimetric ninhydrin assay		VWR Scientific	53501-026	Brown bottle capped with variable volume dispensing unit; adjusts by 100 $\mu$ L increments

## Reagent Preparation

The acid mixture for sample hydrolysis was used directly from ampoules sold by Pierce. Ninhydrin was recrystallized from hot water at an approximate ratio of 1g ninhydrin:2 mL water and dried under high vacuum. Methyl cellosolve was tested for peroxides using a 10% KI in water solution (5:1 cellosolve: KI solution) and filtered through a column of alumina if there was an even slight yellow color development. The following table lists all solutions that must be prepared for the colorimetric ninhydrin assay:

Solution	Reagents Needed	Preparation Procedure	Dispensing Unit
Ninhydrin Solution	<ul style="list-style-type: none"> <li>Recrystallized ninhydrin, 3 g</li> <li>Peroxide free methyl cellosolve</li> </ul>	Dissolve ninhydrin in methyl cellosolve to a total volume of 100 mL	Oxford Dispenser set to 250 $\mu$ L
Stock Cyanide Solution	<ul style="list-style-type: none"> <li>Sodium cyanide, 49 mg</li> <li>Distilled, deionized water</li> </ul>	Dissolve NaCN in water to a total volume of 100 mL	N/A
Stock Acetate Buffer	<ul style="list-style-type: none"> <li>Sodium acetate, 360 g</li> <li>Glacial acetic acid, 66.7 mL</li> <li>Distilled, deionized water</li> </ul>	Dissolve NaOAc and acetic acid to a total volume of 1 L	N/A
Cyanide-Acetate Buffer	<ul style="list-style-type: none"> <li>Stock Cyanide Solution, 2 mL</li> <li>Stock Acetate Buffer</li> </ul>	Dilute cyanide solution with acetate buffer to a total volume of 100 mL	Oxford Dispenser set to 250 $\mu$ L
Diluent	<ul style="list-style-type: none"> <li>Isopropanol</li> <li>Distilled, deionized water</li> </ul>	Combine two reagents in a 1:1 v/v ratio	VWR Dispenser set to 2.5 mL

All solutions used directly in the colorimetric analysis were stored in and dispensed from brown glass bottles under atmospheric conditions. The cyanide-acetate buffer had an unlimited lifetime whereas the ninhydrin solution had to be replaced every six to eight weeks owing to the buildup of peroxides. The dispensers were cleaned by "dispensing" aliquots of warm water through the mechanism followed by acetone; a stream of nitrogen was run through the mechanism to remove any unevaporated acetone. Freshly prepared solutions of the cyanide-acetate buffer and the ninhydrin solution were allowed to sit for approximately one day prior to use as it was found that unusually high blank readings were obtained for analyses conducted immediately after solution preparation.

## Sample Hydrolysis

An aliquot of the sample used for CD measurement was carefully pipetted (using a manufacturer calibrated pipette) into the bottom of a vacuum hydrolysis tube. An aliquot of equal volume of the solvent used to prepare the sample was pipetted into another hydrolysis tube for use as a blank and marked as such. (For ease in analysis, sample volumes were chosen such that the final solutions yielded a ninhydrin color development that required minimal dilution prior to spectrophotometric analysis, yet were not exceptionally small. In general, 75  $\mu\text{L}$  aliquots of sample were used; the ideal sample volume would contain approximately 0.03-0.12  $\mu\text{mol}$  of amino acid). Together, the blank and sample tubes constituted one set for analysis. This was repeated for a total of 3 or 4 sets, with careful attention paid throughout the analysis to ensure equal handling of blank and sample for each set. Approximately 0.5 mL of a 1:1 mixture of hydrochloric and propionic acids was then added to each hydrolysis tube with a disposable Pasteur pipet. (Pierce recommends a ratio of 300  $\mu\text{g}$  sample:1 mL reagent; the 0.5 mL of acid used in this procedure gives a large excess of acid but ensures adequate solution reflux during the hydrolysis procedure.) The hydrolysis tubes were carefully capped by alignment of the threads of the hydrolysis tube and the capping assembly; the cap was then gently turned. It was found that the tubes are very fragile and unforgiving toward an even slight excess of force during capping. Thus the caps were screwed in very slowly and carefully, and the brown O-ring was replaced in instances where it was slightly deformed and difficult to use.

The tubes were placed under high vacuum and degassed. The contents were brought under full vacuum very gradually to ensure that they did not bump into the vacuum line by unscrewing the cap minimally. The tubes were agitated just slightly to begin the degassing process; once much of the gas had been removed, they were shaken well in a vertical position to release any additional gas. The tubes were sealed by screw closure under vacuum, placed in a preheated "Reacta-therm" block, and allowed to hydrolyze for a two hour period. The recommended times for this procedure are 15 minutes at 160  $^{\circ}\text{C}$  or 2 hours at 130  $^{\circ}\text{C}$  (Westall & Hesser, 1974). The block used for this thesis was only able to achieve an approximate temperature of 135  $^{\circ}\text{C}$ ; thus a two hour reaction period was allowed.

After 2 hours the tubes were removed from the heating block and allowed to cool to room temperature. They were placed under high vacuum on a line equipped with a base trap and left until all liquid had been evaporated. Dependent on the strength of the vacuum, this took approximately 1 hour. The filmy residue left in each tube was reconstituted in a known volume of distilled, deionized water, often 250  $\mu\text{L}$ . Complete dissolution to a clear

solution was achieved through vigorous agitation using a "Vortex Genie" at the highest possible speed; no solvent escaped from the tube. The colorimetric ninhydrin assay was performed directly on this solution.

### **Colorimetric Ninhydrin Assay**

The solutions used for the ninhydrin assay were each contained in and dispensed from an automatic dispenser to ensure reproducible aliquots. Before any sample was analyzed, these dispensers were primed by dispensing a number of aliquots until a smooth stream was achieved. This was found to be particularly important for the cyanide-acetate buffer, as it is a very concentrated solution and salts can crystallize on the glass rod of the dispensing mechanism if too much time has elapsed between uses. The ninhydrin solution should be tested periodically for the presence of peroxides as they may build up over time and will interfere with proper color development; the dispenser must be cleaned and a new solution prepared if peroxides are found to be present. This solution can be tested in a fashion similar to that used for the cellosolve alone. However, as the ninhydrin solution itself is yellow in color, it is difficult to detect the presence of small amounts of peroxides. It is therefore recommended that a second test be performed wherein the ninhydrin solution is added to pure water instead of the KI solution; this can then be used for color comparison.

A 250  $\mu\text{L}$  aliquot of the ninhydrin solution and of the cyanide-acetate buffer were each dispensed directly into the hydrolysis tubes, positioning the end of the dispensers below the narrow portion of the hydrolysis tube so that no reagent would be lost. The tubes were then loosely capped with the usual capping apparatus, shaken to homogeneity with a "Vortex Genie," and placed in a boiling water bath. This was most easily accomplished by placing the hydrolysis tubes in an appropriate test tube holder and immersing the entire test tube holder in a large crystallizing dish of boiling water. Color development was allowed to proceed for exactly 15 minutes from the time of introduction into the bath, after which the tubes were removed from the water bath, immediately uncapped, and the solutions diluted with a 2.5 mL aliquot of the isopropanol-water mixture. Care was taken when adding the diluent to ensure that the entire volume passed through the narrow portion of the hydrolysis tubes. These solutions were mixed to homogeneity by vigorous shaking achieved through use of a "Vortex Genie" at its highest setting. It was necessary to tilt the tubes to an approximate angle of 60 degrees from the vertical while shaking so that the entire solution was mixed and aerated; this took approximately 15 to 20 seconds. The solutions were allowed to cool to room temperature.

Absorbance values of blanks and samples were measured in matching 1 cm quartz cells and recorded at 570 nm using a Zeiss spectrophotometer. As the hydrolysis tubes are fairly long, it was not possible to remove their contents with a standard disposable pipet. Therefore nine inch disposable pipets were etched with a file or glass cutter just at the top of the tapered portion and these segments were carefully removed. By gently inserting the end of a nine inch pipet into these segments until a snug fit was achieved it was possible to reach the bottom of the hydrolysis tubes and to therefore remove their entire contents. In some cases it was necessary to carefully dilute the sample solutions (again using the isopropanol-water mixture) to bring the sample absorbance into the ideal optical range of 0.2 to 0.8 absorbance units. This was usually accomplished by pipetting 1.0 mL of developed sample solution into a test tube and mixing it with one dispensing volume of the isopropanol-water mixture, 2.50 mL. Actual sample absorbances were figured by first correcting for dilution when used and then by subtracting the blank absorbance from that of the sample. Net CD sample concentration was determined by comparison of the average observed optical density to calibration curves for each of the amino acids present, for an ammonia standard (for *N*-terminal amides), and for the template.

The vacuum hydrolysis tubes were cleaned immediately after use with a commercially available detergent supplied by Pierce; the tubes were soaked overnight in a solution of the detergent, cleaned with a thin test-tube brush, rinsed, and left to dry, occasionally in an oven. The caps were treated in a similar fashion, although they were never oven dried.

### Calibration Curves

For each of the functional groups that test positive in the ninhydrin assay it was necessary to create a calibration curve of its response to the assay. This was accomplished through the procedure described in the following section. A plot of absorbance versus concentration was created for each amino acid using KaleidaGraph 3.0.1, and the equation of the best linear fit was determined by least squares analysis. Those equations are as follows, where *x* is the concentration (M) and *y* is the absorbance:

$$\text{Ala: } y = 0.0016294 + 21584x$$

$$\text{Lys: } y = 0.0040948 + 24175x$$

$$\text{NH}_3: y = 0.0155350 + 20286x$$

$$\text{Temp: } y = 0.0848650 + 1156.7x$$

Of these, the template equation is the least reliable, as it is founded on a calibration curve containing fewer data points than the others. An alternate equation, for which (0,0) is included as a data point, was generated:

$$\text{Temp': } y = 0.0123040 + 1887.3x$$

### Calculation of Concentration

The concentration of the samples used for CD can be computed by performing the following steps:

1. Determine the average sample absorbance. The blank value should be subtracted from the sample value for each run, appropriately correcting for dilution of the sample when necessary. The resultant numbers are averaged for a final value, Z. Standard deviations (SDs) can be calculated as well.
2. Set up the appropriate equation for comparison to the calibration curves. Each peptide derivative will contain one template and a varying number of amino acid residues. *N*-terminal amides will also contain one NH<sub>3</sub> group. For each amino acid present, the right-hand portion of the corresponding equation above should be multiplied by the number of times that residue appears in the peptide. Absorbance, Z, is equal to the sum of the right-hand portions of the individual equations.
3. Compute the value for x, the concentration of the template derivative in the developed solution. The value obtained in step one, Z, should be used as the absorbance value, or the left-hand portion of the equation. The value of x may be solved algebraically.
4. Make the appropriate corrections to determine the concentration of the template derivative in the original CD sample. This is accomplished by correcting for the volumes used in the assay as well as for the volume of the original aliquots.

### Full Example of Concentration Determination

The following is an example of the full concentration analysis of one template derivative:

Four independent aliquots of the CD sample of Ac-Hel<sub>1</sub>-A<sub>2</sub>-NH<sub>2</sub> were hydrolyzed and assayed colorimetrically as described above. The perchlorate buffer used to prepare the CD sample was used as the blank. 75 μL aliquots were used. After hydrolysis and complete



drying in vacuo, the resultant residues were reconstituted in 250  $\mu\text{L}$  of distilled, deionized water.

It was necessary to dilute the final sample solution, which was accomplished by mixing 1 mL with 2.5 mL of the isopropanol-water mixture to a total of 3.5 mL. The final readings were as follows:

<u>Blank</u>	<u>Sample</u> (after dilution)
0.132	0.384
0.125	0.432
0.118	0.410
0.108	0.428

1. Corrections were made for dilution of the sample solution by multiplying by 3.5 mL/1.0 mL, and the net absorbance was determined:

<u>Blank</u>	<u>Sample</u> (as if not diluted)	<u>Net Absorbance</u>	
0.132	1.344	1.212	Average = Z =
0.125	1.512	1.387	1.3265
0.118	1.435	1.317	SD = 0.084
0.108	1.498	1.390	

2. The equation for comparison to the calibration curve was determined:

$$\begin{aligned} \text{Ala: } y &= (0.0016294 + 21584x) \cdot 2 \\ \text{Temp: } y &= (0.0848650 + 1156.7x) \cdot 1 \\ \text{NH}_3: y &= (0.0155350 + 20286x) \cdot 1 \end{aligned}$$

---


$$\text{Abs} = 0.1036588 + 64610.7 x$$

3. The absorbance of the developed solution was computed using the above equation:

$$\begin{aligned} 1.3265 &= 0.1036588 + 64610.7 x \\ x &= 1.8926 \times 10^{-5} \text{ M} \quad (\text{SD} = 0.1300 \times 10^{-5} \text{ M}) \end{aligned}$$

4. Corrections were made to determine the concentration of the sample used for the CD analysis. After hydrolysis, the sample was reconstituted in 250  $\mu\text{L}$  water, and 3000  $\mu\text{L}$  of reagents were added in the ninhydrin assay to total 3250  $\mu\text{L}$ . The original aliquots were 75  $\mu\text{L}$ :

$$3250 \mu\text{L} \times \frac{1.8926 \times 10^{-5} \text{ mol}}{\text{L}} \times \frac{1}{75 \mu\text{L}} = 8.2013 \times 10^{-4} \text{ M} \\ (\text{SD} = 0.5633 \times 10^{-4} \text{ M})$$

When Temp' was used as the equation representing the calibration curve of the template, the final concentration value obtained was within one standard deviation of the above value.

## ASSAY FOR CONCENTRATION DETERMINATION

### General

All reagents were prepared with careful attention to purity, as described in the preceding section, to eliminate any potential problems owing to reagent contamination. The methyl cellosolve solution was tested every few days for the presence of peroxides; for colorimetric assays performed in solutions with peroxides present, no color development was detected. All solution transfers were conducted using either calibrated pipetmen or automatic dispensers. Manufacturer specifications for the 50-200  $\mu\text{L}$  pipetman were  $\pm 1\%$  in accuracy and  $\pm 0.5\%$  at 50  $\mu\text{L}$  and  $\pm 0.6\%$  at 200  $\mu\text{L}$  in reproducibility; for the 200-1000  $\mu\text{L}$  pipetman, the values were  $\pm 1\%$  in accuracy and  $\pm 0.6\%$  at 200  $\mu\text{L}$  and  $\pm 0.5\%$  at 1000  $\mu\text{L}$  in reproducibility. Manufacturer specifications for the Oxford dispensers gave an accuracy level of  $\pm 1\%$  and a precision level of  $\pm 0.5\%$ . For the VWR dispenser, specification values were  $\pm 0.5\%$  in accuracy and  $\pm 0.1\%$  in repeatability.

Weights of samples were determined on a Mettler Model M5 Micro Gram-Atic Balance, which was exact to four decimals and approximate to six. Specifications were 5  $\mu\text{g}$  in resolution and  $\pm 10 \mu\text{g}$  in linearity. Use of the balance was kindly allowed by the Lippard group at MIT. The balance was serviced yearly.

Standard solutions were prepared by quantitative dissolution into "Class A" volumetric flasks, calibrated to contain at 20  $^{\circ}\text{C}$  and designed to meet the requirements of ASTM specifications E-237 for microflasks. Sizes 5 mL and under conformed with recommendations of the Committee on Microchemical Apparatus of the Analytical Division, American Chemical Society; Analytical Chemistry, 28, page 1993, December 1956.

Tolerance levels were as follows:  $\pm 0.01$  mL for 1 mL flasks,  $\pm 0.015$  mL for 2 mL flasks,  $\pm 0.02$  mL for 5 mL flasks, and 0.02 mL for 10 mL flasks.

### **Preliminary Experiments**

An analytical sample of alanine (H-Ala-OH) in water was used as a sample solution in the developmental stages of the assay. For this solution, alanine was recrystallized from hot water, filtered, dried overnight under high vacuum, crushed into a fine powder and again dried overnight under high vacuum. An aliquot of this was carefully weighed on a microbalance, transferred to a "Class A" volumetric flask, and dissolved in water to a given volume. From this the solution concentration was determined.

Unless the hydrolysis procedure was directly involved, the colorimetric ninhydrin assay was performed as described earlier, but in test tubes rather than the vacuum hydrolysis tubes. Aluminum foil was used to cover the test tubes during color development. All portions of experiments involving hydrolysis were conducted directly in the vacuum hydrolysis tube.

### **Sample Hydrolysis**

Two sets of experiments served as the foundation upon which the exact procedure for sample hydrolysis was established. In the first, aliquots of a solution of alanine of known concentration were lyophilized in the vacuum hydrolysis tubes prior to the addition of the acid mixture and subsequent hydrolysis. After the acid mixture had been removed under high vacuum and the residue resuspended in water, the ninhydrin assay was performed. For this set of samples, color development was minor, only about a few hundredths in absorbance units above those of the corresponding blanks. The ninhydrin assay was performed on the alanine solution in the vacuum hydrolysis tubes without lyophilization or hydrolysis and full color development ensued, eliminating the sample solution, the vacuum hydrolysis tubes and the assay solutions as potential problems. These results indicated that some type of sample loss had occurred, prompting further experimentation to determine the source of such loss. The initial experiment was repeated, but the samples were oven dried rather than lyophilized. Again, the resultant absorbance values were only slightly higher than those of the blanks. In another set of experiments, the sample solution was added to vacuum hydrolysis tubes and the volume levels marked on the outside of the tube. A fraction of each sample was lyophilized, the solutions were warmed to room temperature, and water was added to the tubes to return the volumes to

their original levels. Partial color development ensued following the colorimetric assay that was qualitatively proportional to the fraction of sample solution lyophilized. In an additional experiment, a liquid nitrogen trap was added to the system between the hydrolysis tube and the vacuum port; there was minor color development in both the hydrolysis tube and in the trap. Lyophilization was performed in a round bottom flask as well, with similar results to the above experiments. Finally, a few drops of concentrated HCl were added to the sample solution prior to lyophilization; full color development was observed for these solutions. It was therefore concluded that at neutral pH, alanine was easily removed and lost under high vacuum and that it was necessary to lower the pH of the solution to avoid this problem. It was thus deemed necessary to perform the acid hydrolysis procedure directly on the sample solution.

In the second set of experiments, aliquots of 250  $\mu\text{L}$  of alanine sample with 250, 500, or 1000  $\mu\text{L}$  of the hydrochloric/propionic acid mixture added were subjected to the ninhydrin assay. In all cases, no color development ensued. Thus complete acid removal following hydrolysis was deemed essential.

Results from test solutions on which the hydrolysis procedure was performed and from those for which it was not gave comparable results within standard deviation levels.

### **Colorimetric Ninhydrin Assay**

The importance of aeration and cooling following the 15 minute period of color development was analyzed. Sample solutions were shaken following dilution for periods of approximately 5 seconds (to visual solution homogeneity), exactly 30 seconds, and exactly 45 seconds. Results for all three time periods were the same within standard deviation levels. Sample solutions were cooled following a brief shaking period for approximately 5 minutes (room temperature to touch), 10 minutes, and 40 minutes; no variation in the results was observed. It was therefore determined that precise timing was not necessary for these two steps.

Reproducibility is an extremely important issue and was monitored carefully. Repetitive experiments were performed with four samples per set. Early experiments in which all volume transfers were performed with a pipettoman gave SDs on the order of  $\pm 1-7\%$ . Experiments in which the automatic dispensers were used to apportion reagent solutions gave SDs of  $\pm 1-2\%$ .

## Calibration Curves

Calibration curves were created for the response of alanine, lysine, ammonia, and the template to the ninhydrin assay; for each curve, a stock solution of the sample was created and used to prepare all solutions analyzed for the calibration curves.

## Stock Solutions

For the alanine stock solution, alanine (H-Ala-OH) was first recrystallized from hot water. Approximately 1 g of alanine was suspended in *ca.* 2 mL of water and heated above a steam bath; small quantities of water were added to the hot solution until complete dissolution had been achieved. The solution was allowed to cool to room temperature causing crystals to form. These crystals were filtered from solution, washed with a small amount of cold water, and dried under vacuum overnight. They were then ground to a fine powder and again dried overnight under high vacuum. An elemental combustion analysis was performed on this material both with and without drying to constant weight prior to analysis. For the sample that was dried prior to analysis, the weight loss reported was 0.00 mg. Thus the recrystallization procedure employed was sufficient in ensuring that no residual water remained in the sample. The results of the combustion analysis are as follows:

Element	Expected %	Observed % (sample dried to constant weight)	Observed % (sample not dried)
C	40.44	40.59	40.49
H	7.92	7.74	7.99
N	15.72	15.75	15.64
O *	35.92	35.92	35.88

\* O assumed to be remaining weight percent and is a calculated value.

Using a clean piece of aluminum foil as a weighing boat, 88.907 mg of alanine were weighed on a microbalance and quantitatively transferred to a "Class A" 10 mL volumetric flask by thorough rinsing of the foil boat with distilled, deionized water into the

flask. The solution was made up to its final volume with water, yielding a stock solution of alanine at a concentration of  $9.979 \times 10^{-2}$  M.

A lysine stock solution was prepared in an identical fashion. Lysine (H-Lys-OH • HCl) was recrystallized from hot water, filtered, dried overnight under high vacuum, ground to a powder, and again dried overnight under high vacuum. Precisely 49.005 mg were weighed on a microbalance using a foil weighing boat and quantitatively transferred to a "Class A" 5 mL volumetric flask. The lysine stock solution, when made up to its final volume, had a concentration of  $5.3645 \times 10^{-2}$  M.

The template stock solution was prepared in a similar fashion; template was recrystallized as described earlier. Following recrystallization and thorough drying, 8.772 mg were weighed on a microbalance using a foil weighing boat and quantitatively transferred to a "Class A" 2 mL volumetric flask. The final stock solution had a concentration of  $1.4701 \times 10^{-2}$  M.

The ammonia stock solution was purchased directly from Alfa/ÆSAR as an analytical ammonium ion chromatography standard of  $\text{NH}_4^+\text{Cl}^-$  (Rosin, 1967) in water. This solution was certified against NIST SRM 1212A at a concentration of  $1,000 \pm 5 \mu\text{g/mL}$  in  $\text{NH}_4^+$  ion, or  $5.5535 \times 10^{-2}$  M.

### Data Collection

Unlike the other stock solutions, the template solution required hydrolysis prior to subjection to the ninhydrin assay. 200  $\mu\text{L}$  aliquots were subjected to the hydrolysis procedure outlined earlier and reconstituted in varying quantities of distilled, deionized water. The colorimetric assay was performed on aliquots of these solutions. The amino acid and ammonia stock solutions were serially diluted using the calibrated pipettes and aliquots of these dilutions were subjected to the colorimetric ninhydrin assay as described earlier.

For each concentration, the assay was performed six times and the results averaged. Dilution concentrations and aliquot volumes were chosen to give a color yield within the optimal absorbance range of 0.2 - 0.8 absorbance units so that dilution of the final solutions would not be necessary.

### Calibration Curves and Equations

The results for all of the calibration curves are shown below in graph and table format. The correlation coefficients, R, are shown just below the data.

Conc. Ala in Final Solution	Abs.	Std. Dev.
7.676e-05	1.66	0.5%
4.768e-05	1.03	0.8%
3.473e-05	0.699	0.5%
2.732e-05	0.609	0.6%
1.737e-05	0.357	0.6%
2.251e-05	0.489	1.3%
1.366e-05	0.304	1.6%
1.125e-05	0.251	1.2%
4.241e-05	0.921	1.1%
3.819e-05	0.844	0.9%
3.185e-05	0.701	0.6%
2.941e-05	0.637	1.2%

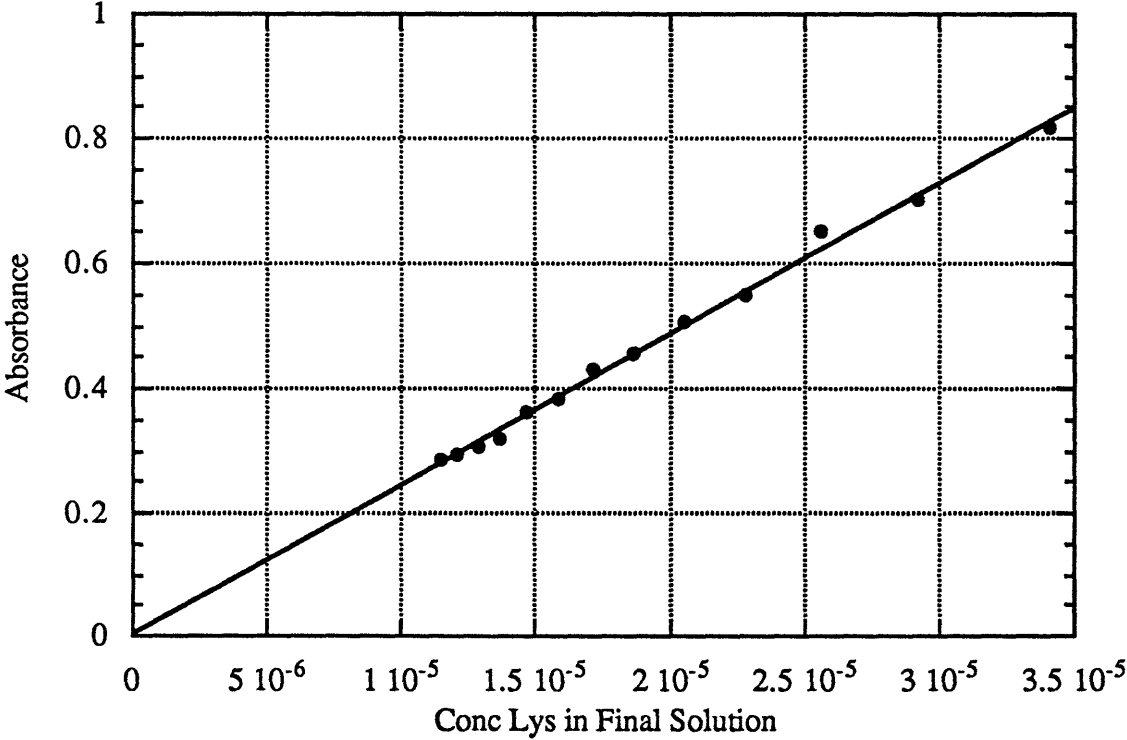
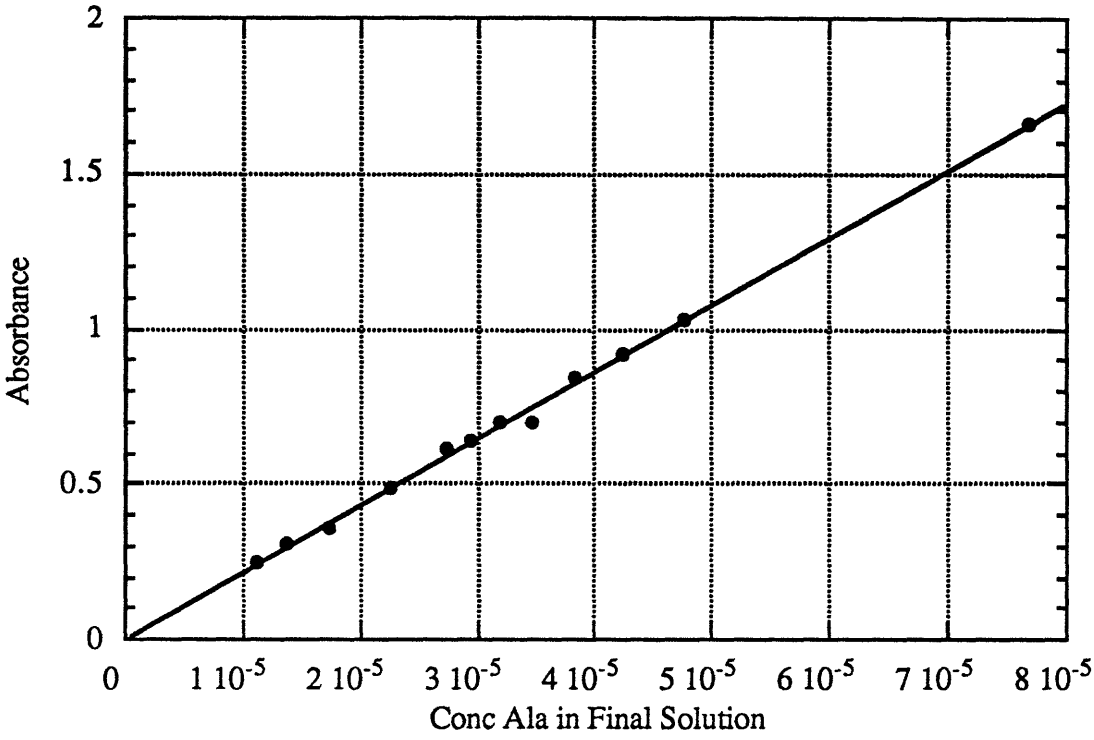
R = 0.99877

Conc. Lys in Final Solution	Abs.	Std. Dev.
2.2798e-05	0.550	0.9%
2.0530e-05	0.505	0.6%
1.8672e-05	0.456	0.9%
2.5631e-05	0.653	2.6%
2.9266e-05	0.704	1.1%
3.4104e-05	0.816	0.6%
1.7122e-05	0.431	0.9%
1.5811e-05	0.384	1.6%
1.4685e-05	0.360	1.9%
1.3709e-05	0.321	0.9%
1.2855e-05	0.307	0.7%
1.2102e-05	0.292	1.0%
1.1431e-05	0.287	0.7%

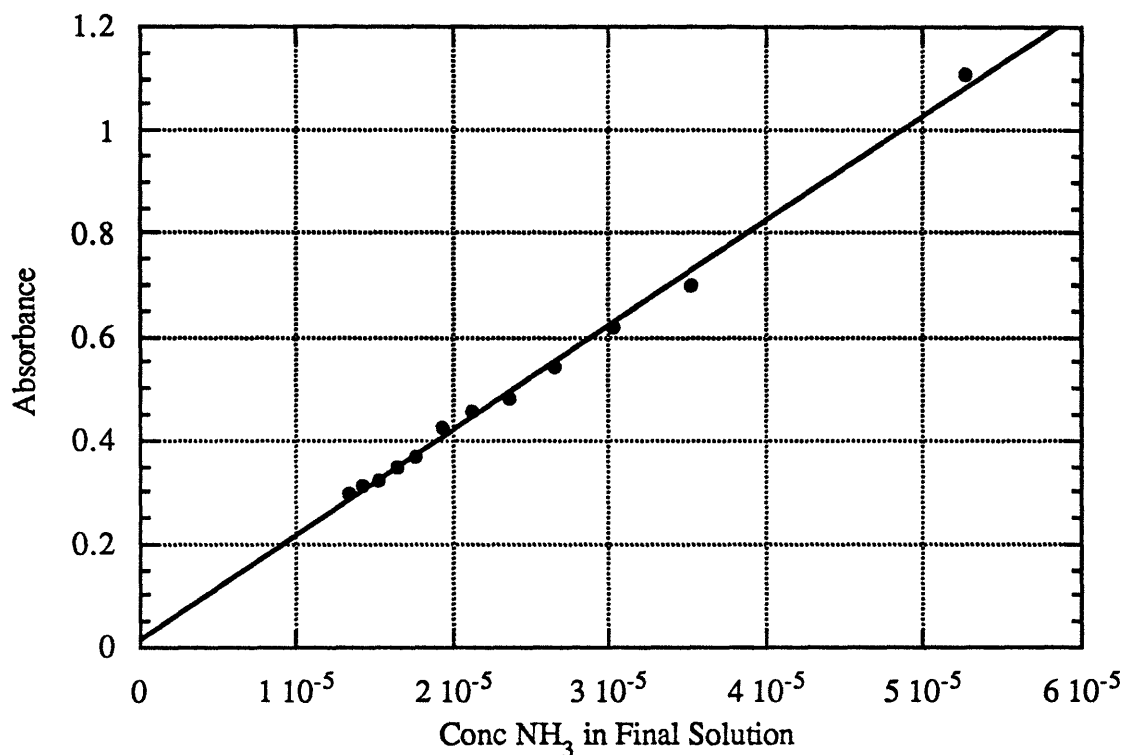
R = 0.99767

Conc. NH <sub>3</sub> in Final Solution	Abs.	Std. Dev.
5.2645e-05	1.11	0.4%
3.5242e-05	0.698	0.6%
3.0243e-05	0.617	0.7%
2.6486e-05	0.540	0.7%
2.3559e-05	0.481	0.6%
2.1215e-05	0.457	0.9%
1.9295e-05	0.424	0.5%
1.7694e-05	0.369	0.5%
1.6338e-05	0.346	0.9%
1.5175e-05	0.324	1.9%
1.4167e-05	0.312	1.6%
1.3284e-05	0.297	1.7%

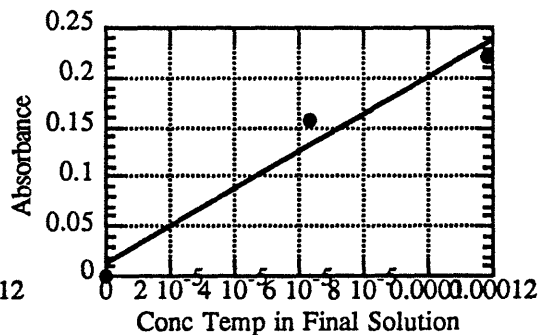
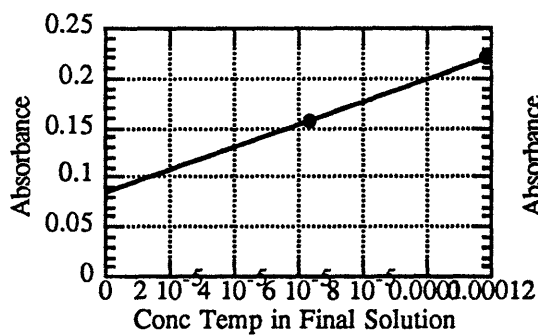
R = 0.99752







Owing to time restrictions, the calibration curve of the template is less comprehensive. The data and curve for the template contribution is given below and to the left. Making the logical assumption that a template concentration of zero gives zero color yield, an alternate calibration curve containing the data point (0,0) may be considered. This, referred to as Temp', is given below and to the right:



Conc. Temp in Final Solution	Abs.	Std. Dev.
6.3229e-5	0.158	7.0%
1.1856e-4	0.222	2.1%

Conc. Temp in Final Solution	Abs.	Std. Dev.
6.3229e-5	0.158	7.0%
1.1856e-4	0.222	2.1%
0.000	0.000	

R= 0.9798

The equations for these curves are:

$$\text{Ala: } y = 0.0016294 + 21584x$$

$$\text{Lys: } y = 0.0040948 + 24175x$$

$$\text{NH}_3: y = 0.0155350 + 20286x$$

$$\text{Temp: } y = 0.0848650 + 1156.7x$$

$$\text{Temp': } y = 0.0123040 + 1887.3x$$

### Validity of Assay/Propagation of Error

As with any analytical procedure, there are both determinate and indeterminate sources of error. The following is a sequential discussion of the errors associated with each step of this assay, followed by an overall evaluation of the error levels.

The initial step of transferring blanks and samples to the vacuum hydrolysis tubes is only as accurate and precise as the calibrated pipetmen; according to manufacturer specifications, this error is no more than  $\pm 1\%$  in accuracy and  $\pm 0.6\%$  in precision. The hydrolysis reagent is added and then removed from the system and thus has no associated errors. A potential source of indeterminate error in the hydrolysis procedure is sample loss, either through degassing or removal of the hydrolysis reagent. When done properly, no solution escapes the hydrolysis tubes during degassing, and all observations indicate that no sample is lost in the removal of the hydrolysis reagent. Reconstitution of the residue following hydrolysis is again subject to the errors associated with the pipetmen used.

Error in the addition of the two reagents for the colorimetric assay is dependent on the inherent errors in the automatic dispensers; an accuracy level of  $\pm 1\%$  and a precision level of  $\pm 0.5\%$  are quoted by the manufacturer. Dilution of the solution immediately after color development again is dependent on the automatic dispenser used; those errors are  $\pm 0.5\%$  in accuracy and  $\pm 0.1\%$  in repeatability. Any further dilutions, when necessary, are subject to the same criteria.

Errors associated with the subsequent comparison of the absorbance value obtained for a given sample to the calibration curves are subject to the errors in the calibration curves. Errors in weight measurements ( $\leq \pm 1\%$ ), in preparation of the stock solutions ( $\leq \pm 1\%$ ), and in dilutions of the stock solutions ( $\leq \pm 1\%$ ) are all factors. In general, individual data points had standard deviations in the range of 0.5-2%.

When taken together, some of the specific errors can be considered unimportant, while others must be regarded as significant. Furthermore, the existence of indeterminate errors cannot be disregarded and must be factored in when making an overall estimate of error. Volume transfer and weight determination errors are so small that they can be ignored. More significant are the indeterminate errors associated with the procedure as a whole. Based on experimental results in this thesis, these errors give rise to standard deviations on the order of  $\pm 5\%$  in absorbance values. When comparison to the calibration curves to determine the sample concentration is taken into consideration, the overall error associated with this assay is at a maximum of  $\pm 7\%$  with a more likely estimate of  $\leq \pm 5\%$ .

## **Appendix A**

### **Development of the Ninhydrin Assay for Concentration Determination**

## INTRODUCTION

The accurate determination of sample concentration in CD studies is of utmost importance as an appropriate calculation of molar ellipticity is completely dependent on this value. A major aim of this thesis has been to develop methodology suitable for the concentration determination of templated derivatives. This appendix presents the development of a ninhydrin assay for this purpose, and demonstrates the high level of accuracy achieved.

Due to the tendency of protein and peptide samples to retain impurities, the accurate determination of their solution concentrations is a nontrivial task. Concentration determination by weight is inappropriate as typical samples are usually prepared from just a few milligrams of compound, which are often highly hydrated. Absorption of tyrosine or tryptophan by UV/Vis spectroscopy under denaturing conditions is frequently used in the determination of protein concentrations (Johnson, 1990), but suffers from a number of disadvantages. The absorption of tyrosine is dependent on its local environment, and the extinction coefficient of tyrosine is low. Its use is particularly problematic for short peptides, as most short peptides of interest do not contain such a chromophore. While a peptide could be designed to contain a tyrosine residue, a strong assumption must be made, that the presence of a tyrosine residue at the end of the peptide does not affect its helicity and has no effect on the CD signal of that peptide. This assumption was invalidated by Baldwin and coworkers (Chakrabartty *et. al.*, 1993), who had previously developed and used a method of tyrosine absorption (Marqusee *et. al.*, 1989), arguing that the standard techniques of amino acid analysis or ninhydrin assay had inherent errors far too large to be acceptable for CD analysis. Error in amino acid analysis is held to be  $\pm 5\%$ , if not more (Marqusee *et. al.*, 1989; Chakrabartty *et. al.*, 1993b). In fact, investigation of this in conjunction with the MIT Biopolymers Laboratory showed the error level to lie in the range of  $\pm 5-10\%$ . As routine amino acid analysis is an automated procedure, it affords little room for improvement.

The ideal assay would be performed directly on an unaltered CD sample, would be sufficiently convenient for routine use, and most importantly would be both precise and accurate. In principle, ninhydrin fulfills all these roles. It is sensitive at the low concentrations used in CD analysis and it is a relatively simple spectrophotometric technique, monitoring in the visible range, where spectral interference is unlikely. Current literature methods for ninhydrin analysis, however, suffer from a lack of both precision and accuracy. Concentrations are based on comparison to an internal standard such as leucine or to a literature extinction coefficient, for which there is more than one value (Hirs,

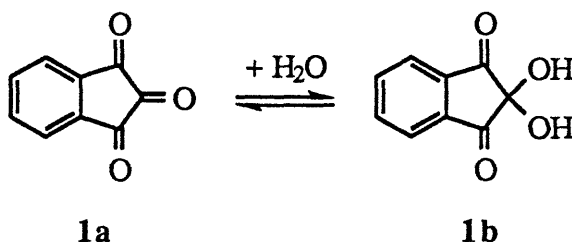
1967; Sarin *et. al.*, 1981). Baldwin and coworkers claim that ninhydrin suffers from an inherent error level of 5-10% and underestimates the concentration by up to 20% (Marqusee *et. al.*, 1989).

For our purposes, only alanine, lysine, and ammonia (for *N*-terminal amides) need be considered. Thus a calibration curve of the ninhydrin response to each of these, as well as to the template, was determined as a means of circumventing many of the problems of the literature methods. In addition, steps were taken to establish an optimal procedure, to determine its tolerance for alterations in protocol, and to demonstrate its reproducibility.

This appendix will first present the relevant history and chemistry of ninhydrin as they bear on the development of an appropriate assay. It will then discuss the development of an optimized procedure. Finally, the precision and accuracy of the current method will be demonstrated in conjunction with the development of the calibration curves.

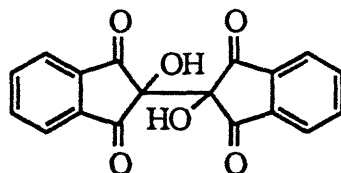
## HISTORY AND CHEMISTRY OF NINHYDRIN

Ninhydrin, 1,2,3-indanetrione or 1,2,3-triketohydrindene, **1a**, was first synthesized by Siegfried Ruhemann in 1910 as an unexpected product in a synthesis aimed at forming a diketone moiety (Ruhemann, 1910a). In water, ninhydrin exists primarily as its hydrate, **1b**; the yellow color observed is most likely due to the trace amount of **1a** present at equilibrium.



Ruhemann discovered shortly thereafter that upon warming with amines and amino acids, "a deep blue colour is produced" (Ruhemann, 1910b) and determined that ninhydrin was a useful reagent in the detection of amino acids (Ruhemann, 1911a). With extensive analysis, Ruhemann (Ruhemann, 1911a; 1911b; 1911c; 1912) was able to discern the fundamental principles of ninhydrin chemistry and to correctly identify the basic structure of the colored product, diketohydrindylidene-diketohydrindamine (DYDA), **2**, which is more commonly known as Ruhemann's purple. Its structure was determined by analogy to the conversion of alloxan to murexide. DYDA has a  $pK_a$  near zero (Friedman & Williams, 1974). While not indefinitely stable (Joullié *et. al.*, 1991), it has previously been shown to





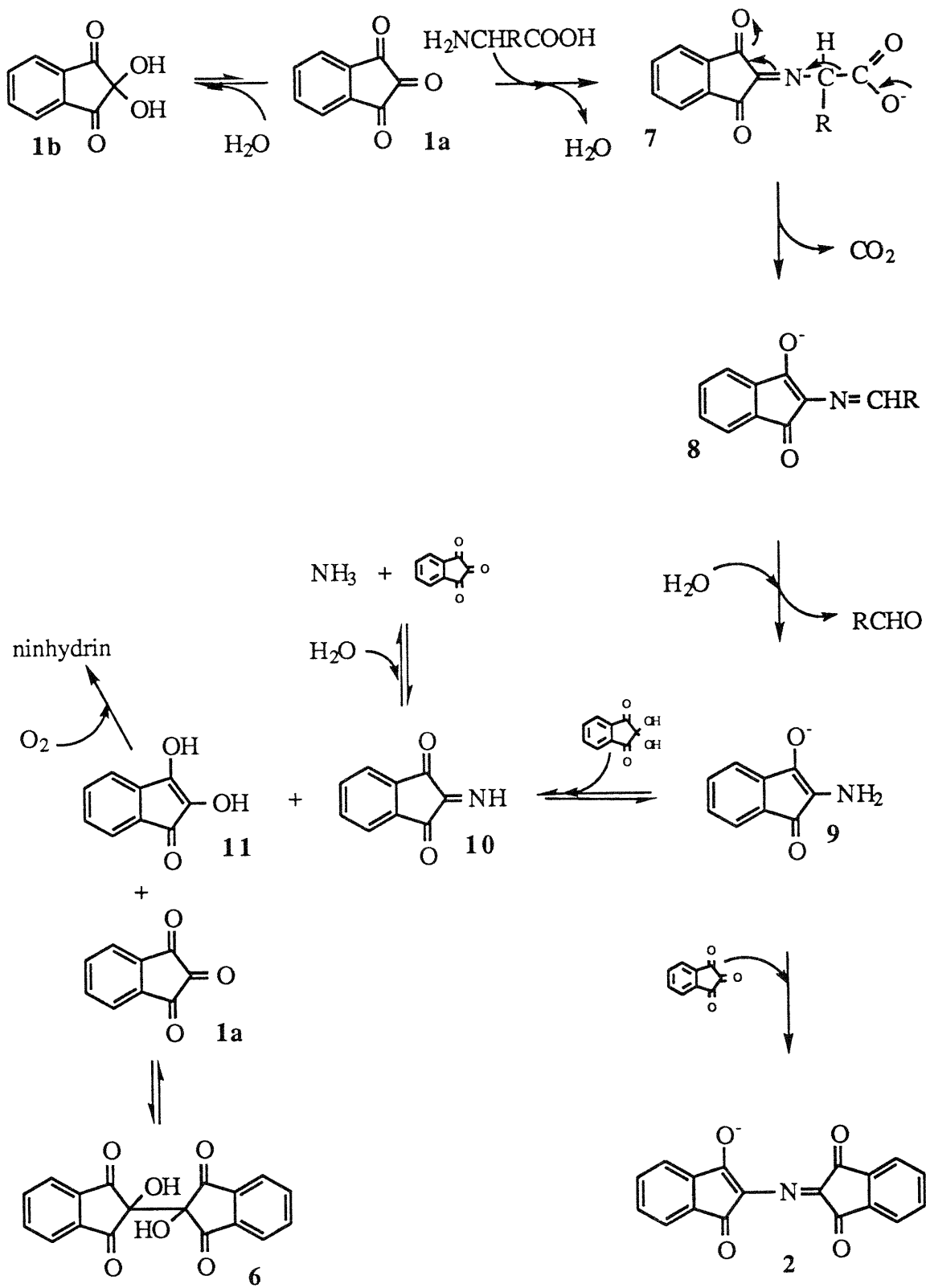
6

Rational optimization of the ninhydrin assay must begin with a thorough understanding of the complex chemistry involved; indeed, many variations of the mechanism of the reaction of ninhydrin with amines and amino acids have been proposed. The first mechanism, albeit an implausible one, was postulated by Ruhemann to explain the reaction of ninhydrin with amino acids. His hypothesis, however, was unable to account for several experimental observations, including the reaction of ninhydrin with ammonium salts, the increased rate of reaction of amino acids relative to amines, and the effects of hydrindantin when present. Since then, numerous mechanisms have been put forth in an effort to explain the observed chemistry of ninhydrin (McCaldin, 1960). Hydrindantin has been postulated to be both an active participant in the mechanism as well as simply part of a side reaction. The formation of an alternate colored compound from the reaction of ninhydrin with imino acids has also been addressed.

The most plausible mechanism for the reaction of ninhydrin with amino acids is given in the following scheme. In this mechanism, the amino acid attacks ninhydrin to form a Schiff's base, **7**, which subsequently decarboxylates to give the aldimine **8**. Hydrolysis yields the amine **9**, which may then undertake one of two pathways. In the first, it condenses with an additional molecule of ninhydrin to give the expected deep blue/purple colored product. In the second, it undergoes a redox reaction with ninhydrin to give adduct **10** and adduct **11**, the enol form of 2-hydroxy-1,3-indanedione, which is occasionally incorrectly referred to as hydrindantin in the literature. **10** may undergo hydrolysis to yield ninhydrin and ammonia. The conjugate base of **11** is red in color, and rapid air oxidation of **11** gives ninhydrin. The red color of the anion of **11** competes with the color of **2**, and air exposure immediately following color development is frequently recommended.

Stein & Moore introduced hydrindantin, **6**, via *in situ* reduction of ninhydrin, in response to the observation of others that little to no color yield was obtained for samples of very low concentration (Moore & Stein, 1948). Additionally, reproducibility was markedly improved with the presence of hydrindantin. Hydrindantin may be generated from ninhydrin by a number of reducing agents, including ascorbic acid, stannous





chloride, and cyanide. It is in rapid equilibrium with ninhydrin and **11** via a retroaldol reaction.

This mechanism explains the need for a reducing agent for the complete development of DYDA. The reducing agent generates hydrindantin, which serves as a redox buffer. In the presence of air, **11** may be irreversibly lost from solution by oxidation to ninhydrin, disabling complete conversion of amine to DYDA. Hydrindantin ensures a constant concentration of **11**, thus driving the equilibrium toward **2**. The red color of the conjugate base of **11** is then depleted by air exposure after color development. The observation of Stein & Moore that ammonia itself does not react with ninhydrin unless hydrindantin is present in solution is also in accordance with the above mechanism.

The reaction of amines with ninhydrin is held to proceed through a similar pathway; formation of the aldimine occurs through loss of a proton rather than decarboxylation. The reaction of imino acids is similar as well, but with a rather different product, accounting for the alternate color produced.

## DEVELOPMENT OF OUR ASSAY

As templated peptides lack a free amino group, it is necessary to hydrolyze the sample prior to the colorimetric assay. The products of this reaction include hydrolyzed template and alanine, and possibly lysine and ammonia, depending on the particular template derivative. This mixture is then subjected to a ninhydrin assay and compared to calibration curves for concentration determination. This section will therefore review the efforts made in establishing both the colorimetric assay as well as the hydrolysis procedure. A brief discussion of ninhydrin assays in the literature will first be presented.

### Ninhydrin Assays in the Literature

The first reproducible quantitative assay was developed by Stein & Moore for use in amino acid analysis (Moore & Stein, 1948). In brief, their procedure involved the preparation of a single solution of ninhydrin and stannous chloride in a 1:1 mixture of methyl cellosolve and 0.2 M citrate buffer. Methyl cellosolve was employed as it was found to have the highest solvating capacity for hydrindantin, which is quite water insoluble. Other workers have noted a decrease in color yield without this solvent present in solution (Rosen *et. al.*, 1962). Solutions for analysis were neutralized, combined with the ninhydrin reagent, developed in a hot water bath, diluted with a 1:1 mixture of water

and isopropanol (necessary to avoid precipitation of the sodium salt of DYDA found for dilution with water only), and monitored at 570 nm.

An extensive analysis of a variety of amine compounds and amino acids showed that different amino acids gave different color yields per mole, a fact that was recognized by Harding many years prior (Harding & MacLean, 1915) and supported by others (Friedman & Williams, 1974; Sheng *et. al.*, 1993). Stein & Moore recognized that a quantitative assay would require that a correction factor be used for the individual amino acids in question.

The procedure of Stein & Moore was later modified (Moore & Stein, 1954) by increasing the strength of the buffer used to eliminate the need to neutralize samples prior to analysis and by adding hydrindantin itself directly to the reagent solution to avoid the precipitation of tin salts. The effective concentration of hydrindantin was increased.

The procedure of Stein & Moore possesses one fundamental problem, however, which is the stability of the ninhydrin reagent. It calls for careful storage under nitrogen and in the dark; solution lifetime under these conditions is still only approximately one week. Other workers (Hirs, 1967) have stressed these storage conditions also, as well as the need to keep the solution chilled. These requirements are primarily due to the presence and stability of hydrindantin in solution, as it is sensitive to atmospheric oxygen, light, and temperature, as well as pH (Joullié *et. al.*, 1991).

Rosen (Rosen, 1957) adapted the procedure to circumvent the problem of reagent degradation. His procedure employs two solutions: one containing ninhydrin in methyl cellosolve and the other an acetate buffer containing a reducing agent, in this case sodium cyanide, which had been shown earlier to adequately reduce ninhydrin (Troll & Cannan, 1953; Yemm & Cocking, 1955). The two solutions are combined immediately before heating, generating the required hydrindantin *in situ* just prior to analysis while avoiding the problem of reagent stability. He reports the two solutions to be indefinitely stable at room temperature.

A somewhat different procedure was introduced as a means by which to maximize color yield (Troll & Cannan, 1953); a primarily organic solution containing phenol and pyridine produced nearly optimal color yields for all but two amino acids. However, a number of disadvantages were noted for this method. It is not convenient for the analysis of aqueous samples (Moore & Stein, 1954), the pH is difficult to control, high water blanks may be obtained, and it requires the routine use of pyridine and phenol (Yemm & Cocking, 1955).

## Development of the Colorimetric Ninhydrin Assay

An early attempt in the development of a suitable ninhydrin assay was founded in the methodology presented by Hirs (Hirs, 1967), whose procedure also contains details for sample hydrolysis and was thus initially chosen for evaluation. The ninhydrin reagent is prepared by the addition of ninhydrin and hydrindantin, then an acetate buffer, to methyl cellosolve, all under nitrogen to avoid oxygen incorporation.

The ninhydrin reagent, prepared in a round bottom flask under nitrogen, was deep wine-red in color. A series of solutions containing alanine and lysine were prepared to serve as trial solutions. Blank readings were found to be quite high, on the order of 0.2-0.3 absorbance units. Directions on the preparation of a similar solution marketed by Pierce suggested that it was necessary to bubble nitrogen through the reagent until it was straw yellow in color. The Hirs reagent was therefore prepared in this fashion, and the blank was significantly lower, i.e. < 0.1 absorbance units.

A set of experiments was then performed to determine the importance of the amount of time allowed for color development in the water bath. Longer times gave only very slightly higher color yields. Protected lysine, in the form of N- $\alpha$ -Boc-Lys-OH, was also evaluated to determine if the  $\epsilon$ -amino group of lysine was reactive toward the ninhydrin reagent, and this was found to be the case.

It was decided at this point to embark on the creation of a calibration curve to which actual samples could be compared. In his procedure, Hirs gives the extinction coefficient of DYDA as  $2 \times 10^{-4} \text{ M}^{-1} \text{ cm}^{-1}$  and suggests the peptide concentration be computed from this and the measured absorbance reading. Alternate values of the extinction coefficient, however, are quoted in the literature (Sarin *et al.*, 1981). Given this and the findings of earlier researchers regarding differential color development for individual amino acids, it was considered more appropriate to generate calibration curves for the determination of sample concentrations. During data collection, however, reproducibility was deemed to be a problem and was thought to be due to an aging solution.

Numerous attempts were made to create a new solution as before by purging the reagent solution with nitrogen, but each attempt yielded a solution of a color different than the original solution and with a blank reading in the range of 0.1-0.2 absorbance units. Solution colors ranged from deep red to bright yellow; there appeared to be no definitive pattern to the observed color changes. Knowing that oxygen can affect significant changes in the ninhydrin reagent, the question arose of whether nitrogen bubbling was in fact purging the solution of oxygen or merely agitating the solution and thereby incorporating atmospheric oxygen. Using apparatus designed to ensure a completely anaerobic system,

an extensive analysis of the role of oxygen incorporation led to the conclusion that the reagent solution is a deep red under anaerobic conditions and fades to a yellow color with oxygen incorporation. The same observations were made for a solution of hydrindantin only. Along these lines, Rosen and coworkers had noted that the cyanide concentration in their procedure was rather important as too little decreases color yield and too much gives a pink color that raised blank levels (Rosen, 1962). Taken together, these observations attest to the fact that the red color of hydrindantin is lost upon its destruction by oxygen.

A suitable batch of reagent was finally prepared and individual steps of the assay analyzed to determine for which it was crucial to be consistent. Only the amount of time the sample spent in the boiling water bath was found to be critical. Variations in the following factors were found to be unimportant: time of shaking prior to color development, time of cooling after color development, order of dilution and cooling, and extent of shaking after color development.

Reproducibility remained a serious problem, however, and was held to be based on the inherent instability of hydrindantin. Furthermore, as described above, it was rather difficult to prepare a suitable batch of reagent. It was clear that the inherent instability of hydrindantin would prove to be a continual problem, even under highly controlled conditions, and made the use of the Hirs procedure inappropriate for routine analysis. Thus the Rosen procedure, in which hydrindantin is not generated until immediately prior to color development, was investigated and found to be suitable.

### **Current Ninhydrin Assay**

Many details both of the development of the current assay and of its execution may be found in the experimental section and will therefore not be discussed in length here. Rather, this section will address the assay as it relates to the preceding discussion.

All attempts were made to ensure the use of reagents of the highest possible purity to avoid any potential problems owing to reagent contamination. As Rosen describes in his procedure, two solutions were prepared. The first consisted of recrystallized ninhydrin in peroxide-free methyl cellosolve, and the second contained sodium cyanide in a sodium acetate buffer. Despite claims by Rosen to the contrary, the ninhydrin solution does not have an indefinite lifetime. Peroxides build up in the solution over time and interfere with proper color development. The ninhydrin solution was therefore monitored regularly for peroxides and replaced when necessary. In addition, consideration was given to volume and weight measurements; calibrated pipettes or automatic dispensers were used for

volume transfers, a microbalance was used for weight measurements, and all solutions were prepared in "Class A" volumetric flasks.

Reproducibility with this procedure was of central importance and was subjected to evaluation prior to further development of this method. Using a stock solution of alanine in water, reproducibility levels were found to be in the acceptable range of  $\pm 1-7\%$  and were improved to  $\pm 1-2\%$  with the introduction of automatic dispensers to aliquot out the reagent solutions. Shaking and cooling times following color development were again varied, with no apparent effects. Vigorous shaking is stressed in some procedures to oxidatively destroy any remaining hydrindantin and thus lower the blank values (Moore & Stein, 1954), but shaking beyond that necessary to achieve solution homogeneity was not found to have any effect.

The above analyses established the relevant variables of the colorimetric assay, yielding a viable, reproducible procedure. Attention was then directed to the hydrolysis procedure.

### Sample Hydrolysis

The hydrolysis procedure of Hirs involves hydrolysis under alkaline conditions in an autoclave followed by neutralization. It was investigated, but with no success. The neutralized solutions gave high blank readings, but more importantly, the sample solutions gave no detectable color yield. Thus a vacuum hydrolysis procedure recommended by Pierce was considered, and the initial results were rather unusual. Following lyophilization, acid hydrolysis, and removal of the hydrolysis reagent under vacuum, the alanine stock solution was put through the colorimetric assay, but no color was observed. The colorimetric assay was performed on the same solution, but without hydrolysis, and found to give full color yield. It was obvious that the sample had somehow been lost, and the source of this loss was investigated. The initial lyophilization step was replaced by oven drying, with the same results. A set of samples was partially lyophilized prior to hydrolysis, and partial color development ensued. Neutral alanine is easily sublimed, explaining why here, under neutral pH, alanine was easily removed and lost under high vacuum. It was thus deemed necessary to lower the pH of the solution to avoid this problem by performing the acid hydrolysis procedure directly on the sample solution. It is probable that the same explanation applies to the oven dried samples, and most likely accounts for the results observed in the Hirs hydrolysis procedure. However, vacuum hydrolysis proved to be the more practical procedure as it was difficult to use the autoclave on a regular basis; the Pierce procedure was therefore chosen over the Hirs method.

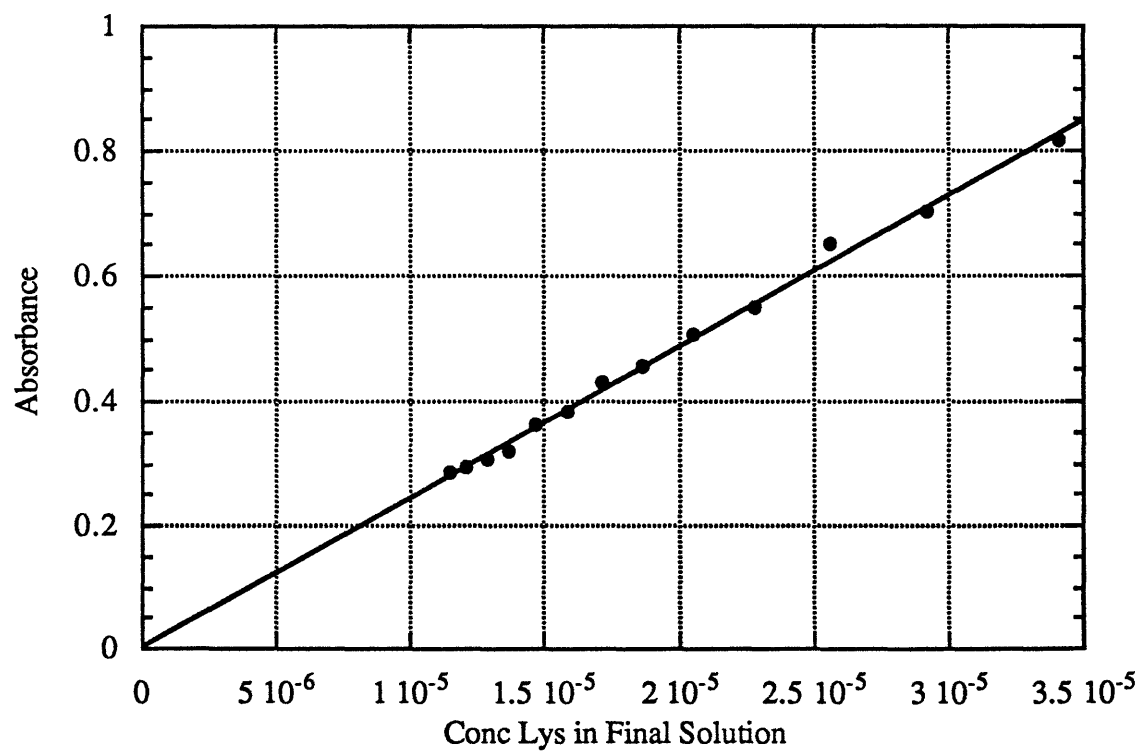
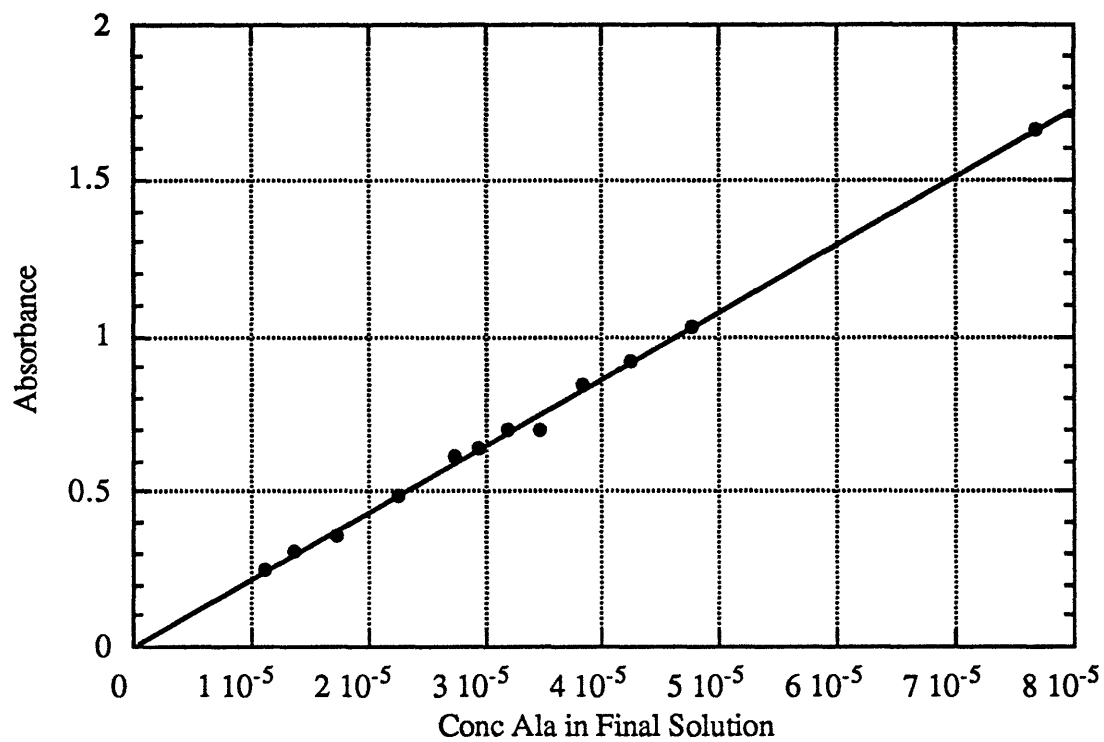
One additional experiment finalized the specifics of the hydrolysis procedure. Aliquots of the alanine solution containing varying quantities of the acid mixture used for hydrolysis were subjected to the ninhydrin assay. In all cases, no color development ensued and complete acid removal following hydrolysis was deemed essential. Poor or no color development at low pH has been previously noted (Moore & Stein, 1948; D'Aniello *et. al.*, 1985). Samples were then reconstituted in a known volume of water.

## **DEMONSTRATION OF PRECISION AND ACCURACY & CREATION OF THE CALIBRATION CURVES**

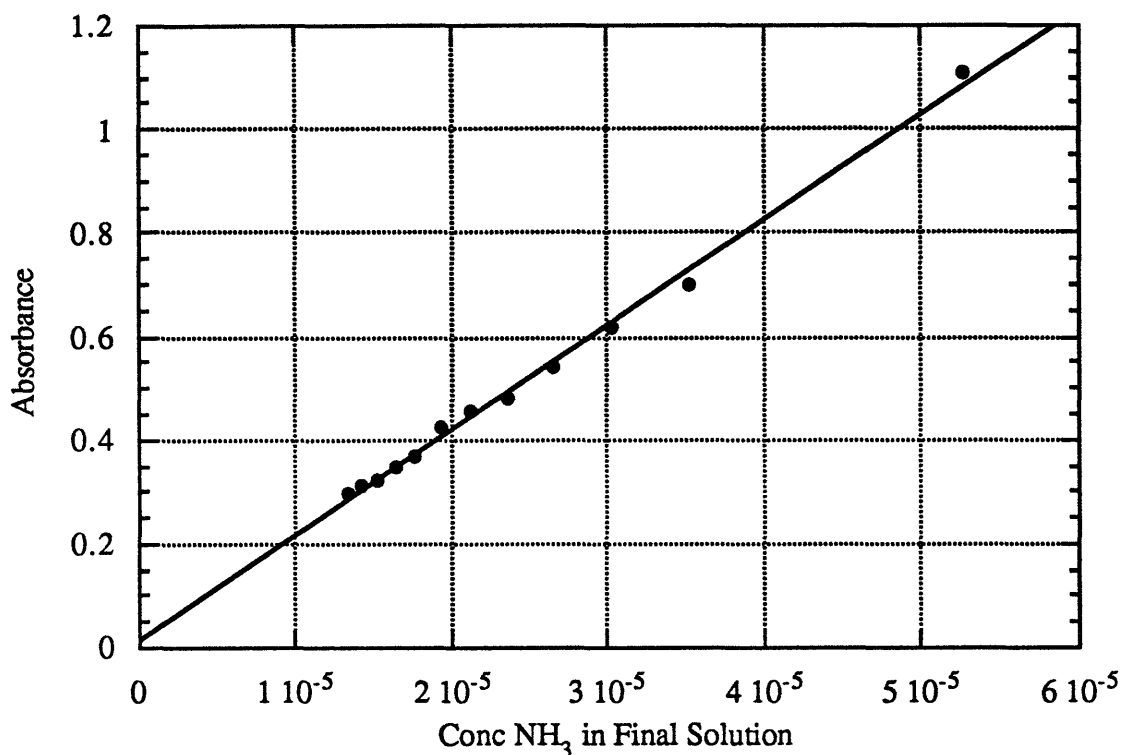
Once the specific details of the assay had been developed, much effort was expended in the development of calibration curves for the response of alanine, lysine, ammonia, and the template to the colorimetric assay. Alanine and lysine were recrystallized and extensively dried prior to dissolution to create a stock solution for analysis. A portion of the recrystallized alanine was subjected to combustion analysis to ensure that no residual water remained in the sample following recrystallization; this was found to be the case. The stock solution of template was prepared in a similar fashion; aliquots were then subsequently hydrolyzed. The stock solution of ammonia was purchased in the form of an analytical standard for ammonium ion. Each stock solution was serially diluted, and the resulting solutions subjected to multiple repeats of the colorimetric assay. The results were averaged, and a plot of absorbance versus concentration was created for each amino acid/amine. The data from actual samples can be compared to these calibration curves for an appropriate concentration determination.

Analysis of a sample therefore involves vacuum hydrolysis directly on the sample solution, removal of the acid mixture and reconstitution in pure water, addition of the ninhydrin reagents, color development, dilution, measurement at 570 nm, and comparison to carefully devised calibration curves.

The calibration curves for alanine, lysine, and ammonia are given below. In general, individual data points had standard deviations in the range of 0.5-2%. The proximity of all the data points to the best-fit line is testimony to the high level of accuracy and precision achieved with this assay.







The assay, in its final, carefully developed form, circumvents previous difficulties associated with quantitative ninhydrin assays and does so with much attention to the minimization of error. Solution instability and hence irreproducibility in the colorimetric assay have been eliminated through the use of stable reagents as introduced by Rosen. Calibration curves have been created for each reactive species to circumvent the problem of differential color development for different amino acids. All materials and reagents are of the highest possible purity and all weights and measurements are made with the most precise and accurate equipment available. Volume transfer and weight determination errors are so small that they can be ignored. More significant are the indeterminate errors associated with the procedure as a whole. Based on experimental results in this thesis, these errors give rise to standard deviations on the order of  $\pm 5\%$  in absorbance values. Values are then compared to the calibration curves to determine the sample concentration; the error in these curves is at a maximum of  $\pm 2\%$ . Use of the calibration curves for the specific amino acids of interest eliminates the low color yield of up to 20% observed by Baldwin and coworkers. Taken together, these considerations give a quantitative ninhydrin assay with an error level of  $\pm 7\%$  at most and a more likely estimate of  $< \pm 5\%$ .

## **Appendix B**

CD Data Analysis: Derivations and Results

### B.1 Determination of the Mole Fraction of the TE State, $\chi_{te}$

The mole fraction of the te state of any given derivative may be determined directly from its t/c ratio, as shown in the following derivation. Tables B.1.1 and B.1.2 show the results of this computation for the alanine series in various mole percentages of TFE.

$$\begin{aligned}
 t/c &= \frac{ts + te}{cs}; \quad te = (cs)(t/c) - ts & \frac{ts}{cs} &= 0.79 \\
 \chi_{te} &= \frac{te}{cs + ts + te} = \frac{te}{(cs)\left(1 + \frac{ts + te}{cs}\right)} = \frac{(cs)(t/c) - ts}{(cs)(1 + t/c)} \\
 &= \frac{(cs)(t/c)}{(cs)(1 + t/c)} - \frac{ts}{(cs)(1 + t/c)} = \frac{t/c}{(1 + t/c)} - \frac{0.79}{(1 + t/c)} \\
 &= \frac{t/c - 0.79 + 1 - 1}{1 + t/c} = \frac{(1 + t/c) - 1.79}{1 + t/c} \\
 \chi_{te} &= 1 - \frac{1.79}{1 + t/c}
 \end{aligned}$$

Mole Percent	Ac-Hel <sub>1</sub> -NH <sub>2</sub>	Ac-Hel <sub>1</sub> -A <sub>1</sub> -NH <sub>2</sub>	Ac-Hel <sub>1</sub> -A <sub>2</sub> -NH <sub>2</sub>	Ac-Hel <sub>1</sub> -A <sub>3</sub> -NH <sub>2</sub>	Ac-Hel <sub>1</sub> -A <sub>4</sub> -NH <sub>2</sub>	Ac-Hel <sub>1</sub> -A <sub>5</sub> -NH <sub>2</sub>	Ac-Hel <sub>1</sub> -A <sub>6</sub> -NH <sub>2</sub>
0	0.37	0.18	0.24	0.26	0.30	0.36	0.40
2				0.28	0.36	0.41	0.55
3	0.38	0.21	0.26				
4				0.37	0.44	0.51	0.79
6	0.44	0.33	0.45	0.51	0.61	0.67	0.85
8				0.66	0.73	0.82	0.90
10	0.56	0.56	0.71	0.74	0.82	0.88	
12				0.81	0.86	0.91	
13	0.63	0.66	0.78				
14				0.83	0.89		
16	0.66	0.71	0.82	0.86	0.91		
18				0.88	0.92		
20	0.68	0.75	0.85	0.89	0.94		

**Table B.1.1:**  $\chi_{te}$  values for the series Ac-Hel<sub>1</sub>-A<sub>n</sub>-NH<sub>2</sub>, n=0-6, calculated from experimental t/c values measured by Dr. K. McClure.

Mole Percent	Ac-Hel <sub>1</sub> -A <sub>1</sub> -OH	Ac-Hel <sub>1</sub> -A <sub>2</sub> -OH	Ac-Hel <sub>1</sub> -A <sub>3</sub> -OH	Ac-Hel <sub>1</sub> -A <sub>4</sub> -OH	Ac-Hel <sub>1</sub> -A <sub>5</sub> -OH	Ac-Hel <sub>1</sub> -A <sub>6</sub> -OH
0	0.00	0.18	0.21	0.24	0.28	0.36
2				0.27	0.32	0.39
3	0.01	0.23	0.28			
4				0.34	0.47	0.55
6	0.10	0.36	0.49	0.56	0.63	0.70
8				0.67	0.74	0.82
10	0.28	0.60	0.68	0.75	0.82	0.89
12				0.79	0.85	0.91
13	0.33	0.67	0.75			
14				0.82	0.88	0.92
16	0.36	0.72	0.78	0.84	0.89	0.93
18				0.86	0.90	0.93
20	0.38	0.74	0.82	0.86	0.92	0.94

**Table B.1.2:**  $\chi_{te}$  values for the series Ac-Hel<sub>1</sub>-A<sub>n</sub>-OH, n=1-6, calculated from experimental t/c values of Chapter 3.

## B.2 Simple Linear Regression in Two Variables: Least Squares Analysis

For a series of equations  $y = \beta_1 x + \beta_0$ , a linear regression analysis to solve for the slope  $\beta_1$  and the intercept  $\beta_0$  simplifies to a least squares analysis. Through the following equations,  $\beta_1$  and  $\beta_0$  may be solved (Mendenhall & Beaver, 1991):

$$\hat{\beta}_1 = \frac{S_{xy}}{S_{xx}} \quad ; \quad \hat{\beta}_0 = \bar{y} - \beta_1 \bar{x} \quad ; \quad \text{std. dev. (ord.)} = \sqrt{\frac{S_{yy} - \beta_1 S_{xy}}{(n-2)}}$$

where

$$S_{xx} = \sum_{i=1}^n (x_i - \bar{x})^2 = \sum_{i=1}^n x_i^2 - \frac{\left(\sum_{i=1}^n x_i\right)^2}{n}$$

$$S_{xy} = \sum_{i=1}^n (x_i - \bar{x})(y_i - \bar{y}) = \sum_{i=1}^n x_i y_i - \frac{\left(\sum_{i=1}^n x_i\right)\left(\sum_{i=1}^n y_i\right)}{n}$$

$$S_{yy} = \sum_{i=1}^n (y_i - \bar{y})^2 = \sum_{i=1}^n y_i^2 - \frac{\left(\sum_{i=1}^n y_i\right)^2}{n}$$

### B.3 Evaluation of the Template Contribution to the Observed CD Signal by Linear Regression Analysis of Ac-Hel<sub>1</sub>-NH<sub>2</sub> in Various Mole Percentages of TFE

The derivative Ac-Hel<sub>1</sub>-NH<sub>2</sub> contains no amino acids but is still able to develop te character and is therefore ideally suited for the determination of the contribution of the template to the overall CD signal of a given template derivative. Its observed CD spectrum is a sum of the contributions of the nonnucleating states, i.e. (cs+ts), and the nucleating state te.

$$\theta_{\text{obs}} = \theta_{\text{te}} \chi_{\text{te}} + \theta_{(\text{cs}+\text{ts})} \chi_{(\text{cs}+\text{ts})}$$

The relative proportions of these states is altered by the addition of TFE. Rearrangement of the above equation gives a standard linear equation in the form of  $y = \beta_1 x + \beta_0$ .

$$\chi_{\text{te}} + \chi_{(\text{cs}+\text{ts})} = 1; \quad \chi_{(\text{cs}+\text{ts})} = 1 - \chi_{\text{te}}$$

$$\theta_{\text{obs}} = \theta_{\text{te}} \chi_{\text{te}} + \theta_{(\text{cs}+\text{ts})} \chi_{(\text{cs}+\text{ts})}$$

$$= \theta_{\text{te}} \chi_{\text{te}} + \theta_{(\text{cs}+\text{ts})} (1 - \chi_{\text{te}})$$

$$= \theta_{\text{te}} \chi_{\text{te}} + \theta_{(\text{cs}+\text{ts})} - \theta_{(\text{cs}+\text{ts})} \chi_{\text{te}}$$

$$\theta_{\text{obs}} = (\theta_{\text{te}} - \theta_{(\text{cs}+\text{ts})}) \chi_{\text{te}} + \theta_{(\text{cs}+\text{ts})}$$

$$\theta_{\text{obs}} = \beta_1 \chi_{\text{te}} + \beta_0 \quad \text{where} \quad \beta_1 = \theta_{\text{te}} - \theta_{(\text{cs}+\text{ts})}; \quad \beta_0 = \theta_{(\text{cs}+\text{ts})}$$

A linear regression analysis on a series of TFE concentrations (and thus a series of  $\chi_{\text{te}}$ ) at each wavelength where the observed ellipticity  $\theta_{\text{obs}}$  is plotted as a function of  $\chi_{\text{te}}$  will yield values for  $\theta_{\text{te}}$  and  $\theta_{(\text{cs}+\text{ts})}$  for each wavelength, where  $\theta_{(\text{cs}+\text{ts})}$  is equal to the intercept and  $\theta_{\text{te}}$  is equal to the slope plus the intercept. Thus the spectra corresponding to the (cs+ts) and the te states of the template can be determined.

This analysis and subsequent analyses were completed through the use of an Excel spreadsheet. The original data was imported into Excel and corrected for baseline discrepancies by subtracting the ellipticity value at 270 nm from the entire spectrum. The appropriate formulas were incorporated into the spreadsheet to perform the least squares analysis. A copy of the spreadsheet is given at the end of this appendix.

#### B.4 Correction for the Template Contribution to the Observed CD Signal

With the above analysis, it is possible to appropriately correct any CD spectrum for the template contribution. Subtracting the contribution of the template from that of a derivative yields a spectrum corresponding to the contribution of the attached peptide only ( $\theta_{\text{peptide}}$ ). Such calculations may be performed as follows, where  $\theta_{T-\text{te}}$  and  $\theta_{T-(\text{cs}+\text{ts})}$  represent the ellipticity of the te and the (cs+ts) states of the template, respectively, and where  $\beta_1$  is the slope and  $\beta_0$  the intercept determined in section B.3. The original data was corrected for baseline discrepancies as above.

$$\begin{aligned}
 \theta_{\text{peptide}} &= \theta_{\text{obs}} - \theta_{T-\text{te}}\chi_{\text{te}} - \theta_{T-(\text{cs}+\text{ts})}\chi_{(\text{cs}+\text{ts})} \\
 &= \theta_{\text{obs}} - \theta_{T-\text{te}}\chi_{\text{te}} - \theta_{T-(\text{cs}+\text{ts})}(1 - \chi_{\text{te}}) \\
 &= \theta_{\text{obs}} - \theta_{T-\text{te}}\chi_{\text{te}} - \theta_{T-(\text{cs}+\text{ts})} + \theta_{T-(\text{cs}+\text{ts})}\chi_{\text{te}} \\
 &= \theta_{\text{obs}} - \theta_{T-\text{te}}\chi_{\text{te}} + \theta_{T-(\text{cs}+\text{ts})}\chi_{\text{te}} - \theta_{T-(\text{cs}+\text{ts})} \\
 &= \theta_{\text{obs}} - \chi_{\text{te}}(\theta_{T-\text{te}} - \theta_{T-(\text{cs}+\text{ts})}) - \theta_{T-(\text{cs}+\text{ts})} \\
 \theta_{\text{peptide}} &= \theta_{\text{obs}} - \chi_{\text{te}}(\beta_1) - \beta_0
 \end{aligned}$$

#### B.5 Calculation of Peptide Limiting Helical and Non-helical CD Spectra by Linear Regression Analysis

The values for  $\theta_{\text{peptide}}$  determined in the previous section represent the CD signals of the peptide portion only of the template derivatives. These spectra are composed of the contribution of the peptides attached to the (cs+ts) state of the template, expected to exhibit random coil spectra, together with the contribution of the peptides attached to the te state of the template, expected to exhibit partially helical spectra. A least squares analysis where  $\theta_{\text{peptide}}$  is plotted as a function of  $\chi_{\text{te}}$  for a TFE series of a given derivative yields the limiting spectra  $\theta_{P-(\text{cs}+\text{ts})}$  and  $\theta_{P-\text{te}}$ , where  $\theta_{P-(\text{cs}+\text{ts})}$  represents the limiting ellipticity of the peptide attached to the (cs+ts) state of the template, and  $\theta_{P-\text{te}}$  is the limiting ellipticity of the peptide attached to the te state of the template. This is demonstrated below.

For linear equation  $\theta_{\text{peptide}} = \text{slope}(\chi_{\text{te}}) + \text{intercept}$

at  $\chi_{(\text{cs+ts})} = 1, \chi_{\text{te}} = 0 \rightarrow \theta_{\text{P-(cs+ts)}} = \text{intercept}$

at  $\chi_{(\text{cs+ts})} = 0, \chi_{\text{te}} = 1 \rightarrow \theta_{\text{P-te}} = \text{slope} + \text{intercept}$

## B.6 Correction of $\theta_{\text{peptide}}$ for the Contributions of Random Coil Ellipticities

The analysis of section B.5 gives reliable values for  $\theta_{\text{P-(cs+ts)}}$ , but only an approximation of  $\theta_{\text{P-te}}$ , especially for the shorter derivatives. When the values of  $\chi_{\text{te}}$  are close together and near to zero, only the intercept may be reliably determined. Thus an alternate method is necessary for the determination of  $\theta_{\text{P-te}}$ .  $\theta_{\text{P-(cs+ts)}}$ , weighted by its mole fraction, must be subtracted from  $\theta_{\text{peptide}}$ , and the resultant value then weighted by the mole fraction  $\chi_{\text{te}}$  to give  $\theta_{\text{P-allte}}$ , the CD spectrum of the peptide if only the te state of the template were present. The equation for this computation follows.

$$\theta_{\text{P-allte}} = \frac{\theta_{\text{peptide}} - ((1 - \chi_{\text{te}})\theta_{\text{P-(cs+ts)}})}{\chi_{\text{te}}}$$

## B.7 Preliminary Calculations of the Ellipticity of a Completely Helical Peptide of Length n; s=1 Analysis

Within the peptide attached to the te state of the template are various substates containing some helical and some random coil residues, owing to fraying effects. As an example, Ac-Hel<sub>1</sub>-A<sub>3</sub>-NH<sub>2</sub> may contain up to four hydrogen bonds. Thus the substates, where h denotes a helical residue and c denotes a random coil residue, are

$$\begin{array}{l} \text{h|ccc} \\ \text{h|hcc} \\ \text{h|hhc} \\ \text{h|hhh} \end{array}$$

where the first residue is necessarily helical by definition of the te state of the template. The contribution of this first hydrogen bond has already been accounted for in the template te state corrections. For  $s_{(\text{Ala})} = 1$ , i.e. the spectra recorded in the absence of TFE, the proportions of these states are equal. In order to analyze the per residue ellipticity of the helical residues, the contribution of the random coil residues must first be determined. This

may be done by simply counting the random coil residues in each state and weighting by the fraction of that particular state.

	<i>Fraction</i>	<i>Correction for <math>\theta_{RC}</math></i>
h ccc	1/4	1/4 x 3 $\theta_{RC}$
h hcc	1/4	1/4 x 2 $\theta_{RC}$
h hhc	1/4	1/4 x 1 $\theta_{RC}$
h hhh	1/4	0

$$\text{where } \theta_{RC} = \frac{\theta_{P-cs+ts}}{n}$$

The helical states may be similarly summed, where  $\theta_{Hn}$  represents the per residue ellipticity for an amino acid in a peptide containing n amino acids.  $\theta_{H0}$ , the ellipticity of the first residue, is not counted as its contribution has already been taken into consideration.

	<i>Fraction</i>	<i>Helical Contribution</i>
hlccc	1/4	0
hlhcc	1/4	1/4 x 1 $\theta_{H1}$
hlhhc	1/4	1/4 x 2 $\theta_{H2}$
hlhhh	1/4	1/4 x 3 $\theta_{H3}$

For a particular derivative,  $\theta_{P-allte}$ , less the summation of the random coil corrections, is equal to the summation of the helical contributions. This is summarized below, where  $\theta_{te3N}$  represents  $\theta_{P-allte}$  for the derivative with 3 alanine residues and an N-terminal amide, i.e. Ac-Hel<sub>1</sub>-A<sub>3</sub>-NH<sub>2</sub>.

$$\begin{aligned} \theta_{te3N} - 1/4(3 + 2 + 1)\theta_{RC} &= 1/4 \times \theta_{H1} + 1/4 \times 2\theta_{H2} + 1/4 \times 3\theta_{H3} \\ 4\theta_{te3N} - 6\theta_{RC} &= \theta_{H1} + 2\theta_{H2} + 3\theta_{H3} \end{aligned} \quad (\text{eq. B.7.1})$$

Such an analysis on Ac-Hel<sub>1</sub>-A<sub>4</sub>-NH<sub>2</sub> gives equation B.7.2.



	<i>Fraction</i>	<i>Correction for <math>\theta_{RC}</math></i>	<i>Helical Contribution</i>
h cccc	1/5	1/5 x 4 $\theta_{RC}$	0
h hccc	1/5	1/5 x 3 $\theta_{RC}$	1/5 x 1 $\theta_{H1}$
h hhcc	1/5	1/5 x 2 $\theta_{RC}$	1/5 x 2 $\theta_{H2}$
h hhhc	1/5	1/5 x 1 $\theta_{RC}$	1/5 x 3 $\theta_{H3}$
h hhhh	1/5	0	1/5 x 4 $\theta_{H4}$

$$\theta_{te4N} - 1/5(4 + 3 + 2 + 1)\theta_{RC} = 1/5 \times \theta_{H1} + 1/5 \times 2\theta_{H2} + 1/5 \times 3\theta_{H3} + 1/5 \times 4\theta_{H4}$$

$$5\theta_{te4N} - 10\theta_{RC} = \theta_{H1} + 2\theta_{H2} + 3\theta_{H3} + 4\theta_{H4} \quad (\text{eq. B.7.2})$$

A similar analysis performed on the longer derivatives of the amide series yields equations B.7.3 and B.7.4.

$$6\theta_{te5N} - 15\theta_{RC} = \theta_{H1} + 2\theta_{H2} + 3\theta_{H3} + 4\theta_{H4} + 5\theta_{H5} \quad (\text{eq. B.7.3})$$

$$7\theta_{te6N} - 21\theta_{RC} = \theta_{H1} + 2\theta_{H2} + 3\theta_{H3} + 4\theta_{H4} + 5\theta_{H5} + 6\theta_{H6} \quad (\text{eq. B.7.4})$$

Equation B.7.1 may be subtracted from B.7.2 to solve for  $\theta_{H4}$ , B.7.2 from B.7.3 to solve for  $\theta_{H5}$ , and B.7.3 from B.7.4 to solve for  $\theta_{H6}$ .

$$\theta_{H4} = \frac{5}{4}\theta_{te4N} - \theta_{te3N} - \theta_{RC}$$

$$\theta_{H5} = \frac{6}{5}\theta_{te5N} - \theta_{te4N} - \theta_{RC}$$

$$\theta_{H6} = \frac{7}{6}\theta_{te6N} - \theta_{te5N} - \theta_{RC}$$

An identical analysis can be performed for the acid series, with the exception that the final residue is always in a "c" conformation as it cannot form a hydrogen bond. The analysis for Ac-Hel<sub>1</sub>-A<sub>3</sub>-OH is shown below, where  $\theta_{te3O}$  represents  $\theta_{P-allte}$  for the derivative with 3 alanine residues and an OH terminus, i.e. Ac-Hel<sub>1</sub>-A<sub>3</sub>-OH. Equation B.7.5 results.

	<i>Fraction</i>	<i>Correction for <math>\theta_{RC}</math></i>	<i>Helical Contribution</i>
h ccc	1/3	1/3 x 3 $\theta_{RC}$	0
h hcc	1/3	1/3 x 2 $\theta_{RC}$	1/3 x 1 $\theta_{H1}$
h hhc	1/3	1/3 x 1 $\theta_{RC}$	1/3 x 2 $\theta_{H2}$

$$\begin{aligned}\theta_{\text{te}3\text{O}} - 1/3(3+2+1)\theta_{\text{RC}} &= 1/3 \times \theta_{\text{H}1} + 1/3 \times 2\theta_{\text{H}2} \\ 3\theta_{\text{te}3\text{O}} - 6\theta_{\text{RC}} &= \theta_{\text{H}1} + 2\theta_{\text{H}2}\end{aligned}\quad (\text{eq. B.7.5})$$

Equations B.7.6, B.7.7, and B.7.8 are generated for the longer derivatives of the acid series.

$$4\theta_{\text{te}4\text{O}} - 10\theta_{\text{RC}} = \theta_{\text{H}1} + 2\theta_{\text{H}2} + 3\theta_{\text{H}3} \quad (\text{eq. B.7.6})$$

$$5\theta_{\text{te}5\text{O}} - 15\theta_{\text{RC}} = \theta_{\text{H}1} + 2\theta_{\text{H}2} + 3\theta_{\text{H}3} + 4\theta_{\text{H}4} \quad (\text{eq. B.7.7})$$

$$6\theta_{\text{te}6\text{O}} - 21\theta_{\text{RC}} = \theta_{\text{H}1} + 2\theta_{\text{H}2} + 3\theta_{\text{H}3} + 4\theta_{\text{H}4} + 5\theta_{\text{H}5} \quad (\text{eq. B.7.8})$$

Equation B.7.5 may be subtracted from B.7.6 to solve for  $\theta_{\text{H}3}$ , B.7.6 from B.7.7 to solve for  $\theta_{\text{H}4}$ , and B.7.7 from B.7.8 to solve for  $\theta_{\text{H}5}$ .

$$\theta_{\text{H}3} = \frac{4}{3}\theta_{\text{te}4\text{O}} - \theta_{\text{te}3\text{O}} - \frac{4}{3}\theta_{\text{RC}}$$

$$\theta_{\text{H}4} = \frac{5}{4}\theta_{\text{te}5\text{O}} - \theta_{\text{te}4\text{O}} - \frac{5}{4}\theta_{\text{RC}}$$

$$\theta_{\text{H}5} = \frac{6}{5}\theta_{\text{te}6\text{O}} - \theta_{\text{te}5\text{O}} - \frac{6}{5}\theta_{\text{RC}}$$

## B.8 Calculations of the Ellipticity of a Completely Helical Peptide of Length $n$ ; Variable $s$ Analysis

A more thorough analysis provides for the inclusion of spectra recorded in various concentrations of TFE, but is also more complicated as varying  $s$  values must be considered. For 0 mole% TFE,  $s_{(\text{Ala})}=1$ , for 2 mole%,  $s_{(\text{Ala})}=1.03$ , for 4 mole%,  $s_{(\text{Ala})}=1.06$ , for 6 mole%,  $s_{(\text{Ala})}=1.15$ , for 6 mole%,  $s_{(\text{Ala})}=1.29$ , and for 10 mole% and higher,  $s_{(\text{Ala})}=1.45$ . The analysis of Ac-Hel<sub>1</sub>-A<sub>4</sub>-NH<sub>2</sub> begins with the correction for the random coil residues in the peptide.

	<i>Relative Weight</i>	<i>Fraction</i>	<i>Correction for <math>\theta_{RC}</math></i>
h cccc	1	$\frac{1}{\Sigma}$	$\frac{1}{\Sigma} \times 4\theta_{RC}$
h hccc	s	$\frac{s}{\Sigma}$	$\frac{s}{\Sigma} \times 3\theta_{RC}$
h hhcc	$s^2$	$\frac{s^2}{\Sigma}$	$\frac{s^2}{\Sigma} \times 2\theta_{RC}$
h hhhc	$s^3$	$\frac{s^3}{\Sigma}$	$\frac{s^3}{\Sigma} \times 1\theta_{RC}$
h hhhh	$s^4$	$\frac{s^4}{\Sigma}$	0
$\Sigma=1+s+s^2+s^3+s^4$			$=\frac{\theta_{RC}}{\Sigma}(4+3s+2s^2+s^3)$

Thus  $\theta_{tecorr4N}$ , denoting the te state peptide of Ac-Hel<sub>1</sub>-A<sub>4</sub>-NH<sub>2</sub> corrected for random coil residues, can be computed for each TFE mole percentage of interest.

$$\theta_{tecorr4N} = \theta_{te4N} - \frac{\theta_{RC}}{\Sigma}(4 + 3s + 2s^2 + s^3)$$

The expression in parenthesis may be denoted F(s):

$$\theta_{tecorr4N} = \theta_{te4N} - \frac{F(s)}{\Sigma}\theta_{RC}$$

The appropriate corrections are detailed in Table B.8.1.

	$\frac{F(s)}{\Sigma}$					
	$s=1$	$s=1.03$	$s=1.06$	$s=1.15$	$s=1.29$	$s=1.45$
Ac-Hel <sub>1</sub> -A <sub>4</sub> -NH <sub>2</sub>	2.00	1.94	1.88	1.72	1.50	1.30
Ac-Hel <sub>1</sub> -A <sub>5</sub> -NH <sub>2</sub>	2.50	2.41	2.33	2.10	1.79	1.50
Ac-Hel <sub>1</sub> -A <sub>6</sub> -NH <sub>2</sub>	3.00	2.88	2.77	2.45	2.03	1.66

**Table B.8.1: Random coil residue corrections for the amide series.**

A similar analysis can be performed on the acid series as exemplified by Ac-Hel<sub>1</sub>-A<sub>4</sub>-OH.

	<i>Relative Weight</i>	<i>Fraction</i>	<i>Correction for <math>\theta_{RC}</math></i>
h cccc	1	$\frac{1}{\Sigma}$	$\frac{1}{\Sigma} \times 4\theta_{RC}$
h hccc	s	$\frac{s}{\Sigma}$	$\frac{s}{\Sigma} \times 3\theta_{RC}$
h hhcc	$s^2$	$\frac{s^2}{\Sigma}$	$\frac{s^2}{\Sigma} \times 2\theta_{RC}$
h hhhc	$s^3$	$\frac{s^3}{\Sigma}$	$\frac{s^3}{\Sigma} \times 1\theta_{RC}$
$\Sigma = 1 + s + s^2 + s^3$		$= \frac{\theta_{RC}}{\Sigma} (4 + 3s + 2s^2 + s^3)$	

The appropriate corrections are detailed in Table B.8.2.

	$\frac{F(s)}{\Sigma}$					
	$s=1$	$s=1.03$	$s=1.06$	$s=1.15$	$s=1.29$	$s=1.45$
Ac-Hel <sub>1</sub> -A <sub>4</sub> -OH	2.50	2.46	2.43	2.33	2.17	2.05
Ac-Hel <sub>1</sub> -A <sub>5</sub> -OH	3.00	2.94	2.88	2.72	2.50	2.30
Ac-Hel <sub>1</sub> -A <sub>6</sub> -OH	3.50	3.41	3.33	3.10	2.79	2.50

**Table B.8.2: Random coil residue corrections for the acid series.**

For each derivative at each concentration of TFE, a general expression may be derived to explain the relationship between the above corrected ellipticities and the contributions of the individual helical residues to that ellipticity. The equations for the amide and acid series follow.

$$\theta_{iecorr4N} = \frac{s}{\Sigma} \theta_{H1'} + \frac{s^2}{\Sigma} \theta_{H2'} + \frac{s^3}{\Sigma} \theta_{H3'} + \frac{s^4}{\Sigma} \theta_{H4'} + (0)\theta_{H5'} + (0)\theta_{H6'}$$

$$\theta_{iecorr5N} = \frac{s}{\Sigma} \theta_{H1'} + \frac{s^2}{\Sigma} \theta_{H2'} + \frac{s^3}{\Sigma} \theta_{H3'} + \frac{s^4}{\Sigma} \theta_{H4'} + \frac{s^5}{\Sigma} \theta_{H5'} + (0)\theta_{H6'}$$

$$\theta_{iecorr6N} = \frac{s}{\Sigma} \theta_{H1'} + \frac{s^2}{\Sigma} \theta_{H2'} + \frac{s^3}{\Sigma} \theta_{H3'} + \frac{s^4}{\Sigma} \theta_{H4'} + \frac{s^5}{\Sigma} \theta_{H5'} + \frac{s^6}{\Sigma} \theta_{H6'}$$

$$\theta_{\text{tecorr}4\text{O}} = \frac{s}{\Sigma} \theta_{\text{H}1'} + \frac{s^2}{\Sigma} \theta_{\text{H}2'} + \frac{s^3}{\Sigma} \theta_{\text{H}3'} + (0) \theta_{\text{H}4'} + (0) \theta_{\text{H}5'} + (0) \theta_{\text{H}6'}$$

$$\theta_{\text{tecorr}5\text{O}} = \frac{s}{\Sigma} \theta_{\text{H}1'} + \frac{s^2}{\Sigma} \theta_{\text{H}2'} + \frac{s^3}{\Sigma} \theta_{\text{H}3'} + \frac{s^4}{\Sigma} \theta_{\text{H}4'} + (0) \theta_{\text{H}5'} + (0) \theta_{\text{H}6'}$$

$$\theta_{\text{tecorr}6\text{O}} = \frac{s}{\Sigma} \theta_{\text{H}1'} + \frac{s^2}{\Sigma} \theta_{\text{H}2'} + \frac{s^3}{\Sigma} \theta_{\text{H}3'} + \frac{s^4}{\Sigma} \theta_{\text{H}4'} + \frac{s^5}{\Sigma} \theta_{\text{H}5'} + (0) \theta_{\text{H}6'}$$

$$\text{where } \theta_{\text{H}n} = \frac{\theta_{\text{H}n'}}{n}$$

These equations may be further simplified by combining  $\theta_{\text{H}1'}$ ,  $\theta_{\text{H}2'}$ , and  $\theta_{\text{H}3'}$  into one term, denoting the results as  $\theta_{\text{short}}$ .

$$\theta_{\text{tecorr}4\text{N}} = \left( \frac{s}{\Sigma} + \frac{s^2}{\Sigma} + \frac{s^3}{\Sigma} \right) \theta_{\text{short}} + \frac{s^4}{\Sigma} \theta_{\text{H}4'} + (0) \theta_{\text{H}5'} + (0) \theta_{\text{H}6'}$$

$$\theta_{\text{tecorr}5\text{N}} = \left( \frac{s}{\Sigma} + \frac{s^2}{\Sigma} + \frac{s^3}{\Sigma} \right) \theta_{\text{short}} + \frac{s^4}{\Sigma} \theta_{\text{H}4'} + \frac{s^5}{\Sigma} \theta_{\text{H}5'} + (0) \theta_{\text{H}6'}$$

$$\theta_{\text{tecorr}6\text{N}} = \left( \frac{s}{\Sigma} + \frac{s^2}{\Sigma} + \frac{s^3}{\Sigma} \right) \theta_{\text{short}} + \frac{s^4}{\Sigma} \theta_{\text{H}4'} + \frac{s^5}{\Sigma} \theta_{\text{H}5'} + \frac{s^6}{\Sigma} \theta_{\text{H}6'}$$

$$\theta_{\text{tecorr}4\text{O}} = \left( \frac{s}{\Sigma} + \frac{s^2}{\Sigma} + \frac{s^3}{\Sigma} \right) \theta_{\text{short}} + (0) \theta_{\text{H}4'} + (0) \theta_{\text{H}5'} + (0) \theta_{\text{H}6'}$$

$$\theta_{\text{tecorr}5\text{O}} = \left( \frac{s}{\Sigma} + \frac{s^2}{\Sigma} + \frac{s^3}{\Sigma} \right) \theta_{\text{short}} + \frac{s^4}{\Sigma} \theta_{\text{H}4'} + (0) \theta_{\text{H}5'} + (0) \theta_{\text{H}6'}$$

$$\theta_{\text{tecorr}6\text{O}} = \left( \frac{s}{\Sigma} + \frac{s^2}{\Sigma} + \frac{s^3}{\Sigma} \right) \theta_{\text{short}} + \frac{s^4}{\Sigma} \theta_{\text{H}4'} + \frac{s^5}{\Sigma} \theta_{\text{H}5'} + (0) \theta_{\text{H}6'}$$

The equations above are all in the form  $y = aV_1 + bV_2 + cV_3 + dV_4$ . Through a multivariable linear regression analysis, it is possible to solve for the variables ( $V_n$ )  $\theta_{\text{H}4'}$ ,  $\theta_{\text{H}5'}$  within the acid series, and  $\theta_{\text{H}4'}$ ,  $\theta_{\text{H}5'}$ , and  $\theta_{\text{H}6'}$  within the amide series. Mathematica was used to set up matrices containing the coefficients a,b,c, and d for various concentrations of TFE and thus various s values. The values for y were the corresponding corrected ellipticities at 222 nm.

## B.9 Examples of the Computational Programs Used to Complete the Above Analyses

The following pages are the Excel spreadsheet used to perform the linear regression analysis on Ac-Hel<sub>1</sub>-NH<sub>2</sub> to determine the template contributions to the observed CD signal. Following that is an example of the multivariable linear regression analysis performed on Mathematica to yield the specific residue contributions of the amide series.

	A	B	C	D	E
1	Wavelength	0 mole% TFE	3 mole% TFE	6 mole% TFE	10 mole% TFE
2					
3	Xte	0.374125874	0.380622837	0.43533123	0.56019656
4					
5	270	0	0	0	0
6	269.8	39.971	25.066	15.55	-3.998
7	269.6	75.946	47.965	29.405	-7.077
8	269.4	108.088	68.784	41.639	-9.296
9	269.2	136.562	87.609	52.328	-10.71
10	269	161.532	104.526	61.545	-11.377
11	268.8	183.164	119.621	69.366	-11.354
12	268.6	201.622	132.981	75.864	-10.697
13	268.4	217.071	144.691	81.116	-9.465
14	268.2	229.675	154.838	85.195	-7.714
15	268	239.599	163.508	88.177	-5.5
16	267.8	247.007	170.787	90.135	-2.882
17	267.6	252.065	176.761	91.145	0.085
18	267.4	254.936	181.516	91.281	3.342
19	267.2	255.786	185.139	90.618	6.833
20	267	254.78	187.715	89.231	10.501
21	266.8	252.081	189.33	87.194	14.289
22	266.6	247.854	190.072	84.582	18.14
23	266.4	242.265	190.025	81.47	21.996
24	266.2	235.477	189.276	77.932	25.801
25	266	227.656	187.911	74.043	29.498
26	265.8	218.965	186.017	69.878	33.03
27	265.6	209.571	176.389	65.512	36.34
28	265.4	199.637	184.632	61.018	39.369
29	265.2	189.327	190.613	56.473	42.063
30	265	178.808	189.759	51.95	37.601
31	264.8	171.363	165.914	47.524	49.959
32	264.6	172.438	180.047	49.02	43.636
33	264.4	178.379	172.984	50.291	29.154
34	264.2	170.118	170.915	51.806	33.479
35	264	161.17	160.87	35.204	24.546
36	263.8	155.467	166.724	33.924	19.767
37	263.6	151.058	172.101	29.446	16.143
38	263.4	141.627	168.548	23.138	33.622
39	263.2	138.714	163.592	28.15	20.065
40	263	142.162	147.988	40.207	6.307
41	262.8	144.861	145.218	53.472	-1.332
42	262.6	152.875	128.388	58.339	-11.708
43	262.4	154.71	125.811	58.546	-12.852
44	262.2	148.024	124.304	63.769	-15.029
45	262	152.734	123.487	67.502	-26.473
46	261.8	152.394	124.012	67.066	-14.194
47	261.6	155.088	124.261	84.8	-2.941
48	261.4	163.614	144.042	94.444	-9.831
49	261.2	169.252	149.825	93.427	-3.534

	A	B	C	D	E
50	261	168.632	142.553	103.168	-15.724
51	260.8	175.324	141.832	122.499	-13.715
52	260.6	183.307	137.034	133.414	-17.562
53	260.4	176.593	134.051	122.733	0.126
54	260.2	168.582	101.67	115.09	-1.229
55	260	166.839	99.891	96.712	-16.206
56	259.8	167.197	92.114	105.607	-21.285
57	259.6	168.062	79.248	107.768	-45.884
58	259.4	159.158	54.437	90.034	-40.589
59	259.2	160.975	37.618	73.895	-35.652
60	259	157.181	26.33	61.719	-43.618
61	258.8	157.211	23.397	49.265	-66.272
62	258.6	146.693	46.545	48.533	-75.016
63	258.4	143.998	57.695	25.468	-91.894
64	258.2	137.47	50.712	24.138	-87.576
65	258	137.314	51.577	11.396	-105.283
66	257.8	138.682	28.67	13.12	-99.964
67	257.6	138.497	24.455	6.272	-91.172
68	257.4	128.488	24.502	11.429	-80.361
69	257.2	130.359	22.705	-3.184	-85.377
70	257	119.456	22.074	-17.857	-93.426
71	256.8	91.135	6.618	-29.496	-91.452
72	256.6	93.568	-15.1	-53.704	-102.014
73	256.4	91.302	-32.481	-53.641	-89.639
74	256.2	97.559	-32.949	-69.945	-88.419
75	256	79.648	-63.021	-75.765	-115.02
76	255.8	62.765	-62.809	-109.094	-138.246
77	255.6	39.393	-74.842	-115.505	-141.09
78	255.4	35.698	-69.397	-114.832	-179.454
79	255.2	36.475	-57.187	-126.672	-186.94
80	255	14.524	-76.567	-145.424	-200.709
81	254.8	8.654	-102.751	-175.072	-220.757
82	254.6	-5.778	-111.81	-203.595	-236.276
83	254.4	-8.22	-108.512	-227.066	-269.545
84	254.2	-38.438	-125.758	-252.153	-306.781
85	254	-57.863	-131.113	-275.853	-328.181
86	253.8	-74.068	-144.353	-292.719	-369.206
87	253.6	-93.99	-171.925	-302.288	-410.623
88	253.4	-122.625	-177.824	-314.553	-428.224
89	253.2	-143.6	-196.993	-338.242	-450.214
90	253	-147.796	-206.317	-359.448	-477.469
91	252.8	-186.439	-234.189	-385.857	-517.472
92	252.6	-210.056	-271.581	-417.746	-555.957
93	252.4	-243.423	-305.085	-433.946	-607.865
94	252.2	-259.713	-318.062	-456.533	-650.422
95	252	-291.191	-351.127	-487.951	-672.502
96	251.8	-337.471	-385.937	-506.879	-709.419
97	251.6	-361.765	-428.806	-531.873	-743.902
98	251.4	-394.308	-451.173	-563.982	-772.446

	A	B	C	D	E
99	251.2	-441.839	-482.27	-599.081	-805.328
100	251	-476.524	-525.195	-640.064	-836.996
101	250.8	-523.498	-546.581	-673.226	-880.454
102	250.6	-565.903	-583.636	-718.238	-934.445
103	250.4	-625.72	-615.131	-755.808	-978.209
104	250.2	-675.151	-652.043	-818.543	-1015.358
105	250	-717.326	-711.674	-884.577	-1058.154
106	249.8	-765.347	-758.896	-923.599	-1104.085
107	249.6	-803.382	-806.8	-978.27	-1163.834
108	249.4	-847.449	-867.148	-1031.461	-1227.91
109	249.2	-908.923	-925.75	-1079.713	-1297.57
110	249	-952.2	-982.745	-1134.374	-1373.246
111	248.8	-997.51	-1034.263	-1186.1	-1434.292
112	248.6	-1052.589	-1096.944	-1230.802	-1490.799
113	248.4	-1080.777	-1171.031	-1285.497	-1579.335
114	248.2	-1139.686	-1239.607	-1340.239	-1608.793
115	248	-1200.765	-1288.186	-1413.659	-1673.206
116	247.8	-1268.869	-1349.987	-1453.709	-1745.685
117	247.6	-1332.405	-1402.135	-1531.846	-1836.785
118	247.4	-1392.496	-1466.652	-1591.244	-1923.275
119	247.2	-1457.281	-1540.644	-1676.261	-2008.354
120	247	-1527.275	-1623.723	-1759.574	-2076.309
121	246.8	-1598.348	-1698.376	-1844.35	-2146.1
122	246.6	-1658.348	-1790.37	-1923.712	-2246.748
123	246.4	-1745.955	-1862.98	-2000.47	-2347.435
124	246.2	-1834.441	-1942.265	-2081.706	-2436.707
125	246	-1909.891	-2041.189	-2153.23	-2531.136
126	245.8	-1989.573	-2142.476	-2253.984	-2620.738
127	245.6	-2065.087	-2231.718	-2344.329	-2697.562
128	245.4	-2146.022	-2320.437	-2438.015	-2801.878
129	245.2	-2234.86	-2409.237	-2538.868	-2910.818
130	245	-2343.035	-2479.634	-2663.075	-3008.755
131	244.8	-2425.149	-2580.41	-2789.473	-3124.92
132	244.6	-2526.906	-2667.012	-2892.772	-3237.664
133	244.4	-2619.409	-2779.268	-3007.789	-3349.486
134	244.2	-2725.016	-2895.135	-3114.304	-3469.486
135	244	-2821.988	-2990.319	-3221.832	-3573.053
136	243.8	-2919.417	-3081.699	-3320.741	-3705.641
137	243.6	-3019.594	-3190.683	-3433.258	-3832.576
138	243.4	-3140.911	-3294.183	-3559.226	-3934.846
139	243.2	-3262.752	-3407.732	-3671.779	-4070.815
140	243	-3366.364	-3502.846	-3798.796	-4203.942
141	242.8	-3490.914	-3614.313	-3916.501	-4318.173
142	242.6	-3599.646	-3744.379	-4063.205	-4438.62
143	242.4	-3733.637	-3867.229	-4177.762	-4543.029
144	242.2	-3849.979	-3987.298	-4310.013	-4690.148
145	242	-4001.743	-4112.713	-4430.791	-4821.832
146	241.8	-4129.494	-4238.384	-4579.545	-4956.96
147	241.6	-4256.118	-4360.706	-4714.682	-5088.193



	A	B	C	D	E
148	241.4	-4392.887	-4477.398	-4833.977	-5231.783
149	241.2	-4533.982	-4615.377	-4968.476	-5379.948
150	241	-4658.141	-4738.067	-5110.849	-5529.685
151	240.8	-4806.199	-4877.257	-5257.22	-5683.406
152	240.6	-4936.522	-5006.588	-5394.623	-5839.161
153	240.4	-5079.347	-5140.167	-5532.085	-5990.209
154	240.2	-5206.24	-5281.187	-5667.487	-6145.234
155	240	-5341.805	-5435.081	-5795.215	-6296.982
156	239.8	-5477.775	-5569.803	-5943.391	-6441.748
157	239.6	-5612.943	-5699.188	-6094.149	-6589.347
158	239.4	-5753.409	-5845.528	-6238.409	-6776.725
159	239.2	-5893.517	-5972.04	-6369.643	-6936.326
160	239	-6022.855	-6121.963	-6521.094	-7099.499
161	238.8	-6177.083	-6259.21	-6663.457	-7257.588
162	238.6	-6331.554	-6400.445	-6812.63	-7409.955
163	238.4	-6470.394	-6540.714	-6966.759	-7565.086
164	238.2	-6634.513	-6676.853	-7112.563	-7730.157
165	238	-6787.317	-6831.24	-7296.495	-7883.384
166	237.8	-6942.719	-6974.452	-7446.885	-8033.448
167	237.6	-7094.299	-7112.168	-7601.756	-8199.118
168	237.4	-7242.016	-7238.901	-7736.034	-8357.159
169	237.2	-7394.147	-7378.555	-7889.46	-8512.356
170	237	-7541.358	-7530.77	-8031.697	-8675.841
171	236.8	-7685.855	-7687.927	-8176.159	-8815.405
172	236.6	-7831.077	-7836.016	-8308.016	-8963.778
173	236.4	-7980.693	-7992.781	-8450.288	-9112.583
174	236.2	-8117.312	-8142.868	-8602.333	-9245.872
175	236	-8258.511	-8289.96	-8749.522	-9392.077
176	235.8	-8412.888	-8420.226	-8877.008	-9561.855
177	235.6	-8563.526	-8535.092	-9017.33	-9704.557
178	235.4	-8716.721	-8679.122	-9145.727	-9863.335
179	235.2	-8859.992	-8835.782	-9281.504	-10015.041
180	235	-8998.019	-8996.897	-9407.986	-10149.594
181	234.8	-9132.727	-9136.861	-9545.603	-10289.195
182	234.6	-9265.213	-9264.158	-9647.109	-10402.81
183	234.4	-9389.115	-9378.889	-9759.1	-10506.024
184	234.2	-9515.555	-9512.899	-9863.359	-10614.238
185	234	-9651.396	-9625.109	-9967.443	-10713.611
186	233.8	-9774.987	-9737.053	-10074.648	-10813.768
187	233.6	-9905.317	-9838.226	-10165.583	-10938.014
188	233.4	-10040.723	-9959.794	-10253.605	-11018.03
189	233.2	-10146.519	-10070.97	-10343.302	-11091.98
190	233	-10256.069	-10179.719	-10437.608	-11166.8
191	232.8	-10386.132	-10274.002	-10503.531	-11225.552
192	232.6	-10507.596	-10347.497	-10594.757	-11282.369
193	232.4	-10631.273	-10442.666	-10668.074	-11334.667
194	232.2	-10724.936	-10537.282	-10742.98	-11383.364
195	232	-10814.466	-10616.812	-10781.679	-11401.311
196	231.8	-10884.288	-10697.021	-10854.091	-11439.91

	A	B	C	D	E
197	231.6	-10980.569	-10779.115	-10894.492	-11457.939
198	231.4	-11073.98	-10820.249	-10940.81	-11489.515
199	231.2	-11147.52	-10863.74	-10978.865	-11500.485
200	231	-11227.317	-10898.955	-11001.636	-11475.531
201	230.8	-11308.331	-10943.31	-11044.392	-11480.432
202	230.6	-11373.75	-11023.384	-11087.817	-11487.428
203	230.4	-11440.642	-11061.324	-11104.547	-11463.514
204	230.2	-11496.845	-11121.336	-11102.267	-11428.981
205	230	-11566.638	-11179.179	-11115.915	-11392.276
206	229.8	-11634.05	-11225.354	-11126.861	-11354.784
207	229.6	-11695.591	-11284.274	-11152.481	-11296.525
208	229.4	-11773.599	-11325.122	-11185.908	-11244.887
209	229.2	-11835.703	-11363.189	-11206.493	-11196.739
210	229	-11898.528	-11412.757	-11217.994	-11145.38
211	228.8	-11959.554	-11470.08	-11215.553	-11051.695
212	228.6	-12010.817	-11529.673	-11235.174	-11015.057
213	228.4	-12069.323	-11567.205	-11230.464	-10925.139
214	228.2	-12161.122	-11595.061	-11229.446	-10877.688
215	228	-12240.837	-11632.876	-11244.314	-10837.423
216	227.8	-12315.177	-11676.725	-11247.251	-10760.9
217	227.6	-12374.793	-11723.874	-11262.002	-10713.164
218	227.4	-12431.982	-11763.825	-11251.789	-10636.267
219	227.2	-12493.702	-11814.985	-11250.205	-10578.743
220	227	-12572.149	-11888.608	-11236.055	-10501.019
221	226.8	-12650.872	-11935.481	-11233.993	-10438.022
222	226.6	-12740.739	-11989.737	-11236.329	-10381.342
223	226.4	-12818.96	-12040.962	-11254.206	-10321.275
224	226.2	-12918.877	-12090.91	-11267.707	-10290.91
225	226	-13019.459	-12163.584	-11281.27	-10230.309
226	225.8	-13125.313	-12243.286	-11289.489	-10195.231
227	225.6	-13244.717	-12317.548	-11294.816	-10139.87
228	225.4	-13373.18	-12396.93	-11307.178	-10086.696
229	225.2	-13498.384	-12472.601	-11340.581	-10017.635
230	225	-13640.79	-12579.568	-11361.715	-9959.222
231	224.8	-13777.927	-12676.698	-11412.104	-9925.972
232	224.6	-13925.414	-12764.882	-11455.36	-9901.585
233	224.4	-14098.341	-12877.839	-11529.901	-9901.973
234	224.2	-14259.224	-13036.455	-11587.562	-9895.352
235	224	-14442.287	-13154.709	-11660.893	-9915.243
236	223.8	-14616.543	-13305.204	-11730.299	-9907.152
237	223.6	-14813.098	-13457.343	-11850.063	-9905.598
238	223.4	-15032.248	-13635.376	-11949.973	-9923.556
239	223.2	-15241.011	-13800.637	-12041.045	-9959.625
240	223	-15487.55	-13969.247	-12175.767	-9997.648
241	222.8	-15740.759	-14171.096	-12313.578	-10041.857
242	222.6	-15999.876	-14406.799	-12461.713	-10104.852
243	222.4	-16261.124	-14668.886	-12607.215	-10168.504
244	222.2	-16518.215	-14908.068	-12772.395	-10241.19
245	222	-16799.916	-15157.243	-12925.521	-10312.421

	A	B	C	D	E
246	221.8	-17117.762	-15423.102	-13129.699	-10442.808
247	221.6	-17446.358	-15650.072	-13337.543	-10537.785
248	221.4	-17766.719	-15936.474	-13585.877	-10650.745
249	221.2	-18094.377	-16225.126	-13786.815	-10809.251
250	221	-18439.432	-16511.695	-14006.25	-10965.979
251	220.8	-18775.428	-16835.499	-14261.221	-11094.605
252	220.6	-19166.563	-17183.654	-14548.806	-11282.334
253	220.4	-19539.832	-17504.035	-14850.873	-11497.189
254	220.2	-19907.947	-17814.679	-15136.876	-11724.587
255	220	-20302.613	-18172.265	-15425.903	-11954.147
256	219.8	-20708.27	-18567.927	-15727.563	-12187.585
257	219.6	-21112.481	-18990.65	-16076.69	-12395.888
258	219.4	-21545.115	-19369.902	-16414.489	-12652.336
259	219.2	-21951.264	-19783.374	-16763.193	-12931.784
260	219	-22369.465	-20184.585	-17116.947	-13228.124
261	218.8	-22821.186	-20626.988	-17509.425	-13519.719
262	218.6	-23267.481	-21060.101	-17891.177	-13882.433
263	218.4	-23709.875	-21502.173	-18266.329	-14205.389
264	218.2	-24149.774	-21976.808	-18658.353	-14526.866
265	218	-24579.033	-22414.958	-19051.777	-14857.326
266	217.8	-25024.729	-22876.857	-19465.927	-15178.735
267	217.6	-25474.584	-23338.675	-19909.939	-15558.63
268	217.4	-25923.84	-23789.831	-20325.941	-15882.739
269	217.2	-26347.737	-24238.246	-20741.845	-16252.202
270	217	-26776.781	-24672.408	-21152.909	-16595.508
271	216.8	-27185.578	-25144.298	-21558.564	-16901.176
272	216.6	-27580.856	-25613.554	-21968.355	-17287.562
273	216.4	-27967.381	-26035.755	-22415.388	-17602.87
274	216.2	-28385.705	-26455.058	-22813.88	-17910.108
275	216	-28769.498	-26872.412	-23211.404	-18226.071
276	215.8	-29137.994	-27299.523	-23603.449	-18567.439
277	215.6	-29453.367	-27648.58	-23971.558	-18873.634
278	215.4	-29768.813	-28078.361	-24338.978	-19213.962
279	215.2	-30037.059	-28441.472	-24710.642	-19535.126
280	215	-30271.852	-28786.23	-25076.333	-19831.524
281	214.8	-30491.235	-29108.431	-25377.109	-20104.692
282	214.6	-30684.709	-29413.769	-25672.925	-20386.954
283	214.4	-30879.069	-29727.505	-25982.589	-20658.415
284	214.2	-31027.945	-29982.042	-26252.066	-20843.726
285	214	-31170.076	-30162.609	-26515.505	-21057.905
286	213.8	-31290.649	-30326.732	-26685.214	-21253.413
287	213.6	-31340.69	-30487.583	-26813.859	-21413.651
288	213.4	-31361.752	-30582.292	-26948.845	-21578.435
289	213.2	-31352.408	-30629.359	-27047.728	-21725.981
290	213	-31295.342	-30711.869	-27071.82	-21801.39
291	212.8	-31167.967	-30682.701	-27050.593	-21851.821
292	212.6	-30991.633	-30649.976	-27032.825	-21866.769
293	212.4	-30768.893	-30562.835	-26998.878	-21862.04
294	212.2	-30533.102	-30397.706	-26916.663	-21815.782

	A	B	C	D	E
295	212	-30240.85	-30141.525	-26808.757	-21706.827
296	211.8	-29958.981	-29882.113	-26635.23	-21577.573
297	211.6	-29504.985	-29601.953	-26424.025	-21467.772
298	211.4	-29034.717	-29158.787	-26151.408	-21295.14
299	211.2	-28529.863	-28737.089	-25859.052	-21067.101
300	211	-27948.041	-28264.785	-25500.718	-20805.651
301	210.8	-27365.469	-27787.849	-25075.691	-20519.001
302	210.6	-26734.461	-27210.173	-24619.077	-20160.161
303	210.4	-25961.184	-26540.212	-24139.011	-19762.552
304	210.2	-25206.947	-25807.71	-23573.439	-19323.167
305	210	-24372.731	-25094.15	-22939.036	-18805.042
306	209.8	-23478.266	-24342.564	-22229.863	-18308.806
307	209.6	-22494.237	-23396.414	-21477.449	-17747.673
308	209.4	-21500.903	-22466.796	-20680.816	-17057.788
309	209.2	-20395.17	-21466.746	-19803.839	-16330.56
310	209	-19311.606	-20396.679	-18864.04	-15565.027
311	208.8	-18150.865	-19241.021	-17854.677	-14749.7
312	208.6	-16892.569	-18053.408	-16795.603	-13889.35
313	208.4	-15542.309	-16781.425	-15678.466	-12933.64
314	208.2	-14135.273	-15464.214	-14493.233	-11970.831
315	208	-12740.165	-14085.949	-13247.651	-10912.865
316	207.8	-11284.397	-12642.408	-11974.003	-9767.325
317	207.6	-9717.56	-11164.45	-10596.813	-8614.668
318	207.4	-8101.845	-9671.166	-9202.725	-7390.362
319	207.2	-6416.436	-8096.439	-7728.261	-6127.455
320	207	-4694.18	-6447.963	-6177.887	-4833.245
321	206.8	-2947.102	-4699.674	-4603.575	-3441.873
322	206.6	-1130.296	-2968.402	-2996.445	-2046.415
323	206.4	688.821	-1178.425	-1293.725	-636.635
324	206.2	2543.357	680.761	435.25	843.695
325	206	4462.15	2540.426	2160.982	2404.302
326	205.8	6392.101	4460.984	3954.675	3978.379
327	205.6	8396.54	6378	5793.363	5597.87
328	205.4	10374.469	8367.287	7728.223	7281.645
329	205.2	12451.376	10266.874	9661.045	8953.129
330	205	14540.407	12318.219	11601.697	10609.052
331	204.8	16591.828	14363.396	13572.921	12394.569
332	204.6	18749.209	16380.184	15613.972	14201.959
333	204.4	20847.459	18467.358	17639.848	16016.751
334	204.2	23008.703	20614.782	19653.075	17874.931
335	204	25089.096	22795.368	21721.003	19766.542
336	203.8	27162.847	24959.635	23828.585	21655.136
337	203.6	29365.584	27138.499	25898.678	23627.169
338	203.4	31453.605	29269.19	28068.862	25545.651
339	203.2	33574.166	31368.587	30124.325	27478.554
340	203	35654.443	33501.981	32196.218	29438.667
341	202.8	37697.775	35519.489	34245.979	31378.36
342	202.6	39695.982	37551.333	36284.835	33224.249
343	202.4	41664.002	39705.43	38263.135	35085.354

	A	B	C	D	E
344	202.2	43666.33	41799.465	40216.749	36978.019
345	202	45565.045	43819.36	42153.507	38800.382
346	201.8	47450.619	45756.415	44106.315	40673.124
347	201.6	49361.646	47689.106	46053.78	42460.405
348	201.4	51070.865	49627.11	47954.003	44273.276
349	201.2	52783.4	51573.251	49774.249	45963.222
350	201	54486.092	53309.415	51560.827	47702.71
351	200.8	56106.752	55034.618	53291.135	49387.956
352	200.6	57696.459	56721.559	55050.303	51049.823
353	200.4	59295.681	58393.262	56654.389	52660.745
354	200.2	60730.396	59957.645	58302.358	54201.858
355	200	62151.877	61478.395	59867.319	55689.534
356	199.8	63498.49	62984.118	61378.764	57206.534
357	199.6	64789.31	64438.794	62834.01	58595.499
358	199.4	66023.17	65788.993	64230.389	59930.683
359	199.2	67198.904	67105.376	65565.218	61209.937
360	199	68315.365	68329.587	66835.827	62431.112
361	198.8	69371.389	69486.735	68039.522	63592.058
362	198.6	70365.81	70575.055	69173.647	64690.62
363	198.4	71297.474	71592.782	70235.514	65724.647
364	198.2	72165.217	72538.149	71222.444	66691.999
365	198	72967.881	73409.383	72131.772	67590.507
366	197.8	73704.303	74204.719	72960.803	68418.038
367	197.6	74373.326	74922.399	73706.874	69172.437
368	197.4	74973.787	75560.641	74367.303	69851.546
369	197.2	75504.521	76117.696	74939.413	70453.218
370	197	75964.381	76591.79	75420.53	70975.304
371	196.8	76352.201	76981.149	75807.968	71415.655
372	196.6	76666.818	77284.016	76099.061	71772.116
373	196.4	76907.076	77498.618	76291.124	72042.538
374	196.2	77071.81	77623.196	76381.491	72224.772
375	196	77159.857	77655.977	76367.468	72316.663
376	195.8	77170.068	77595.188	76246.397	72316.069
377	195.6	77101.279	77439.079	76015.585	72220.827
378	195.4	76952.326	77185.868	75672.358	72028.804
379	195.2	76722.045	76833.797	75214.046	71737.827
380	195	76409.287	76381.102	74637.975	71345.765

	F	G	H	I	J
1	13 mole% TFE	16 mole% TFE	20 mole% TFE	Sum xi or yi	Sum x2i or y2i
2					
3	0.627083333	0.660341556	0.67921147	3.71691286	2.078790078
4					
5	0	0	0	0	0
6	11.94	6.873	6.289	101.691	2713.124951
7	22.778	13.633	12.414	195.064	9841.977464
8	32.555	20.269	18.358	280.397	20042.15289
9	41.312	26.775	24.108	357.984	32182.21804
10	49.09	33.143	29.647	428.106	45322.72601
11	55.929	39.363	34.962	491.051	58698.63006
12	61.87	45.429	40.036	547.105	71699.72179
13	66.955	51.332	44.854	596.554	83854.52377
14	71.224	57.064	49.403	639.685	94812.92037
15	74.718	62.617	53.666	676.785	104331.688
16	77.478	67.983	57.628	708.136	112258.7967
17	79.545	73.154	61.275	734.03	118522.174
18	80.96	78.121	64.591	754.747	123113.2218
19	81.763	82.876	67.562	770.577	126079.4823
20	81.995	87.413	70.172	781.807	127510.5342
21	81.698	91.721	72.406	788.719	127527.5825
22	80.911	95.794	74.25	791.603	126278.2877
23	79.677	99.623	75.687	790.743	123924.7042
24	78.036	103.201	76.704	786.427	120637.4772
25	76.028	106.518	77.284	778.938	116589.4539
26	73.695	109.567	78.351	749.503	109362.631
27	71.078	112.341	72.319	743.55	103548.1212
28	68.217	114.83	57.057	724.76	100312.0109
29	65.153	117.027	43.351	704.007	96956.06574
30	61.927	118.923	52.404	691.372	92817.22912
31	58.58	120.511	45.371	659.222	81660.21058
32	55.153	121.782	13.914	635.99	84525.15528
33	51.687	122.729	57.47	662.694	86158.4266
34	44.993	123.343	48.695	643.349	81565.84495
35	32.326	123.616	68.593	606.325	74727.63891
36	23.699	123.54	58.939	582.06	72806.03225
37	17.799	123.108	50.932	560.587	71631.38962
38	18.316	122.31	57.136	564.697	68692.17581
39	23.1	121.139	49.456	544.216	64853.10624
40	39.211	138.944	62.525	577.344	68519.17677
41	27.708	123.955	68.758	562.64	65794.24371
42	33.104	118.323	78.04	557.361	64581.2091
43	52.871	119.446	73.612	572.144	65837.81594
44	47.58	106.759	94.826	570.233	64308.25595
45	54.534	90.347	85.281	547.412	62243.44018
46	68.735	86.554	80.25	564.817	61958.38301
47	54.466	65.94	93.071	574.685	62669.61314
48	58.159	60.238	103.481	614.147	74253.35974
49	65.883	59.477	81.225	615.555	74310.44746

	F	G	H	I	J
50	87.88	56.423	105.125	648.057	81606.70459
51	86.072	41.178	126.74	679.93	91215.97189
52	80.665	47.27	104.836	668.964	90219.37467
53	73.92	32.598	69.225	609.246	75537.06004
54	62.17	17.65	52.221	516.154	58907.56241
55	55.307	5.936	55.093	463.572	53558.64818
56	54.965	4.063	45.708	448.369	53172.59594
57	44.29	-11.639	40.506	382.351	51982.17109
58	56.616	-10.224	17.524	326.956	41665.23622
59	40.946	-19.624	5.689	263.847	36153.64169
60	21.261	-29.922	-6.194	186.757	32496.62239
61	4.778	-37.07	-30.392	100.917	34402.42419
62	6.064	-58.851	-52.227	61.741	37895.99744
63	-2.87	-56.996	-75.551	-0.15	42121.99781
64	-16.935	-52.89	-95.724	-40.805	41969.13717
65	-42.592	-68.964	-127.663	-144.215	55597.65376
66	-59.527	-63.289	-151.573	-193.881	60742.9373
67	-66.079	-89.957	-169.575	-247.559	69345.51432
68	-101.996	-116.972	-203.882	-338.792	89351.52923
69	-113.233	-127.09	-198.354	-374.174	93126.2456
70	-105.561	-130.985	-221.24	-427.539	101051.6199
71	-104.651	-144.596	-247.776	-520.218	110835.6497
72	-118.778	-170.12	-272.853	-639.001	139771.7437
73	-125.554	-176.492	-306.116	-692.621	160923.8162
74	-164.462	-189.057	-341.729	-789.002	202882.6258
75	-167.563	-207.313	-339.83	-888.864	215825.8538
76	-160.779	-223.984	-374.172	-1006.319	254921.2777
77	-151.411	-235.017	-352.56	-1031.032	242857.7613
78	-180.057	-245.656	-343.947	-1097.645	262547.3495
79	-178.412	-282.858	-353.823	-1149.417	292623.343
80	-199.255	-294.251	-332.763	-1234.445	304523.1147
81	-228.461	-311.527	-360.104	-1390.018	368934.909
82	-259.628	-344.577	-375.823	-1537.487	437195.0682
83	-279.448	-346.592	-401.341	-1640.724	495347.6954
84	-303.775	-400.306	-364.906	-1792.117	560668.8049
85	-313.23	-413.362	-394.02	-1913.622	628569.3283
86	-333.481	-430.608	-407.036	-2051.471	710632.473
87	-366.422	-450.855	-401.936	-2198.039	797469.47
88	-405.513	-480.177	-420.407	-2349.323	900730.4397
89	-433.981	-519.691	-471.306	-2554.027	1057075.088
90	-461.521	-557.784	-515.598	-2725.933	1211555.794
91	-482.1	-571.222	-537.523	-2914.802	1353912.842
92	-493.459	-605.859	-575.8	-3130.458	1543592.222
93	-503.897	-645.711	-597.332	-3337.259	1737801.004
94	-518.497	-693.732	-598.327	-3495.286	1908183.862
95	-553.1	-723.189	-622.91	-3701.97	2115376.295
96	-580.3	-748.618	-676.293	-3944.917	2377584.904
97	-622.611	-784.527	-730.165	-4203.649	2687295.573
98	-653.504	-822.056	-796.331	-4453.8	3010771.001

	F	G	H	I	J
99	-683.992	-854.546	-803.893	-4670.949	3279595.165
100	-732.214	-882.385	-834.291	-4927.669	3623931.241
101	-768.727	-909.646	-889.796	-5191.928	4011367.406
102	-815.439	-956.945	-916.012	-5490.618	4469692.948
103	-865.765	-1014.907	-985.181	-5840.721	5048217.103
104	-918.181	-1029.051	-1038.675	-6147.002	5562801.523
105	-966.926	-1091.669	-1092.634	-6522.96	6243738.982
106	-1035.469	-1149.417	-1139.491	-6876.304	6925513.198
107	-1110.454	-1210.252	-1189.081	-7262.073	7719602.265
108	-1164.831	-1256.836	-1285.994	-7681.629	8632038.782
109	-1214.275	-1332.744	-1335.906	-8094.881	9567937.336
110	-1263.699	-1390.478	-1404.7	-8501.442	10548627.84
111	-1329.532	-1455.622	-1451.136	-8888.455	11521039.34
112	-1396.844	-1522.966	-1546.901	-9337.845	12712086.26
113	-1464.928	-1592.941	-1629.484	-9803.993	14024887.29
114	-1539.478	-1661.392	-1696.645	-10225.84	15228785.33
115	-1647.379	-1730.261	-1764.302	-10717.758	16719732.09
116	-1716.856	-1816.509	-1808.095	-11159.71	18109686.42
117	-1780.62	-1887.978	-1884.782	-11656.551	19749088.65
118	-1857.734	-1971.892	-1905.937	-12109.23	21293286.91
119	-1960.368	-2059.369	-2006.497	-12708.774	23450662.16
120	-2054.031	-2151.243	-2095.719	-13287.874	25615132.95
121	-2142.444	-2251.982	-2240.385	-13921.985	28127383.67
122	-2217.191	-2330.917	-2351.288	-14518.574	30581752.51
123	-2309.432	-2406.336	-2447.383	-15119.991	33144997.3
124	-2406.102	-2481.769	-2524.74	-15707.73	35731424.26
125	-2480.123	-2569.749	-2664.895	-16350.213	38713470.43
126	-2578.315	-2670.151	-2752.453	-17007.69	41850727.79
127	-2706.969	-2765.069	-2855.772	-17666.506	45146590.21
128	-2829.472	-2860.642	-2956.467	-18352.933	48714157.34
129	-2914.425	-2973.598	-3066.354	-19048.16	52456419.29
130	-3034.793	-3093.572	-3188.973	-19811.837	56732677.96
131	-3130.424	-3169.555	-3302.382	-20522.313	60837508.26
132	-3256.315	-3292.604	-3436.467	-21309.74	65602938.88
133	-3395.666	-3403.278	-3528.381	-22083.277	70413806.47
134	-3509.783	-3532.327	-3643.458	-22889.509	75614438.32
135	-3653.676	-3655.528	-3791.448	-23707.844	81139844.38
136	-3810.447	-3787.81	-3934.562	-24560.317	87126749.42
137	-3924.113	-3903.594	-4043.734	-25347.552	92762798.84
138	-4052.902	-4033.592	-4146.951	-26162.611	98761147.95
139	-4172.334	-4162.914	-4258.399	-27006.725	105183869.8
140	-4323.577	-4296.591	-4419.05	-27911.166	112388331.3
141	-4451.074	-4404.622	-4566.044	-28761.641	119296849.7
142	-4608.55	-4540.782	-4649.404	-29644.586	126663199.6
143	-4745.883	-4692.93	-4807.272	-30567.742	134645174.7
144	-4880.124	-4818.714	-4966.653	-31502.929	142997840.9
145	-5006.983	-4965.143	-5093.049	-32432.254	151471999.9
146	-5141.573	-5106.256	-5248.546	-33400.758	160617162.8
147	-5276.172	-5273.037	-5386.694	-34355.602	169907614



	F	G	H	I	J
148	-5428.359	-5431.743	-5576.539	-35372.686	180152136.7
149	-5580.034	-5593.897	-5704.747	-36376.461	190460893.3
150	-5715.608	-5740.865	-5895.725	-37388.94	201231029.2
151	-5875.998	-5881.846	-6039.965	-38421.891	212431292.6
152	-6025.795	-6057.687	-6224.741	-39485.117	224386109
153	-6153.914	-6187.46	-6361.967	-40445.149	235337593.9
154	-6306.551	-6368.529	-6516.667	-41491.895	247677876.8
155	-6457.72	-6519.952	-6645.706	-42492.461	259688815.3
156	-6623.438	-6674.778	-6802.657	-43533.59	272547472.8
157	-6773.405	-6856.285	-6962.659	-44587.976	285910298.5
158	-6961.427	-7027.754	-7096.123	-45699.375	300319415.1
159	-7116.038	-7193.01	-7331.202	-46811.776	315207687.2
160	-7270.847	-7364.041	-7465.652	-47865.951	329511042.1
161	-7406.134	-7523.269	-7624.037	-48910.778	343984644.4
162	-7591.174	-7678.236	-7772.429	-49996.423	359365516.2
163	-7758.238	-7842.631	-7941.806	-51085.628	375182595.7
164	-7920.327	-7999.59	-8098.869	-52172.872	391257707.4
165	-8092.09	-8154.633	-8283.888	-53329.047	408722854.9
166	-8239.466	-8310.65	-8471.316	-54418.936	425555608.9
167	-8413.496	-8464.397	-8647.008	-55532.242	443127921.1
168	-8557.638	-8614.017	-8808.843	-56554.608	459566984
169	-8719.53	-8759.333	-8989.366	-57642.747	477385086.6
170	-8871.529	-8924.489	-9181.988	-58757.672	496022385.4
171	-8994.58	-9086.56	-9375.8	-59822.286	514111197.6
172	-9140.964	-9241.665	-9527.914	-60849.43	531848099.6
173	-9272.13	-9424.682	-9657.528	-61890.685	550087417.7
174	-9429.419	-9563.489	-9828.764	-62930.057	568662201.8
175	-9564.031	-9725.216	-9979.862	-63959.179	587339847.1
176	-9684.339	-9869.107	-10084.106	-64909.529	604782121.1
177	-9807.809	-10002.91	-10216.633	-65847.857	622303355.6
178	-9927.794	-10136.836	-10333.029	-66802.564	640326109.5
179	-10050.844	-10250.315	-10460.487	-67753.965	658528075.5
180	-10145.423	-10363.838	-10601.577	-68663.334	676165141.3
181	-10284.06	-10484.323	-10708.976	-69581.745	694240087.6
182	-10428.759	-10604.409	-10844.447	-70456.905	711768498.6
183	-10542.167	-10719.371	-10975.416	-71270.082	728237568.5
184	-10631.171	-10832.991	-11064.032	-72034.245	743777228.4
185	-10703.554	-10923.219	-11110.843	-72695.175	757257162.4
186	-10817.322	-11023.56	-11216.904	-73458.242	773148948.3
187	-10903.378	-11086.923	-11292.014	-74129.455	787198317.3
188	-11006.329	-11165.201	-11378.715	-74822.397	801823161.9
189	-11086.034	-11233.423	-11466.933	-75439.161	814972695.7
190	-11178.263	-11291.033	-11549.388	-76058.88	828284066.3
191	-11273.417	-11354.378	-11576.486	-76593.498	839790894.9
192	-11293.807	-11422.175	-11591.249	-77039.45	849394205.7
193	-11316.002	-11471.629	-11575.014	-77439.325	857986839.9
194	-11373.974	-11498.441	-11579.636	-77840.613	866720559.3
195	-11425.051	-11529.419	-11587.392	-78156.13	873630812.7
196	-11456.118	-11542.788	-11592.146	-78466.362	880433259.1

	F	G	H	I	J
197	-11471.704	-11573.259	-11547.895	-78704.973	885630733.3
198	-11498.913	-11558.469	-11566.746	-78948.682	891033918.7
199	-11475.617	-11547.522	-11537.793	-79051.542	893240398
200	-11453.711	-11558.451	-11456.026	-79071.627	893589490.4
201	-11442.172	-11534.324	-11384.53	-79137.491	894984750.9
202	-11401.362	-11506.678	-11369.052	-79249.471	897427909.2
203	-11385.566	-11467.327	-11399.37	-79322.29	899040633.4
204	-11351.426	-11435.124	-11371.736	-79307.715	898676811.4
205	-11339.9	-11384.848	-11346.088	-79324.844	899050485.4
206	-11285.846	-11328.188	-11318.161	-79273.244	897896778.9
207	-11242.01	-11284.736	-11244.9	-79200.517	896286829.5
208	-11191.915	-11221.117	-11202.022	-79144.57	895105768.1
209	-11136.527	-11146.429	-11128.433	-79013.513	892265513.5
210	-11091.488	-11083.068	-11032.219	-78881.434	889454234
211	-11046.884	-11012.9	-10963.955	-78720.621	886048180.3
212	-10982.141	-10937.75	-10821.373	-78531.985	882097609.6
213	-10930.896	-10869.26	-10734.543	-78326.83	877806486.7
214	-10852.288	-10791.178	-10692.896	-78199.679	875322583.9
215	-10780.245	-10718.46	-10553.341	-78007.496	871518302.4
216	-10695.277	-10618.681	-10447.676	-77761.687	866606385.2
217	-10621.152	-10515.089	-10392.598	-77602.672	863571355
218	-10584.498	-10426.215	-10295.729	-77390.305	859414279.3
219	-10498.672	-10330.813	-10184.122	-77151.242	854827528.1
220	-10399.111	-10254.41	-10122.571	-76973.923	851679140.3
221	-10305.195	-10152.405	-10028.315	-76744.283	847490644.1
222	-10195.311	-10047.866	-9911.813	-76503.137	843255589.2
223	-10110.076	-9936.99	-9787.371	-76269.84	839246409.8
224	-10026.386	-9865.78	-9704.072	-76164.642	837982581.8
225	-9977.964	-9783.984	-9634.886	-76091.456	837502500.2
226	-9888.132	-9695.118	-9572.726	-76009.295	836974741
227	-9818.585	-9596.378	-9489.867	-75901.781	836087007
228	-9754.288	-9507.066	-9418.325	-75843.663	836354811.4
229	-9676.691	-9446.574	-9348.203	-75800.669	836998943.1
230	-9634.541	-9395.353	-9284.759	-75855.948	839895141.4
231	-9566.777	-9332.525	-9189.131	-75881.134	842350356
232	-9542.551	-9292.424	-9108.275	-75990.491	846496122.6
233	-9517.633	-9252.732	-9046.865	-76225.284	853633796.3
234	-9478.251	-9222.663	-9037.907	-76517.414	862042730.1
235	-9499.83	-9186.452	-9013.579	-76872.993	871796768.7
236	-9501.656	-9162.435	-8948.608	-77171.897	880732625.1
237	-9526.088	-9149.964	-8921.526	-77623.68	893134637.8
238	-9537.874	-9148.71	-8919.529	-78147.266	907398709.7
239	-9542.274	-9149.253	-8881.958	-78615.803	920579894.2
240	-9550.913	-9167.402	-8873.107	-79221.634	937199560.7
241	-9584.031	-9176.805	-8908.164	-79936.29	956477337
242	-9655.28	-9192.025	-8987.109	-80807.654	979440097.9
243	-9735.573	-9243.431	-9072.46	-81757.193	1004472643
244	-9818.43	-9292.559	-9100.01	-82650.867	1028681367
245	-9880.979	-9369.817	-9110.31	-83556.207	1053819278

	F	G	H	I	J
246	-9997.208	-9438.277	-9158.294	-84707.15	1085230675
247	-10085.595	-9534.853	-9202.755	-85794.961	1115558475
248	-10192.196	-9669.819	-9302.621	-87104.451	1151566947
249	-10362.816	-9802.483	-9346.071	-88426.939	1188403039
250	-10528.04	-9944.244	-9431.073	-89826.713	1227749212
251	-10700.501	-10083.679	-9554.679	-91305.612	1269896602
252	-10811.052	-10263.491	-9676.698	-92932.598	1317450496
253	-10987.341	-10419.295	-9842.121	-94640.686	1367080776
254	-11191.753	-10600.11	-9977.399	-96353.351	1417446255
255	-11375.034	-10808.715	-10078.37	-98117.047	1471080684
256	-11598.512	-11029.985	-10280.646	-100100.49	1531371557
257	-11836.601	-11238.448	-10489.32	-102140.08	1594933313
258	-12080.009	-11473.632	-10686.66	-104222.14	1660677690
259	-12383.709	-11718.686	-10904.57	-106436.58	1731069052
260	-12656.937	-11920.938	-11139.231	-108616.23	1802172859
261	-12916.689	-12152.009	-11378.689	-110924.71	1879628671
262	-13171.213	-12427.081	-11606.763	-113306.25	1960349828
263	-13460.079	-12730.726	-11949.908	-115824.48	2045998880
264	-13792.121	-13017.34	-12249.058	-118370.32	2135068811
265	-14078.845	-13328.918	-12539.93	-120850.79	2223393324
266	-14368.993	-13646.945	-12891.43	-123453.62	2317799993
267	-14692.433	-13957.827	-13178.823	-126110.91	2416494717
268	-15027.596	-14289.536	-13472.443	-128711.93	2514933016
269	-15351.014	-14597.494	-13792.752	-131321.29	2615034488
270	-15683.627	-14918.585	-14144.019	-133943.84	2717173770
271	-16034.833	-15269.825	-14464.739	-136559.01	2821224904
272	-16373.429	-15611.599	-14813.348	-139248.7	2929472667
273	-16724.149	-15928.348	-15103.217	-141777.11	3033862183
274	-17061.136	-16260.576	-15405.805	-144292.27	3139690953
275	-17362.28	-16569.042	-15705.111	-146715.82	3243401913
276	-17688.292	-16872.825	-15977.819	-149147.34	3349017843
277	-18010.071	-17179.065	-16308.08	-151444.36	3448230862
278	-18281.296	-17482.737	-16614.757	-153778.9	3552040796
279	-18602.538	-17776.219	-16919.456	-156022.51	3651695592
280	-18944.571	-18060.434	-17188.882	-158159.83	3747677593
281	-19226.173	-18282.354	-17425.529	-160015.52	3832751726
282	-19479.534	-18549.934	-17678.618	-161866.44	3917533975
283	-19729.114	-18766.01	-17912.923	-163655.63	4001380378
284	-19929.346	-18971.838	-18107.245	-165114.21	4070269887
285	-20182.298	-19186.256	-18248.945	-166523.59	4136325553
286	-20356.046	-19377.077	-18465.689	-167754.82	4193444991
287	-20507.753	-19513.284	-18680.579	-168757.4	4239559268
288	-20634.606	-19668.039	-18819.075	-169593.04	4277481483
289	-20733.714	-19768.053	-18937.663	-170194.91	4304026856
290	-20783.989	-19885.598	-19062.331	-170612.34	4321585042
291	-20859.378	-19962.446	-19098.232	-170673.14	4320462337
292	-20861.608	-19994.438	-19119.745	-170516.99	4309380447
293	-20903.721	-20013.305	-19130.15	-170239.82	4291160434
294	-20899.466	-19995.864	-19078.861	-169637.44	4257351132

	F	G	H	I	J
295	-20810.561	-19942.832	-19022.876	-168674.23	4205582137
296	-20707.173	-19836.405	-18935.73	-167533.21	4146340201
297	-20550.815	-19691.45	-18801.495	-166042.5	4069499508
298	-20374.02	-19481.301	-18654.667	-164150.04	3973247159
299	-20156.651	-19264.991	-18440.562	-162055.31	3869771467
300	-19881.261	-18977.299	-18201.247	-159579	3749840608
301	-19584.493	-18647.1	-18021.704	-157001.31	3626901646
302	-19245.126	-18288.291	-17662.913	-153920.2	3484470922
303	-18866.645	-17877.162	-17243.142	-150389.91	3324485402
304	-18397.042	-17466.61	-16842.634	-146617.55	3157727821
305	-17882.823	-16971.5	-16382.249	-142447.53	2979780611
306	-17352.925	-16463.359	-15907.865	-138083.65	2798394947
307	-16757.366	-15889.988	-15389.769	-133152.9	2599789623
308	-16087.408	-15290.834	-14805.199	-127889.74	2397518252
309	-15448.448	-14594.593	-14254.519	-122293.88	2190511375
310	-14711.198	-13860.32	-13641.584	-116350.45	1981705342
311	-13900.291	-13109.102	-12924.008	-109929.66	1768110558
312	-13019.15	-12270.143	-12144.889	-103065.11	1553843756
313	-12109.87	-11389.139	-11358.867	-95793.716	1341658232
314	-11160.171	-10392.186	-10517.672	-88133.58	1135470826
315	-10111.645	-9457.015	-9674.854	-80230.144	940599940.2
316	-9025.253	-8410.166	-8756.353	-71859.905	754805282.9
317	-7862.213	-7330.874	-7826.473	-63113.051	582390653.1
318	-6682.15	-6178.815	-6785.665	-54012.728	427353075
319	-5446.775	-4991.653	-5703.406	-44510.425	291107495.9
320	-4138.616	-3810.79	-4492.521	-34595.202	176971105.5
321	-2791.49	-2506.812	-3260.915	-24251.441	88521827.89
322	-1461.284	-1206.441	-2035.956	-13845.239	30991444.12
323	-83.045	149.661	-698.075	-3051.423	4458791.942
324	1340.54	1603.4	635.359	8082.362	12604984.29
325	2850.483	3075.037	2063.792	19557.172	58655401.5
326	4383.323	4538.998	3486.417	31194.877	144197414.1
327	5952.945	6100.647	4949.171	43168.536	273229712.9
328	7539.233	7697.396	6531.01	55519.263	449132914.4
329	9187.787	9247.513	8059.968	67827.692	668834786.2
330	10847.403	10873.396	9729.727	80519.901	940877792.6
331	12572.647	12494.174	11430.917	93420.452	1264287126
332	14296.179	14169.785	13086.92	106498.208	1641766043
333	16042.532	15861.433	14683.371	119558.752	2067909682
334	17882.124	17587.351	16505.536	133126.502	2561644158
335	19627.728	19388.654	18384.065	146772.456	3110751151
336	21407.878	21111.859	20223.128	160349.068	3710532752
337	23272.904	22910.3	22003.722	174216.856	4378493977
338	25100.446	24693.34	23898.222	188029.316	5097374494
339	26977.413	26500.957	25809.218	201833.22	5869956027
340	28839.122	28294.599	27655.065	215580.095	6693935515
341	30623.601	30107.543	29517.671	229090.418	7555706878
342	32458.745	31892.429	31376.585	242484.158	8461500810
343	34294.757	33678.715	33153.448	255844.841	9416997116

	F	G	H	I	J
344	36120.027	35420.777	34876.444	269077.811	10414358579
345	37868.347	37197.511	36650.694	282054.846	11439637332
346	39649.437	38906.613	38400.147	294942.67	12505254475
347	41331.546	40637.965	40130.19	307664.638	13604832615
348	43032.519	42348.496	41802.319	320108.588	14723419349
349	44720.015	44035.511	43363.862	332213.51	15855411673
350	46450.796	45696.336	44978.03	344184.206	17013550127
351	48128.577	47328.285	46503.643	355780.966	18174807363
352	49778.62	48928.675	48033.085	367258.524	19361940426
353	51354.132	50494.824	49499.077	378352.11	20545757437
354	52891.784	52024.047	51054.987	389163.075	21730760530
355	54389.027	53513.66	52434.417	399524.229	22899115099
356	55843.3	54960.984	53839.784	409711.974	24076903813
357	57252.054	56363.336	55259.253	419532.256	25239766553
358	58612.734	57718.031	56590.714	428894.714	26373812813
359	59922.78	59022.386	57835.788	437860.389	27483638371
360	61179.644	60273.718	59030.003	446395.256	28561004247
361	62380.765	61469.343	60147.792	454487.604	29601719201
362	63523.597	62606.582	61209.819	462145.13	30603528788
363	64605.577	63682.75	62214.725	469353.469	31561658117
364	65624.152	64695.164	63161.139	476098.264	32471383915
365	66576.777	65641.136	64047.694	482365.15	33328051416
366	67460.886	66517.996	64873.026	488139.771	34127095735
367	68273.925	67323.043	65635.761	493407.765	34864060883
368	69013.347	68053.613	66334.534	498154.771	35534620147
369	69676.589	68707.011	66967.987	502366.435	36134599581
370	70261.105	69280.55	67534.737	506028.397	36659997785
371	70764.339	69771.566	68033.432	509126.31	37107010656
372	71183.722	70177.355	68462.698	511645.786	37472048282
373	71516.722	70495.246	68821.167	513572.491	37751771275
374	71760.769	70722.558	69107.472	514892.068	37943105176
375	71913.316	70856.597	69320.245	515590.123	38043262936
376	71971.8	70894.683	69458.12	515652.325	38049785994
377	71933.675	70834.144	69519.729	515064.318	37960557471
378	71796.378	70672.285	69503.706	513811.725	37773829975
379	71557.363	70406.433	69408.682	511880.193	37488260233
380	71214.073	70033.894	69233.3	509255.396	37102937709

	K	L	M	N	O	P
1	Ave x or y					
2		Sxx				
3	0.53098755	0.10515562				
4		Sum xi*yi	Sxy	Slope B1	Intercept Bo	Slope + Int
5	0	0	0	0	0	0
6	14.5272857	45.3220756	-8.6745795	-82.492782	58.329926	-24.162856
7	27.8662857	87.2242136	-16.352342	-155.50612	110.438099	-45.06802
8	40.0567143	125.806574	-23.080743	-219.49129	156.603859	-62.887435
9	51.1405714	161.178813	-28.906234	-274.89006	197.103772	-77.786289
10	61.158	193.443191	-33.875766	-322.14889	232.215049	-89.933839
11	70.1501429	222.70535	-38.036618	-361.71741	262.217584	-99.499825
12	78.1578571	249.070371	-41.435573	-394.04051	287.388461	-106.65205
13	85.222	272.643013	-44.119735	-419.56612	308.006387	-111.55973
14	91.3835714	293.529125	-46.135647	-438.73687	324.347387	-114.38948
15	96.6835714	311.833767	-47.530643	-452.00288	336.691475	-115.31141
16	101.162286	327.659997	-48.351403	-459.80808	345.314654	-114.49343
17	104.861429	341.115846	-48.644946	-462.59959	350.496053	-112.10354
18	107.821	352.303093	-48.458168	-460.82339	352.512482	-108.31091
19	110.082429	361.328528	-47.838267	-454.9283	351.643693	-103.28461
20	111.686714	368.297833	-46.831952	-445.35853	348.16655	-97.191981
21	112.674143	373.313894	-45.486077	-432.55964	342.357928	-90.201714
22	113.086143	376.48364	-43.847698	-416.97913	334.496871	-82.48226
23	112.963286	377.910783	-41.963907	-399.06481	324.861732	-74.203078
24	112.346714	377.701892	-39.881055	-379.25748	313.727716	-65.529766
25	111.276857	375.959459	-37.646922	-358.01151	301.376515	-56.635
26	107.071857	359.843376	-38.133386	-362.63765	299.627935	-63.009715
27	106.221429	362.295732	-32.520062	-309.25653	270.432797	-38.823735
28	103.537143	350.940476	-33.898062	-322.36092	274.706779	-47.654142
29	100.572429	339.110447	-34.708506	-330.06802	275.834436	-54.233579
30	98.7674286	335.759303	-31.350623	-298.1355	257.073666	-41.061831
31	94.1745714	323.066997	-26.971678	-256.49298	230.369152	-26.12383
32	90.8557143	303.281982	-34.420791	-327.33192	264.664889	-62.667031
33	94.6705714	323.292472	-28.589793	-271.88079	239.035886	-32.844903
34	91.907	312.74436	-28.865951	-274.50697	237.666786	-36.840188
35	86.6178571	299.093678	-22.857349	-217.36688	202.036965	-15.329916
36	83.1514286	283.93666	-25.129954	-238.97871	210.04615	-28.932563
37	80.0838571	270.930677	-26.734042	-254.23313	215.078483	-39.154644
38	80.671	277.106626	-22.740451	-216.25521	195.499827	-20.755388
39	77.7451429	265.728089	-23.243832	-221.04223	195.115815	-25.926414
40	82.4777143	289.357376	-17.205101	-163.61561	169.355566	5.73995672
41	80.3771429	277.93047	-20.824366	-198.03379	185.530622	-12.503171
42	79.623	276.798129	-19.153624	-182.14551	176.339999	-5.805512
43	81.7348571	286.082605	-17.718737	-168.50014	171.206336	2.7061925
44	81.4618571	286.774929	-16.011696	-152.26667	162.313563	10.0468938
45	78.2017143	270.480433	-20.188524	-191.98712	180.144485	-11.842635
46	80.6881429	280.225328	-19.685467	-187.20319	180.090707	-7.1124844
47	82.0978571	281.500092	-23.650489	-224.90942	201.521959	-23.38746
48	87.7352857	298.178712	-27.9257	-265.56545	228.747236	-36.818218
49	87.9364286	294.798543	-32.053499	-304.81966	249.791871	-55.027784

	K	L	M	N	O	P
50	92.5795714	317.220884	-26.889316	-255.70974	228.358259	-27.351478
51	97.1328571	332.47141	-28.562955	-271.62558	241.362656	-30.262919
52	95.5662857	321.983106	-33.22845	-315.9931	263.354689	-52.638413
53	87.0351429	285.489203	-38.012839	-361.49128	278.98251	-82.508765
54	73.7362857	237.292503	-36.778846	-349.75635	259.452554	-90.303797
55	66.2245714	209.484474	-36.666487	-348.68786	251.373483	-97.314374
56	64.0527143	199.859658	-38.218699	-363.44895	257.039582	-106.40937
57	54.6215714	161.850604	-41.173018	-391.54368	262.526391	-129.01729
58	46.708	137.376005	-36.233561	-344.57085	229.670833	-114.90002
59	37.6924286	103.321902	-36.777571	-349.74423	223.402262	-126.34197
60	26.6795714	60.6274758	-38.538166	-366.48699	221.279602	-145.20739
61	14.4167143	9.91812965	-43.667541	-415.26589	234.91773	-180.34816
62	8.82014286	-18.830343	-51.614045	-490.83488	269.447352	-221.38752
63	-0.0214286	-55.309937	-55.230289	-525.22432	278.86615	-246.35817
64	-5.8292857	-78.380479	-56.713532	-539.32955	280.54799	-258.78156
65	-20.602143	-141.97274	-65.396368	-621.90084	309.619463	-312.28138
66	-27.697286	-169.56183	-66.613431	-633.47477	308.669929	-324.80484
67	-35.365571	-203.23707	-71.786323	-682.6675	327.122372	-355.54513
68	-48.398857	-262.32631	-82.431971	-783.90458	367.844718	-416.05987
69	-53.453429	-281.45493	-82.773191	-787.14949	364.513149	-422.63634
70	-61.077	-309.97631	-82.958426	-788.91101	357.824928	-431.08609
71	-74.316857	-356.85665	-80.627367	-766.74331	332.814294	-433.92901
72	-91.285857	-423.41401	-84.112436	-799.88532	333.44329	-466.44203
73	-98.945857	-454.96695	-87.193824	-829.18844	341.342884	-487.84556
74	-112.71457	-516.10289	-97.152647	-923.89402	377.861651	-546.03237
75	-126.98057	-564.39532	-92.419601	-878.8841	339.695946	-539.18816
76	-143.75986	-628.23118	-93.888315	-892.85115	330.332987	-562.51816
77	-147.29029	-632.6713	-85.206145	-810.28618	282.96159	-527.32459
78	-156.80643	-672.31836	-89.482532	-850.95341	295.039239	-555.91417
79	-164.20243	-706.97058	-96.644464	-919.06134	323.807704	-595.25364
80	-176.34929	-744.72554	-89.250616	-848.74795	274.32531	-574.42264
81	-198.574	-829.31839	-91.236135	-867.62967	262.126555	-605.50312
82	-219.641	-911.3216	-94.935141	-902.80617	259.737838	-643.06833
83	-234.38914	-970.92626	-99.722238	-948.33009	269.162332	-679.16776
84	-256.01671	-1046.554	-94.962203	-903.06352	223.498771	-679.56475
85	-273.37457	-1112.4903	-96.380802	-916.55399	213.30419	-703.2498
86	-293.06729	-1186.8447	-97.539147	-927.56953	199.460586	-728.10894
87	-314.00557	-1262.7226	-95.591287	-909.04593	168.686501	-740.35943
88	-335.61757	-1347.3019	-99.840677	-949.45642	168.531966	-780.92445
89	-364.861	-1463.5924	-107.43586	-1021.6845	177.64074	-844.04374
90	-389.419	-1565.7189	-118.28237	-1124.8317	207.852606	-916.97905
91	-416.40029	-1661.3613	-113.63768	-1080.662	157.417784	-923.24422
92	-447.20829	-1775.8641	-113.62992	-1080.5882	126.57059	-954.0176
93	-476.75129	-1884.7173	-112.67427	-1071.5002	92.2019807	-979.29822
94	-499.32657	-1970.9657	-115.01235	-1093.7348	81.4329685	-1012.3018
95	-528.85286	-2079.2218	-113.52183	-1079.5603	44.3802178	-1035.1801
96	-563.55957	-2208.8134	-114.11159	-1085.1687	12.6515087	-1072.5172
97	-600.52129	-2351.2525	-119.16719	-1133.246	1.21824158	-1132.0278
98	-636.25714	-2491.0045	-126.09214	-1199.1003	0.45021567	-1198.6501

	K	L	M	N	O	P
99	-667.27843	-2600.0326	-119.81681	-1139.4238	-62.25858	-1201.6824
100	-703.95271	-2734.198	-117.6671	-1118.9806	-109.78795	-1228.7685
101	-741.704	-2877.2916	-120.44242	-1145.3731	-133.52513	-1278.8983
102	-784.374	-3035.4331	-119.98326	-1141.0066	-178.51369	-1319.5203
103	-834.38871	-3227.4854	-126.13525	-1199.5104	-197.46365	-1396.974
104	-878.14314	-3386.6924	-122.71088	-1166.9455	-258.5096	-1425.4551
105	-931.85143	-3586.4549	-122.84439	-1168.2152	-311.54371	-1479.7589
106	-982.32914	-3778.0539	-126.82207	-1206.0418	-341.93599	-1547.9777
107	-1037.439	-3988.6641	-132.59376	-1260.9289	-367.90144	-1628.8304
108	-1097.3756	-4217.8561	-139.00672	-1321.9143	-395.45551	-1717.3699
109	-1156.4116	-4438.2208	-139.93974	-1330.7871	-449.7802	-1780.5673
110	-1214.4917	-4658.1373	-143.97743	-1369.1844	-487.47186	-1856.6562
111	-1269.7793	-4867.2535	-147.59455	-1403.5821	-524.49465	-1928.0768
112	-1333.9779	-5114.558	-156.27852	-1486.1642	-544.84317	-2031.0074
113	-1400.5704	-5371.7041	-165.90586	-1577.7175	-562.82206	-2140.5396
114	-1460.8343	-5597.7449	-167.95113	-1597.1674	-612.75828	-2209.9257
115	-1531.1083	-5866.2257	-175.22965	-1666.3841	-646.27906	-2312.6632
116	-1594.2443	-6103.5313	-177.8642	-1691.4379	-696.1118	-2387.5497
117	-1665.2216	-6371.4658	-181.98236	-1730.6005	-746.29427	-2476.8947
118	-1729.89	-6610.9508	-181.10042	-1722.2134	-815.41611	-2537.6295
119	-1815.5391	-6938.4494	-190.2486	-1809.21	-854.87113	-2664.0812
120	-1898.2677	-7250.598	-194.90228	-1853.4652	-914.10076	-2767.566
121	-1988.855	-7601.8284	-209.42771	-1991.5979	-931.3413	-2922.9392
122	-2074.082	-7924.5457	-215.36362	-2048.0467	-986.5947	-3034.6414
123	-2159.9987	-8247.6923	-219.16533	-2084.1999	-1053.3145	-3137.5144
124	-2243.9614	-8559.3228	-218.71371	-2079.9051	-1139.5577	-3219.4628
125	-2335.7447	-8908.9478	-227.18827	-2160.4957	-1188.5484	-3349.0441
126	-2429.67	-9258.7117	-227.84008	-2166.6943	-1279.1823	-3445.8766
127	-2523.7866	-9616.8281	-236.13334	-2245.5608	-1331.4217	-3576.9826
128	-2621.8476	-9988.422	-243.24302	-2313.1719	-1393.5821	-3706.754
129	-2721.1657	-10362.889	-248.55298	-2363.668	-1466.0874	-3829.7554
130	-2830.2624	-10777.079	-257.23974	-2446.2767	-1531.32	-3977.5967
131	-2931.759	-11153.429	-256.33671	-2437.6891	-1637.3764	-4075.0656
132	-3044.2486	-11583.861	-268.65407	-2554.8237	-1687.669	-4242.4927
133	-3154.7539	-11996.805	-270.85968	-2575.7984	-1787.0369	-4362.8354
134	-3269.9299	-12428.949	-274.90426	-2614.2612	-1881.7897	-4496.0509
135	-3386.8349	-12878.39	-289.81982	-2756.104	-1923.3779	-4679.4819
136	-3508.6167	-13349.82	-308.59727	-2934.6721	-1950.3423	-4885.0145
137	-3621.0789	-13770.757	-311.52252	-2962.4905	-2048.0333	-5010.5238
138	-3737.5159	-14204.379	-312.35842	-2970.4397	-2160.2494	-5130.689
139	-3858.1036	-14654.337	-314.10208	-2987.0213	-2272.0324	-5259.0538
140	-3987.3094	-15151.406	-330.92385	-3146.9917	-2316.296	-5463.2877
141	-4108.8059	-15606.791	-334.71757	-3183.0688	-2418.636	-5601.7047
142	-4234.9409	-16073.597	-332.69089	-3163.7956	-2555.0048	-5718.8004
143	-4366.8203	-16572.66	-341.57	-3248.2335	-2642.0488	-5890.2822
144	-4500.4184	-17077.371	-349.70755	-3325.6192	-2734.556	-6060.1752
145	-4633.1791	-17570.327	-349.20348	-3320.8257	-2869.862	-6190.6877
146	-4771.5369	-18089.608	-354.2209	-3368.5399	-2982.8841	-6351.424
147	-4907.9431	-18604.254	-361.85703	-3441.1574	-3080.7314	-6521.8888



	K	L	M	N	O	P
148	-5053.2409	-19161.389	-378.93301	-3603.5451	-3139.8033	-6743.3484
149	-5196.6373	-19697.518	-382.0696	-3633.3732	-3267.3614	-6900.7345
150	-5341.2771	-20248.309	-395.24686	-3758.6851	-3345.4621	-7104.1472
151	-5488.8416	-20798.157	-396.61077	-3771.6555	-3486.1394	-7257.795
152	-5640.731	-21378.762	-412.65607	-3924.2418	-3557.0075	-7481.2492
153	-5777.8784	-21886.739	-410.86811	-3907.2388	-3703.1833	-7610.4221
154	-5927.4136	-22454.035	-422.35511	-4016.4769	-3794.7143	-7811.1912
155	-6070.3516	-22986.373	-423.40489	-4026.46	-3932.3514	-7958.8114
156	-6219.0843	-23546.884	-431.08953	-4099.5387	-4042.2803	-8141.819
157	-6369.7109	-24117.588	-441.92816	-4202.611	-4138.1768	-8340.7877
158	-6528.4821	-24715.394	-449.59468	-4275.5174	-4258.2356	-8533.753
159	-6687.3966	-25328.251	-471.78091	-4486.5021	-4305.1198	-8791.6219
160	-6837.993	-25892.381	-476.15722	-4528.1196	-4433.6179	-8961.7375
161	-6987.254	-26450.415	-479.40109	-4558.9679	-4566.4988	-9125.4667
162	-7142.3461	-27031.416	-483.9373	-4602.106	-4698.6851	-9300.7911
163	-7297.9469	-27619.112	-493.27995	-4690.9519	-4807.1098	-9498.0617
164	-7453.2674	-28200.245	-497.09979	-4727.2775	-4943.1419	-9670.4194
165	-7618.4353	-28817.843	-500.78307	-4762.3044	-5089.7109	-9852.0153
166	-7774.1337	-29402.772	-506.99483	-4821.3765	-5214.0428	-10035.419
167	-7933.1774	-30002.117	-515.18787	-4899.29	-5331.7154	-10231.005
168	-8079.2297	-30551.718	-521.92545	-4963.3624	-5443.746	-10407.108
169	-8234.6781	-31135.613	-528.03205	-5021.4344	-5568.359	-10589.793
170	-8393.9531	-31737.336	-537.74312	-5113.784	-5678.5975	-10792.382
171	-8546.0409	-32308.11	-543.22082	-5165.8754	-5803.0253	-10968.901
172	-8692.7757	-32856.862	-546.57184	-5197.7426	-5932.8391	-11130.582
173	-8841.5264	-33408.942	-545.75851	-5190.008	-6085.6968	-11275.705
174	-8990.0081	-33964.638	-549.56093	-5226.168	-6214.978	-11441.146
175	-9137.0256	-34513.266	-551.73773	-5246.8688	-6351.0036	-11597.872
176	-9272.7899	-35012.476	-546.32412	-5195.3868	-6514.1041	-11709.491
177	-9406.8367	-35509.377	-544.98506	-5182.6528	-6654.9126	-11837.565
178	-9543.2234	-36009.09	-537.75996	-5113.9441	-6827.7828	-11941.727
179	-9679.1379	-36505.081	-528.56922	-5026.5428	-7010.1062	-12036.649
180	-9809.0477	-36978.585	-519.20963	-4937.5358	-7187.2777	-12124.813
181	-9940.2493	-37459.814	-512.77388	-4876.3336	-7350.9768	-12227.31
182	-10065.272	-37927.718	-515.97843	-4906.808	-7459.8182	-12366.626
183	-10181.44	-38360.301	-516.77515	-4914.3846	-7571.9632	-12486.348
184	-10290.606	-38755.651	-506.3641	-4815.3785	-7733.7004	-12549.079
185	-10385.025	-39086.928	-486.69529	-4628.3336	-7927.4375	-12555.771
186	-10494.035	-39488.192	-482.77973	-4591.0978	-8056.2188	-12647.317
187	-10589.922	-39831.47	-469.65267	-4466.2632	-8218.392	-12684.655
188	-10688.914	-40186.682	-456.92034	-4345.1823	-8381.6761	-12726.858
189	-10777.023	-40504.003	-446.74809	-4248.4472	-8521.1504	-12769.598
190	-10865.554	-40821.232	-434.91304	-4135.8992	-8669.4433	-12805.343
191	-10941.928	-41087.293	-417.09884	-3966.4913	-8835.7708	-12802.262
192	-11005.636	-41299.834	-392.8454	-3735.8479	-9021.947	-12757.795
193	-11062.761	-41479.091	-359.773	-3421.3388	-9246.0724	-12667.411
194	-11120.088	-41667.232	-334.83531	-3184.1885	-9429.3231	-12613.512
195	-11165.161	-41815.653	-315.72043	-3002.4114	-9570.9184	-12573.33
196	-11209.48	-41956.989	-292.3276	-2779.9523	-9733.3602	-12513.313

	K	L	M	N	O	P
197	-11243.568	-42051.784	-260.423	-2476.5486	-9928.5511	-12405.1
198	-11278.383	-42160.34	-239.57268	-2278.2679	-10068.651	-12346.919
199	-11293.077	-42185.616	-210.23156	-1999.2423	-10231.505	-12230.747
200	-11295.947	-42162.751	-176.70112	-1680.3773	-10403.687	-12084.065
201	-11305.356	-42159.572	-138.54978	-1317.569	-10605.743	-11923.312
202	-11321.353	-42182.989	-102.50621	-974.80491	-10803.744	-11778.549
203	-11331.756	-42201.044	-81.895465	-778.80256	-10918.221	-11697.024
204	-11329.674	-42163.132	-51.722786	-491.86897	-11068.497	-11560.366
205	-11332.121	-42138.792	-18.28711	-173.90521	-11239.779	-11413.684
206	-11324.749	-42075.07	18.0355072	171.512539	-11415.82	-11244.308
207	-11314.36	-41993.096	61.3930006	583.829959	-11624.366	-11040.536
208	-11306.367	-41920.905	103.876199	987.833079	-11830.894	-10843.061
209	-11287.645	-41806.583	148.608705	1413.22649	-12038.05	-10624.824
210	-11268.776	-41689.757	195.30238	1857.27004	-12254.964	-10397.694
211	-11245.803	-41560.191	239.478452	2277.37191	-12455.059	-10177.687
212	-11218.855	-41403.003	296.503914	2819.66782	-12716.064	-9896.3957
213	-11189.547	-41250.417	340.154793	3234.77525	-12907.173	-9672.3973
214	-11171.383	-41139.197	383.858914	3650.38901	-13109.694	-9459.3048
215	-11143.928	-40979.347	441.662285	4200.08261	-13374.12	-9174.037
216	-11108.812	-40791.321	499.166788	4746.93406	-13629.375	-8882.4413
217	-11086.096	-40658.953	547.100164	5202.76683	-13848.7	-8645.9336
218	-11055.758	-40500.564	592.7241	5636.63747	-14048.742	-8412.1047
219	-11021.606	-40317.591	648.757935	6169.50329	-14297.535	-8128.0322
220	-10996.275	-40170.571	701.624025	6672.24475	-14539.154	-7866.9089
221	-10963.469	-39991.405	758.854209	7216.48751	-14795.334	-7578.8465
222	-10929.02	-39797.875	824.338415	7839.22367	-15091.55	-7252.3261
223	-10895.691	-39609.582	888.75353	8451.79307	-15383.488	-6931.6953
224	-10880.663	-39498.761	943.715941	8974.46996	-15645.995	-6671.525
225	-10870.208	-39404.639	998.977299	9499.98975	-15914.584	-6414.5945
226	-10858.471	-39301.271	1058.71814	10068.1082	-16204.511	-6136.4026
227	-10843.112	-39180.423	1122.47832	10674.4493	-16511.111	-5836.662
228	-10834.809	-39086.404	1185.63692	11275.0696	-16821.731	-5546.661
229	-10828.667	-39001.669	1247.54268	11863.7757	-17128.184	-5264.4085
230	-10836.564	-38968.792	1309.77257	12455.5643	-17450.314	-4994.7493
231	-10840.162	-38911.444	1380.4935	13128.1002	-17811.02	-4682.9196
232	-10855.784	-38908.766	1441.23839	13705.7668	-18133.376	-4427.6092
233	-10889.326	-38965.578	1509.099	14351.1019	-18509.583	-4158.4808
234	-10931.059	-39056.898	1572.89644	14957.7974	-18873.463	-3915.666
235	-10981.856	-39186.559	1632.04319	15520.2662	-19222.924	-3702.6581
236	-11024.557	-39275.873	1701.44335	16180.242	-19616.064	-3435.8218
237	-11089.097	-39447.275	1769.93277	16831.5568	-20026.444	-3194.8875
238	-11163.895	-39655.788	1839.43701	17492.5223	-20452.207	-2959.6844
239	-11230.829	-39834.245	1909.76728	18161.3432	-20874.276	-2712.933
240	-11317.376	-40081.998	1983.7033	18864.4537	-21334.166	-2469.7127
241	-11419.47	-40389.106	2056.06915	19552.6323	-21801.674	-2249.042
242	-11543.951	-40783.889	2123.96908	20198.3414	-22269.018	-2070.677
243	-11679.599	-41222.652	2189.40004	20820.5712	-22735.063	-1914.4919
244	-11807.267	-41625.612	2260.96905	21501.172	-23224.121	-1722.9494
245	-11936.601	-42029.646	2337.66012	22230.4823	-23740.71	-1510.2281

	K	L	M	N	O	P
246	-12101.021	-42562.363	2416.07916	22976.225	-24301.111	-1324.8859
247	-12256.423	-43064.774	2491.28267	23691.389	-24836.256	-1144.8666
248	-12443.493	-43688.829	2562.55023	24369.1232	-25383.194	-1014.0708
249	-12632.42	-44321.659	2631.94466	25029.0445	-25922.531	-893.48639
250	-12832.388	-44998.107	2698.7589	25664.4289	-26459.88	-795.45093
251	-13043.659	-45714.289	2767.85443	26321.5077	-27020.052	-698.54409
252	-13276.085	-46494.437	2851.61567	27118.0533	-27675.434	-557.38087
253	-13520.098	-47333.68	2919.34604	27762.1498	-28261.454	-499.30415
254	-13764.764	-48180.999	2981.43129	28352.5628	-28819.622	-467.05952
255	-14016.721	-49040.444	3058.48687	29085.3395	-29460.674	-375.3347
256	-14300.07	-50028.543	3123.57011	29704.2626	-30072.663	-368.40078
257	-14591.44	-51038.035	3197.07448	30403.2682	-30735.197	-331.92844
258	-14888.878	-52076.937	3263.72333	31037.0798	-31369.181	-332.10078
259	-15205.226	-53194.884	3321.61501	31587.6132	-31977.855	-390.24192
260	-15516.604	-54288.339	3385.52516	32195.3806	-32611.95	-416.56958
261	-15846.386	-55438.051	3461.58605	32918.6979	-33325.805	-407.10732
262	-16186.607	-56635.414	3528.79365	33557.8231	-34005.393	-447.57024
263	-16546.354	-57928.143	3573.21398	33980.2478	-34589.443	-609.19492
264	-16910.046	-59224.795	3628.37149	34504.78	-35231.654	-726.87435
265	-17264.398	-60491.665	3678.59815	34982.4212	-35839.628	-857.20712
266	-17636.231	-61825.262	3727.07133	35443.3874	-36456.228	-1012.8409
267	-18015.844	-63178.764	3784.56011	35990.0893	-37126.134	-1136.0445
268	-18387.418	-64509.872	3834.55827	36465.5576	-37750.175	-1284.6175
269	-18760.184	-65850.893	3879.0773	36888.9209	-38347.742	-1458.8212
270	-19134.834	-67207.12	3915.39046	37234.2487	-38905.756	-1671.5077
271	-19508.43	-68557.512	3953.62377	37597.8366	-39472.414	-1874.577
272	-19892.672	-69953.647	3985.68075	37902.6894	-40018.528	-2115.8387
273	-20253.873	-71256.173	4025.70656	38283.3234	-40581.841	-2298.5173
274	-20613.181	-72554.089	4063.30927	38640.9145	-41131.026	-2490.1112
275	-20959.403	-73802.414	4101.85943	39007.5155	-41671.908	-2664.3922
276	-21306.763	-75055.012	4140.36954	39373.7357	-42213.727	-2839.9908
277	-21634.908	-76265.961	4149.10608	39456.8177	-42585.987	-3129.1692
278	-21968.415	-77477.069	4177.61514	39727.9307	-43063.452	-3335.5208
279	-22288.93	-78659.546	4186.46611	39812.101	-43428.66	-3616.5593
280	-22594.261	-79789.008	4191.89108	39863.6909	-43761.384	-3897.6936
281	-22859.36	-80761.551	4204.69994	39985.4995	-44091.163	-4105.6634
282	-23123.778	-81744.527	4204.53942	39983.973	-44354.77	-4370.7965
283	-23379.375	-82681.869	4217.23061	40104.6626	-44674.452	-4569.789
284	-23587.744	-83449.037	4224.55206	40174.2875	-44919.791	-4745.503
285	-23789.085	-84202.061	4219.89475	40129.9978	-45097.614	-4967.6163
286	-23964.974	-84875.218	4200.50293	39945.5871	-45175.584	-5229.9967
287	-24108.2	-85431.963	4176.11491	39713.664	-45195.661	-5481.9971
288	-24227.578	-85902.773	4149.02207	39456.0188	-45178.233	-5722.2137
289	-24313.558	-86251.632	4119.74403	39177.593	-45116.372	-5938.7792
290	-24373.191	-86508.242	4084.78618	38845.1538	-44999.484	-6154.3306
291	-24381.877	-86590.902	4034.41	38366.0906	-44753.793	-6387.7027
292	-24359.571	-86550.249	3992.1517	37964.2263	-44518.102	-6553.8759
293	-24319.975	-86462.256	3932.97061	37401.4309	-44179.669	-6778.2379
294	-24233.921	-86200.463	3874.90844	36849.2762	-43800.428	-6951.1513

	K	L	M	N	O	P
295	-24096.318	-85756.808	3807.1069	36204.5029	-43320.459	-7115.9557
296	-23933.315	-85210.365	3747.68151	35639.3843	-42857.384	-7218.0001
297	-23720.356	-84495.48	3671.01753	34910.3317	-42257.308	-7346.9763
298	-23450.006	-83586.113	3575.51513	34002.1311	-41504.714	-7502.5829
299	-23150.758	-82557.138	3492.21377	33209.9589	-40784.833	-7574.8743
300	-22797	-81332.023	3402.44026	32356.2384	-39977.76	-7621.5217
301	-22428.758	-80060.837	3304.90222	31428.6794	-39116.996	-7688.3163
302	-21988.6	-78511.642	3218.06903	30602.9204	-38238.37	-7635.4496
303	-21484.273	-76741.672	3113.49714	29608.4715	-37206.002	-7597.5308
304	-20945.364	-74850.718	3001.37555	28542.2271	-36100.931	-7558.7043
305	-20349.647	-72738.493	2899.37285	27572.2104	-34990.148	-7417.9374
306	-19726.235	-70541.021	2779.67733	26433.9401	-33762.329	-7328.3885
307	-19021.842	-68066.867	2635.66306	25064.4054	-32330.73	-7266.3241
308	-18269.963	-65395.319	2512.54351	23893.5736	-30957.154	-7063.58
309	-17470.554	-62577.361	2359.16423	22434.9803	-29383.249	-6948.2685
310	-16621.493	-59563.206	2217.43639	21087.1888	-27818.528	-6731.3394
311	-15704.238	-56300.97	2070.31309	19688.0881	-26158.367	-6470.2793
312	-14723.587	-52799.428	1926.86313	18323.9199	-24453.361	-6129.4409
313	-13684.817	-49102.572	1762.69848	16762.7608	-22585.634	-5822.8731
314	-12590.511	-45194.253	1603.58121	15249.6009	-20687.86	-5438.2588
315	-11461.449	-41165.301	1435.90698	13655.0667	-18712.12	-5057.0529
316	-10265.701	-36878.637	1278.07836	12154.1614	-16719.409	-4565.2477
317	-9016.1501	-32411.04	1101.20443	10472.1406	-14576.726	-4104.5858
318	-7716.104	-27737.76	942.326036	8961.25236	-12474.417	-3513.1651
319	-6358.6321	-22864.773	769.708192	7319.7058	-10245.305	-2925.599
320	-4942.1717	-17770.502	599.11916	5697.45267	-7967.4482	-2269.9955
321	-3464.4916	-12444.296	432.91767	4116.92381	-5650.5269	-1533.6031
322	-1977.8913	-7099.4099	252.239619	2398.72697	-3251.5854	-852.85847
323	-435.91757	-1538.0586	82.2089817	781.784014	-851.03515	-69.251137
324	1154.62314	4203.72686	-87.906747	-835.96814	1598.51182	762.543677
325	2793.88171	10143.7909	-240.824	-2290.1676	4009.93222	1719.76458
326	4456.411	16153.6827	-410.40862	-3902.8691	6528.78593	2625.91679
327	6166.93371	22349.9517	-572.00352	-5439.5906	9055.28861	3615.698
328	7931.32329	28756.2018	-723.8357	-6883.4715	11586.361	4702.88947
329	9689.67029	35129.9032	-885.75685	-8423.2955	14162.3354	5739.03982
330	11502.843	41713.1965	-1041.8686	-9907.8741	16763.8008	6855.9267
331	13345.7789	48425.1096	-1179.9874	-11221.345	19304.1732	8082.82853
332	15214.0297	55212.9542	-1336.2686	-12707.534	21961.5718	9254.03829
333	17079.8217	61987.4594	-1496.7496	-14233.663	24637.7196	10404.0566
334	19018.0717	69061.6701	-1626.8452	-15470.835	27232.8924	11762.0576
335	20967.4937	76189.9203	-1744.4268	-16589.002	29776.0473	13187.0452
336	22907.0097	83268.3327	-1875.0263	-17830.966	32375.0309	14544.0645
337	24888.1223	90494.1732	-2012.8087	-19141.237	35051.881	15910.6437
338	26861.3309	97716.024	-2125.2021	-20210.067	37592.6247	17382.5579
339	28833.3171	104954.702	-2216.2255	-21075.674	40024.2374	18948.5639
340	30797.1564	112150.598	-2319.7493	-22060.155	42510.8243	20450.669
341	32727.2026	119243.187	-2400.9726	-22832.566	44851.0111	22018.4447
342	34640.594	126277.791	-2478.278	-23567.718	47154.759	23587.0408
343	36549.263	133275.535	-2574.8911	-24486.481	49551.2798	25064.7984

	K	L	M	N	O	P
344	38439.6873	140197.659	-2679.3086	-25479.462	51968.9645	26489.5023
345	40293.5494	147015.533	-2752.0788	-26171.486	54190.2825	28018.7968
346	42134.6671	153791.216	-2819.6701	-26814.26	56372.7053	29558.4455
347	43952.0911	160463.999	-2902.0935	-27598.083	58606.3297	31008.2466
348	45729.7983	167015.817	-2957.8582	-28128.389	60665.6228	32537.2336
349	47459.0729	173369.203	-3032.0352	-28833.792	62769.4573	33935.6656
350	49169.1723	179697.673	-3059.8555	-29098.354	64620.0363	35521.6818
351	50825.8523	185823.948	-3091.3159	-29397.535	66435.5772	37038.0426
352	52465.5034	191887.913	-3121.7916	-29687.349	68229.1164	38541.767
353	54050.3014	197741.142	-3159.1181	-30042.314	70002.3963	39960.0821
354	55594.725	203484.922	-3155.8261	-30011.008	71530.1968	41519.1885
355	57074.8899	208969.709	-3172.6834	-30171.316	73095.483	42924.1671
356	58530.282	214376.641	-3175.3165	-30196.356	74564.1712	44367.8151
357	59933.1794	219598.418	-3167.9874	-30126.658	75930.06	45803.4016
358	61270.6734	224581.971	-3155.7829	-30010.597	77205.927	47195.3297
359	62551.4841	229349.112	-3149.304	-29948.984	78454.0221	48505.0376
360	63770.7509	233895.595	-3134.7292	-29810.382	79599.6927	49789.3105
361	64926.8006	238207.421	-3119.8395	-29668.785	80680.5561	51011.771
362	66020.7329	242291.787	-3101.5237	-29494.607	81682.0022	52187.3948
363	67050.4956	246140.913	-3079.9362	-29289.317	82602.7582	53313.4414
364	68014.0377	249747.021	-3055.2306	-29054.374	83441.5484	54387.1748
365	68909.3071	253102.328	-3027.562	-28791.253	84197.1039	55405.8513
366	69734.253	256199.061	-2997.0811	-28501.388	84868.1353	56366.7472
367	70486.8236	259029.432	-2963.9488	-28186.31	85453.4031	57267.0935
368	71164.9673	261585.669	-2928.313	-27847.423	85951.6021	58104.1793
369	71766.6336	263859.993	-2890.3306	-27486.221	86361.475	58875.2536
370	72289.771	265844.62	-2850.1593	-27104.204	86681.7658	59577.562
371	72732.33	267531.787	-2807.9459	-26702.766	86911.1663	60208.4004
372	73092.2551	268913.691	-2763.8519	-26283.445	87048.437	60764.9924
373	73367.4987	269982.573	-2718.027	-25847.663	87092.2858	61244.6232
374	73556.0097	270730.651	-2670.628	-25396.912	87041.4538	61644.5419
375	73655.7319	271150.13	-2621.8072	-24932.64	86894.6534	61962.0132
376	73664.6179	271233.244	-2571.7215	-24456.34	86650.6298	62194.2901
377	73580.6169	270972.217	-2520.5239	-23969.465	86308.1041	62338.6396
378	73401.675	270359.262	-2468.3676	-23473.473	85865.797	62392.3239
379	73125.7419	269386.603	-2415.4072	-22969.835	85322.4381	62352.6035
380	72750.7709	268046.477	-2361.7989	-22460.035	84676.77	62216.7347

```

y = {-29351.773,-30680.845,-32160.145,-32180.654,-32593.891
-32048.11,-59763.652,-62237.165,-62659.355,-63273.138,
-62633.595,-64569.801,-86691.081,-79299.269,-74192.928,
-82915.648,-88088.955}

```

```

x = {{0.600,0.200,0.000,0.000},
      {0.599,0.213,0.000,0.000},
      {0.598,0.224,0.000,0.000},
      {0.593,0.260,0.000,0.000},
      {0.574,0.312,0.000,0.000},
      {0.550,0.368,0.000,0.000},

```

```

      {0.501,0.167,0.167,0.000},
      {0.491,0.175,0.179,0.000},
      {0.484,0.181,0.192,0.000},
      {0.456,0.200,0.230,0.000},
      {0.410,0.223,0.287,0.000},
      {0.358,0.240,0.348,0.000},

```

```

      {0.429,0.143,0.143,0.143},
      {0.414,0.148,0.151,0.155},
      {0.401,0.150,0.160,0.169},
      {0.360,0.158,0.182,0.209},
      {0.299,0.162,0.210,0.270}}

```

```

z =Inverse[(Transpose[x].x)].(Transpose[x].y)

```

```

r = y - x.z

```

```

error = Transpose[r].r

```

```

q = Inverse[(Transpose[x].x)]

```

```

{-29351.773, -30680.845, -32160.145, -32180.654,
-32593.891, -32048.11, -59763.652, -62237.165,
-62659.355, -63273.138, -62633.595, -64569.801,
-86691.081, -79299.269, -74192.928, -82915.648,
-88088.955}

```

```
{{0.6, 0.2, 0., 0.}, {0.599, 0.213, 0., 0.},  
  {0.598, 0.224, 0., 0.}, {0.593, 0.26, 0., 0.},  
  {0.574, 0.312, 0., 0.}, {0.55, 0.368, 0., 0.},  
  {0.501, 0.167, 0.167, 0.}, {0.491, 0.175, 0.179, 0.},  
  {0.484, 0.181, 0.192, 0.}, {0.456, 0.2, 0.23, 0.},  
  {0.41, 0.223, 0.287, 0.}, {0.358, 0.24, 0.348, 0.},  
  {0.429, 0.143, 0.143, 0.143},  
  {0.414, 0.148, 0.151, 0.155},  
  {0.401, 0.15, 0.16, 0.169},  
  {0.36, 0.158, 0.182, 0.209},  
  {0.299, 0.162, 0.21, 0.27}}  
  
{-77731., 46567.9, -154099., -171104.}  
  
{7973.28, 5961.1, 3891.82, 1806.21, -2505.44, -6433.01,  
  -2862.7, -4636.88, -3879.3, -1698.58, 3077.92,  
  5708.08, -13499.6, -4220.54, 3564.51, 1516.63, 6167.59}  
  
5.0796 108  
  
{{4.35256, -9.39539, 0.0373372, -0.840139},  
  {-9.39539, 22.5443, -1.93172, 1.6936},  
  {0.0373372, -1.93172, 4.33459, -2.3728},  
  {-0.840139, 1.6936, -2.3728, 7.59437}}
```

## References



- Abderhalden, E., Schmidt, H. S. (1913) *Hoppe Seyler's Zeit. Physiol. Chem.* **85**, 143-147.
- Adler, A. J., Greenfield, N. J., Fasman, G. D. (1973) In *Methods in Enzymology* **27**, pp 675-735, C. H. W. Hirs, ed., Academic Press, Inc., New York.
- Albert, J. S., Hamilton, A. D. (1995) *Biochemistry* **34**, 984-990.
- Allen, T. A. (1993) Ph.D. Thesis, Massachusetts Institute of Technology.
- Barlow, D. J., Thornton, J. M. (1988) *J. Mol. Biol.* **201**, 601-619.
- Bayley, P. M., Nielsen, E. B., Schellman, J. A. (1969) *J. Chem. Phys.* **73**, 228-243.
- Bell, J. A., Becktel, W. J., Sauer, U., Baase, W. A., Matthews, B. W. (1992) *Biochemistry* **31**, 3590-3596.
- Ben-Naim, A. (1964) *Israel J. Chem.* **2**, 278-279.
- Bierzynski, A., Baldwin, R. L. (1982) *J. Mol. Biol.* **162**, 173-186.
- Bierzynski, A., Kim, P. S., Baldwin, R. L. (1982) *Proc. Natl. Acad. Sci. USA* **79**, 2470-2474.
- Blaber, M., Zhang, X. J., Matthews, B. W. (1993) *Science* **260**, 1637-1640.
- Blout, E. R., Karlson, R. H., Doty, P., Hargitay, B. (1954) *J. Am. Chem. Soc.* **76**, 4492-4493.
- Blout, E. R., Karlson, R. H. (1956) *J. Am. Chem. Soc.* **78**, 941-946.
- Boyd, J. G. (1989) Ph.D. Thesis, Massachusetts Institute of Technology.
- Brown, J. E., Klee, W. A. (1971) *Biochemistry* **10**, 470-476.
- Bundi, A., Wüthrich, K. (1979) *Biopolymers* **18**, 285-297.
- Calvin, M., Hermans, J., Scheraga, H. A. (1960) *J. Am. Chem. Soc.* **81**, 5048-5050.
- Cammers-Goodwin, A., Allen, T. J., Oslick, S. L., McClure, K. F., Lee, J. H., Kemp, D. S. (1996) *J. Am. Chem. Soc.*, in press.
- Chakrabarty, A., Schellman, J. A., Baldwin, R. L. (1991) *Nature* **351**, 586-588.
- Chakrabarty, A., Kortemme, T., Padmanabhan, S., Baldwin, R. L. (1993) *Biochemistry* **32**, 5560-5565.
- Chakrabarty, A., Kortemme, T., Baldwin, R. L. (1994) *Protein Sci.* **3**, 843-852.
- Chang, C. T., Wu, C. C., Yang, J. T. (1978) *Anal. Biochem.* **91**, 13-31.
- Chen, Y. H., Yang, J. T. (1971) *Biochem. Biophys. Res. Commun.* **44**, 1285-1291.
- Chen, Y. H., Yang, J. T., Martinez, H. M. (1972) *Biochemistry* **11**, 4120-4131.

- Chen, Y. H., Yang, J. T., Chau, K. H. (1974) *Biochemistry* **13**, 3350-3359.
- Crabbé, P. (1972) ORD and CD in Chemistry and Biochemistry: An Introduction, pp 11-13, Academic Press, New York.
- Curran, T. P. (1988) Ph.D. Thesis, Massachusetts Institute of Technology.
- D'Aniello, A., D'Onofrio, G., Pischetola, M., Strazzullo, L. (1985) *Anal. Biochem.* **144**, 610-611.
- Davidson, B., Fasman, G. D. (1967) *Biochemistry* **6**, 1616-1629.
- Doty, P., Holtzer, A. M., Bradbury, J. H., Blout, E. R. (1954) *J. Am. Chem. Soc.* **76**, 4493-4494.
- Doty, P., Yang, J. T. (1956) *J. Am. Chem. Soc.* **78**, 498-500.
- Doty, P., Bradbury, J. H., Holtzer, A. M. (1956) *J. Am. Chem. Soc.* **78**, 947-954.
- Doty, P., Wada, A., Yang, J. T., Blout, E. R. (1957) *J. Poly. Sci.* **23**, 851-861.
- Doty, P., Imahori, K., Klemperer, E. (1958) *Proc. Natl. Acad. Sci. USA* **44**, 424-431.
- Eberhardt, E. S., Loh, S. N., Hinck, A. P., Raines, R. T. (1992) *J. Am. Chem. Soc.* **114**, 5437-5439.
- Epand, R. M., Scheraga, H. A. (1968) *Biochemistry* **7**, 2864-2872.
- Fairman, R., Shoemaker, K. R., York, E. J., Stewart, J. M., Baldwin, R. L. (1989) *Proteins: Struc. Func. Genetics* **5**, 1-7.
- Fairman, R., Shoemaker, K. R., York, E. J., Stewart, J. M., Baldwin, R. L. (1990) *Biophys. Chem.* **37**, 107-119.
- Fairman, R., Armstrong, K. M., Shoemaker, K. R., York, E. J., Stewart, J. M., Baldwin, R. L. (1991) *J. Mol. Biol.* **221**, 1395-1401.
- Fasman, G. D., Lindblow, C., Bodenheimer, E. (1964) *Biochemistry* **3**, 155-166.
- Fillipi, B., Borin, G., Moretto, V., Marchiori, F. (1978) *Biopolymers* **17**, 2545-2559.
- Fitts, D. D., Kirkwood, J. G. (1956) *Proc. Natl. Acad. Sci. USA* **42**, 33-36.
- Forood, B., Feliciano, E. J., Nambiar, K. P. (1993) *Proc. Natl. Acad. Sci. USA* **90**, 838-842.
- Friedman, M., Williams, L. D. (1974) *Bioorganic Chem.* **3**, 267-280.
- Gans, P. J., Pingchiang, C. L., Manning, M. C., Woody, R. W., Kallenbach, N. R. (1991) *Biopolymers* **31**, 1605-1614.
- Goodman, M., Verdini, A. S., Toniolo, C., Phillips, W. D., Bovey, F. A. (1969) *Proc. Natl. Acad. Sci. USA* **64**, 444-450.

- Goodman, M., Naider, F., Rupp, R. (1971) *Bioorg. Chem.* **1**, 310-328.
- Goodman, M., Toniolo, C., Naider, F. (1974) In *Peptides, Polypeptides, and Proteins*, pp 308-319, E. R. Blout, F. A. Bovey, M. Goodman, N. Lotan, eds., John Wiley & Sons, Inc., New York.
- Gratzer, W. B., Doty, P. (1963) *J. Am. Chem. Soc.* **85**, 1193-1197.
- Greenfield, N., Fasman, G. D. (1969) *Biochemistry* **8**, 4108-4116.
- Grigg, R., Malone, J. F., Mongkolaussavaratana, T., Thianpatanagul, S. (1986) *J. Chem. Soc., Chem. Commun.*, 421-422.
- Grigg, R., Malone, J. F., Mongkolaussavaratana, T., Thianpatanagul, S. (1989) *Tetrahedron* **45**, 3849-3862.
- Groebke, K., Renold, P., Tsang, K. Y., Allen, T. J., McClure, K. F., Kemp, D. S. (1996) *Proc. Natl. Acad. Sci. USA*, in press.
- Harding, V. J., MacLean, R. M. (1915) *J. Biol. Chem.* **20**, 217-230.
- Hermans, J., Scheraga, H. A. (1959) *Biochem. Biophys. Acta* **36**, 534-535.
- Hirs, C. H. W. (1967) In *Methods in Enzymology* **11**, pp 325-329, C. H. W. Hirs, ed., Academic Press, Inc., New York.
- Holzwarth, G., Gratzer, W. B., Doty, P. (1962) *J. Am. Chem. Soc.* **84**, 3194-3196.
- Holzwarth, G., Doty, P. (1965) *J. Am. Chem. Soc.* **87**, 218-228.
- Idelson, M., Blout, E. R. (1957) *J. Am. Chem. Soc.* **79**, 3948-3955.
- Jasanoff, A., Fersht, A. R. (1994) *Biochemistry* **33**, 2129-2135.
- Johnson, W. C. (1985) In *Methods of Biochemical Analysis* **31**, pp 61-163, D. Glick, ed., John Wiley & Sons, Inc., New York.
- Johnson, W. C. (1988) In *Ann. Rev. Biophys. Biophys. Chem* **17**, pp 145-166, D. M. Engelman, ed., Annual Reviews, Inc., Palo Alto, California.
- Johnson, W. C. (1990) *Proteins: Struc. Func. Genetics* **7**, 205-214.
- Joullié, M. M., Thompson, T. R., Nemeroff, N. H. (1991) *Tetrahedron* **47**, 8791-8830.
- Katchalski, E., Sela, M. (1958) *Adv. Prot. Chem.* **13**, 243-492.
- Kemp, D. S., Curran, T. P. (1988) *Tett. Lett.* **29**, 4935-4938.
- Kemp, D. S., Curran, T. P., Boyd, J. G., Allen, T. J. (1991a) *J. Org. Chem.* **56**, 6683-6697.
- Kemp, D. S., Boyd, J. G., Muendel, C. C. (1991b) *Nature* **352**, 451-454.

- Kemp, D. S., Curran, T. P., Davis, W. M., Boyd, J. G., Muendel, C. (1991c) *J. Org. Chem.* **56**, 6672-6682.
- Kemp, D. S., Allen, T. J., Oslick, S. L. (1995) *J. Am. Chem. Soc.* **117**, 6641-6657.
- Kemp, D. S., Allen, T. J., Oslick, S. L., Boyd, J. G. (1996a) *J. Am. Chem. Soc.*, in press.
- Kemp, D. S., Oslick, S. L., Allen, T. J. (1996b) *J. Am. Chem. Soc.*, in press.
- Kim, P. S., Bierzynski, A. Baldwin, R. L. (1982) *J. Mol. Biol.* **162**, 187-199.
- Lifson, S., Roig, A. (1961) *J. Chem. Phys.* **34**, 1963-1974.
- Lord, R. S., Cox, D. J. (1973) *Biopolymers* **12**, 2359-2373.
- Lyu, P. C., Marky, L. A., Kallenbach, N. R. (1989) *J. Am. Chem. Soc.* **111**, 2733-2734.
- Lyu, P. C., Liff, M. I., Marky, L. A., Kallenbach, N. R. (1990) *Science* **250**, 669-673.
- Lyu, P. C., Wang, P. C., Liff, M. I., Kallenbach, N. R. (1991) *J. Am. Chem. Soc.* **113**, 3568-3572.
- Manning, M. C., Illangasekare, M., Woody, R. W. (1988) *Biophys. Chem.* **31**, 77-86.
- Manning, M. C., Woody, R. W. (1991) *Biopolymers* **31**, 569-586.
- Marqusee, S., Baldwin, R. L. (1987) *Proc. Natl. Acad. Sci USA* **84**, 8898-8902.
- Marqusee, S., Robbins, V. H., Baldwin, R. L. (1989) *Proc. Natl. Acad. Sci USA* **86**, 5286-5290.
- Mattice, W. L. (1974) *Biopolymers* **13**, 169-183.
- Mattice, W. L., Harrison, W. H. (1975) *Biopolymers* **14**, 2025-2033.
- McCaldin, D. J. (1960) *Chem. Rev.* **60**, 39-51.
- McClure, K. F., Renold, P., Kemp, D. S. (1995) *J. Org. Chem.* **60**, 454-457.
- Mendenhall, W., Beaver, R. J. (1991) Introduction to Probability and Statistics, pp 398-410, PWS-Kent Publishing Company, Boston.
- Merutka, G., Stellwagen, E. (1989) *Biochemistry* **28**, 352-357.
- Merutka, G., Lipton, W., Schalongo, W., Park, S., Stellwagen, E. (1990) *Biochemistry* **29**, 894-898.
- Miick, S. M., Martinez, G. V., Fiori, W. R., Todd, A. P., Millhauser, G. L. (1992) *Nature* **359**, 653-655.
- Moffitt, W. (1956a) *J. Chem. Phys.* **25**, 467-478.

- Moffitt, W. (1956b) *Proc. Natl. Acad. Sci USA* **42**, 736-746.
- Moffitt, W., Yang, J. T. (1956) *Proc. Natl. Acad. Sci USA* **42**, 596-603.
- Moffitt, W., Fitts, D. D., Kirkwood, J. G. (1957) *Proc. Natl. Acad. Sci USA* **43**, 723-730.
- Moore, S., Stein, W. H. (1948) *J. Biol. Chem.* **176**, 367-388.
- Moore, S., Stein, W. H. (1954) *J. Biol. Chem.* **211**, 907-913.
- Nelson, J. W., Kallenbach, N. R. (1986) *Proteins: Struc. Func. Genetics* **1**, 211-217.
- O'Neil, K. T., DeGrado, W. F. (1990) *Science* **250**, 646-651.
- Osterhout, J. J., Baldwin, R. L., York, E. J., Stewart, J. M., Dyson, H. J., Wright, P. E. (1989) *Biochemistry* **28**, 7059-7064.
- Padmanabhan, S., Marqusee, S., Ridgeway, T., Laue, T. M., Baldwin, R. L. (1990) *Nature* **344**, 268-270.
- Padmanabhan, S., York, E. J., Gera, L., Stewart, J. M., Baldwin, R. L. (1994) *Biochemistry* **33**, 8604-8609.
- Park, S., Shalongo, W., Stellwagen, E. (1993a) *Biochemistry* **32**, 7048-7053.
- Park, S., Shalongo, W., Stellwagen, E. (1993b) *Biochemistry* **32**, 12901-12905.
- Pauling, L., Corey, R. B. (1951) *Proc. Natl. Acad. Sci. USA* **37**, 235-240.
- Poland, D., Scheraga, H. A. (1969) *Biopolymers* **7**, 887-908.
- Radzicka, A., Acheson, S. A., Wolfenden, R. (1992) *Bioorg. Chem.* **20**, 382-386.
- Rohl, C. A., Scholtz, J. M., York, E. J., Stewart, J. M., Baldwin, R. L. (1992) *Biochemistry* **31**, 1263-1269.
- Rosen, H. (1957) *Arch. Biochem. Biophys.* **67**, 10-15.
- Rosen, H., Berard, C. W., Levenson, S. M. (1962) *Anal. Biochem.* **4**, 213-221.
- Rosin, J. (1967) Reagent Chemicals and Standards, pp 8, 36-37, D. Van Nostrand Company, Inc., Princeton, New Jersey.
- Ruhemann, S. (1910a) *J. Chem. Soc.* **97**, 1438-1449.
- Ruhemann, S. (1910b) *J. Chem. Soc.* **97**, 2025-2031.
- Ruhemann, S. (1911a) *J. Chem. Soc.* **99**, 792-800.
- Ruhemann, S. (1911b) *J. Chem. Soc.* **99**, 1306-1310.
- Ruhemann, S. (1911c) *J. Chem. Soc.* **99**, 1486-1510.

- Ruhemann, S. (1912) *J. Chem. Soc.* **101**, 780-788.
- Sarin, V. K., Kent, S. B. H., Tam, J. P., Merrifield, R. B. (1981) *Anal. Biochem.* **117**, 147-157.
- Schellman, J. A., Oriel, P. (1962) *J. Chem. Phys.* **37**, 2114-2124.
- Schneider, H., Kresheck, G. C., Scheraga, H. A. (1965) *J. Phys. Chem.* **69**, 4310-4324.
- Scheraga, H. A. (1960) *Ann. N.Y. Acad. Sci.* **84**, 608-616.
- Scheraga, H. A. (1978) *Pure & Appl. Chem.* **50**, 315-324.
- Scholtz, J. M., York, E. J., Stewart, J. M., Baldwin, R. L. (1991a) *J. Am. Chem. Soc.* **113**, 5102-5104.
- Scholtz, J. M., Qian, H., York, E. J., Stewart, J. M., Baldwin, R. L. (1991b) *Biopolymers* **31**, 1463-1470.
- Scholtz, J. M., Marqusee, S., Baldwin, R. L., York, E. J., Stewart, J. M., Santoro, M., Bolen, D. W. (1991c) *Proc. Natl. Acad. Sci. USA* **88**, 2854-2858.
- Scholtz, J. M., Baldwin, R. L. (1993) *Biochemistry* **32**, 4604-4608.
- Schönberg, A., Singer, E. (1978) *Tetrahedron* **34**, 1285-1300.
- Serrano, L., Neira, J. L., Sancho, J., Fersht, A. R. (1992a) *Nature* **356**, 453-455.
- Serrano, L., Sancho, J., Hirshberg, M., Fersht, A. R. (1992b) *J. Mol. Biol.* **227**, 544-559.
- Sheng, S., Kraft, J. J., Schuster, S. M. (1993) *Anal. Biochem.* **211**, 242-249.
- Shoemaker, K. R., Kim, P. S., Brems, D. N., Marqusee, S., York, E. J., Chaiken, I. M., Stewart, J. M., Baldwin, R. L. (1985) *Proc. Natl. Acad. Sci. USA* **82**, 2349-2353.
- Shoemaker, K. R., Kim, P. S., York, E. J., Stewart, J. M., Baldwin, R. L. (1987) *Nature* **326**, 563-567.
- Shoemaker, K. R., Fairman, R., Schultz, D. A., Robertson, A. D., York, E. J., Stewart, J. M., Baldwin, R. L. (1990) *Biopolymers* **29**, 1-11.
- Sueki, M., Lee, S., Powers, S. P., Denton, J. B., Konishi, Y., Scheraga, H. A. (1984) *Macromolecules* **17**, 148-155.
- Tinoco, I. (1960) *J. Chem. Phys.* **33**, 1332-1338.
- Tinoco, I. (1962) *Adv. Chem. Phys.* **4**, 113-160.
- Tinoco, I., Woody, R. W., Bradley, D. F. (1963) *J. Chem. Phys.* **38**, 1317-1325.
- Todd, A. P., Millhauser, G. L. (1991) *Biochemistry* **30**, 5515-5523.

- Toniolo, C., Bonora, G. M. (1976) *Can. J. Chem.* **54**, 70-76.
- Toniolo, C., Bonora, G. M., Salardi, S., Mutter, M. (1979) *Macromolecules* **12**, 620-625.
- Troll, W., Cannan, R. K. (1953) *J. Biol. Chem.* **200**, 803-811.
- Vdovenko, V. M., Gurikov, Y. V., Legin, E. K. (1967) *Doklady Akad. Nauk. SSSR* **172**, 126-129.
- Vila, J., Williams, R. L., Grant, J. A., Wojcik, J., Scheraga, H. A. (1992) *Proc. Natl. Acad. Sci. USA* **89**, 7821-7825.
- Westall, F., Hesser, H. (1974) *Anal. Biochem.* **61**, 610-613.
- Woody, R. W., Tinoco, I. (1967) *J. Chem. Phys.* **46**, 4927-4945.
- Woody, R. W. (1985) In *The Peptides* **7**, pp 15-114, V. J. Hruby, ed., Academic Press, Inc., New York.
- Woody, R. W. (1994) In *Circular Dichroism: Principles and Applications*, pp 473-496, K. Nakanishi, N. Berova, R. W. Woody, eds., VCH Publishers, Inc., New York.
- Woody, R. W. (1995) In *Methods in Enzymology* **246**, pp 34-71, C. H. W. Hirs, S. N. Timasheff, eds., Academic Press, Inc., New York.
- Wüthrich, K. (1986) *NMR of Proteins and Nucleic Acids*, pp 162-166, John Wiley & Sons, Inc., New York.
- Yang, J. T., Doty, P. (1957) *J. Am. Chem. Soc.* **79**, 761-775.
- Yang, J. T., Wu, C. C., Martinez, H. M. (1986) In *Methods in Enzymology*, pp 208-269, C. H. W. Hirs, S. N. Timasheff, eds., Academic Press, Inc., New York.
- Yemm, E. W., Cocking, E. C. (1955) *Analyst* **80**, 209-213.
- Zhou, H. X., Lyu, P. C., Wemmer, P. C., Kallenbach, N. R. (1994) *Proteins: Struct. Func. Genetics* **18**, 1-7.
- Zimm, B. H., Bragg, J. K. (1959) *J. Chem. Phys.* **31**, 526-535.